

UNCLASSIFIED

AD NUMBER
AD025162
NEW LIMITATION CHANGE
TO Approved for public release, distribution unlimited
FROM Distribution authorized to U.S. Gov't. agencies and their contractors; Administrative/Operational Use; 30 SEP 1953. Other requests shall be referred to Office of Naval Research, One Liberty Center, 875 North Randolph Street, arlington, VA 22203-1995.
AUTHORITY
ONR ltr, 26 Oct 1977

THIS PAGE IS UNCLASSIFIED

# Armed Services Technical Information Agency

# AD

PLEASE RETURN THIS COPY TO:

ARMED SERVICES TECHNICAL INFORMATION AGENCY  
DOCUMENT SERVICE CENTER  
Knott Building, Dayton 2, Ohio

*Because of our limited supply you are requested to return this copy as soon as it has served your purposes so that it may be made available to others for reference use. Your cooperation will be appreciated.*

# 25162

NOTICE: WHEN GOVERNMENT OR OTHER DRAWINGS, SPECIFICATIONS OR OTHER DATA ARE USED FOR ANY PURPOSE OTHER THAN IN CONNECTION WITH A DEFINITELY RELATED GOVERNMENT PROCUREMENT OPERATION, THE U. S. GOVERNMENT THEREBY INCURS NO RESPONSIBILITY, NOR ANY OBLIGATION WHATSOEVER; AND THE FACT THAT THE GOVERNMENT MAY HAVE FORMULATED, FURNISHED, OR IN ANY WAY SUPPLIED THE SAID DRAWINGS, SPECIFICATIONS, OR OTHER DATA IS NOT TO BE REGARDED BY IMPLICATION OR OTHERWISE AS IN ANY MANNER LICENSING THE HOLDER OR ANY OTHER PERSON OR CORPORATION, OR CONVEYING ANY RIGHTS OR PERMISSION TO MANUFACTURE, USE OR SELL ANY PATENTED INVENTION THAT MAY IN ANY WAY BE RELATED THERETO.

Reproduced by

DOCUMENT SERVICE CENTER

KNOTT BUILDING, DAYTON, 2, OHIO

# UNCLASSIFIED

AD No. 25 / 62

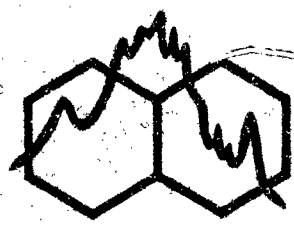
ASTIA FILE COPY

LABORATORY OF MOLECULAR STRUCTURE AND SPECTRA  
DEPARTMENT OF PHYSICS • THE UNIVERSITY OF CHICAGO

# TECHNICAL REPORT

1952 - 1953

PART TWO



For the period  
1 April 1952 to 30 September 1953:  
OFFICE OF NAVAL RESEARCH  
CONTRACT N60RI-20, TASK ORDER IX  
PROJECT NR 019 101

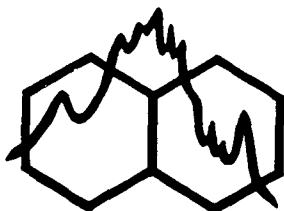
For the period  
24 June 1952 to 30 September 1953:  
OFFICE OF ORDNANCE RESEARCH  
CONTRACT DA-11-022-ORD-1002  
PROJECT TB2-0001 (505)

**LABORATORY OF MOLECULAR STRUCTURE AND SPECTRA**  
**DEPARTMENT OF PHYSICS • THE UNIVERSITY OF CHICAGO**

**TECHNICAL REPORT**

**1952 - 1953**

**PART TWO**



For the period  
1 April 1952 to 30 September 1953:  
OFFICE OF NAVAL RESEARCH  
CONTRACT N60RI-20, TASK ORDER IX  
PROJECT NR 019-101

For the period  
24 June 1952 to 30 September 1953:  
OFFICE OF ORDNANCE RESEARCH  
CONTRACT DA-11-022-ORD-1002  
PROJECT TB2-0001 (505)

Lithoprinted in U.S.A.  
**EDWARDS BROTHERS, INC.**  
ANN ARBOR, MICHIGAN

## PERSONNEL

### Faculty

- †\*\* Professor R. S. Mulliken, Director<sup>o#</sup>
- \* Professor W. G. Brown, Associate Deputy Director (from 16 September 1952)<sup>#</sup>
- †\* Associate Professor J. R. Platt<sup>o</sup>
- †\*\* Assistant Professor C. C. J. Roothaan, Associate Deputy Director<sup>#</sup>
- \* Visiting Associate Professor C. Reid (from 9 December 1952)<sup>\*</sup>

### Research Associates

- †\* Dr. K. Ruedenberg
- †\* Dr. Y. Tanaka (to 31 August 1952)
- \* Dr. P. G. Wilkinson (from 1 September 1952)

### Student Assistants

- † Mr. R. A. Bonic (from 8 October 1952 to 17 April 1953)
- †\* Mr. Charles E. Cohn (to 30 September 1952)
- \* Mr. Paul W. Engler (from 23 March 1953)
- †\* Mr. Norman S. Ham (from 1 October 1952)
- † Mr. David M. G. Lawrey (to 15 June 1952)
- \* Mr. Paul A. Michael (17 October 1952 to 23 February 1953)
- †\* Mr. Morton Schagrin (to 10 August 1952)
- † Mr. Charles W. Scherr (from 1 December 1952)

### Computation Staff

- †\* Mr. Walter Jaunzemis
- † Mr. Tracy J. Kinyon
- † Mrs. Gudrun Lenkersdorf (from 22 June 1953)
- \* Mr. Philip I. Merryman, Jr. (from 21 October 1952)

### Secretarial Staff

- †\*\* Mr. H. H. Brimmer, II, Administrative Secretary and Editor
- †\*\* Mrs. Eugenia Y. K. Bautista (from 23 September 1952)
- †\*\* Mr. William A. Lester, Jr. (from 30 April 1953)
- †\*\* Miss Arline T. Johnson (from 16 June 1952 to 5 January 1953)
- †\*\* Mr. Joel T. Rosenthal (from 6 January 1953 to 17 April 1953)

### Associated Scientific Personnel

- Mr. James E. Faulkner (to April 1953)
- Mr. Joe S. Ham, Jr., AEC Predoctoral Fellow, 1951-53
- Mr. Norman S. Ham, CSIRO Predoctoral Fellow, 1952-54 (from September 1952)
- Mr. William L. Lichten, AEC Predoctoral Fellow, 1951-53 (from January 1953)
- Dr. Harden M. McConnell, NRC Postdoctoral Fellow, 1950-52 (to May 1952)
- Mr. A. D. McLean, Australian Canteen Fellow, 1952-55 (from September 1952)
- Dr. W. J. Potts, Jr., AEC Predoctoral Fellow, 1950-52 (to December 1952)
- Dr. A. V. Stuart, Shell Development Company (from September to October 1952)

† Normally engaged under or associated with Office of Naval Research contract.

\* Normally engaged under or associated with Office of Ordnance Research contract.

\* Normally engaged under or associated with Office of Scientific Research (Air Research and Development Command) contract.

<sup>o</sup> On leave of absence for the academic year 1952-53. Professor Mulliken is for the most part at Oxford University, England, under a Fulbright Award. Professor Platt is at King's College, University of London, and other scientific centers in Europe under a Guggenheim Memorial Foundation Grant.

<sup>#</sup> During Professor's Mulliken absence Professor W. G. Brown of the Department of Chemistry is Deputy Director for the research contract with OOR, and Professor C. C. J. Roothaan is Deputy Director for those with ONR and OSR (ARDC).

<sup>\*</sup> On leave of absence from the Department of Chemistry, University of British Columbia.

TABLE OF CONTENTS

FOREWORD . . . . .	vii
PROGRESS REPORTS	
1. Theoretical Work in Progress . . . . .	xi
2. Experimental Work in Progress. . . . .	xiii
3. Progress Report on the Investigation of Integrals between Slater Atomic Orbitals and their Application in Molecular Calculations . . . . .	xiv
4. Progress Report on Xenon Emission Continua . . . . .	xxii
TECHNICAL PAPERS	
12. K. Ruedenberg, C. C. J. Roothaan, and W. Jaunzemis: A Study of Two-Center Integrals Useful in Calculations on Molecular Structure. III. A Unified Treatment of the Hybrid, Coulomb, and One-Electron Integrals <sup>†</sup> [ <u>J. Chem. Phys.</u> <u>22</u> , 000 (1954)]. . . . .	137
13. C. W. Scherr: Corrigenda: Free-Electron Network Model for Conjugated Systems. II. Numerical Calculations <sup>†</sup> . . . . .	259
14. P.-O. Löwdin: Studies of Atomic Self-Consistent Fields. I. Calculation of Slater Functions <sup>†</sup> [ <u>Phys. Rev.</u> <u>90</u> , 120 (1953)] . . . . .	260
15. C. W. Scherr: On the Use of a Single Scale Factor in Atomic Wavefunctions. I <sup>†</sup> [ <u>J. Chem. Phys.</u> <u>21</u> , 1237 (1953)] . . . . .	276
16. C. W. Scherr: On the Use of a Single Scale Factor in Atomic Wavefunctions. II. Application to Overlap Integrals <sup>†</sup> [ <u>J. Chem. Phys.</u> <u>21</u> , 1241 (1953)] . . . . .	286
17. N. Muller, L. W. Pickett, and R. S. Mulliken: Hyper- conjugation in $C_6H_7^+$ and Other Hydrocarbon Ions <sup>†</sup> [ <u>J. Chem. Phys.</u> <u>21</u> , 1400 (1953)] . . . . .	290
18. C. Reid: $n-\pi$ Emission Spectra* [ <u>J. Chem. Phys.</u> <u>21</u> , 1906 (1953)] . . . . .	293
19. C. Reid: The Aromatic Carbonium Ions* [ <u>J. Am. Chem. Soc.</u> <u>76</u> , 000 (1954)]. . . . .	295
20. W. J. Potts, Jr: Low-Temperature Absorption Spectra of Selected Olefins in the Farther Ultraviolet Region* . . . . .	303
21. W. J. Potts, Jr: Low-Temperature Absorption Spectra of Benzene, Toluene, and Para-Xylene in the Farther Ultraviolet Region* . . . . .	320
22. C. Reid and R. S. Mulliken: Molecular Compounds and their Spectra. IV. The Pyridine-Iodine System* [ <u>J. Am. Chem. Soc.</u> <u>76</u> , 000 (1954)]. . . . .	334
DISTRIBUTION LIST. . . . .	351

<sup>†</sup>Work assisted by the Office of Naval Research under Task Order IX of Contract N6ori-20 with The University of Chicago.

\*Work assisted by the Office of Ordnance Research under Project TB2-0001 (505) of Contract DA-11-022-ORD-1002 with The University of Chicago.

## FOREWORD

Six previous comprehensive TECHNICAL REPORTS have been issued under Contract N6ori-20, Task Order IX, Project 019 101, with the Office of Naval Research: A Quarterly Report for the period 1 June 1947 to 31 August 1947; an Annual Report (in two parts) for the period from 1 September 1947 to 31 August 1948; a Report (in two parts) for the period 1 September 1948 to 31 March 1950; a Report (in two parts) for the period 1 April 1950 to 31 March 1951; and a Report (in two parts) for the period 1 April 1951 to 31 March 1952.

The present Report is being issued in an as yet undetermined number of parts, published jointly under this Laboratory's contract with the Office of Naval Research as well as under Contract Number DA-11-022-ORD-1002, ORD Project Number TB2-0001 (505), with the Office of Ordnance Research. Part One covered roughly the period 1 April 1952 to 31 March 1953 for the contract with the Office of Naval Research, and the period 24 June 1952 to 23 June 1953 for the contract with the Office of Ordnance Research. The present Part Two covers roughly the period 1 April 1952 to 30 September 1953 for the former contract, and the period 24 June 1952 to 30 September 1953 for the latter.

This Part Two contains complete texts of finished articles recently published, now in press, or shortly to go to press, covering research partly or wholly supported by one or both of the two contracts. In addition, it contains, as a new and experimental feature, Progress Reports on various activities of the Laboratory, reflecting the status as of the time of going to press; these Progress Reports, to be included in future reports as activities and timeliness indicate, replace former sections of this Foreword entitled "Summary of Papers in Present Report", "Work in Progress", and "Associated Activities".

For an account of the general program and a survey of the equipment and apparatus on hand and in use, reference may be made to this TECHNICAL REPORT, 1948-49, Part One, and 1952-53, Part One, p. x. For a note on the reorganization of these Reports, reference may be made to this TECHNICAL REPORT, 1952-53, Part One, p. ix.

PROGRESS REPORTS

## THEORETICAL WORK IN PROGRESS

### 1. Computation of Molecular Integrals

Work now in progress on the problem of computing molecular integrals is reviewed in a separate Progress Report on this subject (see p. xiv).

### 2. Free-Electron Network Model

The free-electron network model for conjugated organic molecules, which had been proposed in four research papers by K. Ruedenberg, C. W. Scherr, and J. R. Platt,<sup>1</sup> has been further developed. Dr. Ruedenberg has succeeded in showing that this theory is in essential respects equivalent to the semiempirical LCAO theory most commonly used for the study of conjugated systems. A further investigation by Mr. Norman S. Ham and Dr. Ruedenberg has provided a numerical substantiation of the theoretical calculations. Professor J. R. Platt has investigated more closely the model of O. Schmidt,<sup>2</sup> i.e., the behavior of electrons in a box of the shape of the organic molecule. Although this box model does not contain any assumption concerning the molecular framework, very typical properties of the  $\pi$ -electron densities have been found.

The three investigations will be published in subsequent issues of this TECHNICAL REPORT and of the JOURNAL OF CHEMICAL PHYSICS. Work on these theories is being continued. In particular, applications to heteroatoms and inclusion of electronic interaction are being carried out.

### 3. Ultraviolet Spectra of Aromatic Systems

Extensive analyses have been made and are being continued by Professor Platt on the wavelength shifts in the ultraviolet spectra of aromatic systems produced by chemical substitution. The shifts are a combination of two independent terms, one a product of the directing power of the substituent with some local property of the aromatic eigenfunction, and the other a product of the ionization potential of the substituent with some other local property of the aromatic eigenfunction. These two terms provide accurate empirical predictions of the wavelength shifts, but their theoretic interpretation is not yet clear.

<sup>1</sup>This TECHNICAL REPORT, 1952-53, pp. 18, 58, 88, and 97 [J. Chem. Phys. 21, 1565, 1582, 1597, and 1413 (1953)].

<sup>2</sup>Ber. deut. chem. Ges. 73A, 97 (1940).

## PROGRESS REPORTS

### 4. Structural Formulas of the Boron Hydrides

Professor Platt has devised a new method for writing the structural formulas of the boron hydrides, and it will appear shortly.

### 5. Long-Wavelength Spectra of Polyacetylenes

Studies have been made by Professor Platt on the interpretation of the long-wavelength spectra of polyacetylenes and will be published shortly. Other molecules whose spectral interpretations are also being studied include ethylene, the thermochromic dianthrones, and the convex peri-condensed hydrocarbons.

### 6. Calculations on the First-Row Atoms

Comprehensive calculations on the first-row atoms have been completed, using single-term Slater wavefunctions for the 1s, 2s, and 2p atomic orbitals with arbitrary effective nuclear charges for the three orbitals. Determined were the best Z-values and the corresponding energies of the first-row atoms in their neutral, singly ionized, doubly ionized, and triply ionized states, arising from any distribution of the outer electrons over 2s and 2p orbitals. These results will form the subject of a paper to be written in the near future. The calculations were carried out under the direction of Dr. C. C. J. Roothaan, primarily by Mr. Robert Bonic (until 17 April) and Mrs. Gudrun Lenkersdorf (since 22 June); smaller portions of the results were obtained by predoctoral students C. W. Scherr and A. D. McLean.

### 7. Molecular Complexes and Hyperconjugation

Professor Mulliken has been continuing his studies on molecular complexes and their spectra, and on hyperconjugation especially in radicals and ions.

---

Some of the aforementioned activities are being supported under Project NR 019 101 of Contract N6ori-20, Task Order IX, with the Office of Naval Research, others under Project TB2-0001(505) of Contract DA-11-022-ORD-1002 with the Office of Ordnance Research.

30 November 1953

## EXPERIMENTAL WORK IN PROGRESS

### 1. Xenon-Emission Continua

Work now in progress on xenon-emission continua is reviewed in a separate Progress Report on this subject (see p. xxii).

### 2. Vacuum Ultraviolet Spectra of Organic Compounds

The last 101 vacuum ultraviolet spectra of organic compounds taken by Klevens, Platt, and co-workers from 1945 to 1950 have now been reduced and will be published in a forthcoming issue of this Laboratory's TECHNICAL REPORTS. Plans are being made to study polarization of transitions in this region by the method of stream double refraction, using the new photoelectric spectrophotometer which was described in the last issue of this TECHNICAL REPORT.

### 3. Naphthalene Vapor

Mr. William L. Lichten, predoctoral student, is constructing apparatus for studying magnetic and optical properties of a beam of naphthalene vapor in the triplet state.

### 4. Molecular Complexes

Dr. Dennis F. Evans (from Lincoln College, Oxford University), Research Associate on this Laboratory's OOR contract, is undertaking an experimental program in the field of molecular complexes. He is planning to continue the study of pyridine-iodine complexes begun by Professor C. Reid (see paper in this TECHNICAL REPORT), and is now studying the near vacuum ultraviolet spectrum of iodine in the vapor state and in "inert" solvents.

A study of iodine complexes in rigid glasses at liquid-nitrogen temperature, and in solutions under 2,000 atmospheres pressure, has recently been completed by Mr. Joe S. Ham. A doctoral dissertation covering this work is nearing completion and will appear in a subsequent issue of this TECHNICAL REPORT.

---

These research activities are being supported under Project TB2-0001(505) of Contract DA-11-022-ORD-1002 with the Office of Ordnance Research.

30 November 1953

· PROGRESS REPORT ON THE INVESTIGATION OF INTEGRALS BETWEEN SLATER ATOMIC  
ORBITALS AND THEIR APPLICATION IN MOLECULAR CALCULATIONS

1. Coulomb Integrals

The 28 Coulomb integrals between the ten basic charge distributions<sup>1</sup> arising from Slater orbitals with quantum numbers 1 and 2 have been evaluated for the argument values:

$$\bar{\rho} = 0.(0.02) 10.0, \quad \bar{\tau} = -0.9(0.1) 0.9$$

The calculations were directed by Assistant Professor C. C. J. Roothaan and were carried out on IBM punched-card machines at Iowa State College, Ames, Iowa, after certain auxiliary functions had been previously computed by hand. The information is at present stored on punched cards. Aside from a simple factor, each of the 48 conventional Coulomb integrals is a linear combination with simple numerical coefficients of at most five basic Coulomb integrals; in 27 cases the linear combination comprises only one term (see reference 1, Eq. (30)). The computation of all required linear combinations is planned for the near future.

It is intended to have tables printed from punched cards by a card-governed electrical typewriter as soon as feasible at the Watson Laboratory of the IBM Corporation in New York. Such tables should provide a fair copy for photolithographic reproduction in form of a separate volume in the series of TECHNICAL REPORTS issued by this Laboratory.

2. Exchange Integrals

Numerical investigations of the Exchange integrals under the direction of Dr. K. Ruedenberg were carried out by Mr. Tracy Kinyon, full-time computer, and by Mr. Walter Jaunzemis, part-time student computer, beginning in April, 1952. The possible use of large-scale electronic digital computers was studied with the assistance of Mr. Philip Merryman, Research Aid for electronic computing. The investigations had a three-fold objective:

- (1) to test the feasibility of the proposed method<sup>2</sup> and to study the

<sup>1</sup>See C. C. J. Roothaan, J. Chem. Phys. **19**, 1445 (1951).

<sup>2</sup>K. Ruedenberg, J. Chem. Phys. **19**, 1459 (1951).

PROGRESS REPORTS

numerical problems involved in its application;

(2) to study the problems connected with tabulation, in particular to consider the feasibility of satisfactory interpolation;

(3) to study the application of automatic computing machines for the evaluation of Exchange integrals.

The Exchange integrals, it will be recalled, are expressed as an infinite convergent series:

$$I = C_I(I_0 + I_1 + I_2 + \dots)$$

where  $C_I$  is a simple factor and each  $I_\ell$  is a function of four parameters  $\alpha$ ,  $\bar{\alpha}$ ,  $\beta$ , and  $\bar{\beta}$ . It was decided first to investigate the procedure of evaluating the  $I_\ell$ 's by means of the auxiliary functions  $B_j^{M\ell}(\beta)$ ,  $\phi_{n\bar{n}}^{M\ell}(\alpha, \bar{\alpha})$ , i.e., by the formula

$$I_\ell = \sum_{n=0}^N \sum_{\bar{n}=0}^{\bar{N}} \omega_n^\ell(\beta) \bar{\omega}_{\bar{n}}^\ell(\bar{\beta}) \phi_{n\bar{n}}^{M\ell}(\alpha, \bar{\alpha}),$$

where

$$\omega_n^\ell(\beta) = \sum_{j=0}^J \omega_{nj} B_j^{M\ell}(\beta),$$

[see reference 2, Eqs. (1,16,17, and 19)]. Since the functions  $\phi_{n\bar{n}}^{M\ell}(\alpha, \bar{\alpha})$  were expected to present the most difficult problems, they were considered first. In accordance with the general recurrence procedure, the following functions were successively computed:

$$A_n(x), G_n(x), \phi_{n\bar{n}}^{00}(\alpha, \bar{\alpha}), \phi_{n\bar{n}}^{0\ell}(\alpha, \bar{\alpha}).$$

Together with the functions  $\phi_{n\bar{n}}^{00}$ , the following related functions were investigated:

$$\phi_{n\bar{n}}^* = e^{\alpha + \bar{\alpha}} \phi_{n\bar{n}}^{00}, \quad \Psi_{n\bar{n}} = \frac{\alpha^{n+1} \bar{\alpha}^{\bar{n}+1}}{n! \bar{n}!} \phi_{n\bar{n}}^{00}, \quad \Psi_{n\bar{n}}^* = e^{\alpha + \bar{\alpha}} \Psi_{n\bar{n}}.$$

In distinction from the functions  $\phi_{n\bar{n}}^{00}$ , the  $\Psi_{n\bar{n}}$ 's, and the  $\Psi_{n\bar{n}}^*$ 's have the advantage that their orders of magnitude do not increase with increasing values of the indices  $n$ ,  $\bar{n}$ . Hence they are more convenient for numerical work than the functions  $\phi_{n\bar{n}}^{00}$ , and  $\phi_{n\bar{n}}^*$ . Furthermore, the functions  $\Psi_{n\bar{n}}$ ,  $\Psi_{n\bar{n}}^*$ , and  $\phi_{n\bar{n}}^*$  are more easily interpolated than the functions  $\phi_{n\bar{n}}^{00}$ . All four functions,  $\phi_{n\bar{n}}^{00}$ ,  $\phi_{n\bar{n}}^*$ ,  $\Psi_{n\bar{n}}$ , and  $\Psi_{n\bar{n}}^*$ , were computed for the following values of the arguments:

PROGRESS REPORTS

$$\begin{aligned} \rho = 0.2 & \quad \text{and} \quad \tau = 0(0.1)1 ; \\ \rho = 1.0 & \quad \text{and} \quad \tau = 0(0.1)1 ; \\ \rho = 3.0 & \quad \text{and} \quad \tau = 0, 0.5, 0.9 ; \\ \rho = 6.0 & \quad \text{and} \quad \tau = 0(0.1)1 ; \\ \tau = 0, \rho = 0(0.2)1(0.25)5.5(0.5)7 . \end{aligned}$$

The computations were carried out for the values  $n, \bar{n} = 0(1)10$  of the indices and, in general, for ten significant figures. For the values  $n, \bar{n} = 0, 1, 4, 7$ , graphs were drawn and difference tables were constructed. Also the functions  $(\bar{n}/\alpha)\Psi_{n\bar{n}}, [(n/\alpha) + (\bar{n}/\alpha)]\Psi_{n\bar{n}}, [\bar{a} \ln \frac{1}{2}(1-\tau)]\Psi_{n\bar{n}}$ , were investigated for interpolation purposes.

No serious difficulties were found in computing these functions or the necessary auxiliary functions  $A_n(x), G_n(x)$ . However, it had to be concluded that in all these functions interpolation requires a very close mesh of entries, a fact which would lead to very voluminous tables.

Subsequently the functions  $A_{n\bar{n}}, \phi_{n\bar{n}}^{0l}, \phi_{n\bar{n}}^{Ml}$  were computed for the argument values

$$\begin{aligned} \rho = 0.2 & \quad \text{and} \quad \tau = 0, 0.9 ; \\ \rho = 1.0 & \quad \text{and} \quad \tau = 0, 0.9 ; \\ \rho = 6.0 & \quad \text{and} \quad \tau = 0, 0.9 . \end{aligned}$$

It was found that, in each step of the recurrence procedure, one to two significant figures were lost so that the recursion could only be carried out for a limited number of  $l$  and  $M$  values. The number of significant figures remaining for different  $l$  and  $M$  values are given in the following table:

$\rho$	$\tau$	$M = 0$						$M = 1$					$M = 2$			
		$l=0$	$l=1$	$l=2$	$l=3$	$l=4$	$l=5$	$l=6$	$l=1$	$l=2$	$l=3$	$l=4$	$l=5$	$l=2$	$l=3$	$l=4$
0.2	0.0	9	5-6	1-3	0			4-5	0							
0.2	0.0	9	2-5	0												
1.0	0.0	9-10	8	6	4-6	1-4	0	6-7	3-5	2-5	0		2-5			
1.0	0.9	8-9	3-7	1-6	0			4-6	0							
6.0	0.0	8	7	6	5-6	4-5	3-4	2	6-7	5-6	4-5	3-4	2-5	4	3	2
6.0	0.9	9	6-8	3-7	2-6	1-4	0									

It was found that the loss of figures increases with increasing  $\tau$  and decreases with increasing  $\rho$ . For large values of  $\tau$ , the loss becomes more serious with increasing  $\bar{n}$ , whereas it is fairly independent of  $n$ .

Moreover it turned out that, in raising the indices  $l$  and  $M$ , the last significant digit slowly moves towards the decimal point, while the total value of the functions becomes smaller; i.e., one loses figures "on the left and on the right." Hence the functions  $\phi_{n\bar{n}}^{Ml}$  for higher values of  $M$  and  $l$  have fewer significant figures and fewer

PROGRESS REPORTS

decimal places than those for lower M and  $\ell$ , from which they were computed.

It was now decided to find out how these results would affect the evaluation of an Exchange integral as a whole.

For this purpose the functions  $B_j^{M\ell}$  had to be computed first. The following procedure was found to be practical:  $B_0^{M9}$  and  $B_0^{M10}$  were computed by series expansion, which proved more convenient than the use of explicit formulas. Then  $B_0^{M8}$ ,  $B_0^{M7}$ , ...  $B_0^{M0}$  were obtained by descending recursion, and  $B_j^{M\ell}$  by ascending recursion. Actually the functions

$$b_j^{M\ell} = \left[ \frac{(\ell-M)!}{(\ell+M)!} \frac{1}{2(2\ell+1)} \right]^{\frac{1}{2}} B_j^{M\ell} = \frac{(\ell-M)!}{(\ell+M)!} \frac{1}{2} \int_{-1}^1 d\eta P_\ell^M(\eta) (1-\eta^2)^{M/2} e^{\beta\eta} \eta^j$$

proved to be most convenient for numerical work.

After the functions  $b_j^{M\ell}$  were computed for a number of argument values, the evaluation of a number of integrals was undertaken. In all cases (16 different integrals were considered) it was found that the loss of decimal places, which occurs in raising the indices  $\ell$  and M of the  $\phi$ -functions is not compensated by other factors so that the  $\phi$ -functions with highest  $\ell$ -values determine the last significant decimal place. The number of significant figures in the total integral is less than the number of significant figures in the largest term.

The integral  $[1s_a 1s_b | 1s_a 1s_b]$  was furthermore computed for the values:

$$\begin{aligned} \tau = 0, & \quad \rho = 0(.2)3, 1(0.25)5.5 ; \\ \rho = 1, & \quad \tau = 0(0.1)1 . \end{aligned}$$

Difference tables were constructed, and it proved to be possible to interpolate this total integral to five decimal places.

Furthermore the integral  $[2s_a 2s_b | 2s_a 2s_b]$  was evaluated for  $\alpha = \bar{\alpha} = 1(1)6$ ,  $\beta = 0(0.5)\alpha$ ,  $\bar{\beta} = 0(0.5)\alpha$  in order to obtain an insight in the convergence of the series which becomes infinite for  $\beta \neq 0$  and  $\bar{\beta} \neq 0$ . The convergence was found to be satisfactory for all possible values of  $\beta$ ,  $\bar{\beta}$  (one must have  $\beta \leq \alpha$ ,  $\bar{\beta} \leq \bar{\alpha}$ ). Furthermore the  $\beta$ -dependence and  $\bar{\beta}$ -dependence of the integral was studied, and graphs were drawn. The simplest behavior resulted when the integral was divided by  $\zeta = \frac{1}{4}(\zeta_a + \zeta_b + \bar{\zeta}_a + \bar{\zeta}_b)$  and when the resulting expression was considered as a function of

$$\rho = \frac{1}{2}(\alpha + \bar{\alpha}), \quad \tau = (\alpha - \bar{\alpha})/(\alpha + \bar{\alpha}), \quad \tau' = \alpha/\beta, \quad \tau'' = \bar{\alpha}/\bar{\beta} .$$

Here, as always, it was observed that interpolation proved to be very much easier in

PROGRESS REPORTS

the total integral than in the auxiliary functions.

In view of the unpleasant information obtained for the  $\phi$ -functions, it was now decided to investigate a different method of computing the  $I_\ell$ 's, i.e., a numerical integration proposed by Dr. Ruedenberg. In this method the functions  $B_j^{M\ell}$  are computed as before;  $I_\ell$  is then given by the integral

$$I_\ell = \int_1^\infty d\xi (\xi^2 - 1)^{-1} [P_\ell^M(\xi)]^{-2} \int_1^\xi dx P_\ell^M(x) (x-1)^{M/2} e^{-\alpha x} \omega^\ell(\beta, x) \\ \times \int_1^\xi dx P_\ell^M(x) (x^2 - 1)^{M/2} e^{-\bar{\alpha} x} \bar{\omega}^\ell(\bar{\beta}, x),$$

where

$$\omega^\ell(\beta, x) = \sum_{n=0}^N x^n \omega_n^\ell(\beta),$$

which follows from Eqs. (1.17), (3.12) of reference 2. The three successive single integrations were carried out numerically. The method proved to be straightforward, and no significant figures were lost. Transforming the interval  $x = (1 \rightarrow \infty)$  into the interval  $x = (1 \rightarrow 0)$  and taking steps of 0.0., the integral  $[2s_a 2s_b | 2s_a 2s_b]$  was found correct to five decimal places. Since, in a numerical integration of this type, most of the time is spent calculating the integrand, it was concluded that this method would be very much facilitated if the following table were available:

- |  |                             |
|--|-----------------------------|
| (1) An interpolatable table of the $B_j^{M\ell}(\beta)$  | } for $t = 0(0.01)1$ (say). |
| (2) A table of $P_\ell^M(1/t) [(1/t)^2 - 1]^{M/2}$       |                             |
| (3) A table of $[P_\ell^M(1/t)]^{-2} [(1/t)^2 - 1]^{-1}$ |                             |

Then, for a particular integral, only the functions

$$e^{-\alpha/t}, \quad e^{-\bar{\alpha}/t}, \quad \omega_n^\ell(1/t), \quad \bar{\omega}_n^\ell(1/t) \quad (*)$$

would have to be calculated before starting the integration proper. Moreover, in one molecular problem the same functions of the type (\*) will occur in several integrals.

In view of the great complexity of the calculations involved in the Exchange integrals, the possible use of an electronic digital computer had been investigated simultaneously. It was concluded that these machines offer the best existing method of carrying out such complicated computations. It was however realized that the inordinate loss of significant figures as well as the extreme variations in the order of magnitude of the intermediate results, both of which are characteristic of the  $\phi$ -function method, create very unpleasant problems for machine operation, namely

## PROGRESS REPORTS

scaling and multiple precision. On the other hand, the numerical integration procedure should be well suited for a machine.

The  $\phi$ -functions theoretically offer one advantage: they can be tabulated as two-parameter functions. The numerical integration method on the other hand, furnishes the total integral in one step; i.e., it yields directly four-parameter functions which would lead to very voluminous tables and therefore do not seem suitable for tabulation. It was however already mentioned that the  $\phi$ -functions are difficult to interpolate and, therefore, are not ideal for tabulation either. Furthermore, our investigation of electronic computing techniques seems to indicate that future molecular computations may rely rather on subroutines executed within the machine than on printed interpolatable tables. For these reasons a tabulation of the  $\phi$ -functions loses a great deal of its attractiveness.

It was therefore decided to prepare a code for the numerical integration method for an electronic digital computer in order to learn how well this method would work on a machine. Although a flow chart for the  $\phi$ -functions had already been made, it was decided to wait with the preparation of a code for them. If the numerical integration by an electronic machine would work out well, and if it should prove to be superior in simplicity to anything which can be expected from the  $\phi$ -function method, then, it is felt, a computation and tabulation of  $\phi$ -functions is likely to be inadvisable. Rather it might be preferable to consider the preparation of the following tables:

(1) A table of total exchange integrals (computed by numerical integration) for a very wide mesh of entries to serve as a guide for the general behavior of the integrals;

(2) A closer tabulation for such selected intervals and/or special values of the arguments as may prove to be very frequently used;

(3) In case one wants to make provision for a facile evaluation without an electronic computer: a tabulation of the three kinds of simple functions which, as was outlined before, would make it possible to evaluate (by numerical integration) an exchange integral by hand without excessive labor.

### 3. Hybrid Integrals and One-Electron Integrals

The investigation of the hybrid integrals has resulted in a paper entitled "A Unified Treatment of the Hybrid, Coulomb, and One-Electron Integrals", by K. Ruedenberg, C. C. J. Roothaan, and W. Jaunzemis, which appears in this TECHNICAL REPORT.

## PROGRESS REPORTS

A method of dealing with the integrals has been developed which permitted an entirely general solution of the problem. The treatment is based on a new type of auxiliary functions, called  $C_{\alpha\beta}^{\gamma\delta\epsilon}$ , and it has been possible to express the two-center one-electron integrals as well in terms of these auxiliary functions--with the only exception of the nuclear attraction integrals of the type  $\int dV\chi_a\chi_a'/r_b$ , for which independent formulas are given. Pilot computations are being started at present. It is anticipated that the final calculations will probably be carried out on an electronic digital computer; they shall furnish tables for one-electron integrals and tables for the auxiliary functions occurring in the hybrid integrals.

#### 4. Application of Machine Computing Techniques to Molecular Calculations

In view of the rapid improvements made in the last few years in the reliability and power of electronic digital computers, it appears to be likely that future molecular calculations will largely be carried out by means of such machines. Since the techniques which are now being developed in the field of automatic machine computing will therefore have to be considered in planning future work, a study of this new field was initiated by Mr. P. Merryman, Dr. K. Ruedenberg, and Dr. C. C. J. Roothaan. The possibilities of the new machines have also been recognized by other researchers; pioneer work is being done in particular by Dr. S. F. Boys, who for several years has been working with the EDSAC computer in Cambridge, England.

The most immediate consequence is, of course, that calculations whose complexity makes them forbidding for hand computation are now within the range of possibility. The most obvious examples are the integrals between the atomic orbitals. It may be expected that codes can be prepared which will allow the evaluation of an integral of this kind for a particular set of parameter values in a matter of minutes, so that it may become possible to obtain a large number of them when required, e.g., if a diatomic molecular problem is to be solved for many values of the interatomic distance in order to construct a potential curve. Another important example is the solution of secular equations of very high order; such equations up to the order forty are now being solved, and it can be expected that equations of higher order will become soluble, by automatic methods. This fact will facilitate the superposition of more atomic orbitals to form molecular orbitals than appeared to be possible until now, and it will also permit taking into account a greater amount of configurational interaction than was hitherto feasible.

## PROGRESS REPORTS

Another development to be mentioned is the tendency of those working with high-speed computing machines to rely more on subroutines executed within the machine than upon interpolatable tables in order to obtain values of complicated as well as simple functions. It is generally considered more economical to generate these values in the machine, by a subroutine, whenever required than to store an interpolatable table in the memory of the machine. This fact seems to indicate that, with such computers, one will want to solve molecular problems individually and in total; that is, the four steps of the LCAO procedure (evaluation of the necessary integrals, construction of the energy matrix elements in terms of the integrals, solution of the eigenvalue equation of this matrix, computation of certain physical quantities from the eigenvalues and eigenfunctions) will be combined into one master code which would contain such intermediary steps as the evaluation of integrals in form of subroutines. Boys has already taken some steps along this path. It must be admitted that total molecular codes will require a large fast machine memory; but in view of the rapid progress being made at present; the latter can be expected to become available. In light of the foregoing it appears then that the calculation of molecular problems will presumably move away from integral tables and that, instead of such tables, a library of codes required in molecular calculations (e.g., codes for integrals, for the construction of matrix elements, for the solution of secular equations, for the calculation of dipole moments, etc.) will prove to be the appropriate tool in conjunction with an electronic digital computer.

Finally it should be pointed out that the high-speed large-scale computing machines will facilitate the handling and use of numerical wavefunctions, e.g., SCF atomic orbitals, as contrasted with analytical functions. Indeed, it is likely that even the execution of numerical Hartree-type SCF calculations for three-dimensional molecular orbitals will come within range of possibility.

The conclusions presented here are, of course, preliminary in nature and will undoubtedly give way to more precise formulations as experience with the new computing machines accumulates.

---

The research on molecular integrals hereabove described is being supported in part under Project NR 019 101 of Contract N6ori-20, Task Order IX, with the Office of Naval Research, and in part under Project R-351-40-4 of Contract AF 18(600)-471 with the Air Research and Development Command.

30 November 1953

K. Ruedenberg

## PROGRESS REPORT ON XENON EMISSION CONTINUA

Recently Dr. Yoshio Tanaka of the Air Force Cambridge Research Center discovered a continuous emission in xenon and krypton excited by microwave energy.<sup>1</sup> This continuum spreads to the red from the  $1,470\text{\AA}$  xenon resonance line and is quite intense up to approximately  $1,850\text{\AA}$ .

In the original experiments at the Air Force Laboratory, an electrodeless pyrex tube was waxed to the slit of a vacuum spectrograph, and xenon was stressed through the tube at approximately 10mm pressure. Owing to the high cost of xenon, experiments were conducted at the Air Force Laboratory and also in this Laboratory to produce a sealed-off tube with a lithium-fluoride or a calcium-fluoride window. Great difficulty was experienced initially with small amounts of impurities which gave rise to the intense fourth positive group emission-band system of carbon monoxide overlapping the continuum. It proved to be possible to remove these impurities by means of a getter of magnesium-aluminum-barium alloy, and a number of sealed-off tubes were prepared with various pressures of xenon.

These tubes have apparently limitless life, but their usefulness is reduced to about 100 hours' operating time by solarization of the lithium-fluoride or calcium-fluoride windows. The relative intensity of the xenon emission continuum increases with pressure to a maximum intensity at about 200mm pressure. Above this pressure, increasing absorption by weak xenon van der Waals molecules begins to reduce the intensity. This is in agreement with the work of McLennan and Turnbull<sup>2</sup> on the pressure broadening in absorption of the  $1,470\text{\AA}$  resonance line. Also, the extent of the continuum is reduced at the higher pressures, particularly on the short-wavelength end. The useful range of the emission in 200mm of xenon photographed on the Harrison 21-foot vacuum spectrograph is  $1,520$  to  $1,850\text{\AA}$ , with a maximum in intensity near  $1,650\text{\AA}$ .

In the region  $1,900$ - $6,000\text{\AA}$ , the mercury  $2,537\text{\AA}$  and  $2,483\text{\AA}$  lines appear. At  $3,080\text{\AA}$  is a weak and diffuse emission-band system which is favored by a pressure of 190mm, and from  $2,400$  to  $7,000\text{\AA}$  is another weak emission continuum with a region of

<sup>1</sup>Y. Tanaka and M. Zelikoff, Bull. Am. Phys. Soc. **28**, No. 6, 29 (1953).

<sup>2</sup>J. C. McLennan and R. Turnbull, Proc. Roy. Soc. (London) **A139**, 683 (1933), **A129**, 266 (1930).

## PROGRESS REPORTS

relatively low emission near  $5,300\text{\AA}$ , and one observable maximum near  $4,700\text{\AA}$ . The entire region above  $3,800\text{\AA}$  is overlapped by many atomic emission lines of xenon. The intensity of this continuum is at least twenty times weaker than the vacuum ultraviolet continuum.

The characteristics of the xenon emission are such that it should be possible to use the vacuum ultraviolet continuum in the third order of a diffraction grating without the use of a disperser. The third order of the continuum would fall from  $4,560$  to  $5,550\text{\AA}$  where Eastman SWR plates are insensitive, and the second order falling in this region is very weak. This vacuum ultraviolet continuum has already been used in this laboratory to photograph the absorption of ethylene, deuterio-ethylene, and carbon dioxide in the first order from  $1,520$  to  $1,850\text{\AA}$ . These absorption experiments have shown that the xenon continuum is more suitable for absorption spectroscopy than the Lyman continuum due to its more even intensity distribution and its ease of production. The use of the third order of the Harrison 21-foot grating in absorption spectroscopy is very important since the theoretical resolving power would be tripled, and many observed bands might then be resolvable.

At present a half-wave dipole antenna is used to couple the microwave energy to the discharge tube. Since this results in a considerable loss of available power, a microwave cavity has been constructed in cooperation with Professor Hutchison of the Department of Chemistry and Mr. Gale Flesher of the Department of Electrical Engineering, Illinois Institute of Technology. This tunable resonance cavity was designed to resonate in the  $TM_{010}$  mode of oscillation at 2,464 megacycles per second; it is cylindrical in shape, the discharge tube being located along the axis to coincide with the maximum electric-field intensity. In its present form, the cavity will resonate in the  $TE_{112}$  mode at one end of the tuning range and in the  $TM_{010}$  mode on the other end. Some modifications are still necessary to improve the efficiency of the cavity. In its final assembly, a crystal detector and a microammeter will be employed to monitor the power output, and a double stub tuner will be located on the input power cable to secure satisfactory impedance matching.

The xenon continuum may be somewhat similar to the Hopfield emission continuum in helium from  $584\text{\AA}$  to  $1,000\text{\AA}$ . The latter is due at least in part to a transition from a stable excited state  $^1\Sigma_u^+$ , to the unstable ground state  $^1\Sigma_g^+$ ; the excited state results from a combination of a normal  $^1S$  atom with an excited  $^1P$  atom. In xenon, a combination of an excited  $^3P$  atom with an unexcited  $^1S$  atom may result in the formation

## PROGRESS REPORTS

of a stable excited state, probably  ${}^3\Sigma_u^+$ , which can combine optically with the unstable ground state,  ${}^1\Sigma_g^+$ .

The continuum which appears in the 2,400-7,000Å region is very similar to that produced by a high-voltage condensed discharge in xenon, reported by LaPorte.<sup>3</sup> This continuum as it appears on LaPorte's published plates, extends from 2,900Å to 6,000Å and shows two maxima, one at about 4,700Å and another at about 5,800Å. In microwave excitation, the intensity maximum at 5,800Å is not observed although there is a region of relatively weak emission near 5,300Å, in agreement with LaPorte. It seems possible that under the microwave-excitation conditions, the long wavelength maximum has been shifted beyond 7,000Å, which would then be out of the region of measurement. The diffuse band shaded toward the violet with its head near 3,080Å is not observed in the published photographs of LaPorte.

No ultraviolet and visible transitions of molecular xenon have been identified. It is conceivable that upper states in xenon exist other than that suggested above and that these can combine with a repulsive lower state in a manner similar to the transition in the vacuum ultraviolet. It is fairly clear that the long wavelength continua are not just parts of the tail of the vacuum ultraviolet continuum, since maxima of intensity occur in each, and at widely different positions in the spectrum, namely at 1,650Å and at 4,700Å.

---

The aforementioned research is being supported under Project TB2-0001(505) of Contract DA-11-022-ORD-1002 with the Office of Ordnance Research.

30 November 1953

P. G. Wilkinson

---

<sup>3</sup>M. LaPorte, *J. phys. radium* 9, 228 (1938), 6, 164 (1945).

TECHNICAL PAPERS

A STUDY OF TWO-CENTER INTEGRALS USEFUL IN CALCULATIONS ON MOLECULAR STRUCTURE.

III. A UNIFIED TREATMENT OF THE HYBRID, COULOMB, AND ONE-ELECTRON INTEGRALS<sup>†</sup>

Klaus Ruedenberg, C. C. J. Roothaan, and Walter Jaunzemis  
Laboratory of Molecular Structure and Spectra  
Department of Physics  
The University of Chicago  
Chicago 37, Illinois

INTRODUCTION

IN RECENT YEARS it has become recognized that in calculations on molecular structure the exact values of all integrals between atomic orbitals (AO's) must be taken into account in order to draw meaningful conclusions from the initial assumptions through detailed calculations. It has further been realized that these integrals require systematic investigation in order that the present unsatisfactory state in this field may be clarified. Several studies have therefore been made recently on this subject.<sup>1</sup>

In two previous publications, two of us presented a study of all the two-center integrals between Slater AO's except the so-called hybrid integrals.<sup>2,3</sup> Referring the reader to these papers we shall not repeat the introductory remarks given there. We shall use certain concepts and results from these papers, quoting reference 2 as (I) and reference 3 as (II).

The principal object of the present paper is a completely general treatment of the hybrid integrals

$$[\chi'_a \chi''_a | \chi_a \chi_b] = \int dV_1 \int dV_2 \chi'_a(1) \chi''_a(1) (1/r_{12}) \chi_a(2) \chi_b(2), \quad (\text{A.1})$$

where  $\chi_a, \chi'_a, \chi''_a$  denote three different Slater AO's on atom  $\underline{a}$ , and  $\chi_b$  denotes a Slater AO on atom  $\underline{b}$ . The Slater AO's used here have the form

$$(n\ell m) = (2\zeta)^{n+\frac{1}{2}} [(2n)!]^{-\frac{1}{2}} r^{n-1} e^{-\zeta r} S_{\ell m}(\theta, \varphi), \quad (\text{A.2})$$

---

<sup>†</sup>This work was assisted by the Office of Naval Research under Task Order IX of Contract N6ori-20 with The University of Chicago.

<sup>1</sup>See the bibliography.

<sup>2</sup>C. C. J. Roothaan, J. Chem. Phys. **19**, 1445 (1951).

<sup>3</sup>K. Ruedenberg, J. Chem. Phys. **19**, 1459 (1951).

where  $S_{\ell m}(\theta, \varphi)$  denotes a normalized, real spherical harmonic [see (I), Eqs. (9,10), and (II), Eq. (1.3)]. If we use  $a_H$ , the Bohr radius, as the unit of length, then the parameter  $\zeta$  is defined by

$$\zeta = Z/n, \quad (\text{A.3})$$

where  $n$  is the principal quantum number and  $Z$  is the effective nuclear charge. We propose for the parameter  $\zeta$  the name orbital exponent.

Unfortunately there exists some confusion in the literature due to different choices of the unit of energy. We propose therefore that the symbol  $[\chi'_a \chi''_a | \chi_a \chi_b]$  always be used to denote the integral on the right-hand side of (A.1), regardless of which unit of energy is used. From this convention it follows then that the contribution to the energy matrix corresponding to the integral (A.1) is given by

$[\chi'_a \chi''_a | \chi_a \chi_b]$  if the energy is expressed in units of  $e^2/a_H$  (Hartree and present authors), and by  $2[\chi'_a \chi''_a | \chi_a \chi_b]$  if the energy is expressed in units of  $e^2/2a_H$  (Parr, Brennan and Mulligan). We consider the foregoing convention more satisfactory than the suggestion of Brennan and Mulligan,<sup>4</sup> who make the meaning of the symbol  $[\chi'_a \chi''_a | \chi_a \chi_b]$  dependent upon the choice of energy units.

The orbital exponents of the four orbitals are entirely arbitrary in our discussion, which is therefore wider in scope than the treatments given by Kotani, Amemiya, and Simose<sup>5</sup> and by Brennan and Mulligan.<sup>4</sup> A new method is developed which involves only one type of auxiliary functions. It appears to be simpler than any of those previously suggested, and from the following exposition it should be a straight-forward matter to apply it to any hybrid integral involving Slater AO's. The explicit results are given for all hybrid integrals involving 1s, 2s, 2p AO's.

It is furthermore shown that the coulomb integrals, overlap integrals, kinetic-energy integrals, and one type of nuclear-attraction integrals can also be very simply expressed in terms of the new auxiliary functions, so that a unified treatment of these five types of integrals has been achieved.

Section 1 of this paper deals with the hybrid integrals; Section 2 treats in a general way the integrals of paper (I), that is, the coulomb integrals and one-

<sup>4</sup>See (7) in the bibliography.

<sup>5</sup>See (8) in the bibliography.

electron integrals; Sections 3 and 4 provide an analysis of the new auxiliary functions; Section 5 collects some useful facts about the exponential integral and certain related functions; and finally the bibliography surveys the literature on the hybrid integrals.

### 1. HYBRID INTEGRALS

#### a. Charge Distributions; Classification of the Hybrid Integrals

The Slater AO's which enter (A.1) are functions of coordinates having the origins  $\underline{a}$  and  $\underline{b}$ , respectively; the orientation of these two coordinate systems is explained in (I), Eq. (1), and in (II), Eq. (1.4) and Fig. 1. Following the method employed in (I) and (II) we call

$$\chi'_a(1)\chi''_a(1) \quad (1.1)$$

and

$$\chi_a(2)\chi_b(2) \quad (1.2)$$

the charge distributions occupied by the two electrons.<sup>6</sup>

The symmetry group of our two-center problem is the two-dimensional rotation-reflection group  $C_{\infty v}$ . Consequently, it is useful to write the charge distributions (1.1,2) as linear combinations of certain basic charge distributions, that is, charge distributions which belong to irreducible representations of  $C_{\infty v}$ ; it is also said that these basic charge distributions are of a particular species (a particular irreducible representation) and subspecies (classifying the different members within the same irreducible representation). The species and subspecies determine the dependence of the basic charge distributions on  $\varphi$ , the azimuth around the ab-axis; this dependence is given in Table I.

The charge distributions (1.1) are products of two Slater AO's on the same center  $\underline{a}$ . Convenient basic charge distributions  $\Omega_a$  for this case are, as is shown in (I) (Section: Charge Distributions on Atoms), given by<sup>7</sup>

<sup>6</sup> $\chi_a(1)$  is an abbreviation for  $\chi_a(x_{a1}, y_{a1}, z_{a1})$ , etc.

<sup>7</sup>In the case of the hybrid integrals there occurs only one one-center charge distribution,  $\Omega_a$ ; this distribution is characterized by the three integers N,L,M. In the case of the coulomb integrals, treated in Section 2, there occur two one-center charge distributions,  $\Omega_a$  and  $\Omega_b$ ; we shall characterize these distributions

RUEDENBERG, ROTHAAAN, AND JAUNZEMIS

$$[NLM] = [(2L+1)/4\pi]^{1/2} [2(2\zeta_a)^L / (N+L+1)!] r_a^{N-1} e^{-2\zeta_a r_a} S_{LM}(\theta_a, \varphi), \quad (1.3)$$

where  $S_{LM}(\theta, \varphi)$  denotes a normalized, real spherical harmonic [see (I), Eqs. (10) and (11)], and where

$$\zeta_a = \frac{1}{2}(\zeta'_a + \zeta''_a) \quad (1.4)$$

is the average orbital exponent of the AO's  $\chi'_a$  and  $\chi''_a$ .

TABLE I.  
DEPENDENCE OF THE BASIC CHARGE DISTRIBUTIONS ON THE AZIMUTH  $\varphi$   
FOR THE DIFFERENT SPECIES AND SUBSPECIES OF  $C_{\infty v}$

Species	Subspecies	Dependence on $\varphi$
$\Sigma$	—	independent of $\varphi$
$\Pi$	$\Pi$	$\cos\varphi$
	$\bar{\Pi}$	$\sin\varphi$
$\Delta$	$\Delta$	$\cos 2\varphi$
	$\bar{\Delta}$	$\sin 2\varphi$
$\Phi$	$\Phi$	$\cos 3\varphi$
	$\bar{\Phi}$	$\sin 3\varphi$

The explicit expansions of the charge distributions (1.1) in terms of the basic charge distributions (1.3) are given in Table II, for all the possible products of the AO's  $1s, 2s, 2p\sigma, 2p\pi, 2p\bar{\pi}$ . This table is taken from the more general formulas in (I), Eqs. (12). It is seen that the basic charge distributions  $1S, 2S, 3S, 2P\Sigma, 2P\Pi, 2P\bar{\Pi}, 3P\Sigma, 3P\Pi, 3P\bar{\Pi}, 3D\Sigma, 3D\Pi, 3D\bar{\Pi}, 3D\Delta, 3D\bar{\Delta}$  are required for this purpose.

It should be stressed that this method of expanding the one-center charge distributions into basic charge distributions provides the most economical way of

---

then by  $N_a, L_a, M$  and  $N_b, L_b, M$  respectively (it is not necessary to write also  $M_a$  and  $M_b$ , since the integrals with  $M_a \neq M_b$  vanish).

TWO-CENTER INTEGRALS. III

dealing with integrals involving charge distributions of the type (1.1).<sup>8</sup>

TABLE II.  
EXPANSION OF THE ONE-CENTER CHARGE DISTRIBUTIONS  
IN TERMS OF BASIC CHARGE DISTRIBUTIONS

$$\begin{array}{l}
 1s'_a 1s''_a = \zeta'_a{}^{3/2} \zeta''_a{}^{3/2} \tau_a^{-3} [1S_a] \\
 1s'_a 2s''_a = (\sqrt{3}/2) \zeta'_a{}^{3/2} \zeta''_a{}^{5/2} \tau_a^{-4} [2S_a] \\
 2s'_a 2s''_a = \zeta'_a{}^{5/2} \zeta''_a{}^{5/2} \tau_a^{-5} [3S_a] \\
 \left. \begin{array}{l} 1s'_a 2p\sigma''_a \\ 1s'_a 2p\pi''_a \\ 1s'_a 2p\bar{\pi}''_a \end{array} \right\} = \zeta'_a{}^{3/2} \zeta''_a{}^{5/2} \tau_a^{-4} \left\{ \begin{array}{l} [2P\Sigma_a] \\ [2P\Pi_a] \\ [2P\bar{\Pi}_a] \end{array} \right. \\
 \left. \begin{array}{l} 2s'_a 2p\sigma''_a \\ 2s'_a 2p\pi''_a \\ 2s'_a 2p\bar{\pi}''_a \end{array} \right\} = (5/2\sqrt{3}) \zeta'_a{}^{5/2} \zeta''_a{}^{5/2} \tau_a^{-5} \left\{ \begin{array}{l} [3P\Sigma_a] \\ [3P\Pi_a] \\ [3P\bar{\Pi}_a] \end{array} \right. \\
 \left. \begin{array}{l} 2p\sigma'_a 2p\sigma''_a \\ 2p\sigma'_a 2p\pi''_a \\ 2p\sigma'_a 2p\bar{\pi}''_a \\ 2p\pi'_a 2p\pi''_a \\ 2p\pi'_a 2p\bar{\pi}''_a \\ 2p\bar{\pi}'_a 2p\bar{\pi}''_a \end{array} \right\} = \zeta'_a{}^{5/2} \zeta''_a{}^{5/2} \tau_a^{-5} \left\{ \begin{array}{l} [3S_a] + 3[3D\Sigma_a] \\ (3\sqrt{3}/2)[3D\Pi_a] \\ (3\sqrt{3}/2)[3D\bar{\Pi}_a] \\ [3S_a] - (3/2)[3D\Sigma_a] + (3\sqrt{3}/2)[3D\Delta_a] \\ (3\sqrt{3}/2)[3D\bar{\Delta}_a] \\ [3S_a] - (3/2)[3D\Sigma_a] - (3\sqrt{3}/2)[3D\Delta_a] \end{array} \right.
 \end{array}$$

<sup>8</sup>This statement is illustrated by the fact that Barnett and Coulson in their paper [see (12) in the bibliography], where they used the charge distributions (1.1) directly, list 90 hybrid integrals as being essentially different; whereas we, using the basic charge distributions (1.3), find that actually 79 integrals are sufficient. This difference is due in particular to the fact that the six products of

The charge distributions (1.2) are products of two Slater AO's on different centers, namely a and b. Convenient basic charge distributions  $\Omega_{ab}$  for this case are given in (II), Eqs. (1.5-11) and Table I. Since we consider only the AO's 1s, 2s, 2p $\sigma$ , 2p $\pi$ , 2p $\bar{\pi}$  on the centers a and b, an actual decomposition for the charge distributions (1.2) in terms of basic charge distributions occurs only for the three products where both factors are  $\pi$ -AO's, as is shown in Table III of this paper. The basic two-center charge distributions which we shall need are listed in Table IV. They are expressed in the elliptic (prolate spheroidal) coordinates  $\xi, \eta, \varphi$ , and multiplied by  $(\frac{1}{2}R)^2(\xi-\eta)$ ; the inclusion of this factor will later prove useful. The elliptic coordinates are defined by<sup>9</sup>

$$\xi = (r_a + r_b)/R, \quad \eta = (r_a - r_b)/R, \quad \varphi = \varphi_a = \varphi_b, \quad (1.5)$$

so that

$$\left. \begin{aligned} r_a &= \frac{1}{2}R(\xi + \eta), \quad r_b = \frac{1}{2}R(\xi - \eta), \\ r_a \cos \theta_a &= \frac{1}{2}R(1 + \xi\eta), \quad r_b \cos \theta_b = \frac{1}{2}R(1 - \xi\eta), \\ r_a \sin \theta_a &= r_b \sin \theta_b = \frac{1}{2}R[(\xi^2 - 1)(1 - \eta^2)]^{\frac{1}{2}}, \end{aligned} \right\} \quad (1.5')$$

where R is the internuclear distance ab.

TABLE III.  
EXPANSION OF THE  $\pi$ -AO PRODUCT CHARGE DISTRIBUTIONS  
IN TERMS OF BASIC CHARGE DISTRIBUTIONS

$2p\pi_a 2p\pi_b = 2p\pi_a 2p\pi_b \Sigma + 2p\pi_a 2p\pi_b \Delta$
$2p\bar{\pi}_a 2p\bar{\pi}_b = 2p\pi_a 2p\pi_b \Sigma - 2p\pi_a 2p\pi_b \Delta$
$2p\pi_a 2p\bar{\pi}_b = 2p\bar{\pi}_a 2p\pi_b = 2p\pi_a 2p\pi_b \bar{\Delta}$

2p AO's can be expressed in terms of five basic charge distributions (see Table II). Similarly, among the 30 hybrid integrals listed by Brennan and Mulligan [see (7) in the bibliography], only 24 are independent.

<sup>9</sup>This definition coincides with the one given in (I), Eqs. (2) and (3), but differs from the one given in (II), Eq. (18), by the sign of  $\eta$ .

TWO-CENTER INTEGRALS. III

TABLE IV.

THE BASIC TWO-CENTER CHARGE DISTRIBUTIONS  $\Omega_{ab}$

$\Omega_{ab}$	$(\frac{1}{2}R)^2(\xi-\eta)\Omega_{ab}$
	10 $\Sigma$ -type distributions:
$1s_a 1s_b$	$(\zeta_a^{3/2} \zeta_b^{-1/2} \rho_b^2 / 4\pi) e^{-\rho\xi - \tau\rho\eta} (\xi - \eta)$
$1s_a 2s_b$	$(\zeta_a^{3/2} \zeta_b^{-1/2} \rho_b^3 / 8\sqrt{3}\pi) e^{-\rho\xi - \tau\rho\eta} (\xi - \eta)^2$
$2s_a 1s_b$	$(\zeta_a^{5/2} \zeta_b^{-3/2} \rho_b^3 / 8\sqrt{3}\pi) e^{-\rho\xi - \tau\rho\eta} (\xi + \eta) (\xi - \eta)$
$2s_a 2s_b$	$(\zeta_a^{5/2} \zeta_b^{-3/2} \rho_b^4 / 48\pi) e^{-\rho\xi - \tau\rho\eta} (\xi + \eta) (\xi - \eta)^2$
$1s_a 2p\sigma_b$	$(\zeta_a^{3/2} \zeta_b^{-1/2} \rho_b^3 / 8\pi) e^{-\rho\xi - \tau\rho\eta} (\xi - \eta) (1 - \xi\eta)$
$2p\sigma_a 1s_b$	$(\zeta_a^{5/2} \zeta_b^{-3/2} \rho_b^3 / 8\pi) e^{-\rho\xi - \tau\rho\eta} (\xi - \eta) (1 + \xi\eta)$
$2s_a 2p\sigma_b$	$(\zeta_a^{5/2} \zeta_b^{-3/2} \rho_b^4 / 16\sqrt{3}\pi) e^{-\rho\xi - \tau\rho\eta} (\xi + \eta) (\xi - \eta) (1 - \xi\eta)$
$2p\sigma_a 2s_b$	$(\zeta_a^{5/2} \zeta_b^{-3/2} \rho_b^4 / 16\sqrt{3}\pi) e^{-\rho\xi - \tau\rho\eta} (\xi - \eta)^2 (1 + \xi\eta)$
$2p\sigma_a 2p\sigma_b$	$(\zeta_a^{5/2} \zeta_b^{-3/2} \rho_b^4 / 16\pi) e^{-\rho\xi - \tau\rho\eta} (\xi - \eta) (1 + \xi\eta) (1 - \xi\eta)$
$2p\pi_a 2p\pi_b \Sigma$	$(\zeta_a^{5/2} \zeta_b^{-3/2} \rho_b^4 / 32\pi) e^{-\rho\xi - \tau\rho\eta} (\xi - \eta) (\xi^2 - 1) (1 - \eta^2)$
	6 $\Pi$ -type distributions:
$1s_a 2p\pi_b$	$(\zeta_a^{3/2} \zeta_b^{-1/2} \rho_b^3 / 8\pi) e^{-\rho\xi - \tau\rho\eta} (\xi - \eta) [(\xi^2 - 1)(1 - \eta^2)]^{\frac{1}{2}} \cos\varphi$
$2p\pi_a 1s_b$	$(\zeta_a^{5/2} \zeta_b^{-3/2} \rho_b^3 / 8\pi) e^{-\rho\xi - \tau\rho\eta} (\xi - \eta) [(\xi^2 - 1)(1 - \eta^2)]^{\frac{1}{2}} \cos\varphi$
$2s_a 2p\pi_b$	$(\zeta_a^{5/2} \zeta_b^{-3/2} \rho_b^4 / 16\sqrt{3}\pi) e^{-\rho\xi - \tau\rho\eta} (\xi + \eta) (\xi - \eta) [(\xi^2 - 1)(1 - \eta^2)]^{\frac{1}{2}} \cos\varphi$
$2p\pi_a 2s_b$	$(\zeta_a^{5/2} \zeta_b^{-3/2} \rho_b^4 / 16\sqrt{3}\pi) e^{-\rho\xi - \tau\rho\eta} (\xi - \eta)^2 [(\xi^2 - 1)(1 - \eta^2)]^{\frac{1}{2}} \cos\varphi$
$2p\sigma_a 2p\pi_b$	$(\zeta_a^{5/2} \zeta_b^{-3/2} \rho_b^4 / 16\pi) e^{-\rho\xi - \tau\rho\eta} (\xi - \eta) (1 + \xi\eta) [(\xi^2 - 1)(1 - \eta^2)]^{\frac{1}{2}} \cos\varphi$
$2p\pi_a 2p\sigma_b$	$(\zeta_a^{5/2} \zeta_b^{-3/2} \rho_b^4 / 16\pi) e^{-\rho\xi - \tau\rho\eta} (\xi - \eta) (1 - \xi\eta) [(\xi^2 - 1)(1 - \eta^2)]^{\frac{1}{2}} \cos\varphi$

TABLE IV (continued)

$\Omega_{ab}$	$(\frac{1}{2}R)^2(\xi-\eta)\Omega_{ab}$
<p>6 <math>\Pi</math>-type distributions:                  replace every <math>\pi</math> AO in the above list by a <math>\bar{\pi}</math> AO, and <math>\cos\varphi</math> by <math>\sin\varphi</math>.</p>	
$2p\pi_a 2p\pi_b \Delta$	<p>1 <math>\Delta</math>-type distribution:  <math>(\zeta_a^{5/2} \zeta_b^{-3/2} \rho_b^4 / 32\pi) e^{-\rho\xi - \tau\rho\eta} (\xi-\eta)(\xi^2-1)(1-\eta^2) \cos 2\varphi</math></p>
<p>1 <math>\bar{\Delta}</math>-type distribution:                  replace <math>2p\pi_a 2p\pi_b \Delta</math> by <math>2p\pi_a 2p\pi_b \bar{\Delta}</math>, and <math>\cos 2\varphi</math> by <math>\sin 2\varphi</math>.</p>	

In Table IV  $\zeta_a, \zeta_b, n_a, n_b$  are the orbital exponents and principal quantum numbers of the AO's  $\chi_a$  and  $\chi_b$ . The basic charge distributions are further considered as functions of the parameters  $\rho_a$  and  $\rho_b$ , defined by

$$\rho_a = \zeta_a R, \quad \rho_b = \zeta_b R; \quad (1.6)$$

finally, the parameters  $\rho$  and  $\tau$ , occurring in the factor  $e^{-\rho\xi - \tau\rho\eta}$ , are defined in terms of  $\rho_a$  and  $\rho_b$  by

$$\left. \begin{aligned} \rho &= \frac{1}{2}(\rho_a + \rho_b) = \frac{1}{2}(\zeta_a + \zeta_b)R, \\ \tau &= (\rho_a - \rho_b) / (\rho_a + \rho_b) = (\zeta_a - \zeta_b) / (\zeta_a + \zeta_b), \end{aligned} \right\} \quad (1.7)$$

so that  $\rho_a$  and  $\rho_b$  can also be written in terms of  $\rho$  and  $\tau$ , namely

$$\rho_a = (1+\tau)\rho, \quad \rho_b = (1-\tau)\rho. \quad (1.7')$$

Obviously, we may consider the basic charge distributions  $\Omega_{ab}$  as either functions of  $\rho_a$  and  $\rho_b$ , or as functions of  $\rho$  and  $\tau$ . The former choice is more useful for the mathematical analysis of the hybrid integrals, and will be adhered to throughout this paper; the latter choice, however, is more useful from the point of view of the numerical tabulation of the auxiliary functions in which we shall express the hybrid

integrals.

From Table IV it can easily be verified that the basic charge distributions  $\Omega_{ab}$  satisfy the general formula

$$\left(\frac{1}{2}R\right)^2(\xi-\eta)\Omega_{ab} = \zeta_a^{n_a+\frac{1}{2}} \zeta_b^{-n_a+\frac{1}{2}} \rho_b^{n_a+n_b} e^{-\rho\xi-\tau\rho\eta} \times p(\xi+\eta, \xi-\eta, 1+\xi\eta, 1-\xi\eta) [(\xi^2-1)(1-\eta^2)]^{q+\frac{1}{2}M} \begin{cases} \cos M\varphi \\ \sin M\varphi \end{cases} \quad (1.8)$$

where  $q$  is a non-negative integer, and  $p(u, v, x, y)$  is a homogeneous polynomial in  $u, v, x, y$  of the degree  $n_a+n_b-2q-M-1$ . Actually, in all our cases, due to the restriction to  $1s, 2s$ , and  $2p$  AO's,  $p$  consists of only one term; further  $q = 0$ , except for  $2p\pi_a 2p\pi_b \Sigma$ , in which case  $q = 1$ . The  $\Sigma$ -type distributions are independent of  $\varphi$ , hence the upper choice of (1.8) applies with  $M = 0$ ; for  $\Pi$ - and  $\Delta$ - (or  $\bar{\Pi}$ - and  $\bar{\Delta}$ -) type distributions the upper (lower) choice applies with  $M = 1$  and  $M = 2$ , respectively. The validity of Eq. (1.8) can of course be proven in general; however, since this proof is somewhat lengthy, though not difficult, we shall omit it here.

By means of the Tables II and III any hybrid integral involving AO's with principal quantum numbers 1 and/or 2 can immediately be expressed in terms of a few integrals between basic charge distributions; if  $\Omega_a$  and  $\Omega_{ab}$  are the basic charge distributions, then such a basic hybrid integral has the form

$$[\Omega_a | \Omega_{ab}] = \int dV_1 \int dV_2 \Omega_a(1) \Omega_{ab}(2) / r_{12} \quad (1.9)$$

So, for instance

$$\begin{aligned} [1s'_a 2s''_a | 1s_a 2p\sigma_b] &= (\sqrt{3}/2) \zeta_a^{3/2} \zeta_a^{5/2} \tau_a^{-4} [2s_a | 1s_a 2p\sigma_b], \\ [2p\sigma'_a 2p\sigma''_a | 2p\pi_a 2p\pi_b] &= \zeta_a^{5/2} \zeta_a^{5/2} \tau_a^{-5} \\ &\times \{ [3s_a | 2p\pi_a 2p\pi_b \Sigma] + [3s_a | 2p\pi_a 2p\pi_b \Delta] \\ &+ 3[3D\Sigma_a | 2p\pi_a 2p\pi_b \Sigma] + 3[3D\Sigma_a | 2p\pi_a 2p\pi_b \Delta] \}. \end{aligned}$$

Since the basic charge distributions  $\Omega_a$  and  $\Omega_{ab}$  are classified according to their species and subspecies with respect to the group  $C_{\infty v}$ , we may conclude [see (II), Theorem II] as follows:

Theorem. The integral  $[\Omega_a | \Omega_{ab}]$  vanishes if  $\Omega_a$  and  $\Omega_{ab}$  belong to (i) different species, (ii) the same species, but different subspecies. Furthermore, the

integral is independent of the subspecies.

As a corollary to this theorem we conclude that, in order that the integral  $[\Omega_a | \Omega_{ab}]$  shall not vanish,  $\Omega_a$  and  $\Omega_{ab}$  must both be of the same type (both of  $\Sigma$ -type,  $\Pi$ -type,  $\bar{\Pi}$ -type, etc.); and that an integral involving  $\bar{\Pi}$ - (or  $\bar{\Delta}$ -) type distributions has the same value as the integral involving the corresponding  $\Pi$ - (or  $\Delta$ -) type distributions.

In our example  $[1s'_a 2s''_a | 1s_a 2p\sigma_b]$  we conclude, since  $2S_a$  and  $1s_a 2p\sigma_b$  are both of  $\Sigma$ -type, that this integral does not vanish. In our example  $[2p\sigma'_a 2p\sigma''_a | 2p\pi_a 2p\pi_b]$  the integrals between  $\Sigma$ -type and  $\Delta$ -type distributions vanish, so that this integral reduces to

$$[2p\sigma'_a 2p\sigma''_a | 2p\pi_a 2p\pi_b] = \zeta'_a{}^{5/2} \zeta''_a{}^{5/2} \zeta_a^{-5} \{ [3S_a | 2p\pi_a 2p\pi_b \Sigma] + 3[3D\Sigma_a | 2p\pi_a 2p\pi_b \Sigma] \} .$$

We can now classify the basic hybrid integrals as being of  $\Sigma$ -type,  $\Pi$ -type, or  $\Delta$ -type. On the other hand, a further classification is suggested according to whether  $\Omega_a$  is S-, P-, or D-type [see Eq. (1.3)], that is, whether  $\Omega_a$  is a charge distribution of (mono)pole, dipole, or quadrupole character. We are thus led to the classification of the basic hybrid integrals as exhibited in Table V.

TABLE V.  
CLASSIFICATION AND ENUMERATION OF THE BASIC HYBRID INTEGRALS

Number of basic charge distributions $\Omega_a$			Number of basic charge distributions $\Omega_{ab}$		Number of basic hybrid integrals $[\Omega_a   \Omega_{ab}]$					
	S	P	D			S	P	D	Total	
$\Sigma$	3	2	1	$\Sigma$	10	$\Sigma$	30	20	10	60
$\Pi$		2	1	$\Pi$	6	$\Pi$		12	6	18
$\Delta$			1	$\Delta$	1	$\Delta$			1	1
						Total	30	32	17	79

TWO-CENTER INTEGRALS. III

b. First Integration

The integration over the coordinates of electron 1 in Eq. (1.9) leads to the functions

$$U_{\Omega_a}(2) = \int dV_1 \Omega_a(1)/r_{12}, \quad (1.10)$$

which are the electrostatic potentials of the charge distributions  $\Omega_a$ . We substitute for  $\Omega_a$  the general expression [NLM] as given by Eq. (1.3) and for  $1/r_{12}$  the Laplace expansion<sup>10</sup>

$$1/r_{12} = \sum_{\ell=0}^{\infty} [4\pi/(2\ell+1)] (r_{<}/r_{>})^{\ell+1} \sum_{m=-\ell}^{\ell} S_{\ell m}(\theta_{a1}, \varphi_1) S_{\ell m}(\theta_{a2}, \varphi_2), \quad (1.11)$$

where  $r_{<}$  means the smaller one of  $r_{a1}$  and  $r_{a2}$ , and  $r_{>}$  the larger one. Carrying out the integration in the spherical coordinates  $r_{a1}, \theta_{a1}, \varphi_1$ , we obtain immediately the result

$$U_{\text{NLM}}(2) = [4\pi/(2L+1)]^{\frac{1}{2}} [2^L (2\zeta_a)^{N+2} / (N+L+1)!] S_{\text{LM}}(\theta_{a2}, \varphi_2) \times \int_0^{\infty} dr_{a1} (r_{<}/r_{>})^{L+1} r_{a1}^{N+1} e^{-2\zeta_a r_{a1}},$$

or

$$U_{\text{NLM}}(2) = [4\pi/(2L+1)]^{\frac{1}{2}} 2^{L+1} \zeta_a S_{\text{LM}}(\theta_{a2}, \varphi_2) U_{\text{NL}}(r_{a2}), \quad (1.12)$$

where

$$U_{\text{NL}}(r_{a2}) = [(2\zeta_a)^{N+1} / (N+L+1)!] \int_0^{\infty} dr_{a1} (r_{<}/r_{>})^{L+1} r_{a1}^{N+1} e^{-2\zeta_a r_{a1}}. \quad (1.13)$$

Carrying out the substitutions

$$t = r_{a1}/r_{a2}, \quad s = 2\zeta_a r_{a2}, \quad (1.14)$$

we obtain for (1.13)

$$U_{\text{NL}}(r_{a2}) = [s^{N+1} / (N+L+1)!] \left[ \int_0^1 dt e^{-st} t^{N+L+1} + \int_1^{\infty} dt e^{-st} t^{N-L} \right],$$

or

---

<sup>10</sup>Usually the Laplace expansion is given in terms of the complex spherical harmonics  $Y_{\ell m}(\theta, \varphi)$  [see (II), Eq. (4.18) and ref. 24]; the expansion (1.11) in terms of the real spherical harmonics  $S_{\ell m}(\theta, \varphi)$  is readily obtained from this one.

$$U_{NL}(r_{a2}) = [s^{N+1}/(N+L+1)!][(N+L+1)!/s^{N+L+2} - A_{N+L+1}(s) + A_{N-L}(s)] , \quad (1.15)$$

where<sup>11</sup>

$$A_n(s) = (n!/s^{n+1})e^{-s} \sum_{k=0}^n s^k/k! . \quad (1.16)$$

We rewrite (1.15) in the form

$$U_{NL}(r_{a2}) = s^{-L-1}(1-e^{-s} \sum_{k=0}^{N+L} u_k s^k) , \quad (1.17)$$

with

$$\left. \begin{aligned} u_k &= 1/k! \text{ for } 0 \leq k \leq 2L , \\ u_k &= (1/k!) - (N-L)!/(N+L+1)!(k-2L-1)! \text{ for } 2L+1 \leq k \leq N+L . \end{aligned} \right\} \quad (1.18)$$

Substitution of (1.17) into (1.12) yields the potentials  $U_{NLM}(2)$ . For all the basic charge distributions occurring in Table II the results were already derived in (I) and are given there in Eqs. (33); in order to write these potentials in the present notation we have to make the substitution  $\sigma = \frac{1}{2}s$ . The purpose of the present derivation is to establish the general fact that (1.17) and therefore also (1.12) contains negative powers of  $r_{a2}$  only in the form

$$s^{-L-1}[1-e^{-s} \sum_{k=0}^{2L} (s^k/k!)] \quad (1.19)$$

which will be essential for our further conclusions. (It may be noted that  $\sum_{k=0}^{L+1}$  would be sufficient in (1.19) to insure that  $U_{NLM}(2)$  remains finite for  $r_{a2} = 0$ .)

In order to prepare the potentials  $U_{NLM}(2)$  for the second integration we express them in the elliptic coordinates  $\xi, \eta, \varphi$ . We define the new parameter

$$\bar{\rho}_a = \zeta_a R = \frac{1}{2}(\zeta'_a + \zeta''_a)R , \quad (1.20)$$

so that [see Eqs. (1.5', 14)]

$$s = \bar{\rho}_a (\xi + \eta) . \quad (1.21)$$

Furthermore we note that the factor  $S_{LM}$  in (1.12) can be written

<sup>11</sup>Concerning the functions  $A_n(x)$ , see Section 5a of this paper.

TWO-CENTER INTEGRALS. III

$$S_{LM}(\theta_{a2}, \varphi_2) \sim \sin^M \theta_{a2} P_L^{(M)}(\cos \theta_{a2}) \begin{cases} \cos M\varphi_2 \\ \sin M\varphi_2 \end{cases}$$

$$= [(\xi^2-1)(1-\eta^2)]^{\frac{1}{2}M} (\xi+\eta)^{-M} P_L^{(M)}[(1+\xi\eta)/(\xi+\eta)] \begin{cases} \cos M\varphi_2 \\ \sin M\varphi_2 \end{cases}; \quad (1.22)$$

considering Eqs (1.12,17,21,22) we obtain for the potentials  $U_{NLM}$  the general relation

$$\frac{1}{2}R(\xi+\eta)U_{NLM}(2) = \bar{\rho}_a^{-L}(\xi+\eta)^{-2L} [1 - e^{-\bar{\rho}_a(\xi+\eta)} \sum_{k=0}^{N+L} u_k \bar{\rho}_a^k (\xi+\eta)^k]$$

$$\times p'(\xi+\eta, 1+\xi\eta) [(\xi^2-1)(1-\eta^2)]^{\frac{1}{2}M} \begin{cases} \cos M\varphi_2 \\ \sin M\varphi_2 \end{cases}, \quad (1.23)$$

where  $p'(x,y)$  is a homogeneous polynomial in  $x,y$  of the degree  $L-M$ . The inclusion of the factor  $(\frac{1}{2}R)(\xi+\eta)$  in (1.23) will prove useful later.

In Table VI are given the explicit expressions of the type (1.23) for the 10 basic charge distributions which are needed; these expressions are readily obtained from those given in (I), Eq. (33).

c. Second Integration

The second integration is carried out in elliptic coordinates. The volume element is given by

$$dV_2 = (R^3/8)(\xi^2-\eta^2)d\xi d\eta d\varphi_2, \quad (1.24)$$

so that the basic hybrid integrals have the general form

$$[\Omega_a | \Omega_{ab}] = \int_1^\infty d\xi \int_{-1}^1 d\eta \int_0^{2\pi} d\varphi_2 [\frac{1}{2}R(\xi+\eta)U_{\Omega_a}(2)] [(\frac{1}{2}R)^2(\xi-\eta)\Omega_{ab}(2)], \quad (1.25)$$

where the expressions  $(\frac{1}{2}R)^2(\xi-\eta)\Omega_{ab}(2)$  and  $\frac{1}{2}R(\xi+\eta)U_{\Omega_a}(2)$  are to be taken from Tables IV and VI, respectively.

Now  $U_{\Omega_a}(2)$  and  $\Omega_{ab}(2)$  contain  $\varphi_2$  in the form  $\cos M\varphi_2$  or  $\sin M\varphi_2$ : hence the integration over  $\varphi_2$  can be carried out immediately. Since

$$\left. \begin{aligned} \int_0^{2\pi} d\varphi_2 &= 2\pi, \\ \int_0^{2\pi} d\varphi_2 \cos m\varphi_2 &= \int_0^{2\pi} d\varphi_2 \sin m\varphi_2 = 0, \\ \int_0^{2\pi} d\varphi_2 \cos m\varphi_2 \cos n\varphi_2 &= \int_0^{2\pi} d\varphi_2 \sin m\varphi_2 \sin n\varphi_2 = \pi \delta_{mn}, \\ \int_0^{2\pi} d\varphi_2 \cos m\varphi_2 \sin n\varphi_2 &= 0, \end{aligned} \right\} \quad (1.26)$$

TABLE VI.

 POTENTIALS OF THE TEN BASIC ONE-CENTER CHARGE DISTRIBUTIONS  $\Omega_a$ 

$\Omega_a$	$\frac{1}{2}R(\xi+\eta)U_{\Omega_a}$
	(Mono)pole Potentials (L = 0)
[1S <sub>a</sub> ]	$1 - e^{-\bar{\rho}_a(\xi+\eta)} [1 + (1/2)\bar{\rho}_a(\xi+\eta)]$
[2S <sub>a</sub> ]	$1 - e^{-\bar{\rho}_a(\xi+\eta)} [1 + (2/3)\bar{\rho}_a(\xi+\eta) + (1/6)\bar{\rho}_a^2(\xi+\eta)^2]$
[3S <sub>a</sub> ]	$1 - e^{-\bar{\rho}_a(\xi+\eta)} [1 + (3/4)\bar{\rho}_a(\xi+\eta) + (1/4)\bar{\rho}_a^2(\xi+\eta)^2 + (1/24)\bar{\rho}_a^3(\xi+\eta)^3]$
	Dipole Potentials (L = 1)
$\left. \begin{array}{l} [2P\Sigma_a] \\ [2P\Pi_a] \\ [2P\bar{\Pi}_a] \end{array} \right\}$	$2\bar{\rho}_a^{-1}(\xi+\eta)^{-2} \{1 - e^{-\bar{\rho}_a(\xi+\eta)} [ \sum_{k=0}^2 (\bar{\rho}_a^k/k!) (\xi+\eta)^k + (1/8)\bar{\rho}_a^3(\xi+\eta)^3 ]\}$ $\times \begin{cases} (1+\xi\eta) \\ [(\xi^2-1)(1-\eta^2)]^{\frac{1}{2}} \cos\varphi \\ [(\xi^2-1)(1-\eta^2)]^{\frac{1}{2}} \sin\varphi \end{cases}$
$\left. \begin{array}{l} [3P\Sigma_a] \\ [3P\Pi_a] \\ [3P\bar{\Pi}_a] \end{array} \right\}$	$2\bar{\rho}_a^{-1}(\xi+\eta)^{-2} \{1 - e^{-\bar{\rho}_a(\xi+\eta)} [ \sum_{k=0}^2 (\bar{\rho}_a^k/k!) (\xi+\eta)^k$ $+ (3/20)\bar{\rho}_a^3(\xi+\eta)^3 + (1/40)\bar{\rho}_a^4(\xi+\eta)^4 ]\}$ $\times \begin{cases} (1+\xi\eta) \\ [(\xi^2-1)(1-\eta^2)]^{\frac{1}{2}} \cos\varphi \\ [(\xi^2-1)(1-\eta^2)]^{\frac{1}{2}} \sin\varphi \end{cases}$
	Quadrupole Potentials (L = 2)
$\left. \begin{array}{l} [3D\Sigma_a] \\ [3D\Pi_a] \\ [3D\bar{\Pi}_a] \\ [3D\Delta_a] \\ [3D\bar{\Delta}_a] \end{array} \right\}$	$2\bar{\rho}_a^{-2}(\xi+\eta)^{-4} \{1 - e^{-\bar{\rho}_a(\xi+\eta)} [ \sum_{k=0}^4 (\bar{\rho}_a^k/k!) (\xi+\eta)^k + (1/144)\bar{\rho}_a^5(\xi+\eta)^5 ]\}$ $\times \begin{cases} [3(1+\xi\eta)^2 - (\xi+\eta)^2] \\ 2\sqrt{3}(1+\xi\eta)[(\xi^2-1)(1-\eta^2)]^{\frac{1}{2}} \cos\varphi \\ 2\sqrt{3}(1+\xi\eta)[(\xi^2-1)(1-\eta^2)]^{\frac{1}{2}} \sin\varphi \\ \sqrt{3}(\xi^2-1)(1-\eta^2) \cos 2\varphi \\ \sqrt{3}(\xi^2-1)(1-\eta^2) \sin 2\varphi \end{cases}$

TWO-CENTER INTEGRALS. III

where  $m \neq 0$ ,  $n \neq 0$ , we obtain here once more the result already stated on the ground of group theoretical considerations, namely: in order that the integral  $[\Omega_a | \Omega_{ab}]$  shall not vanish,  $\Omega_a$  and  $\Omega_{ab}$  must be of the same type (both  $\Sigma$ -type,  $\Pi$ -type,  $\bar{\Pi}$ -type, etc.); and an integral involving  $\bar{\Pi}$ - (or  $\bar{\Delta}$ -) type distributions has the same value as the integral involving the corresponding  $\Pi$ - (or  $\Delta$ -) type distributions. We see further from (1.26) that the integration over  $\varphi_2$  yields  $2\pi$  for integrals of  $\Sigma$ -type, and  $\pi$  for integrals of  $\Pi$ - and  $\Delta$ - type.

Substituting the general expressions (1.8) and (1.23) into (1.25) and carrying out the integration over  $\varphi_2$ , we obtain for the non-vanishing basic hybrid integrals the general formula

$$[\Omega_a | \Omega_{ab}] = \zeta_a^{n_a + \frac{1}{2}} \zeta_b^{-n_a + \frac{1}{2}} \bar{\rho}_a^{-L} \rho_b^{n_a + n_b} \int_1^\infty d\xi \int_{-1}^1 d\eta (\xi + \eta)^{-2L} [1 - e^{-\bar{\rho}_a(\xi + \eta)} \sum_{k=0}^{N+L} u_k \bar{\rho}_a^k (\xi + \eta)^k] \times e^{-\rho \xi - \tau \rho \eta} p''(\xi + \eta, \xi - \eta, 1 + \xi \eta, 1 - \xi \eta) [(\xi^2 - 1)(1 - \eta^2)]^{q+M}, \quad (1.27)$$

where  $p''(u, v, x, y)$  is a homogeneous polynomial in  $u, v, x, y$  of the degree  $n_a + n_b + L - 2q - 2M - 1$ . Actually, the polynomial  $p''$  consists of only one term in all cases except for the integrals involving the distribution  $3D\Sigma_a$ , in which case  $p''$  consists of two terms. For instance, for  $[2P\Pi_a | 2p\sigma_a 2p\pi_b]$  we find  $p'' = (1/8)(\xi - \eta)(1 + \xi \eta)$ ,  $q = 0$ , and for  $[3D\Sigma_a | 2p\pi_a 2p\pi_b \Sigma]$  we find  $p'' = (1/8)(\xi - \eta)[3(1 + \xi \eta)^2 - (\xi + \eta)^2]$ ,  $q = 1$ .

If we now expand the polynomial  $p''$  in terms of its four arguments  $\xi + \eta, \xi - \eta, 1 + \xi \eta, 1 - \xi \eta$ , then the integral (1.27) can be written as a linear combination with numerical coefficients of expressions of the type<sup>12</sup>

$$I_{\lambda\beta}^{\gamma\delta\epsilon} = \zeta_a^{n_a + \frac{1}{2}} \zeta_b^{-n_a + \frac{1}{2}} \bar{\rho}_a^{-L} \rho_b^{n_a + n_b} \int_1^\infty d\xi \int_{-1}^1 d\eta [1 - e^{-\bar{\rho}_a(\xi + \eta)} \sum_{k=0}^{N+L} u_k \bar{\rho}_a^k (\xi + \eta)^k] e^{-\rho \xi - \tau \rho \eta} (\xi + \eta)^\lambda (\xi - \eta)^\beta (1 + \xi \eta)^\gamma (1 - \xi \eta)^\delta (\xi^2 - 1)^\epsilon (1 - \eta^2)^\epsilon, \quad (1.28)$$

where

<sup>12</sup>According to Eq. (1.28), the  $I_{\lambda\beta}^{\gamma\delta\epsilon}$ 's are, apart from the factor  $\zeta_a^{n_a + \frac{1}{2}} \zeta_b^{-n_a + \frac{1}{2}}$ , functions of the three parameters  $\bar{\rho}_a, \rho_a, \rho_b$ . They further depend of course on the set of indices  $\lambda, \beta, \gamma, \delta, \epsilon$ , but also on the numbers  $u_k$ , which are determined by  $L$  and  $M$ . This dependence of  $L$  and  $M$  is not indicated by the symbol  $I_{\lambda\beta}^{\gamma\delta\epsilon}$ ; however, this does not lead to any difficulties, since  $I_{\lambda\beta}^{\gamma\delta\epsilon}$  is only used as the symbol for an intermediate result, and does not occur in any of the tables designed for practical use.

RUEDENBERG, ROTHAN, AND JAUNZEMIS

$$\left. \begin{aligned} \epsilon &= q+M, \\ \lambda+\beta+\gamma+\delta &= n_a+n_b-L-2q-2M-1, \end{aligned} \right\} \quad (1.29)$$

so that

$$\lambda+\beta+\gamma+\delta+2\epsilon = n_a+n_b-L-1. \quad (1.29')$$

Obviously  $\beta, \gamma, \delta, \epsilon$  are non-negative integers, whereas  $\lambda$  is restricted to the range

$$-2L \leq \lambda \leq n_a+n_b-L-2q-2M-1, \quad (1.30)$$

so that in general  $\lambda \geq 0$ .

We shall deal first with those integrals  $I_{\lambda\beta}^{\gamma\delta\epsilon}$  which can be evaluated by a term by term integration. This is certainly possible if  $L = 0$ , since then  $\lambda \geq 0$ ; however, in many cases where  $\lambda < 0$  it is still possible in spite of the singularity of  $(\xi+\eta)^\lambda$  for  $\xi+\eta = 0$ , as will be discussed below.

The functions  $I_{\lambda\beta}^{\gamma\delta\epsilon}$  depend on the three parameters  $\bar{\rho}_a, \rho_a, \rho_b$ . It is useful, however, to consider instead  $\rho^*_a, \rho_a, \rho_b$ , as the primary parameters, where  $\rho^*_a$  is given by

$$\rho^*_a = 2\bar{\rho}_a + \rho_a = (\zeta'_a + \zeta''_a + \zeta_a)R. \quad (1.31)$$

In analogy to (1.7), we define the secondary parameters  $\rho^*$  and  $\tau^*$  by

$$\left. \begin{aligned} \rho^* &= \frac{1}{2}(\rho^*_a + \rho_b) = \frac{1}{2}(\zeta'_a + \zeta''_a + \zeta_a + \zeta_b)R, \\ \tau^* &= (\rho^*_a - \rho_b) / (\rho^*_a + \rho_b) = (\zeta'_a + \zeta''_a + \zeta_a - \zeta_b) / (\zeta'_a + \zeta''_a + \zeta_a + \zeta_b), \end{aligned} \right\} \quad (1.32)$$

so that

$$\rho^*_a = (1+\tau^*)\rho^*, \quad \rho_b = (1-\tau^*)\rho^*, \quad (1.32')$$

and also

$$\rho^* = \rho + \bar{\rho}_a, \quad \tau^*\rho^* = \tau\rho + \bar{\rho}_a. \quad (1.32'')$$

We define further another secondary parameter  $\mu$  by

$$\mu = (\rho^*_a - \rho_a) / 2\rho_b = \bar{\rho}_a / \rho_b = \zeta'_a / \zeta_b = (\zeta'_a + \zeta''_a) / 2\zeta_b. \quad (1.33)$$

In view of Eqs. (1.31-33), we may write for the integral (1.28)

TWO-CENTER INTEGRALS. III

$$I_{\lambda\beta}^{\gamma\delta\epsilon} = \zeta_a^{n_a+\frac{1}{2}} \zeta_b^{-n_a+\frac{1}{2}} \mu^{-L} \rho_b^{\lambda+\beta+\gamma+\delta+2\epsilon+1} \\ \times \int_1^\infty d\xi \int_{-1}^1 d\eta [e^{-\rho\xi-\tau\rho\eta} - e^{-\rho^*\xi-\tau^*\rho^*\eta} \sum_{k=0}^{N+L} u_k \mu^k \rho_b^k (\xi+\eta)^k] \\ \times (\xi+\eta)^\lambda (\xi-\eta)^\beta (1+\xi\eta)^\gamma (1-\xi\eta)^\delta (\xi^2-1)^\epsilon (1-\eta^2)^\epsilon. \quad (1.34)$$

Defining now the two-parameter functions

$$C_{\alpha\beta}^{\gamma\delta\epsilon}(\rho_a, \rho_b) = (-1)^{\beta+\delta+\epsilon} (\frac{1}{2}\rho_b)^{\alpha+\beta+\gamma+\delta+2\epsilon+1} \int_1^\infty d\xi \int_{-1}^1 d\eta e^{-\rho\xi-\tau\rho\eta} \\ \times (\xi+\eta)^\alpha (\xi-\eta)^\beta (1+\xi\eta)^\gamma (1-\xi\eta)^\delta (\xi^2-1)^\epsilon (1-\eta^2)^\epsilon, \quad (1.35)$$

we may write for (1.34)

$$I_{\lambda\beta}^{\gamma\delta\epsilon} = (-1)^{\beta+\delta+\epsilon} 2^{\lambda+\beta+\gamma+\delta+2\epsilon+1} \zeta_a^{n_a+\frac{1}{2}} \zeta_b^{-n_a+\frac{1}{2}} \mu^{-L} \\ \times [C_{\lambda\beta}^{\gamma\delta\epsilon}(\rho_a, \rho_b) - \sum_{\alpha=0}^{N+L} u_\alpha (2\mu)^\alpha C_{\lambda+\alpha, \beta}^{\gamma\delta\epsilon}(\rho_a^*, \rho_b)] . \quad (1.36)$$

Remembering that each basic hybrid integral is a linear combination of a few functions  $I_{\lambda\beta}^{\gamma\delta\epsilon}$ , we see that the basic hybrid integrals for which the term by term integration is possible, have the general form

$$[\Omega_a | \Omega_{ab}] = \zeta_a^{n_a+\frac{1}{2}} \zeta_b^{-n_a+\frac{1}{2}} \mu^{-L} [H_0(\rho_a, \rho_b) - \sum_{\alpha=0}^{N+L} \mu^\alpha H_\alpha(\rho_a^*, \rho_b)], \quad (1.37)$$

where each function  $H_\alpha(\rho_a, \rho_b)$  is a simple linear combination of C-functions with numerical coefficients.

We return now to the question of the possibility of a term by term integration; this method is valid provided all the functions  $C_{\alpha\beta}^{\gamma\delta\epsilon}$  which occur in Eq. (1.36) are defined by converging integrals as given by (1.35). This is clearly the case if  $\alpha \geq 0$ . It is furthermore shown in Section 4 that for  $\alpha < 0$  the integral (1.35) still converges if

$$\alpha + \gamma + 2\epsilon + 1 \geq 0; \quad (1.38)$$

consequently, Eqs. (1.36, 37) hold if

$$\lambda + \gamma + 2\epsilon + 1 \geq 0. \quad (1.39)$$

The basic hybrid integrals for which all the occurring functions  $I_{\lambda\beta}^{\gamma\delta\epsilon}$  satisfy (1.39) are said to form the first class; whereas those for which some of the functions  $I_{\lambda\beta}^{\gamma\delta\epsilon}$  do not satisfy (1.39) belong to the second class. The validity of the general

expression (1.37) is therefore proved for the basic hybrid integrals of the first class.

With the help of Tables IV and VI it is easily established that all but three of our 79 basic hybrid integrals belong to the first class; the three integrals of the second class are

$$[\exists D \Sigma_a | 1s_b \chi_b], \text{ with } \chi_b = 1s_b, 2s_b, 2p\sigma_b. \quad (1.40)$$

For these integrals we shall prove that the general expression (1.37) is still valid; however, in this case the H-functions are not any more simple linear combination of C-functions with numerical coefficients, but with coefficients depending on  $\rho_a$  and  $\rho_b$  (or  $\rho_a^*$  and  $\rho_b$ ).

Returning to the expression (1.28), we observe that the integral  $I_{\lambda\beta}^{\gamma\delta\epsilon}$  always converges, regardless of whether its indices satisfy (1.39) or not. Namely in the integrand the negative powers of  $\xi+\eta$  occur only in  $v_\lambda[\bar{\rho}_a(\xi+\eta)]$ , where [see Eq. (1.18)]

$$v_\lambda(x) = x^\lambda (1 - e^{-x} \sum_{k=0}^{-\lambda-1} x^k/k!); \quad (1.41)$$

$v_\lambda[\bar{\rho}_a(\xi+\eta)]$  is a well-behaved function in the entire domain of  $\xi$  and  $\eta$ , even at the critical point  $\xi+\eta = 0$ , since

$$\lim_{x \rightarrow 0} v_\lambda(x) = \lim_{x \rightarrow 0} x^\lambda e^{-x} (e^x - \sum_{k=0}^{-\lambda-1} x^k/k!) = 1/(-\lambda)!$$

Obviously, the functions  $v_\lambda(x)$  are defined for  $\lambda \leq -1$ . Making use of Eqs. (1.31,41) we may write for (1.28)

$$\begin{aligned} I_{\lambda\beta}^{\gamma\delta\epsilon} &= \zeta_a^{n_a+\frac{1}{2}} \zeta_b^{-n_b+\frac{1}{2}} \mu^{-L} \rho_b^{\lambda+\beta+\gamma+\delta+2\epsilon+1} \\ &\times \{\bar{\rho}_a^{-\lambda} \int_1^\infty d\xi \int_{-1}^1 d\eta v_\lambda[\bar{\rho}_a(\xi+\eta)] e^{-\rho\xi-\tau\rho\eta} (\xi-\eta)^\beta (1+\xi\eta)^\gamma (1-\xi\eta)^\delta (\xi^2-1)^\epsilon (1-\eta^2)^\epsilon \\ &- \sum_{\alpha=-\lambda}^{N+L} u_\alpha \mu^\alpha \rho_b^\alpha \int_1^\infty d\xi \int_{-1}^1 d\eta e^{-\rho^*\xi-\tau^*\rho^*\eta} (\xi+\eta)^{\lambda+\alpha} (\xi-\eta)^\beta (1+\xi\eta)^\gamma (1-\xi\eta)^\delta (\xi^2-1)^\epsilon (1-\eta^2)^\epsilon\}. \end{aligned} \quad (1.42)$$

We define the three-parameter functions

$$\begin{aligned} C_{\lambda\beta}^{\gamma\delta\epsilon}(\bar{\rho}_a, \rho_a, \rho_b) &= (-1)^{\beta+\delta+\epsilon} \bar{\rho}_a^{-\lambda} (\frac{1}{2}\rho_b)^{\lambda+\beta+\gamma+\delta+2\epsilon+1} \\ &\int_1^\infty d\xi \int_{-1}^1 d\eta v_\lambda[\bar{\rho}_a(\xi+\eta)] e^{-\rho\xi-\tau\rho\eta} (\xi-\eta)^\beta (1+\xi\eta)^\gamma (1-\xi\eta)^\delta (\xi^2-1)^\epsilon (1-\eta^2)^\epsilon; \end{aligned} \quad (1.43)$$

this definition is valid for  $\lambda \leq -1$ . Making use of Eq. (1.35), we may write for (1.42)

TWO-CENTER INTEGRALS. III

$$I_{\lambda\beta}^{\gamma\delta\epsilon} = (-1)^{\beta+\delta+\epsilon} 2^{\lambda+\beta+\gamma+\delta+2\epsilon+1} \zeta_a^{n_a+\frac{1}{2}} \zeta_b^{-n_a+\frac{1}{2}} \mu^{-L} \\ \times [C_{\lambda\beta}^{\gamma\delta\epsilon}(\bar{\rho}_a, \rho_a, \rho_b) - \sum_{\alpha=-\lambda}^{N+L} u_\alpha (2\mu)^\alpha C_{\lambda+\alpha, \beta}^{\gamma\delta\epsilon}(\rho^*_a, \rho_b)] . \quad (1.44)$$

Eq. (1.44) is to be used as the starting point for the basic hybrid integrals of the second class. However, for many integrals of the first class Eq. (1.44) can still be used, namely as long as these integrals give rise to I-functions with  $\lambda \leq -1$ . In these cases the C-functions can be expressed in terms of C-functions by means of

$$C_{\lambda\beta}^{\gamma\delta\epsilon}(\bar{\rho}_a, \rho_a, \rho_b) = C_{\lambda\beta}^{\gamma\delta\epsilon}(\rho_a, \rho_b) - \sum_{\alpha=0}^{-\lambda-1} [(2\mu)^\alpha / \alpha!] C_{\lambda+\alpha, \beta}^{\gamma\delta\epsilon}(\rho^*_a, \rho_b) ; \quad (1.45)$$

substitution of (1.45) into (1.44) yields once more (1.36).

We observe now that for the integrals (1.40) the I-functions occur in the combination

$$\left. \begin{aligned} &3I_{-4, \beta}^{2\delta 0} - I_{-2, \beta}^{0\delta 0} , \text{ with} \\ &\beta = 1 , \delta = 0 \text{ for } \chi_b = 1s_b , \\ &\beta = 2 , \delta = 0 \text{ for } \chi_b = 2s_b , \\ &\beta = 1 , \delta = 1 \text{ for } \chi_b = 2p\delta_b . \end{aligned} \right\} \quad (1.46)$$

Now in Section 1d the following relation is proved:<sup>13</sup>

$$3C_{-4, \beta}^{2\delta 0} - C_{-2, \beta}^{0\delta 0} \\ = [-\rho_a \rho_b^{-1} C_{-3, \beta}^{0\delta 1} + 2\rho_b^{-1} C_{-2, \beta}^{1\delta 0} + \delta \rho_b^{-1} C_{-2, \beta}^{0, \delta-1, 1}] \\ - [-\rho_a \rho_b^{-1} C_{-3, \beta}^{0\delta 1} + 2\rho_b^{-1} C_{-2, \beta}^{1\delta 0} + \delta \rho_b^{-1} C_{-2, \beta}^{0, \delta-1, 1}]^* \\ - 2\mu [C_{-3, \beta}^{0\delta 1} - \rho_a \rho_b^{-1} C_{-2, \beta}^{0\delta 1} + 2\rho_b^{-1} C_{-1, \beta}^{1\delta 0} + \delta \rho_b^{-1} C_{-1, \beta}^{0, \delta-1, 1}]^* \\ - 2\mu^2 [2C_{-2, \beta}^{0\delta 1} - \rho_a \rho_b^{-1} C_{-1, \beta}^{0\delta 1} + 2\rho_b^{-1} C_{0\beta}^{1\delta 0} + \delta \rho_b^{-1} C_{0\beta}^{0, \delta-1, 1} + C_{0\beta}^{0\delta 0}]^* \\ - 4\mu^3 C_{-1, \beta}^{2\delta 0} . \quad (1.47)$$

<sup>13</sup>In Eq. (1.47), and also for the analysis in the following sections, we have adopted, unless stated otherwise, the following convention concerning the arguments. (1) The arguments of the C-functions are always  $\bar{\rho}_a, \rho_a, \rho_b$ . (2) The arguments of the C-functions are  $\rho_a, \rho_b$ , if the symbol C is used, and  $\rho^*_a, \rho_b$  if the symbol C\* is used.

According to Eq. (1.44), the "easy" part of the I-functions in (1.46) yields, combined with the expression (1.47), an expression of the form (1.37).

The explicit formulas for the H-functions of (1.37) in terms of the C-functions (1.35) are given in Table VII for all the 79 basic hybrid integrals. The C-functions themselves will be dealt with in Sections 3 and 4.

At this point we wish to call attention to the fact that we have not dealt with the integrals of the second class in a general way, but have considered only the explicit cases arising from the restriction to 1s, 2s, and 2p AO's. However, we feel confident that for all possible cases formulas of the type (1.47) can be found by the procedure outlined in the next section 4d, in particular by appropriate use of the noteworthy relations (1.54, 54'). In other words, Eq. (1.47) is probably the first member of a more general family of relations. Nevertheless, since within the scope of the present program only three integrals of the second class arose, we did not deem it worth while to investigate this class in a more general way.

d. Proof of Eq. (1.47)

I

From the identity

$$(1+\xi\eta) + (1-\xi\eta) = 2$$

follow the relations<sup>13</sup>

$$\rho_b C_{\alpha\beta}^{\gamma\delta\epsilon} + C_{\alpha\beta}^{\gamma, \delta+1, \epsilon} = C_{\alpha\beta}^{\gamma+1, \delta\epsilon}, \quad (1.48)$$

$$\rho_b C_{\lambda\beta}^{\gamma\delta\epsilon} + C_{\lambda\beta}^{\gamma, \delta+1, \epsilon} = C_{\lambda\beta}^{\gamma+1, \delta\epsilon}. \quad (1.49)$$

Similarly, from the identity

$$(1+\xi\eta)^2 + (\xi^2-1)(1-\eta^2) = (\xi+\eta)^2$$

follows

$$C_{\alpha\beta}^{\gamma\delta\epsilon} = C_{\alpha\beta}^{\gamma-2, \delta, \epsilon+1} + C_{\alpha+2, \beta}^{\gamma-2, \delta\epsilon}; \quad (1.50)$$

also

---

(3) The symbol \* outside an expression in brackets applies to all the symbols inside those brackets; that is, not only is every C to be considered as C\*, but also  $\rho_a^-$  is to be considered as  $\rho_a^*$ .

TWO-CENTER INTEGRALS. III

TABLE VII

THE 79 HYBRID INTEGRALS IN TERMS OF THE AUXILIARY FUNCTIONS  $C_{\alpha\beta}^{\gamma\delta\epsilon}$   
 The last column of this table contains common factors with which the expressions  
 in terms of C-functions have to be multiplied in order to yield the H-functions.

L = 0 , M = 0 : Monopole Integrals

$[\Omega_a   \Omega_{ab}]$	$H_0$	$H_1$	$H_2$	cf
$[1S_a   1s_a 1s_b]$	$C_{01}^{000}$	$C_{11}^{000}$		-2
$[1S_a   1s_a 2s_b]$	$C_{02}^{000}$	$C_{12}^{000}$		$2/\sqrt{3}$
$[1S_a   2s_a 1s_b]$	$C_{11}^{000}$	$C_{21}^{000}$		$-2/\sqrt{3}$
$[1S_a   2s_a 2s_b]$	$C_{12}^{000}$	$C_{22}^{000}$		$2/3$
$[1S_a   1s_a 2p\sigma_b]$	$C_{01}^{010}$	$C_{11}^{010}$		2
$[1S_a   2p\sigma_a 1s_b]$	$C_{01}^{100}$	$C_{11}^{100}$		-2
$[1S_a   2s_a 2p\sigma_b]$	$C_{11}^{010}$	$C_{21}^{010}$		$2/\sqrt{3}$
$[1S_a   2p\sigma_a 2s_b]$	$C_{02}^{100}$	$C_{12}^{100}$		$2/\sqrt{3}$
$[1S_a   2p\sigma_a 2p\sigma_b]$	$C_{01}^{110}$	$C_{11}^{110}$		2
$[1S_a   2p\pi_a 2p\pi_b \Sigma]$	$C_{01}^{001}$	$C_{11}^{001}$		1
$[2S_a   1s_a 1s_b]$	$3C_{01}^{000}$	$4C_{11}^{000}$	$2C_{21}^{000}$	$-2/3$
$[2S_a   1s_a 2s_b]$	$3C_{02}^{000}$	$4C_{12}^{000}$	$2C_{22}^{000}$	$2/3\sqrt{3}$
$[2S_a   2s_a 1s_b]$	$3C_{11}^{000}$	$4C_{21}^{000}$	$2C_{31}^{000}$	$-2/3\sqrt{3}$
$[2S_a   2s_a 2s_b]$	$3C_{12}^{000}$	$4C_{22}^{000}$	$2C_{32}^{000}$	$2/9$
$[2S_a   1s_a 2p\sigma_b]$	$3C_{01}^{010}$	$4C_{11}^{010}$	$2C_{21}^{010}$	$2/3$
$[2S_a   2p\sigma_a 1s_b]$	$3C_{01}^{100}$	$4C_{11}^{100}$	$2C_{21}^{100}$	$-2/3$
$[2S_a   2s_a 2p\sigma_b]$	$3C_{11}^{010}$	$4C_{21}^{010}$	$2C_{31}^{010}$	$2/3\sqrt{3}$
$[2S_a   2p\sigma_a 2s_b]$	$3C_{02}^{100}$	$4C_{12}^{100}$	$2C_{22}^{100}$	$2/3\sqrt{3}$
$[2S_a   2p\sigma_a 2p\sigma_b]$	$3C_{01}^{110}$	$4C_{11}^{110}$	$2C_{21}^{110}$	$2/3$
$[2S_a   2p\pi_a 2p\pi_b \Sigma]$	$3C_{01}^{001}$	$4C_{11}^{001}$	$2C_{21}^{001}$	$1/3$

## RUEDENBERG, ROOTHAAN, AND JAUNZEMIS

TABLE VII (continued)

$[\Omega_a   \Omega_{ab}]$	$H_0$	$H_1$	$H_2$	$H_3$	cf
$[3S_a   1s_a 1s_b]$	$6C_{01}^{000}$	$9C_{11}^{000}$	$6C_{21}^{000}$	$2C_{31}^{000}$	-1/3
$[3S_a   1s_a 2s_b]$	$6C_{02}^{000}$	$9C_{12}^{000}$	$6C_{22}^{000}$	$2C_{32}^{000}$	$1/3\sqrt{3}$
$[3S_a   2s_a 1s_b]$	$6C_{11}^{000}$	$9C_{21}^{000}$	$6C_{31}^{000}$	$2C_{41}^{000}$	$-1/3\sqrt{3}$
$[3S_a   2s_a 2s_b]$	$6C_{12}^{000}$	$9C_{22}^{000}$	$6C_{32}^{000}$	$2C_{42}^{000}$	1/9
$[3S_a   1s_a 2p\sigma_b]$	$6C_{01}^{010}$	$9C_{11}^{010}$	$6C_{21}^{010}$	$2C_{31}^{010}$	1/3
$[3S_a   2p\sigma_a 1s_b]$	$6C_{01}^{100}$	$9C_{11}^{100}$	$6C_{21}^{100}$	$2C_{31}^{100}$	-1/3
$[3S_a   2s_a 2p\sigma_b]$	$6C_{11}^{010}$	$9C_{21}^{010}$	$6C_{31}^{010}$	$2C_{41}^{010}$	$1/3\sqrt{3}$
$[3S_a   2p\sigma_a 2s_b]$	$6C_{02}^{100}$	$9C_{12}^{100}$	$6C_{22}^{100}$	$2C_{32}^{100}$	$1/3\sqrt{3}$
$[3S_a   2p\sigma_a 2p\sigma_b]$	$6C_{01}^{110}$	$9C_{11}^{110}$	$6C_{21}^{110}$	$2C_{31}^{110}$	1/3
$[3S_a   2p\pi_a 2p\pi_b \Sigma]$	$6C_{01}^{001}$	$9C_{11}^{001}$	$6C_{21}^{001}$	$2C_{31}^{001}$	1/6

L = 1 , M = 0 : Dipole Integrals of  $\Sigma$ -character

$[\Omega_a   \Omega_{ab}]$	$H_0$	$H_1$	$H_2$	$H_3$	cf
$[2P\Sigma_a   1s_a 1s_b]$	$C_{-2,1}^{100}$	$2C_{-1,1}^{100}$	$2C_{01}^{100}$	$C_{11}^{100}$	-2
$[2P\Sigma_a   1s_a 2s_b]$	$C_{-2,2}^{100}$	$2C_{-1,2}^{100}$	$2C_{02}^{100}$	$C_{12}^{100}$	$2/\sqrt{3}$
$[2P\Sigma_a   2s_a 1s_b]$	$C_{-1,1}^{100}$	$2C_{01}^{100}$	$2C_{11}^{100}$	$C_{21}^{100}$	$-2/\sqrt{3}$
$[2P\Sigma_a   2s_a 2s_b]$	$C_{-1,2}^{100}$	$2C_{02}^{100}$	$2C_{12}^{100}$	$C_{22}^{100}$	2/3
$[2P\Sigma_a   1s_a 2p\sigma_b]$	$C_{-2,1}^{110}$	$2C_{-1,1}^{110}$	$2C_{01}^{110}$	$C_{11}^{110}$	2
$[2P\Sigma_a   2p\sigma_a 1s_b]$	$C_{-2,1}^{200}$	$2C_{-1,1}^{200}$	$2C_{01}^{200}$	$C_{11}^{200}$	-2
$[2P\Sigma_a   2s_a 2p\sigma_b]$	$C_{-1,1}^{110}$	$2C_{01}^{110}$	$2C_{11}^{110}$	$C_{21}^{110}$	$2/\sqrt{3}$
$[2P\Sigma_a   2p\sigma_a 2s_b]$	$C_{-2,2}^{200}$	$2C_{-1,2}^{200}$	$2C_{02}^{200}$	$C_{12}^{200}$	$2/\sqrt{3}$
$[2P\Sigma_a   2p\sigma_a 2p\sigma_b]$	$C_{-2,1}^{210}$	$2C_{-1,1}^{210}$	$2C_{01}^{210}$	$C_{11}^{210}$	2
$[2P\Sigma_a   2p\pi_a 2p\pi_b \Sigma]$	$C_{-2,1}^{101}$	$2C_{-1,1}^{101}$	$2C_{01}^{101}$	$C_{11}^{101}$	1

TWO-CENTER INTEGRALS. III

TABLE VII (continued)

$[\Omega_a   \Omega_{ab}]$	$H_0$	$H_1$	$H_2$	$H_3$	$H_4$	cf
$[3P\Sigma_a   1s_a 1s_b]$	$5C_{-2,1}^{100}$	$10C_{-1,1}^{100}$	$10C_{01}^{100}$	$6C_{11}^{100}$	$2C_{21}^{100}$	-2/5
$[3P\Sigma_a   1s_a 2s_b]$	$5C_{-2,2}^{100}$	$10C_{-1,2}^{100}$	$10C_{02}^{100}$	$6C_{12}^{100}$	$2C_{22}^{100}$	$2/5\sqrt{3}$
$[3P\Sigma_a   2s_a 1s_b]$	$5C_{-1,1}^{100}$	$10C_{01}^{100}$	$10C_{11}^{100}$	$6C_{21}^{100}$	$2C_{31}^{100}$	$-2/5\sqrt{3}$
$[3P\Sigma_a   2s_a 2s_b]$	$5C_{-1,2}^{100}$	$10C_{02}^{100}$	$10C_{12}^{100}$	$6C_{22}^{100}$	$2C_{32}^{100}$	2/15
$[3P\Sigma_a   1s_a 2p\sigma_b]$	$5C_{-2,1}^{110}$	$10C_{-1,1}^{110}$	$10C_{01}^{110}$	$6C_{11}^{110}$	$2C_{21}^{110}$	2/5
$[3P\Sigma_a   2p\sigma_a 1s_b]$	$5C_{-2,1}^{200}$	$10C_{-1,1}^{200}$	$10C_{01}^{200}$	$6C_{11}^{200}$	$2C_{21}^{200}$	-2/5
$[3P\Sigma_a   2s_a 2p\sigma_b]$	$5C_{-1,1}^{110}$	$10C_{01}^{110}$	$10C_{11}^{110}$	$6C_{21}^{110}$	$2C_{31}^{110}$	$2/5\sqrt{3}$
$[3P\Sigma_a   2p\sigma_a 2s_b]$	$5C_{-2,2}^{200}$	$10C_{-1,2}^{200}$	$10C_{02}^{200}$	$6C_{12}^{200}$	$2C_{22}^{200}$	$2/5\sqrt{3}$
$[3P\Sigma_a   2p\sigma_a 2p\sigma_b]$	$5C_{-2,1}^{210}$	$10C_{-1,1}^{210}$	$10C_{01}^{210}$	$6C_{11}^{210}$	$2C_{21}^{210}$	2/5
$[3P\Sigma_a   2p\pi_a 2p\pi_b \Sigma]$	$5C_{-2,1}^{101}$	$10C_{-1,1}^{101}$	$10C_{01}^{101}$	$6C_{11}^{101}$	$2C_{21}^{101}$	1/5

L = 1 , M = 1 : Dipole Integrals of  $\Pi$ -character

$[\Omega_a   \Omega_{ab}]$	$H_0$	$H_1$	$H_2$	$H_3$	$H_4$	cf
$[2P\Pi_a   1s_a 2p\pi_b]$	$C_{-2,1}^{001}$	$2C_{-1,1}^{001}$	$2C_{01}^{001}$	$C_{11}^{001}$		1
$[2P\Pi_a   2p\pi_a 1s_b]$	$C_{-2,1}^{001}$	$2C_{-1,1}^{001}$	$2C_{01}^{001}$	$C_{11}^{001}$		1
$[2P\Pi_a   2s_a 2p\pi_b]$	$C_{-1,1}^{001}$	$2C_{01}^{001}$	$2C_{11}^{001}$	$C_{21}^{001}$		$1/\sqrt{3}$
$[2P\Pi_a   2p\pi_a 2s_b]$	$C_{-2,2}^{001}$	$2C_{-1,2}^{001}$	$2C_{02}^{001}$	$C_{12}^{001}$		$-1/\sqrt{3}$
$[2P\Pi_a   2p\sigma_a 2p\pi_b]$	$C_{-2,1}^{101}$	$2C_{-1,1}^{101}$	$2C_{01}^{101}$	$C_{11}^{101}$		1
$[2P\Pi_a   2p\pi_a 2p\sigma_b]$	$C_{-2,1}^{011}$	$2C_{-1,1}^{011}$	$2C_{01}^{011}$	$C_{11}^{011}$		-1
$[3P\Pi_a   1s_a 2p\pi_b]$	$5C_{-2,1}^{001}$	$10C_{-1,1}^{001}$	$10C_{01}^{001}$	$6C_{11}^{001}$	$2C_{21}^{001}$	1/5
$[3P\Pi_a   2p\pi_a 1s_b]$	$5C_{-2,1}^{001}$	$10C_{-1,1}^{001}$	$10C_{01}^{001}$	$6C_{11}^{001}$	$2C_{21}^{001}$	1/5
$[3P\Pi_a   2s_a 2p\pi_b]$	$5C_{-1,1}^{001}$	$10C_{01}^{001}$	$10C_{11}^{001}$	$6C_{21}^{001}$	$2C_{31}^{001}$	$1/5\sqrt{3}$
$[3P\Pi_a   2p\pi_a 2s_b]$	$5C_{-2,2}^{001}$	$10C_{-1,2}^{001}$	$10C_{02}^{001}$	$6C_{12}^{001}$	$2C_{22}^{001}$	$-1/5\sqrt{3}$
$[3P\Pi_a   2p\sigma_a 2p\pi_b]$	$5C_{-2,1}^{101}$	$10C_{-1,1}^{101}$	$10C_{01}^{101}$	$6C_{11}^{101}$	$2C_{21}^{101}$	1/5
$[3P\Pi_a   2p\pi_a 2p\sigma_b]$	$5C_{-2,1}^{011}$	$10C_{-1,1}^{011}$	$10C_{01}^{011}$	$6C_{11}^{011}$	$2C_{21}^{011}$	-1/5

RUEDENBERG, ROOTHAAN, AND JAUNZEMIS

TABLE VII

L = 2 , M = 0 : Quadrupole

$[\Omega_a   \Omega_{ab}]$	$H_0$	$H_1$	$H_2$
$[3D\Sigma_a   1s_a 1s_b]$	$\rho_b^{-1} [9\rho_a C_{-3,1}^{001}$ $-18C_{-2,1}^{100}]$	$\rho_b^{-1} [-18\rho_b C_{-3,1}^{001}$ $+18\rho_a C_{-2,1}^{001}$ $-36C_{-1,1}^{100}]$	$\rho_b^{-1} [-36\rho_b C_{-2,1}^{001}$ $+18\rho_a C_{-1,1}^{001}$ $-36C_{01}^{100}]$
$[3D\Sigma_a   1s_a 2s_b]$	$\rho_b^{-1} [9\rho_a C_{-3,2}^{001}$ $-18C_{-2,2}^{100}]$	$\rho_b^{-1} [-18\rho_b C_{-3,2}^{001}$ $+18\rho_a C_{-2,2}^{001}$ $-36C_{-1,2}^{100}]$	$\rho_b^{-1} [-36\rho_b C_{-2,2}^{001}$ $+18\rho_a C_{-1,2}^{001}$ $-36C_{02}^{100}]$
$[3D\Sigma_a   1s_a 2p\sigma_b]$	$\rho_b^{-1} [9\rho_a C_{-3,1}^{011}$ $-18C_{-2,1}^{110}$ $-9C_{-2,1}^{001}]$	$\rho_b^{-1} [-18\rho_b C_{-3,1}^{011}$ $+18\rho_a C_{-2,1}^{011}$ $-36C_{-1,1}^{110}$ $-18C_{-1,1}^{001}]$	$\rho_b^{-1} [-36\rho_b C_{-2,1}^{011}$ $+18\rho_a C_{-1,1}^{011}$ $-36C_{01}^{110}$ $-18C_{01}^{001}]$
$[3D\Sigma_a   2s_a 2s_b]$	$27C_{-3,2}^{200} - 9C_{-1,2}^{000}$	$54C_{-2,2}^{200} - 18C_{02}^{000}$	$54C_{-1,2}^{200} - 18C_{12}^{000}$
$[3D\Sigma_a   2s_a 1s_b]$	$27C_{-3,1}^{200} - 9C_{-1,1}^{000}$	$54C_{-2,1}^{200} - 18C_{01}^{000}$	$54C_{-1,1}^{200} - 18C_{11}^{000}$
$[3D\Sigma_a   2p\sigma_a 2p\sigma_b]$	$27C_{-4,1}^{310} - 9C_{-2,1}^{110}$	$54C_{-3,1}^{310} - 18C_{-1,1}^{110}$	$54C_{-2,1}^{310} - 18C_{01}^{110}$
$[3D\Sigma_a   2p\sigma_a 1s_b]$	$27C_{-4,1}^{300} - 9C_{-2,1}^{100}$	$54C_{-3,1}^{300} - 18C_{-1,1}^{100}$	$54C_{-2,1}^{300} - 18C_{01}^{100}$
$[3D\Sigma_a   2s_a 2p\sigma_b]$	$27C_{-3,1}^{210} - 9C_{-1,1}^{010}$	$54C_{-2,1}^{210} - 18C_{01}^{010}$	$54C_{-1,1}^{210} - 18C_{11}^{010}$
$[3D\Sigma_a   2p\sigma_b 2s_a]$	$27C_{-4,2}^{300} - 9C_{-2,2}^{100}$	$54C_{-3,2}^{300} - 18C_{-1,2}^{100}$	$54C_{-2,2}^{300} - 18C_{02}^{100}$
$[3D\Sigma_a   2p\pi_a 2p\pi_b \Sigma]$	$27C_{-4,1}^{201} - 9C_{-2,1}^{001}$	$54C_{-3,1}^{201} - 18C_{-1,1}^{001}$	$54C_{-2,1}^{201} - 18C_{01}^{001}$

TWO-CENTER INTEGRALS. III

(continued)

Integrals of  $\Sigma$ -character

$H_3$	$H_4$	$H_5$	cf
$-36c_{-1,1}^{001}$	$-18c_{01}^{200}$	$-6c_{11}^{200}$	
$-24c_{11}^{000}$	$+6c_{21}^{000}$	$+2c_{31}^{000}$	1/9
$-36c_{-1,2}^{001}$	$-18c_{02}^{200}$	$-6c_{12}^{200}$	
$-24c_{12}^{000}$	$+6c_{22}^{000}$	$+2c_{32}^{000}$	-1/9 $\sqrt{3}$
$-36c_{-1,1}^{011}$	$-18c_{01}^{210}$	$-6c_{11}^{210}$	
$-24c_{11}^{010}$	$+6c_{21}^{010}$	$+2c_{31}^{010}$	-1/9
$36c_{02}^{200}-12c_{22}^{000}$	$18c_{12}^{200}-6c_{32}^{000}$	$6c_{22}^{200}-2c_{42}^{000}$	1/27
$36c_{01}^{200}-12c_{21}^{000}$	$18c_{11}^{200}-6c_{31}^{000}$	$6c_{21}^{200}-2c_{41}^{000}$	-1/9 $\sqrt{3}$
$36c_{-1,1}^{310}-12c_{11}^{110}$	$18c_{01}^{310}-6c_{21}^{110}$	$6c_{11}^{310}-2c_{31}^{110}$	1/9
$36c_{-1,1}^{300}-12c_{11}^{100}$	$18c_{01}^{300}-6c_{21}^{100}$	$6c_{11}^{300}-2c_{31}^{100}$	-1/9
$36c_{01}^{210}-12c_{21}^{010}$	$18c_{11}^{210}-6c_{31}^{010}$	$6c_{21}^{210}-2c_{41}^{010}$	1/9 $\sqrt{3}$
$36c_{-1,2}^{300}-12c_{12}^{100}$	$18c_{02}^{300}-6c_{22}^{100}$	$6c_{12}^{300}-2c_{32}^{100}$	1/9 $\sqrt{3}$
$36c_{-1,1}^{201}-12c_{11}^{001}$	$18c_{01}^{201}-6c_{21}^{001}$	$6c_{11}^{201}-2c_{31}^{001}$	1/18

TABLE VII (continued)  
 $L = 2, M = 1$  : Quadrupole Integrals of  $\Pi$ -character

$[\Omega_a   \Omega_{ab}]$	$H_0$	$H_1$	$H_2$	$H_3$	$H_4$	$H_5$	cf
$[3D\Pi_a   1s_a 2p\pi_b]$	$9C_{-4,1}^{101}$	$18C_{-3,1}^{101}$	$18C_{-2,1}^{101}$	$12C_{-1,1}^{101}$	$6C_{01}^{101}$	$2C_{11}^{101}$	$1/3\sqrt{5}$
$[3D\Pi_a   2p\pi_a 1s_b]$	$9C_{-4,1}^{101}$	$18C_{-3,1}^{101}$	$18C_{-2,1}^{101}$	$12C_{-1,1}^{101}$	$6C_{01}^{101}$	$2C_{11}^{101}$	$1/3\sqrt{5}$
$[3D\Pi_a   2s_a 2p\pi_b]$	$9C_{-3,1}^{101}$	$18C_{-2,1}^{101}$	$18C_{-1,1}^{101}$	$12C_{01}^{101}$	$6C_{11}^{101}$	$2C_{21}^{101}$	$1/9$
$[3D\Pi_a   2p\pi_a 2s_b]$	$9C_{-4,2}^{101}$	$18C_{-3,2}^{101}$	$18C_{-2,2}^{101}$	$12C_{-1,2}^{101}$	$6C_{02}^{101}$	$2C_{12}^{101}$	$-1/9$
$[3D\Pi_a   2p\sigma_a 2p\pi_b]$	$9C_{-4,1}^{201}$	$18C_{-3,1}^{201}$	$18C_{-2,1}^{201}$	$12C_{-1,1}^{201}$	$6C_{01}^{201}$	$2C_{11}^{201}$	$1/3\sqrt{5}$
$[3D\Pi_a   2p\pi_a 2p\sigma_b]$	$9C_{-4,1}^{111}$	$18C_{-3,1}^{111}$	$18C_{-2,1}^{111}$	$12C_{-1,1}^{111}$	$6C_{01}^{111}$	$2C_{11}^{111}$	$-1/3\sqrt{5}$

$L = 2, M = 2$  : Quadrupole Integral of  $\Delta$ -character

$[\Omega_a   \Omega_{ab}]$	$H_0$	$H_1$	$H_2$	$H_3$	$H_4$	$H_5$	cf
$[3D\Delta_a   2p\pi_a 2\pi_b \Delta]$	$9C_{-4,1}^{002}$	$18C_{-3,1}^{002}$	$18C_{-2,1}^{002}$	$12C_{-1,1}^{002}$	$6C_{01}^{002}$	$2C_{11}^{002}$	$-1/12\sqrt{5}$

TWO-CENTER INTEGRALS. III

$$C_{\lambda\beta}^{\gamma\delta\epsilon} = C_{\lambda\beta}^{\gamma-2,\delta,\epsilon+1} + C_{\lambda+2,\beta}^{\gamma-2,\delta\epsilon} - [(2\mu)^{-\lambda-2}/(-\lambda-2)!]C_{0\beta}^{\gamma-2,\delta\epsilon} - [(2\mu)^{-\lambda-1}/(-\lambda-1)!]C_{1\beta}^{\gamma-2,\delta\epsilon}, \quad (1.51)$$

which holds for  $\lambda < -2$ , and

$$\left. \begin{aligned} C_{-2,\beta}^{\gamma\delta\epsilon} &= C_{-2,\beta}^{\gamma-2,\delta,\epsilon+1} + C_{0\beta}^{\gamma-2,\delta\epsilon} - C_{0\beta}^{\gamma-2,\delta\epsilon} - 2\mu C_{1\beta}^{\gamma-2,\delta\epsilon}, \\ C_{-1,\beta}^{\gamma\delta\epsilon} &= C_{-1,\beta}^{\gamma-2,\delta,\epsilon+1} + C_{1\beta}^{\gamma-2,\delta\epsilon} - C_{1\beta}^{\gamma-2,\delta\epsilon}. \end{aligned} \right\} (1.51')$$

II

The functions  $v_\lambda(x)$ , defined by Eq. (1.41), have the property

$$(d/dx)v_\lambda(x) = \lambda v_{\lambda-1}(x), \quad (1.52)$$

whence

$$(\lambda+1)\bar{\rho}_a^{-\lambda} v_\lambda[\bar{\rho}_a(\xi+\eta)] = \left\{ \frac{\partial/\partial\xi}{\partial/\partial\eta} \right\} \bar{\rho}_a^{-\lambda-1} v_{\lambda+1}[\bar{\rho}_a(\xi+\eta)], \quad (1.53)$$

which suggests partial integration of this factor in (1.43). We consider only the case  $\epsilon > 0$ ; then the integrated parts vanish for the boundary values, namely for  $\eta = \pm 1$  in the case of a partial integration with respect to  $\eta$ , or for  $\xi = 1$ , and of course also for  $\xi = \infty$ , in the case of a partial integration with respect to  $\xi$ . Hence we obtain

$$-(\lambda+1)C_{\lambda\beta}^{\gamma\delta\epsilon} = (-1)^{\beta+\delta+\epsilon} \bar{\rho}_a^{-\lambda-1} (\frac{1}{2}\rho_b)^{\lambda+\beta+\gamma+\delta+2\epsilon+1} \int_1^\infty d\xi \int_{-1}^1 d\eta v_{\lambda+1}[\bar{\rho}_a(\xi+\eta)] \left\{ \frac{\partial/\partial\xi}{\partial/\partial\eta} \right\} e^{-\rho\xi-\tau\rho\eta} (\xi-\eta)^\beta (1+\xi\eta)^\gamma (1-\xi\eta)^\delta (\xi^2-1)^\epsilon (1-\eta^2)^\epsilon;$$

adding these two equations, and carrying out the indicated differentiations, we obtain

$$\begin{aligned} -(\lambda+1)\rho_b C_{\lambda\beta}^{\gamma\delta\epsilon} &= -\rho_a C_{\lambda+1;\beta}^{\gamma\delta\epsilon} + 2\epsilon C_{\lambda+2,\beta}^{\gamma,\delta+1,\epsilon-1} + \gamma C_{\lambda+2,\beta}^{\gamma-1,\delta\epsilon} + \delta C_{\lambda+2,\beta}^{\gamma,\delta-1,\epsilon} \\ &- [(2\mu)^{-\lambda-2}/(-\lambda-2)!][2\epsilon C_{0\beta}^{\gamma,\delta+1,\epsilon-1} + \gamma C_{0\beta}^{\gamma-1,\delta\epsilon} + \delta C_{0\beta}^{\gamma,\delta-1,\epsilon}]^*, \end{aligned} \quad (1.54)$$

which holds for  $\lambda < -2$ , and

$$\begin{aligned} \rho_b C_{-2,\beta}^{\gamma\delta\epsilon} &= -\rho_a C_{-1,\beta}^{\gamma\delta\epsilon} + 2\epsilon C_{0\beta}^{\gamma,\delta+1,\epsilon-1} + \gamma C_{0\beta}^{\gamma-1,\delta\epsilon} + \delta C_{0\beta}^{\gamma,\delta-1,\epsilon} \\ &- [2\epsilon C_{0\beta}^{\gamma,\delta+1,\epsilon-1} + \gamma C_{0\beta}^{\gamma-1,\delta\epsilon} + \delta C_{0\beta}^{\gamma,\delta-1,\epsilon}]^*. \end{aligned} \quad (1.54')$$

RUEDENBERG, ROTHAN, AND JAUNZEMIS

We turn now to the actual problem of expressing  $3C_{-4,\beta}^{2\delta 0} - C_{-2,\beta}^{0\delta 0}$  in terms of C-functions. We observe that for both C-functions

$$\lambda + \gamma + 2\epsilon + 1 = -1 .$$

This we compare with the condition (1.39). Apparently, if we succeed in converting  $3C_{-4,\beta}^{2\delta 0} - C_{-2,\beta}^{0\delta 0}$  into C-functions in which  $\lambda, \gamma, \text{ or } \epsilon$  is raised by at least one, then we can expand this new expression in terms of C-functions using Eq. (1.45).

First, we apply (1.51) to  $C_{-4,\beta}^{2\delta 0}$  so that

$$3C_{-4,\beta}^{2\delta 0} - C_{-2,\beta}^{0\delta 0} = 3C_{-4,\beta}^{0\delta 1} + 2C_{-2,\beta}^{0\delta 0} - 6\mu^2 C_{0\beta}^{*0\delta 0} - 4\mu^3 C_{1\beta}^{*0\delta 0} .$$

Next, we apply (1.54) to  $C_{-4,\beta}^{0\delta 1}$ , obtaining

$$\begin{aligned} 3C_{-4,\beta}^{2\delta 0} - C_{-2,\beta}^{0\delta 0} &= -\rho_a \rho_b^{-1} C_{-3,\beta}^{0\delta 1} + 2\rho_b^{-1} (\rho_b C_{-2,\beta}^{0\delta 0} + C_{-2,\beta}^{0,\delta+1,0}) + \delta \rho_b^{-1} C_{-2,\beta}^{0,\delta-1,1} \\ &\quad - 2\mu^2 \rho_b^{-1} [3\rho_b C_{0\beta}^{0\delta 0} + 2C_{0\beta}^{0,\delta+1,0} + \delta C_{0\beta}^{0,\delta-1,1}] - 4\mu^3 C_{1\beta}^{*0\delta 0} . \end{aligned}$$

Finally, making use of Eq. (1.48,49), we obtain

$$\begin{aligned} 3C_{-4,\beta}^{2\delta 0} - C_{-2,\beta}^{0\delta 0} &= -\rho_a \rho_b^{-1} C_{-3,\beta}^{0\delta 1} + 2\rho_b^{-1} C_{-2,\beta}^{1\delta 0} + \delta \rho_b^{-1} C_{-2,\beta}^{0,\delta-1,1} \\ &\quad - 2\mu^2 [C_{0\beta}^{0\delta 0} + 2\rho_b^{-1} C_{0\beta}^{1\delta 0} + \delta \rho_b^{-1} C_{0\beta}^{0,\delta-1,1}] - 4\mu^3 C_{1\beta}^{*0\delta 0} . \end{aligned} \quad (1.55)$$

We note that all the C-functions occurring at the right-hand side of Eq. (1.55) satisfy the condition (1.39). We can therefore now make use of the expansion (1.45). When this is done, then  $\rho_a \rho_b^{-1}$  appears as a multiplier of C-functions and C\*-functions. Keeping in mind the desired form (1.37), we substitute for  $\rho_a$ , when it occurs in connection with the C\*-functions

$$\rho_a = \rho_a^* - 2\mu \rho_b , \quad (1.56)$$

a relation which is readily obtained from Eqs. (1.31,33). We obtain then for (1.55)

TWO-CENTER INTEGRALS. III

$$\begin{aligned}
 & 3C_{-4,\beta}^{2\delta 0} - C_{-2,\beta}^{0\delta 0} \\
 & = -\rho_a \rho_b^{-1} C_{-3,\beta}^{0\delta 1} + 2\rho_b^{-1} C_{-2,\beta}^{1\delta 0} + \delta \rho_b^{-1} C_{-2,\beta}^{0,\delta-1,1} \\
 & - [-\rho_a \rho_b^{-1} C_{-3,\beta}^{0\delta 1} + 2\rho_b^{-1} C_{-2,\beta}^{1\delta 0} + \delta \rho_b^{-1} C_{-2,\beta}^{0,\delta-1,1}] * \\
 & - 2\mu [C_{-3,\beta}^{0\delta 1} - \rho_a \rho_b^{-1} C_{-2,\beta}^{0\delta 1} + 2\rho_b^{-1} C_{-1,\beta}^{1\delta 0} + \delta \rho_b^{-1} C_{-1,\beta}^{0,\delta-1,1}] * \\
 & - 2\mu^2 [2C_{-2,\beta}^{0\delta 1} - \rho_a \rho_b^{-1} C_{-1,\beta}^{0\delta 1} + 2\rho_b^{-1} C_{0\beta}^{1\delta 0} + \delta \rho_b^{-1} C_{0\beta}^{0,\delta-1,1} + C_{0\beta}^{0\delta 0}] * \\
 & - 4\mu^3 [C_{-1,\beta}^{0\delta 1} + C_{1\beta}^{0\delta 0}] * . \tag{1.57}
 \end{aligned}$$

If Eq. (1.50) is now applied to the term with  $\mu^3$ , then Eq. (1.57) becomes identical with (1.47).

e. Discussion of the general result (1.37)

The general basic hybrid integral (1.9) depends upon the four parameters  $R, \zeta_a, \zeta_b, \zeta_a$ . But Eq. (1.37) shows that they can all be very simply formulated in terms of the two-parameter functions  $H_\alpha$ . Each integral has of course its individual set of  $N+L+1$  functions  $H_\alpha$  so that there exist altogether 336 H-functions for the 79 basic hybrid integrals. Table VII shows however that each of these 336 H-functions is a very simple linear combination of a few out of only 122 C-functions. This situation suggests a tabulation of the auxiliary functions  $C_{\alpha\beta}^{\gamma\delta\epsilon}$ , in particular since these functions are also very useful for other types of integrals, as will be shown in Section 2.

The C-functions will be discussed in Sections 3 and 4. Section 3 deals with those for which  $\alpha \geq 0$ , and Section 4 with those for which  $\alpha < 0$ ; it is not surprising that these two types differ quite radically. In these sections general recurrence methods are developed for the computation of any C-function. By their means the explicit formulas are given in Tables XIII, XIV, and XV; they make it possible to compute spot values of the listed hybrid integrals as long as numerical tables of the C-functions are not yet available. The course of calculation followed in finding the explicit formulas is described in Sections 3 and 4.

Special attention should be paid to the limiting case  $R \rightarrow 0$ , i.e. the centers a and b coincide, and the hybrid integrals reduce to one-center integrals. It is

seen from Eqs. (1.6,31) that in this case  $\rho_a \rightarrow 0$ ,  $\rho_b \rightarrow 0$ ,  $\rho_a^* \rightarrow 0$ . Now each two-parameter function  $C_{\alpha\beta}^{\gamma\delta\epsilon}(\rho_a, \rho_b)$ , and therefore also each function  $H_\alpha(\rho_a, \rho_b)$ , is discontinuous for  $\rho_a = \rho_b = 0$ , since the numerical value still depends upon the limiting ratio  $\rho_b/\rho_a$ ; this is more fully discussed at the end of Section 3. However if we consider  $\rho, \tau$  as the arguments instead of  $\rho_a, \rho_b$ , then the C-functions are well-behaved in the entire domain  $0 \leq \rho < \infty$ ,  $-1 \leq \tau \leq 1$ ; this is the reason why for numerical tabulation the parameters  $\rho, \tau$  are more suitable than  $\rho_a, \rho_b$ , although the latter are more useful for the analytical derivations in this paper.

The values of the hybrid integrals for  $R \rightarrow 0$  must of course be in agreement with the formulas given in (I), Eqs. (34b), which were obtained as the limiting case for the coulomb integrals. In making this comparison, the following points should be kept in mind:

(1) The one-center charge distributions  $\text{Lim}_{R \rightarrow 0} \Omega_{ab}$  of the hybrid integrals should be expanded in terms of the basic one-center charge distributions  $\text{Lim}_{R \rightarrow 0} \Omega_b$  of the coulomb integrals. This expansion is done by means of (I), Eqs. (27). The parameter  $\tau$  occurring in those equations has precisely the same meaning which it has in this paper for the hybrid integrals.

(2) The one-center integrals between basic one-center charge distributions are given by (I), Eqs. (34b). Let us denote the parameters  $\zeta$  and  $\tau$  occurring in those equations by  $\bar{\zeta}$  and  $\bar{\tau}$ , as we have also done in Section 2 of this paper. By means of the following equations we can now carry out the transition from the hybrid integral parameters  $\zeta_a, \zeta_b, \tau, \tau^*, \mu$  to the coulomb integral parameters  $\bar{\zeta}, \bar{\tau}, \tau$ :

$$\left. \begin{aligned} \zeta_a &= (1+\tau)(1-\bar{\tau})\bar{\zeta} , \\ \zeta_b &= (1-\tau)(1-\bar{\tau})\bar{\zeta} , \\ 1-\tau^* &= \frac{1}{2}(1-\tau)(1-\bar{\tau}) , \\ (1-\tau^*)\mu &= \frac{1}{2}(1+\bar{\tau}) . \end{aligned} \right\} \quad (1.58)$$

As an example, we shall carry out the indicated comparison for  $\text{Lim}_{R \rightarrow 0} [1S_a | 2p\sigma_a 2p\sigma_b]$ . From (I), Eqs. (27,34b) we find

TWO-CENTER INTEGRALS. III

$$\begin{aligned} \lim_{R \rightarrow 0} [1S_a | 2p\sigma_a 2p\sigma_b] &= (1-\tau^2)^{5/2} \lim_{R \rightarrow 0} \{ [1S_a | 3S_b] + 3[1S_a | 3D\Sigma_b] \} \\ &= (1/32)(1-\tau^2)^{5/2}(1-\bar{\tau}^2)(14-7\bar{\tau}-\bar{\tau}^2+3\bar{\tau}^3-\bar{\tau}^4)\zeta. \end{aligned}$$

On the other hand, using Eqs. (1.37,58) and Tables VII and XV, we find

$$\begin{aligned} \lim_{R \rightarrow 0} [1S_a | 2p\sigma_a 2p\sigma_b] &= 2(1+\tau)^{5/2}(1-\tau)^{-3/2}(1-\bar{\tau}) \lim_{R \rightarrow 0} [C_{01}^{110} - C_{01}^*{}^{110} - C_{11}^*{}^{110}] \zeta \\ &= (1+\tau)^{5/2}(1-\tau)^{-3/2}(1-\bar{\tau}) \left[ \frac{1}{2}(1-\tau)^4 - \frac{1}{2}(1-\tau^*)^4 - \mu(1-\tau^*)^5 \right] \zeta \\ &= (1-\tau^2)^{5/2}(1-\bar{\tau}) \left[ \frac{1}{2} - (1/32)(1-\bar{\tau})^4 - (1/32)(1-\bar{\tau})^4(1+\bar{\tau}) \right] \zeta \\ &= (1/32)(1-\tau^2)^{5/2}(1-\bar{\tau}^2)(14-7\bar{\tau}-\bar{\tau}^2+3\bar{\tau}^3-\bar{\tau}^4)\zeta. \end{aligned}$$

In this fashion, we compared all the hybrid integrals for  $R \rightarrow 0$  with the results of (I), and found agreement throughout.

2. COULOMB INTEGRALS AND ONE-ELECTRON INTEGRALS

a. Coulomb Integrals

In paper (I) it is shown in detail [see (I), Eq. (30)] how the general coulomb integral

$$[\chi'_a \chi''_a | \chi'_b \chi''_b] = \int dV_1 \int dV_2 \chi'_a(1) \chi''_a(1) (1/r_{12}) \chi'_b(2) \chi''_b(2) \quad (2.1)$$

can be expressed in terms of the basic coulomb integrals

$$[\Omega_a | \Omega_b] = \int dV_1 \int dV_2 \Omega_a(1) (1/r_{12}) \Omega_b(2) , \quad (2.2)$$

where  $\Omega_a$  and  $\Omega_b$  denote basic charge distributions on a and b of the type (1.3), namely<sup>7</sup>

$$\left. \begin{aligned} \Omega_a = [N_a L_a M] &= [(2L_a+1)/4\pi]^{\frac{1}{2}} [2^{L_a} (2\zeta_a)^{N_a+2} / (N_a+L_a+1)!] \\ &\quad \times r_a^{N_a-1} e^{-2\zeta_a r_a} S_{L_a M}(\theta_a, \varphi) , \\ \Omega_b = [N_b L_b M] &= [(2L_b+1)/4\pi]^{\frac{1}{2}} [2^{L_b} (2\zeta_b)^{N_b+2} / (N_b+L_b+1)!] \\ &\quad \times r_b^{N_b-1} e^{-2\zeta_b r_b} S_{L_b M}(\theta_b, \varphi) , \end{aligned} \right\} \quad (2.3)$$

with

$$\left. \begin{aligned} \zeta_a &= \frac{1}{2}(\zeta'_a + \zeta''_a) , \\ \zeta_b &= \frac{1}{2}(\zeta'_b + \zeta''_b) . \end{aligned} \right\} \quad (2.4)$$

Since the basic coulomb integral (2.2) differs from the basic hybrid integral (1.9) only in the appearance of the charge distribution  $\Omega_b$  in lieu of the charge distribution  $\Omega_{ab}$ , it follows immediately that the integral (2.2) can be written in the form

$$[\Omega_a | \Omega_b] = \int_1^\infty d\xi \int_{-1}^1 d\eta \int_0^{2\pi} d\varphi [(\frac{1}{2}R(\xi+\eta)) U_{\Omega_a}(2)] [(\frac{1}{2}R)^2(\xi-\eta) \Omega_b(2)] , \quad (2.5)$$

which is analogous to Eq. (1.25). In Eq. (2.5) the potential is precisely the same as in Eq. (1.25), namely the potential for which Eq. (1.23) gives the general expression and Table VI furnishes the particular expressions in specific cases.

In order to be able to perform the integration (2.5) we must express the distributions  $\Omega_b$  in elliptic coordinates. The resulting expressions are given in Table VIII

TWO-CENTER INTEGRALS. III

for all those basic charge distributions  $\Omega_b$  which are needed.

TABLE VIII  
THE BASIC ONE-CENTER CHARGE DISTRIBUTIONS  $\Omega_b$

$\Omega_b$	$(\frac{1}{2}R)^2(\xi-\eta)\Omega_b$
6 $\Sigma$ -type Distributions:	
$1S_b$	$(\xi_b/4\pi)\bar{\rho}_b^2 e^{-\bar{\rho}_b(\xi-\eta)} (\xi-\eta)$
$2S_b$	$(\xi_b/12\pi)\bar{\rho}_b^3 e^{-\bar{\rho}_b(\xi-\eta)} (\xi-\eta)^2$
$3S_b$	$(\xi_b/48\pi)\bar{\rho}_b^4 e^{-\bar{\rho}_b(\xi-\eta)} (\xi-\eta)^3$
$2P\Sigma_b$	$(\xi_b/8\pi)\bar{\rho}_b^3 e^{-\bar{\rho}_b(\xi-\eta)} (\xi-\eta)(1-\xi\eta)$
$3P\Sigma_b$	$(\xi_b/40\pi)\bar{\rho}_b^4 e^{-\bar{\rho}_b(\xi-\eta)} (\xi-\eta)^2(1-\xi\eta)$
$3D\Sigma_b$	$(\xi_b/144\pi)\bar{\rho}_b^4 e^{-\bar{\rho}_b(\xi-\eta)} (\xi-\eta)[3(1-\xi\eta)^2 - (\xi-\eta)^2]$
3 $\Pi$ -type Distributions:	
$2\Pi_b$	$(\xi_b/8\pi)\bar{\rho}_b^3 e^{-\bar{\rho}_b(\xi-\eta)} (\xi-\eta)[(\xi^2-1)(1-\eta^2)]^{\frac{1}{2}} \cos\varphi$
$3\Pi_b$	$(\xi_b/40\pi)\bar{\rho}_b^4 e^{-\bar{\rho}_b(\xi-\eta)} (\xi-\eta)^2[(\xi^2-1)(1-\eta^2)]^{\frac{1}{2}} \cos\varphi$
$3D\Pi_b$	$(\xi_b/24\sqrt{3}\pi)\bar{\rho}_b^4 e^{-\bar{\rho}_b(\xi-\eta)} (\xi-\eta)(1-\xi\eta)[(\xi^2-1)(1-\eta^2)]^{\frac{1}{2}} \cos\varphi$
3 $\bar{\Pi}$ -type Distributions:	
Replace $\Pi$ by $\bar{\Pi}$ in the above listed charge distributions, and $\cos\varphi$ by $\sin\varphi$ .	
1 $\Delta$ -type Distribution:	
$3D\Delta_b$	$(\xi_b/48\sqrt{3}\pi)\bar{\rho}_b^4 e^{-\bar{\rho}_b(\xi-\eta)} (\xi-\eta)(\xi^2-1)(1-\eta^2) \cos 2\varphi$
1 $\bar{\Delta}$ -type Distribution:	
Replace $\Delta$ by $\bar{\Delta}$ in the above listed charge distribution, and $\cos 2\varphi$ by $\sin 2\varphi$ .	

From this table, which is analogous to Table IV for the distributions  $\Omega_{ab}$ , it is seen that the  $\Omega_b$ 's satisfy the general formula

$$(\frac{1}{2}R)^2(\xi-\eta)\Omega_b = \zeta_b \bar{\rho}_b^{N_b+1} e^{-\bar{\rho}_b(\xi-\eta)} p''(\xi-\eta, 1-\xi\eta) [(\xi^2-1)(1-\eta^2)]^{\frac{1}{2}M} \begin{cases} \cos M\varphi, \\ \sin M\varphi, \end{cases} \quad (2.6)$$

where  $p''(x,y)$  is a homogeneous polynomial in  $x,y$  of the degree  $N_b-M$ , and  $\bar{\rho}_b$  is defined by

$$\bar{\rho}_b = R\zeta_b = \frac{1}{2}(\zeta'_b + \zeta''_b)R. \quad (2.7)$$

It is not difficult to verify that the relation (2.6) is generally valid.

In order that the integral  $[\Omega_a | \Omega_b]$  does not vanish, both charge distributions,  $\Omega_a$  and  $\Omega_b$ , must belong to the same species and subspecies of  $C_{\infty v}$  [see (I)]. In such a case we obtain, by substituting (1.23) and (2.6) into (2.5) and carrying out the integration over  $\varphi$ , the general form

$$[\Omega_a | \Omega_b] = \zeta_b \bar{\rho}_a^{-L_a} \bar{\rho}_b^{N_b+1} \int_1^\infty d\xi \int_{-1}^1 d\eta (\xi+\eta)^{-2L_a} [1 - e^{-\bar{\rho}_a(\xi+\eta)} \sum_{k=0}^{N_a+L_a} u_k \bar{\rho}_a^k (\xi+\eta)^k] \times e^{-\bar{\rho}_b(\xi-\eta)} p'''(\xi+\eta, \xi-\eta, 1+\xi\eta, 1-\xi\eta) [(\xi^2-1)(1-\eta^2)]^M, \quad (2.8)$$

where  $p'''(u,v,x,y)$  is a polynomial in  $u,v,x,y$  of the degree  $N_b+L_a-2M$ . If this polynomial is expressed in terms of the four arguments  $\xi+\eta, \xi-\eta, 1+\xi\eta, 1-\xi\eta$ , then the integral (2.5) can be written as a linear combination with numerical coefficients, of expressions of the type

$$I_{\lambda\beta}^{\gamma\delta\epsilon} = \zeta_b \bar{\rho}_a^{-L_a} (2\bar{\rho}_b)^{N_b+1} \int_1^\infty d\xi \int_{-1}^1 d\eta [1 - e^{-\bar{\rho}_a(\xi+\eta)} \sum_{k=0}^{N_a+L_a} u_k \bar{\rho}_a^k (\xi+\eta)^k] \times e^{-\bar{\rho}_b(\xi-\eta)} (\xi+\eta)^\lambda (\xi-\eta)^\beta (1+\xi\eta)^\gamma (1-\xi\eta)^\delta (\xi^2-1)^\epsilon (1-\eta^2)^\epsilon, \quad (2.9)$$

where

$$\left. \begin{aligned} \epsilon &= M, \\ \lambda + \beta + \gamma + \delta &= N_b - L_a - 2M, \end{aligned} \right\} \quad (2.10)$$

so that

$$\lambda + \beta + \gamma + \delta + 2\epsilon = N_b - L_a. \quad (2.10')$$

Obviously  $\beta, \gamma, \delta, \epsilon$  are integers  $\geq 0$ , whereas  $\lambda$  is restricted to the range

TWO-CENTER INTEGRALS. III

$$-2L_a \leq \lambda \leq N_b - L_a - 2M, \quad (2.11)$$

so that in general  $\lambda \geq 0$ .

The integrals  $\bar{I}_{\lambda\beta}^{\gamma\delta\epsilon}$ , defined by (2.9), are analogous to the integrals  $I_{\lambda\beta}^{\gamma\delta\epsilon}$ , defined by (1.28). As a matter of fact,  $\bar{I}_{\lambda\beta}^{\gamma\delta\epsilon}$  is obtained from  $I_{\lambda\beta}^{\gamma\delta\epsilon}$  by replacing the factor  $\zeta_a^{n_a+\frac{1}{2}} \zeta_b^{-n_a+\frac{1}{2}}$  by  $\bar{\zeta}_b$  and furthermore changing consistently all other parameters and indices in the following manner:

$$\left. \begin{aligned} \bar{\rho}_a \rightarrow \bar{\rho}_a, \rho_a \rightarrow 0, \rho_b \rightarrow 2\bar{\rho}_b; \\ n_a + n_b \rightarrow N_b + 1, N \rightarrow N_a, L \rightarrow L_a. \end{aligned} \right\} \quad (2.12)$$

Again, we shall deal first with the integrals  $\bar{I}_{\lambda\beta}^{\gamma\delta\epsilon}$  which can be evaluated by a term by term integration. In section 1 we introduced  $\rho_a^*, \rho_a, \rho_b$  as parameters for  $I_{\lambda\beta}^{\gamma\delta\epsilon}$  instead of  $\bar{\rho}_a, \rho_a, \rho_b$ . Keeping in mind Eq. (1.31) and the parameter changes (2.12), we see that by the same token the integrals  $\bar{I}_{\lambda\beta}^{\gamma\delta\epsilon}$  should be considered as functions of  $2\bar{\rho}_a, 0, 2\bar{\rho}_b$ . Furthermore, we define the secondary parameters  $\bar{\rho}$  and  $\bar{\tau}$  by

$$\left. \begin{aligned} \bar{\rho} &= \frac{1}{2}(\bar{\rho}_a + \bar{\rho}_b) = \frac{1}{4}(\zeta'_a + \zeta''_a + \zeta'_b + \zeta''_b)R, \\ \bar{\tau} &= (\bar{\rho}_a - \bar{\rho}_b)/(\bar{\rho}_a + \bar{\rho}_b) = (\zeta'_a + \zeta''_a - \zeta'_b - \zeta''_b)/(\zeta'_a + \zeta''_a + \zeta'_b + \zeta''_b), \end{aligned} \right\} \quad (2.13)$$

so that

$$\bar{\rho}_a = (1 + \bar{\tau})\bar{\rho}, \quad \bar{\rho}_b = (1 - \bar{\tau})\bar{\rho}. \quad (2.13')$$

We define further a parameter  $\bar{\mu}$ , analogous to  $\mu$  of (1.33), by

$$\bar{\mu} = \bar{\rho}_a/2\bar{\rho}_b = \bar{\zeta}_a/2\bar{\zeta}_b = (\zeta'_a + \zeta''_a)/2(\zeta'_b + \zeta''_b). \quad (2.14)$$

From Eqs. (1.31, 32, 33) and (2.13, 14) it is clear that, if we extend the parameter change (2.12) to the parameters  $\rho_a^*, \rho, \tau, \rho^*, \tau^*, \mu$  of section 1, we obtain

$$\left. \begin{aligned} \rho_a^* \rightarrow 2\bar{\rho}_a, \rho \rightarrow \bar{\rho}_b, \rho^* \rightarrow 2\bar{\rho}; \\ \tau \rightarrow -1, \tau^* \rightarrow \bar{\tau}, \mu \rightarrow \bar{\mu}. \end{aligned} \right\} \quad (2.15)$$

In view of Eqs. (2.13, 14), we find for the integral (2.9), in analogy to (1.34)

$$\begin{aligned} \bar{I}_{\lambda\beta}^{\gamma\delta\epsilon} &= \bar{\xi}_b \bar{\mu}^{-L_a} (2\bar{\rho}_b)^{\lambda+\beta+\gamma+\delta+2\epsilon+1} \\ &\times \int_1^\infty d\xi \int_{-1}^1 d\eta [e^{-\bar{\rho}_b(\xi-\eta)} - e^{-2\bar{\rho}_b\xi-2\bar{\rho}_b\eta} \sum_{k=0}^{N_a+L_a} u_k \bar{\mu}^k (2\bar{\rho}_b)^k (\xi+\eta)^k] \\ &\times (\xi+\eta)^\lambda (\xi-\eta)^\beta (1+\xi\eta)^\gamma (1-\xi\eta)^\delta (\xi^2-1)^\epsilon (1-\eta^2)^\epsilon. \end{aligned} \quad (2.16)$$

If we make use now of the two-parameter C-functions (1.35), we may write for (2.16)

$$\begin{aligned} \bar{I}_{\lambda\beta}^{\gamma\delta\epsilon} &= (-1)^{\beta+\delta+\epsilon} 2^{\lambda+\beta+\gamma+\delta+2\epsilon+1} \bar{\xi}_b \bar{\mu}^{-L_a} \\ &\times [C_{\lambda\beta}^{\gamma\delta\epsilon}(0, 2\bar{\rho}_b) - \sum_{\alpha=0}^{N_a+L_a} u_\alpha (2\bar{\mu})^\alpha C_{\lambda+\alpha, \beta}^{\gamma\delta\epsilon}(2\bar{\rho}_a, 2\bar{\rho}_b)], \end{aligned} \quad (2.17)$$

and consequently the basic coulomb integrals for which the term by term integration is possible, have the general form

$$[\Omega_a | \Omega_b] = \bar{\xi}_b \bar{\mu}^{-L_a} [H_0(0, 2\bar{\rho}_b) - \sum_{\alpha=0}^{N_a+L_a} \bar{\mu}^\alpha H_\alpha(2\bar{\rho}_a, 2\bar{\rho}_b)], \quad (2.18)$$

where each function  $H_\alpha$  is a simple linear combination of C-functions with numerical coefficients. The term by term integration of the integrals  $\bar{I}_{\lambda\beta}^{\gamma\delta\epsilon}$  is valid if the condition (1.39) is satisfied. Accordingly, the basic coulomb integrals are also to be divided into integrals of the first class and integrals of the second class. It is easily seen from Tables VI and VIII that the second class consists of the integrals involving the charge distribution  $\exists\Delta\Sigma_a$ . Indeed, Eq. (1.47) now has a considerably simpler form since, according to Eq. (2.12), one must put  $\rho_a = 0$  in Eq. (1.55). Consequently, the seven C-functions with  $\gamma\delta\epsilon = 0\delta 1$  are eliminated from Eq. (1.57), and the corresponding changes must be made in Eq. (1.47).

The coulomb integrals have the convenient property that it is arbitrary which one of the charge distributions is to be considered as  $\Omega_a$  (i.e., as forming the potential  $U_{\Omega_a}$ ), and which one is to be considered as  $\Omega_b$  (i.e., acting as charge distribution in the field of the potential). For instance, the integral between  $\exists S$  and  $\exists\Delta\Sigma$  on two centers can be evaluated as  $[\exists S_a | \exists\Delta\Sigma_b]$  or as  $[\exists\Delta\Sigma_a | \exists S_b]$ . Accordingly, for each basic coulomb integral there are two possible expansions of the type (2.18) with two different sets of H-functions. In Table IX, which gives the explicit expressions of the H-functions in terms of C-functions for all the 28 basic coulomb integrals, only one expansion is given for each integral, namely always the simpler one. In particular, application of Eq. (1.47) is avoided wherever possible; this was always feasible, except for the integral  $[\exists\Delta\Sigma_a | \exists\Delta\Sigma_b]$ .

TWO-CENTER INTEGRALS. III

TABLE IX

THE 28 COULOMB INTEGRALS IN TERMS OF THE AUXILIARY FUNCTIONS  $C_{\alpha\beta}^{\gamma\delta\epsilon}$   
 The last column of this table contains common factors with which the expressions  
 in terms of C-functions have to be multiplied in order to yield the H-functions.

L = 0 , M = 0 : Monopole Integrals

$[\Omega_a   \Omega_b]$	$H_0$	$H_1$	$H_2$	$H_3$	$H_4$	$H_5$	cf
$[1S_a   1S_b]$	$C_{01}^{000}$	$C_{11}^{000}$					-1/2
$[1S_a   2S_b]$	$C_{02}^{000}$	$C_{12}^{000}$					1/6
$[1S_a   3S_b]$	$C_{03}^{000}$	$C_{13}^{000}$					-1/24
$[1S_a   2P\Sigma_b]$	$C_{01}^{010}$	$C_{11}^{010}$					1/4
$[1S_a   3P\Sigma_b]$	$C_{02}^{010}$	$C_{12}^{010}$					-1/20
$[1S_a   3D\Sigma_b]$	$3C_{01}^{020}$	$3C_{11}^{020}$					-1/72
	$-C_{03}^{000}$	$-C_{13}^{000}$					
$[2S_a   2S_b]$	$3C_{02}^{000}$	$4C_{12}^{000}$	$2C_{22}^{000}$				1/18
$[2S_a   3S_b]$	$3C_{03}^{000}$	$4C_{13}^{000}$	$2C_{23}^{000}$				-1/72
$[2S_a   2P\Sigma_b]$	$3C_{01}^{010}$	$4C_{11}^{010}$	$2C_{21}^{010}$				1/12
$[2S_a   3P\Sigma_b]$	$3C_{02}^{010}$	$4C_{12}^{010}$	$2C_{22}^{010}$				-1/60
$[2S_a   3D\Sigma_b]$	$9C_{01}^{020}$	$12C_{11}^{020}$	$6C_{21}^{020}$				-1/216
	$-3C_{03}^{000}$	$-4C_{13}^{000}$	$-2C_{23}^{000}$				
$[3S_a   3S_b]$	$6C_{03}^{000}$	$9C_{13}^{000}$	$6C_{23}^{000}$	$2C_{33}^{000}$			-1/144
$[3S_a   2P\Sigma_b]$	$6C_{01}^{010}$	$9C_{11}^{010}$	$6C_{21}^{010}$	$2C_{31}^{010}$			1/24
$[3S_a   3P\Sigma_b]$	$6C_{02}^{010}$	$9C_{12}^{010}$	$6C_{22}^{010}$	$2C_{32}^{010}$			-1/120
$[3S_a   3D\Sigma_b]$	$18C_{01}^{020}$	$27C_{11}^{020}$	$18C_{21}^{020}$	$6C_{31}^{020}$			-1/432
	$-6C_{03}^{000}$	$-9C_{13}^{000}$	$-6C_{23}^{000}$	$-2C_{33}^{000}$			

RUEDENBERG, ROOTHAAN, AND JAUNZEMIS

TABLE IX

L = 1 , M = 0 : Dipole

$[\Omega_a   \Omega_b]$	$H_0$	$H_1$	$H_2$
$[2P\Sigma_a   2P\Sigma_b]$	$C_{-2,1}^{110}$	$2C_{-1,1}^{110}$	$2C_{01}^{110}$
$[2P\Sigma_a   3P\Sigma_b]$	$C_{-2,2}^{110}$	$2C_{-1,2}^{110}$	$2C_{02}^{110}$
$[2P\Sigma_a   3D\Sigma_b]$	$3C_{-2,1}^{120}$ $-C_{-2,3}^{100}$	$6C_{-1,1}^{120}$ $-2C_{-1,3}^{100}$	$6C_{01}^{120}$ $-2C_{03}^{100}$
$[3P\Sigma_a   3P\Sigma_b]$	$5C_{-2,2}^{110}$	$10C_{-1,2}^{110}$	$10C_{02}^{110}$
$[3P\Sigma_a   3D\Sigma_b]$	$15C_{-2,1}^{120}$ $-5C_{-2,3}^{100}$	$30C_{-1,1}^{120}$ $-10C_{-1,3}^{100}$	$30C_{01}^{120}$ $-10C_{03}^{100}$

L = 1 , M = 1 : Dipole

$[\Omega_a   \Omega_b]$	$H_0$	$H_1$	$H_2$
$[2P\Pi_a   2P\Pi_b]$	$C_{-2,1}^{001}$	$2C_{-1,1}^{001}$	$2C_{01}^{001}$
$[2P\Pi_a   3P\Pi_b]$	$C_{-2,2}^{001}$	$2C_{-1,2}^{001}$	$2C_{02}^{001}$
$[2P\Pi_a   3D\Pi_b]$	$C_{-2,1}^{011}$	$2C_{-1,1}^{011}$	$2C_{01}^{011}$
$[3P\Pi_a   3P\Pi_b]$	$5C_{-2,2}^{001}$	$10C_{-1,2}^{001}$	$10C_{02}^{001}$
$[3P\Pi_a   3D\Pi_b]$	$5C_{-2,1}^{011}$	$10C_{-1,1}^{011}$	$10C_{01}^{011}$

L = 2 , M = 0 : Quadrupole

$[\Omega_a   \Omega_b]$	$H_0$	$H_1$	$H_2$
$[3D\Sigma_a   3D\Sigma_b]$	$18\rho_b^{-1} [ 3C_{-2,1}^{120}$ $+3C_{-2,1}^{011}$ $-C_{-2,3}^{100} ]$	$36\rho_b^{-1} [ 3C_{-1,1}^{120}$ $+3C_{-1,1}^{011}$ $-C_{-1,3}^{100} ]$	$36\rho_b^{-1} [ 3C_{01}^{120}$ $+3C_{01}^{011}$ $-C_{03}^{100} ]$

TWO-CENTER INTEGRALS. III

(continued)

Integrals of  $\Sigma$ -character

$H_3$	$H_4$	$H_5$	cf
$c_{11}^{110}$			1/4
$c_{12}^{110}$			-1/20
$3c_{11}^{120}$			-1/72
$-c_{13}^{120}$			
$6c_{12}^{110}$	$2c_{22}^{110}$		-1/100
$18c_{11}^{120}$	$6c_{21}^{120}$		-1/360
$-6c_{13}^{100}$	$-2c_{23}^{100}$		

Integrals of  $\Pi$ -character

$H_3$	$H_4$	$H_5$	cf
$c_{11}^{001}$			1/8
$c_{12}^{001}$			-1/40
$c_{11}^{011}$			-1/24 $\sqrt{3}$
$6c_{12}^{001}$	$2c_{22}^{001}$		-1/200
$6c_{11}^{011}$	$2c_{21}^{011}$		-1/120 $\sqrt{3}$

Integral of  $\Sigma$ -character

$H_3$	$H_4$	$H_5$	cf
$24[ 3c_{11}^{020}$	$6[-3c_{21}^{020}$	$2[-3c_{31}^{020}$	-1/1296
$-c_{13}^{000}]$	$+c_{23}^{000}$	$+c_{33}^{000}$	
	$+9c_{01}^{220}$	$+9c_{11}^{220}$	
	$-3c_{03}^{200}]$	$-3c_{13}^{200}]$	

TABLE IX (continued)

L = 2, M = 1 : Quadrupole Integral of  $\Pi$ -character

$[\Omega_a   \Omega_b]$	$H_0$	$H_1$	$H_2$	$H_3$	$H_4$	$H_5$	cf
$[\Delta \Pi_a   \Delta \Pi_b]$	$9C_{-4,1}^{111}$	$18C_{-3,1}^{111}$	$18C_{-2,1}^{111}$	$12C_{-1,1}^{111}$	$6C_{01}^{111}$	$2C_{11}^{111}$	-1/216

L = 2, M = 2 : Quadrupole Integral of  $\Delta$ -character

$[\Omega_a   \Omega_b]$	$H_0$	$H_1$	$H_2$	$H_3$	$H_4$	$H_5$	cf
$[\Delta \Delta_a   \Delta \Delta_b]$	$9C_{-4,1}^{002}$	$18C_{-3,1}^{002}$	$18C_{-2,1}^{002}$	$12C_{-1,1}^{002}$	$6C_{01}^{002}$	$2C_{11}^{002}$	-1/864

Note Concerning the Use of the H-Functions in Eq. (2.18)

The present table furnishes the  $H_u$ 's as functions of  $\rho_a$  and  $\rho_b$ ; e.g., for the integral  $[\Delta \Sigma_a | \Delta \Sigma_b]$  one finds

$$H_0(\rho_a, \rho_b) = -(72\rho_b)^{-1} [3C_{-2,1}^{120}(\rho_a, \rho_b) + 3C_{-2,1}^{011}(\rho_a, \rho_b) - C_{-2,3}^{100}(\rho_a, \rho_b)], \text{ etc.}$$

Before using these expressions in Eq. (2.18), one has to perform in each  $H_u(\rho_a, \rho_b)$  the substitutions  $(\rho_a \rightarrow 0, \rho_b \rightarrow 2\bar{\rho}_b)$  or  $(\rho_a \rightarrow 2\bar{\rho}_a, \rho_b \rightarrow 2\bar{\rho}_b)$  respectively, as indicated in Eq. (2.18).

TWO-CENTER INTEGRALS. III

It should be noted that 66 C-functions are needed in order to express the 28 coulomb integrals. This situation compares unfavorably with the case of the hybrid integrals where we had 122 C-functions for 79 integrals. Since the coulomb integral expansions of Table IX and the hybrid integral expansions of Table VII have 35 C-functions in common, the total number of C-functions occurring in Tables VII and IX is 153. This state of affairs is shown in Table X. Explicit expressions for all the necessary C-functions are listed in Tables XIII, XIV, XV.<sup>14</sup>

TABLE X  
NUMBER OF C-FUNCTIONS USED FOR THE HYBRID  
AND COULOMB INTEGRALS

	79 hybrid integrals	28 coulomb integrals	hybrid and coulomb integrals together
$\alpha \geq 0$	63	44	88
$\alpha < 0$	59	22	65
Total	122	66	153

If the explicit formulas for the C-functions, as given in Tables XIII, XIV, and XV, are substituted into the expansions in terms of C-functions as given in Table IX, then we must of course obtain the formulas which were given in (I), Eqs. (34, 34a, 34b). This is indeed the case. In order to make the transition, we observe that our present parameters  $\bar{\rho}_a, \bar{\rho}_b, \bar{\rho}, \bar{\tau}$ , defined by Eqs. (1.20) and (2.7,13), were designated in (I) by  $\rho_a, \rho_b, \rho, \tau$ . Furthermore, according to Eq. (2.14) we must replace  $\bar{\mu}$  by

$$\bar{\mu} = \bar{\rho}_a / 2\bar{\rho}_b = \frac{1}{2}(1+\bar{\tau}) / (1-\bar{\tau}) = \frac{1}{2}[(\bar{\kappa}+1)/(\bar{\kappa}-1)]^{\frac{1}{2}}, \quad (2.19)$$

where

$$\bar{\kappa} = \frac{1}{2}(\bar{\tau}+1/\bar{\tau}); \quad (2.20)$$

this parameter  $\bar{\kappa}$  was designated in (I) by  $\kappa$ . It is to be noted that the exponential integral functions, which occur in the C-functions for  $\alpha < 0$ , do not occur in the explicit formulas (34, 34a, 34b) of (I). Indeed, if the indicated transition is carried

<sup>14</sup>Tables XIII, XIV, and XV (as well as Table XII) will be found at the end of Section 5, preceding the Bibliography.

out, then the exponential integral functions are found to cancel out in the final results.

We wish to mention that the formulas (34, 34a, 34b) of (I) have all been rechecked by the present method, which is somewhat different from the method employed in (I). Besides a few misprints, only one error was found; all corrections have been previously reported.<sup>15</sup>

b. One-Electron Integrals Expressible in Terms of C-Functions

If the overlap integrals [see (I), Eq. (4)]

$$(\chi_a | \chi_b) = \int dV \chi_a \chi_b \quad (2.21)$$

are expressed in elliptic coordinates, it is seen at once that they are linear combinations of C-functions with  $\alpha \geq 0$ . In paper (I) it was furthermore shown that the nuclear-attraction integrals [See (I), Eq. (6)]

$$(\chi_a | 1/r_a | \chi_b) = \int dV \chi_a (1/r_a) \chi_b, \quad (2.22)$$

and the kinetic-energy integrals [See (I), Eq. (5)]

$$(\chi_a | -\frac{1}{2}\Delta | \chi_b) = -\frac{1}{2} \int dV \chi_a \Delta \chi_b, \quad (2.23)$$

can be expressed in terms of overlap integrals [See (I), Eqs. (22, 23)]. Hence these integrals are also expressible in terms of C-functions with  $\alpha \geq 0$ . It is also useful to introduce the parameter

$$v = \zeta_a / \zeta_b = \rho_a / \rho_b = (1+\tau)/(1-\tau). \quad (2.24)$$

In Tables XI, XIa, and XIb are listed the expansions in terms of C-functions for the overlap integrals (2.21), the nuclear-attraction integrals (2.22), and the kinetic-energy integrals (2.23), respectively. It may be noted that Table XI does not contain overlap integrals involving Os and lp AO's, as did Eqs. (25) of (I); their function has been taken over by appropriate C-functions.

c. Nuclear-Attraction Integrals not Expressible in Terms of C-Functions

The nuclear-attraction integrals (see (I), Eq. (7))

$$[a | \chi_b \chi'_b] = (\chi_b | 1/r_a | \chi'_b) = \int dV \chi_b (1/r_a) \chi'_b \quad (2.25)$$

can be expressed in terms of the basic integrals

<sup>15</sup>THIS TECHNICAL REPORT, 1951-52, Part Two, Paper 10; 1952-53, p. 101.

TWO-CENTER INTEGRALS. III

TABLE XI

THE ONE-ELECTRON INTEGRALS  $(\chi_a | M | \chi_b)$  IN TERMS OF THE AUXILIARY FUNCTIONS  $C_{\alpha\beta}^{\gamma\delta\epsilon}$

(a) Overlap Integrals
$(1s_a   1s_b) = -2v^{3/2} C_{11}^{000}$
$(1s_a   2s_b) = (2/\sqrt{3}) v^{3/2} C_{12}^{000}$
$(2s_a   2s_b) = (2/3) v^{5/2} C_{22}^{000}$
$(1s_a   2p\sigma_b) = 2v^{3/2} C_{11}^{010}$
$(2s_a   2p\sigma_b) = (2/\sqrt{3}) v^{5/2} C_{21}^{010}$
$(2p\sigma_a   2p\sigma_b) = 2v^{5/2} C_{11}^{110}$
$(2p\pi_a   2p\pi_b) = v^{5/2} C_{11}^{001}$

(b) Nuclear-Attraction Integrals
$(1s_a   1/r_a   1s_b) = -2\zeta_a v^{1/2} C_{01}^{000}$
$(1s_a   1/r_a   2s_b) = (2/\sqrt{3}) \zeta_a v^{1/2} C_{02}^{000}$
$(2s_a   1/r_a   1s_b) = -(2/\sqrt{3}) \zeta_a v^{3/2} C_{11}^{000}$
$(2s_a   1/r_a   2s_b) = (2/3) \zeta_a v^{3/2} C_{12}^{000}$
$(1s_a   1/r_a   2p\sigma_b) = 2\zeta_a v^{1/2} C_{01}^{010}$
$(2p\sigma_a   1/r_a   1s_b) = -2\zeta_a v^{3/2} C_{01}^{100}$
$(2s_a   1/r_a   2p\sigma_b) = (2/\sqrt{3}) \zeta_a v^{3/2} C_{11}^{010}$
$(2p\sigma_a   1/r_a   2s_b) = (2/\sqrt{3}) \zeta_a v^{3/2} C_{02}^{100}$
$(2p\sigma_a   1/r_a   2p\sigma_b) = 2\zeta_a v^{3/2} C_{01}^{110}$
$(2p\pi_a   1/r_a   2p\pi_b) = \zeta_a v^{3/2} C_{01}^{001}$

(c) Kinetic-Energy Integrals
$(1s_a   -\frac{1}{2}\Delta   1s_b) = -\zeta_a^2 v^{1/2} (2C_{01}^{000} - vC_{11}^{000})$
$(1s_a   -\frac{1}{2}\Delta   2s_b) = (1/\sqrt{3}) \zeta_a^2 v^{1/2} (2C_{02}^{000} - vC_{12}^{000})$
$(2s_a   -\frac{1}{2}\Delta   2s_b) = -(1/3) \zeta_a^2 v^{1/2} (2C_{02}^{000} - 4vC_{12}^{000} + v^2 C_{22}^{000})$
$(1s_a   -\frac{1}{2}\Delta   2p\sigma_b) = \zeta_a^2 v^{1/2} (2C_{01}^{010} - vC_{11}^{010})$
$(2s_a   -\frac{1}{2}\Delta   2p\sigma_b) = -(1/\sqrt{3}) \zeta_a^2 v^{1/2} (2C_{01}^{010} - 4vC_{11}^{010} + v^2 C_{21}^{010})$
$(2p\sigma_a   -\frac{1}{2}\Delta   2p\sigma_b) = \zeta_a^2 v^{3/2} (4C_{01}^{110} - vC_{11}^{110})$
$(2p\pi_a   -\frac{1}{2}\Delta   2p\pi_b) = (1/2) \zeta_a^2 v^{3/2} (4C_{01}^{001} - vC_{11}^{001})$

$$[a|\Omega_b] = \int dV \Omega_b / r_a, \quad (2.26)$$

as was shown in (I), Eqs. (28). It was further shown in (I) that the integral  $[a|\Omega_b]$  vanishes unless  $\Omega_b$  is of  $\Sigma$ -type, and that the integrals  $[a|NLO_b]$  are intimately connected with potentials  $U_{NLM}$  [see (I), Eq. (32)]. Since the difference in notation of (I) and the present paper may become somewhat confusing at this point, we shall show this connection here once more. Instead of  $[a|\Omega_b]$  we shall first evaluate  $[\Omega_a|b]$ , and make the proper change  $a \rightleftharpoons b$  in the final result. Now  $[\Omega_a|b]$  is just the potential  $U_{\Omega_a}(2)$ , as given by (1.10), evaluated at the point  $b$ , i.e.,  $r_{a2} = R$ ,  $\theta_{a2} = 0$ . Since  $S_{LM}(0, \varphi) = [(2L+1)/4\pi]^{\frac{1}{2}} \delta_{MO}$ , we find from Eqs. (1.12, 17)

$$[NLM_a|b] = 2^{L+1} \zeta_a \sigma^{-L-1} (1 - e^{-\sigma} \sum_{k=0}^{N+L} u_k \sigma^k) \delta_{MO},$$

where  $\sigma = 2\zeta_a R$ , and  $u_k$  is defined by (1.18). Exchanging now  $a$  and  $b$ , and putting  $2\zeta_b R = 2\bar{\rho}_b$  [see Eq. (2.7)], we find the general result

$$[a|NLM_b] = \zeta_b \bar{\rho}_b^{-L-1} [1 - e^{-2\bar{\rho}_b} \sum_{k=0}^{N+L} u_k (2\bar{\rho}_b)^k] \delta_{MO}. \quad (2.27)$$

The explicit expressions for Eq. (2.27), which arise from AO's with the principal quantum numbers 1 and 2, were already given in (I), Eqs. (31); the parameters  $\zeta$  and  $\rho$  of those equations are here designated by  $\zeta_b$  and  $\bar{\rho}_b$ , respectively.

In the present derivation of the connection between the potentials  $U_{\Omega_a}$  and the integrals  $[a|\Omega_b]$ , the integrals were derived from the potentials, whereas in (I) the potentials were derived from the integrals.

TWO-CENTER INTEGRALS. III

3. THE FUNCTIONS  $C_{\alpha\beta}^{\gamma\delta\epsilon}$  FOR  $\alpha \geq 0$

a. General Remarks

The functions  $C_{\alpha\beta}^{\gamma\delta\epsilon}(\rho_a, \rho_b)$  were defined by Eq. (1.35), namely

$$C_{\alpha\beta}^{\gamma\delta\epsilon}(\rho_a, \rho_b) = (-1)^{\beta+\delta+\epsilon} \left(\frac{1}{2}\rho_b\right)^{\alpha+\beta+\gamma+\delta+2\epsilon+1} \int_1^\infty d\xi \int_{-1}^1 d\eta e^{-\rho\xi-\tau\rho\eta} \\ \times (\xi+\eta)^\alpha (\xi-\eta)^\beta (1+\xi\eta)^\gamma (1-\xi\eta)^\delta (\xi^2-1)^\epsilon (1-\eta^2)^\epsilon, \quad (3.1)$$

with

$$\rho = \frac{1}{2}(\rho_a + \rho_b), \quad \tau = (\rho_a - \rho_b)/(\rho_a + \rho_b). \quad (3.2)$$

For  $\alpha \geq 0$  we can express  $C_{\alpha\beta}^{\gamma\delta\epsilon}(\rho_a, \rho_b)$  in terms of the functions  $A_n(\rho)$  and  $B_n(\tau\rho)$  (see Section 5a), by first multiplying out the polynomial in  $\xi$  and  $\eta$  before integrating. A more elegant access to the functions  $C_{\alpha\beta}^{\gamma\delta\epsilon}(\rho_a, \rho_b)$  for  $\alpha \geq 0$  is provided by the following system of recurrence formulas.

b. Recurrence Relations for  $C_{\alpha\beta}^{000}$

We observe that

$$C_{\alpha\beta}^{000}(\rho_a, \rho_b) = \frac{1}{2}(-1)^\alpha \rho_b^{\alpha+\beta+1} \partial_a^\alpha \partial_b^\beta \int_1^\infty d\xi \int_{-1}^1 d\eta e^{-\rho\xi-\tau\rho\eta}, \quad (3.3)$$

where

$$\partial_a = \partial/\partial\rho_a, \quad \partial_b = \partial/\partial\rho_b. \quad (3.4)$$

Carrying out the integration we obtain for (3.3)

$$C_{\alpha\beta}^{000}(\rho_a, \rho_b) = 2(-1)^{\alpha+1} \rho_b^{\alpha+\beta+1} \partial_a^\alpha \partial_b^\beta (e^{-\rho_a} - e^{-\rho_b}) / (\rho_a^2 - \rho_b^2). \quad (3.5)$$

By virtue of the identity

$$\partial_a^\alpha \partial_b^\beta (e^{-\rho_a} - e^{-\rho_b}) = \sum_{i=0}^\alpha \sum_{j=0}^\beta \binom{\alpha}{i} \binom{\beta}{j} [\partial_a^{i+1} \partial_b^j (\rho_a^2 - \rho_b^2)] \\ \times [\partial_a^{\alpha-i-1} \partial_b^{\beta-j} (e^{-\rho_a} - e^{-\rho_b}) / (\rho_a^2 - \rho_b^2)] \quad (3.6)$$

we find the recurrence relation<sup>16</sup>

<sup>16</sup>For  $\alpha \leq 1$  and  $\beta \leq 1$  there occur in Eq. (3.7) C-functions with negative indices with vanishing coefficients. Such terms should simply be omitted, which is easily seen to be correct by applying Eq. (3.6) to these special cases.

$$\begin{aligned}
 c_{\alpha\beta}^{000} = (\kappa-1) \{ & \alpha \rho_a \rho_b^{-1} c_{\alpha-1,\beta}^{000} + \beta c_{\alpha,\beta-1}^{000} \\
 & - \frac{1}{2} \alpha (\alpha-1) c_{\alpha-2,\beta}^{000} + \frac{1}{2} \beta (\beta-1) c_{\alpha,\beta-2}^{000} \\
 & - \rho_b^{\alpha+\beta-1} [\delta_{\beta 0} e^{-\rho_a} - \delta_{\alpha 0} (-1)^\beta e^{-\rho_b}] \} , \quad (3.7)
 \end{aligned}$$

where

$$\kappa = \frac{1}{2} [\tau + (1/\tau)] = (\rho_a^2 + \rho_b^2) / (\rho_a^2 - \rho_b^2) . \quad (3.8)$$

For the three simplest cases Eq. (3.7) yields

$$\left. \begin{aligned}
 c_{00}^{000} &= -(\kappa-1) \rho_b^{-1} (e^{-\rho_a} - e^{-\rho_b}) , \\
 c_{10}^{000} &= (\kappa-1) (\rho_a \rho_b^{-1} c_{00}^{000} - e^{-\rho_a}) , \\
 c_{01}^{000} &= (\kappa-1) (c_{00}^{000} - e^{-\rho_b}) .
 \end{aligned} \right\} \quad (3.9)$$

We make use of Eqs. (3.9) to derive the following relations, which we shall need in Section 4:

$$\left. \begin{aligned}
 \rho_a c_{01}^{000} - \rho_b c_{10}^{000} &= (\kappa-1) (\rho_b e^{-\rho_a} - \rho_a e^{-\rho_b}) , \\
 \rho_b c_{01}^{000} - \rho_a c_{10}^{000} + 2\rho_b c_{00}^{000} &= (\kappa-1) (\rho_a e^{-\rho_a} - \rho_b e^{-\rho_b}) .
 \end{aligned} \right\} \quad (3.10)$$

c. Recurrence Relations for the Upper Index Triple

The following recurrence formulas serve to obtain the functions  $c_{\alpha\beta}^{\gamma\delta\epsilon}$  for which the upper indices are different from zero. Each of these formulas corresponds to an identity in  $\xi$  and  $\eta$ . Thus the identities

$$\begin{aligned}
 1 \pm \xi\eta &= 1 \pm \frac{1}{4} [(\xi+\eta)^2 - (\xi-\eta)^2] , \\
 (\xi^2-1)(1-\eta^2) &= -1 + \frac{1}{2} [(\xi+\eta)^2 + (\xi-\eta)^2] - (1/16) [(\xi+\eta)^2 - (\xi-\eta)^2]^2 , \\
 (1+\xi\eta)(1-\xi\eta) &= 1 - (1/16) [(\xi+\eta)^2 - (\xi-\eta)^2] , \\
 1 + \xi\eta + 1 - \xi\eta &= 2 , \\
 (\xi^2-1)(1-\eta^2) - (1+\xi\eta)(1-\xi\eta) &= -2 + \frac{1}{2} [(\xi+\eta)^2 + (\xi-\eta)^2] , \\
 (\xi^2-1)(1-\eta^2) + (1+\xi\eta)^2 &= (\xi\pm\eta)^2 ,
 \end{aligned}$$

TWO-CENTER INTEGRALS. III

$$(1+\xi\eta)^2 + (1-\xi\eta)^2 + 2(1+\xi\eta)(1-\xi\eta) = 4 ,$$

yield the following recurrence relations, respectively:

$$2C_{\alpha\beta}^{\gamma+1,\delta\epsilon} = \rho_b C_{\alpha\beta}^{\gamma\delta\epsilon} + \rho_b^{-1}(C_{\alpha+2,\beta}^{\gamma\delta\epsilon} - C_{\alpha,\beta+2}^{\gamma\delta\epsilon}) , \quad (3.11)$$

$$2C_{\alpha\beta}^{\gamma,\delta+1,\epsilon} = -\rho_b C_{\alpha\beta}^{\gamma\delta\epsilon} + \rho_b^{-1}(C_{\alpha+2,\beta}^{\gamma\delta\epsilon} - C_{\alpha,\beta+2}^{\gamma\delta\epsilon}) , \quad (3.12)$$

$$4C_{\alpha\beta}^{\gamma\delta,\epsilon+1} = \rho_b^2 C_{\alpha\beta}^{\gamma\delta\epsilon} - 2(C_{\alpha+2,\beta}^{\gamma\delta\epsilon} + C_{\alpha,\beta+2}^{\gamma\delta\epsilon}) \\ + \rho_b^{-2}(C_{\alpha+4,\beta}^{\gamma\delta\epsilon} - 2C_{\alpha+2,\beta+2}^{\gamma\delta\epsilon} + C_{\alpha,\beta+4}^{\gamma\delta\epsilon}) , \quad (3.13)$$

$$4C_{\alpha\beta}^{\gamma+1,\delta+1,\epsilon} = -\rho_b^2 C_{\alpha\beta}^{\gamma\delta\epsilon} + \rho_b^{-2}(C_{\alpha+4,\beta}^{\gamma\delta\epsilon} - 2C_{\alpha+2,\beta+2}^{\gamma\delta\epsilon} + C_{\alpha,\beta+4}^{\gamma\delta\epsilon}) , \quad (3.14)$$

$$C_{\alpha\beta}^{\gamma+1,\delta\epsilon} - C_{\alpha\beta}^{\gamma,\delta+1,\epsilon} = \rho_b C_{\alpha\beta}^{\gamma\delta\epsilon} , \quad (3.15)$$

$$2(C_{\alpha\beta}^{\gamma\delta,\epsilon+1} - C_{\alpha\beta}^{\gamma+1,\delta+1,\epsilon}) = \rho_b^2 C_{\alpha\beta}^{\gamma\delta\epsilon} - C_{\alpha+2,\beta}^{\gamma\delta\epsilon} - C_{\alpha,\beta+2}^{\gamma\delta\epsilon} , \quad (3.16)$$

$$C_{\alpha\beta}^{\gamma+2,\delta\epsilon} - C_{\alpha\beta}^{\gamma\delta,\epsilon+1} = C_{\alpha+2,\beta}^{\gamma\delta\epsilon} , \quad (3.17)$$

$$C_{\alpha\beta}^{\gamma,\delta+2,\epsilon} - C_{\alpha\beta}^{\gamma\delta,\epsilon+1} = C_{\alpha,\beta+2}^{\gamma\delta\epsilon} , \quad (3.18)$$

$$C_{\alpha\beta}^{\gamma+2,\delta\epsilon} + C_{\alpha\beta}^{\gamma,\delta+2,\epsilon} - 2C_{\alpha\beta}^{\gamma+1,\delta+1,\epsilon} = \rho_b^2 C_{\alpha\beta}^{\gamma\delta\epsilon} . \quad (3.19)$$

The Eqs. (3.11,12,13) permit us to raise each of the three upper indices independently; Eq. (3.14) permits us to raise  $\gamma$  and  $\delta$  simultaneously. The Eqs. (3.15-18) serve to transfer raised units between the various upper indices. So Eq. (3.15) converts one raised unit of  $\gamma$  into one raised unit of  $\delta$ , and vice versa; Eq. (3.16) converts one raised unit of  $\epsilon$  into one raised unit of  $\gamma$  plus one raised unit of  $\delta$ , and vice versa; and Eqs. (3.17,18) convert one raised unit of  $\epsilon$  into two raised units of  $\gamma$  or  $\delta$ , and vice versa. Finally, Eq. (3.19) may be useful as a check.

The Eqs. (3.11-19) are of course not the only possible recurrence relations for raising the upper indices; they are however rather simple relations, particularly Eqs. (3.15,17,18).

Fig. 1 represents in diagrammatic form a possible scheme for successively raising the upper indices, and at the same time checking the obtained results. The scheme was constructed using mostly the particularly simple relations (3.15,17,18). It appears to be useful to group together the C-functions which have the same upper

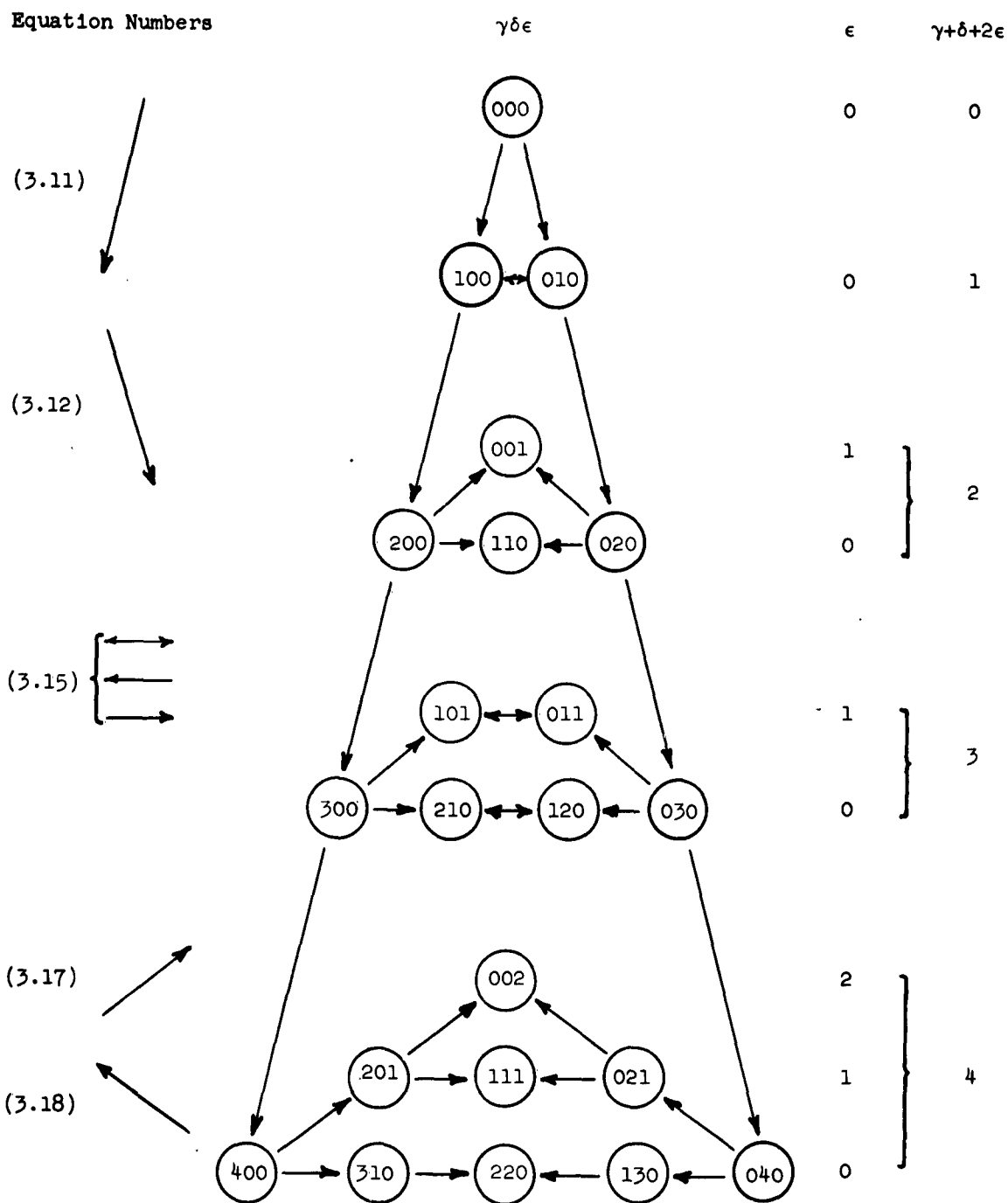


Fig. 1. A Possible Scheme for Raising the Upper Indices

index sum  $\gamma+\delta+2\epsilon$ ; such a group is then conveniently subdivided according to the different values of  $\epsilon$ . In order to calculate C-functions with the same upper index sum, say  $n$ , from each other, we need also C-functions of the group  $n-1$  if Eq. (3.15) is used, and  $n-2$  if Eq. (3.17) or (3.18) is used. Finally, it should be noted that parallel arrows in Fig. 1 represent the same equation; this also applies to arrows which are not drawn in Fig. 1, e.g., an arrow from 310 to 111 would represent Eq. (3.17). Another set of parallel arrows which is not shown at all in Fig. 1 is a set of vertical arrows representing Eq. (3.16), e.g., from 310 to 201.

In the last analysis the methods described for raising the upper indices amount of course to making the decomposition

$$(1+\xi\eta)^\gamma(1-\xi\eta)^\delta(\xi^2-1)^\epsilon(1-\eta^2)^\epsilon = \sum_{ij} a_{ij} \gamma^{\delta\epsilon} (\xi+\eta)^i (\xi-\eta)^j,$$

where the coefficients  $a_{ij} \gamma^{\delta\epsilon}$  are constants. But the described systematic arrangement of successive steps appears more convenient.

#### d. The Total Recurrence Procedure

From the foregoing it appears that two units of the lower index sum  $\alpha+\beta$  are consumed in order to raise the upper index sum  $\gamma+\delta+2\epsilon$  by one unit. Now from Tables VII, IX, and XI it is seen that the maximum value of the upper index sum is 4, and that this occurs for the index pairs  $(\alpha,\beta) = (0,1)$  and  $(\alpha,\beta) = (1,1)$ . Furthermore, it is seen that the maximum value of "lower sum plus two times upper sum" is 10. For the calculation of the needed C-functions we therefore used the following scheme (see Fig. 2). First the functions  $C_{\alpha\beta}^{000}$  (i.e., upper sum = 0) were calculated by means of Eq. (3.7) for all index pairs  $\alpha,\beta$  which are entered in Fig. 2. Then, in subsequent steps, the C-functions with upper sum = 1, 2, 3, 4 were calculated by means of Eqs. (3.11-19) for all the index pairs  $\alpha,\beta$  situated above and to the left of the lines marked 1, 2, 3, 4, respectively, in Fig. 2. In this manner explicit formulas were calculated for the 260 C-functions with  $\alpha \geq 0$  which are listed in Table XIIa. They were needed in order to establish the 88 among them which appear in Tables VII, IX, and XI. The explicit formulas for these 88 are given in Table XIII. Formulas for the 172 others can be made available upon demand.

#### e. The Limiting Cases $\rho = 0$ and $\tau = 0$

For  $\rho = 0$  and  $\tau = 0$  the formulas of Table XIII cannot be employed directly for numerical computations. Tables XIV and XV give the formulas for the functions  $C_{\alpha\beta}^{\gamma\delta\epsilon}$  for these two limiting cases. All these formulas were calculated in two ways. The

RUEDENBERG, ROOTHAAN, AND JAUNZEMIS

	00	01	02	03	04	05	06	07	08	09
	10	11	12	13	14	15	16	17	18	19
4	20	21	22	23	24	25	26	27		
	30	31	32	33	34	35	36	37		
3	40	41	42	43	44	45				
	50	51	52	53	54	55				
2	60	61	62	63						
	70	71	72	73						
1	80	81								
	90	91								

Fig. 2. List of Lower Indices  $\alpha, \beta$  Occurring in the Course of the Recurrence Procedure Represented in Fig. 1

first way consisted in calculating the limits of the expressions given in Table XIII by expanding the exponentials. The second way for the case  $\tau = 0$  was the method described in 3a: the functions  $C_{\alpha\beta}^{\gamma\delta\epsilon}$  were expressed in terms of the functions  $A_n(\rho)$  and  $B_n(\tau\rho) = B_n(0) = [1 + (-1)^n]/(n+1)$ . For the case  $\rho = 0$  the second way was the direct integration, leading to the general result

$$\lim_{\rho \rightarrow 0} C_{\alpha\beta}^{\gamma\delta\epsilon}(\rho_a, \rho_b) = c_{\gamma+\delta}^{\epsilon} (-1)^{\beta+\epsilon} (\alpha+\beta+\gamma+\delta+2\epsilon)! \left[\frac{1}{2}(1-\tau)\right]^{\alpha+\beta+\gamma+\delta+2\epsilon+1}, \quad (3.20)$$

where the constants  $c_w^{\epsilon}$  are defined by

$$c_w^{\epsilon} = \int_{-1}^1 dt (1-t^2)^{\epsilon} t^w, \quad (3.21)$$

$$c_w^{\epsilon} = 2^{2\epsilon+1} \epsilon! w! \left(\frac{1}{2}w+\epsilon\right)! / \left(\frac{1}{2}w\right)! (w+2\epsilon+1)! \quad (3.21')$$

for  $w$  even, and

$$c_w^{\epsilon} = 0 \quad (3.21'')$$

for  $w$  odd.

To prove Eq. (3.20) we substitute  $\rho_b = (1-\tau)\rho$  in (3.1) and multiply  $\rho^{\alpha+\beta+\gamma+\delta+2\epsilon+1}$  into the integrand. Putting  $\rho\xi = x$  we then obtain

TWO-CENTER INTEGRALS. III

$$C_{\alpha\beta}^{\gamma\delta\epsilon} = (-1)^{\beta+\delta+\epsilon} [\frac{1}{2}(1-\tau)]^{\alpha+\beta+\gamma+\delta+2\epsilon+1} \int_{\rho}^{\infty} dx \int_{-1}^1 d\eta e^{-x-\tau\rho\eta} \\ \times (x+\rho\eta)^{\alpha}(x-\rho\eta)^{\beta}(\rho+x\eta)^{\gamma}(\rho-x\eta)^{\delta}(x^2-\rho^2)^{\epsilon}(1-\eta^2)^{\epsilon},$$

so that, letting  $\rho \rightarrow 0$ ,

$$\lim_{\rho \rightarrow 0} C_{\alpha\beta}^{\gamma\delta\epsilon} = (-1)^{\beta+\epsilon} [\frac{1}{2}(1-\tau)]^{\alpha+\beta+\gamma+\delta+2\epsilon+1} \int_0^{\infty} dx e^{-x} x^{\alpha+\beta+\gamma+\delta+2\epsilon} \\ \times \int_{-1}^1 d\eta (1-\eta^2)^{\epsilon} \eta^{\gamma+\delta}, \quad (3.22)$$

whence (3.20). It may be noted that it is the factor  $\rho_b^{\alpha+\beta+\gamma+\delta+2\epsilon+1}$  in (3.1) which keeps the functions  $C_{\alpha\beta}^{\gamma\delta\epsilon}$  finite for  $\rho \rightarrow 0$ .

The agreement obtained by using two different methods for calculating the limiting cases is a further check on the derivations of the explicit formulas for the general case.

We can also see now why for a numerical tabulation of the C-functions we should use the parameters  $\rho, \tau$  rather than  $\rho_a, \rho_b$ . Namely the function  $C_{\alpha\beta}^{\gamma\delta\epsilon}(\rho_a, \rho_b)$  is discontinuous at the point  $\rho_a = \rho_b = 0$  in the  $\rho_a, \rho_b$ -plane; but, considered as a function of  $\rho$  and  $\tau$ ,  $C_{\alpha\beta}^{\gamma\delta\epsilon}$  is well-behaved for the entire range  $0 \leq \rho < \infty$ ,  $-1 \leq \tau \leq 1$ .

4. THE FUNCTIONS  $C_{\alpha\beta}^{\gamma\delta\epsilon}$  FOR  $\alpha < 0$ 

 a. Condition for Convergence

The definition of the functions  $C_{\alpha\beta}^{\gamma\delta\epsilon}$  by the integral (3.1) shows that for  $\alpha < 0$  the integrand becomes infinite at the point  $\xi = 1, \eta = -1$ , so that the question arises as to whether or not the integration extending to this critical point in the  $\xi, \eta$ -plane yields a finite result. It will be shown that the condition for convergence, which limits the possible negative values of  $\alpha$ , is

$$\alpha + \gamma + 2\epsilon + 1 \geq 0. \quad (4.1)$$

This result was already used in Sections 1 and 2; the relation (4.1) is identical with (1.38).

To derive the condition (4.1), we divide the area of integration in the  $\xi, \eta$ -plane into the areas I and II as shown in Fig. 3. For the area I we introduce polar

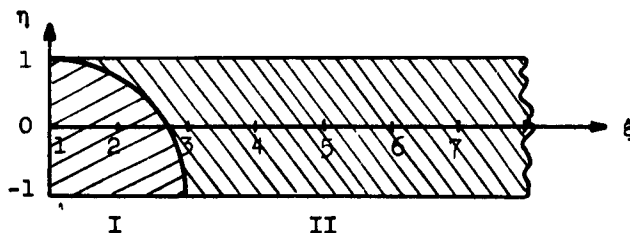


Fig. 3. Area of Integration.

coordinates  $r, \varphi$ :

$$\xi - 1 = r \cos \varphi, \quad \eta + 1 = r \sin \varphi, \quad (4.2)$$

so that the integral (3.1) becomes

$$\begin{aligned} C_{\alpha\beta}^{\gamma\delta\epsilon}(\rho_a, \rho_b) &= (-1)^{\beta+\delta+\epsilon} \left(\frac{1}{2\rho_b}\right)^{\alpha+\beta+\gamma+\delta+2\epsilon+1} \left\{ e^{-\rho_b} \int_0^2 dr r^{\alpha+\gamma+2\epsilon+1} \int_0^{\frac{1}{2}\pi} d\varphi e^{-r(\rho \cos \varphi + \tau \rho \sin \varphi)} \right. \\ &\quad \times (\cos \varphi + \sin \varphi)^\alpha (2 + r \cos \varphi - r \sin \varphi)^\beta (-\cos \varphi + \sin \varphi + r \cos \varphi \sin \varphi)^\gamma \\ &\quad \times (2 + r \cos \varphi - r \sin \varphi - r^2 \cos \varphi \sin \varphi)^\delta [\cos \varphi \sin \varphi (2 + r \cos \varphi) (2 + r \sin \varphi)]^\epsilon \\ &\quad \left. + \int_{-1}^1 d\eta \int_1^\infty \frac{d\xi}{1 + \sqrt{4 - (1 + \eta)^2}} e^{-\rho \xi - \tau \rho \eta} \right. \\ &\quad \left. \times (\xi + \eta)^\alpha (\xi - \eta)^\beta (1 + \xi \eta)^\gamma (1 - \xi \eta)^\delta (\xi^2 - 1)^\epsilon (1 - \eta^2)^\epsilon \right\}. \quad (4.3) \end{aligned}$$

It is easily seen that the second integral in (4.3) is always convergent. To investigate the convergence of the first integral, we expand the integrand in a power series

TWO-CENTER INTEGRALS. III

with respect to  $r$ ; this yields for the first integral

$$\int_0^2 dr r^{\alpha+\gamma+2\epsilon+1} \int_0^{\frac{1}{2}\pi} d\varphi (\cos\varphi+\sin\varphi)^\alpha \sum_{k=0}^{\infty} r^k p_k(\rho_a, \rho_b, \cos\varphi, \sin\varphi), \quad (4.4)$$

where each  $p_k(u, v, x, y)$  is a polynomial in  $u, v, x, y$ . Clearly, the infinite series in (4.4) is uniformly convergent; hence a sufficient condition for the convergence of (4.4) is that the integrals

$$\int_0^2 dr r^{\alpha+\gamma+2\epsilon+1+k} \quad \text{and} \quad \int_0^{\frac{1}{2}\pi} d\varphi (\cos\varphi+\sin\varphi)^\alpha p_k(\rho_a, \rho_b, \cos\varphi, \sin\varphi)$$

converge for all values of  $k$ . Now

$$\cos\varphi+\sin\varphi = \sqrt{2}\cos(\varphi-\frac{1}{4}\pi) > 0 \quad \text{for} \quad 0 \leq \varphi \leq \frac{1}{2}\pi;$$

hence  $(\cos\varphi+\sin\varphi)^\alpha$  introduces no singularity inspite of  $\alpha < 0$ , and consequently all the integrals over  $\varphi$  converge. On the other hand, the integrals over  $r$  converge if

$$\alpha+\gamma+2\epsilon+1 \geq 0,$$

so that (4.1) is indeed a sufficient condition for convergence.

It is conceivable that the expression (4.4) might still be convergent if the condition (4.1) is violated. Namely, if we evaluate  $p_0(\rho_a, \rho_b, \cos\varphi, \sin\varphi)$ , we find

$$(\cos\varphi+\sin\varphi)^\alpha p_0(\rho_a, \rho_b, \cos\varphi, \sin\varphi) = (-1)^{\gamma_2\beta+\delta+\epsilon+\frac{1}{2}(\alpha+\gamma)} \cos^\alpha(\varphi+\frac{1}{4}\pi) \cos^\gamma(\varphi-\frac{1}{4}\pi) \sin 2\varphi$$

The functions  $\cos(\varphi+\frac{1}{4}\pi)$ ,  $\cos(\varphi-\frac{1}{4}\pi)$ , and  $\sin 2\varphi$  are plotted in Fig. 4. From these plots it is obvious that

$$\int_0^{\frac{1}{2}\pi} d\varphi (\cos\varphi+\sin\varphi)^\alpha p_0(\rho_a, \rho_b, \cos\varphi, \sin\varphi) \begin{cases} \neq 0, & \gamma \text{ even,} \\ = 0, & \gamma \text{ odd.} \end{cases}$$

Consequently, if  $\gamma$  is odd, the expression (4.4) might still yield a finite result if

$$\alpha+\gamma+2\epsilon+2 = 0.$$

But in that case the integral (4.3) is at most conditionally convergent, i.e. it depends on how we reach the point  $\xi = 1, \eta = -1$  in the  $\xi\eta$ -plane whether the integral (4.3) converges at all and/or what numerical value will result. Moreover, when we attempted, in a few simple cases, to use the relation

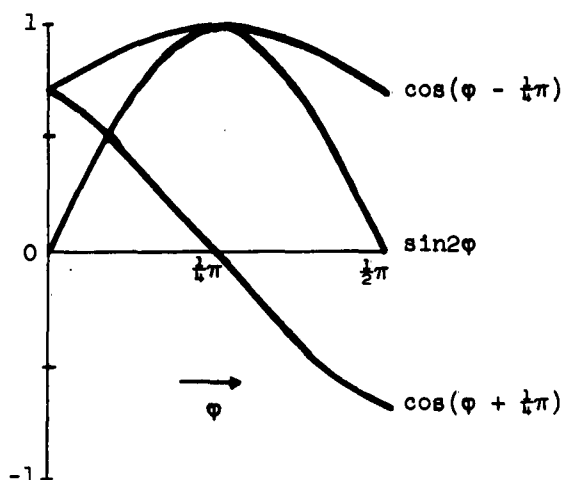


Fig. 4. The functions  $\cos(\varphi + \frac{1}{4}\pi)$ ,  $\cos(\varphi - \frac{1}{4}\pi)$ , and  $\sin 2\varphi$ .

$$C_{\alpha-1,\beta}^{\gamma\delta\epsilon}(\rho_a, \rho_b) = \rho_b^{-1} \int_{\rho_a}^{\infty} dt C_{\alpha\beta}^{\gamma\delta\epsilon}(t, \rho_b), \quad (4.5)$$

which follows from the definition (3.1), in order to lower the index  $\alpha$  beyond the value consistent with the condition (4.1), the right-hand side of Eq. (4.5) was found to be divergent. It was therefore considered inadvisable to pursue further the problems connected with those C-functions which have  $\alpha + \gamma + 2\epsilon < 0$ , in particular since we were successful in Sections 1 and 2 in expressing all hybrid and coulomb integrals in terms of C-functions satisfying the condition (4.1), which are regularly convergent.

In the following subsections we shall show that the latter type of C-functions (with  $\alpha < 0$ ) can all be expressed by the general formula

$$C_{\alpha\beta}^{\gamma\delta\epsilon}(\rho_a, \rho_b) = D_{\alpha\beta}^{\gamma\delta\epsilon}(\rho_a, \rho_b) + E_{\alpha\beta}^{\gamma\delta\epsilon}(\rho_a, \rho_b)F(\rho_a, \rho_b) + (-1)^{\gamma+\delta} E_{\alpha\beta}^{\gamma\delta\epsilon}(-\rho_a, -\rho_b)G(\rho_a, \rho_b), \quad (4.6)$$

or, suppressing the explicit arguments,

$$C_{\alpha\beta}^{\gamma\delta\epsilon} = D_{\alpha\beta}^{\gamma\delta\epsilon} + E_{\alpha\beta}^{\gamma\delta\epsilon}F + \bar{E}_{\alpha\beta}^{\gamma\delta\epsilon}G, \quad (4.6')$$

where

$$\bar{E}_{\alpha\beta}^{\gamma\delta\epsilon}(\rho_a, \rho_b) = (-1)^{\gamma+\delta} E_{\alpha\beta}^{\gamma\delta\epsilon}(-\rho_a, -\rho_b). \quad (4.7)$$

The functions  $D_{\alpha\beta}^{\gamma\delta\epsilon}$  have a structure very similar to the C-functions with  $\alpha \geq 0$ ; each function  $E_{\alpha\beta}^{\gamma\delta\epsilon}$  consists of a finite series of powers (positive, zero, or negative) of

TWO-CENTER INTEGRALS. III

$\rho_a$  and  $\rho_b$ , multiplied by  $e^{\rho_b}$ ; finally, the functions F and G, which do not depend upon the indices  $\alpha, \beta, \gamma, \delta, \epsilon$ , are expressible in terms of exponential integrals and logarithms.

**b. The Functions  $C_{-1, \beta}^{000}$**

We start from Eq. (4.5) for  $\alpha = \beta = \gamma = \delta = \epsilon = 0$ , yielding

$$C_{-1,0}^{000}(\rho_a, \rho_b) = \rho_b^{-1} \int_{\rho_a}^{\infty} dt C_{00}^{000}(t, \rho_b) ; \quad (4.8)$$

substituting for  $C_{00}^{000}$  the expression (3.5) we find

$$\begin{aligned} C_{-1,0}^{000}(\rho_a, \rho_b) &= \rho_b^{-1} \int_{\rho_a}^{\infty} dt (e^{-t} - e^{-\rho_b}) [(t + \rho_b)^{-1} - (t - \rho_b)^{-1}] \\ &= e^{\rho_b} \rho_b^{-1} \int_{\rho_a + \rho_b}^{\infty} dt e^{-t} t^{-1} - e^{-\rho_b} \rho_b^{-1} \int_{\rho_a - \rho_b}^{\infty} dt [(e^{-t} - 1)t^{-1} + (t + 2\rho_b)^{-1}], \end{aligned}$$

or

$$C_{-1,0}^{000}(\rho_a, \rho_b) = A_0(\rho_b)F(\rho_a, \rho_b) + A_0(-\rho_b)G(\rho_a, \rho_b) , \quad (4.9)$$

where the function  $A_0$  is defined by Eqs. (5.1,2) and

$$\left. \begin{aligned} G(\rho_a, \rho_b) &= - \int_{\rho_a + \rho_b}^{\infty} dt e^{-t} t^{-1} , \\ F(\rho_a, \rho_b) &= - \int_{\rho_a - \rho_b}^{\infty} dt [(e^{-t} - 1)t^{-1} + (t + 2\rho_b)^{-1}] . \end{aligned} \right\} \quad (4.10)$$

Note that F and G are well-behaved functions of both arguments except for  $\rho_a = \rho_b = 0$  ; for that special case the value of  $C_{-1,0}^{000}$  is found by the limiting process  $\rho_a \rightarrow 0$  ,  $\rho_b \rightarrow 0$  . The functions F and G can be expressed in terms of exponential integrals and logarithms [see Section 5], namely

$$\left. \begin{aligned} G(\rho_a, \rho_b) &= \text{Ei}(-\rho_a - \rho_b) , \\ F(\rho_a, \rho_b) &= \text{Ei}(-\rho_a + \rho_b) - \log|\rho_a - \rho_b| + \log(\rho_a + \rho_b) . \end{aligned} \right\} \quad (4.11)$$

For the derivatives  $\partial_b F$  and  $\partial_b G$  we find from Eqs. (4.11; 5.14), or also directly from Eqs. (4.10):

$$\left. \begin{aligned} \partial_b G(\rho_a, \rho_b) &= e^{-\rho_a - \rho_b} (\rho_a + \rho_b)^{-1} , \\ \partial_b F(\rho_a, \rho_b) &= - e^{-\rho_a + \rho_b} (\rho_a - \rho_b)^{-1} + (\rho_a + \rho_b)^{-1} + (\rho_a - \rho_b)^{-1} . \end{aligned} \right\} \quad (4.12)$$

Having obtained an explicit expression for  $C_{-1,0}^{000}$  in Eqs. (4.9,10), we proceed now to the functions  $C_{-1, \beta}^{000}$ . We shall repeatedly make use of the following relation,

which follows immediately from the definition (3.1):

$$\rho_b^{-\alpha-\beta-\beta'-\gamma-\delta-2\epsilon-1} C_{\alpha,\beta+\beta'}^{\gamma\delta\epsilon} = \partial_b^\beta \rho_b^{-\alpha-\beta'-\gamma-\delta-2\epsilon-1} C_{\alpha\beta'}^{\gamma\delta\epsilon} . \quad (4.13)$$

Eq. (4.13) permits us to calculate  $C_{-1,\beta}^{000}$  by successive differentiations of  $C_{-1,0}^{000}$ , namely, putting  $\alpha = -1, \beta' = \gamma = \delta = \epsilon = 0$ , we obtain

$$\rho_b^{-\beta} C_{-1,\beta}^{000} = \partial_b^\beta C_{-1,0}^{000} . \quad (4.14)$$

If we substitute in Eq. (4.14) for  $C_{-1,0}^{000}$  the expression (4.9), we see that, because of Eqs. (4.12;5.1) the result may be written in the form

$$\rho_b^{-\beta} C_{-1,\beta}^{000} = A_\beta(-\rho_b)G + (-1)^\beta A_\beta(\rho_b)F + \rho_b^{-\beta} D_{-1,\beta}^{000} , \quad (4.15)$$

where the functions  $D_{-1,\beta}^{000}(\rho_a, \rho_b)$  do not contain any exponential integrals or logarithms. Hence we have proved the validity of Eq. (4.6) for the functions  $C_{-1,\beta}^{000}$ , namely

$$C_{-1,\beta}^{000}(\rho_a, \rho_b) = D_{-1,\beta}^{000}(\rho_a, \rho_b) + E_{-1,\beta}^{000}(\rho_a, \rho_b)F(\rho_a, \rho_b) + E_{-1,\beta}^{000}(-\rho_a, -\rho_b)G(\rho_a, \rho_b) ; \quad (4.16)$$

the functions  $E_{-1,\beta}^{000}$  are actually only functions of  $\rho_b$ , and are given by

$$E_{-1,\beta}^{000}(\rho_a, \rho_b) = (-\rho_b)^\beta A_\beta(\rho_b) . \quad (4.17)$$

We observe that Eq. (4.9) implies that

$$D_{-1,0}^{000} = 0 ; \quad (4.18)$$

we shall now proceed to find a recurrence scheme for the functions  $D_{-1,\beta}^{000}$ . We start with the relation

$$\begin{aligned} \rho_b^{-\beta-2} [C_{-1,\beta+2}^{000} + (\beta+2)C_{-1,\beta+1}^{000}] - \rho_b^{-\beta} [C_{-1,\beta}^{000} + \beta C_{-1,\beta-1}^{000}] \\ = \rho_b^{-\beta-2} [D_{-1,\beta+2}^{000} + (\beta+2)D_{-1,\beta+1}^{000}] - \rho_b^{-\beta} [D_{-1,\beta}^{000} + \beta D_{-1,\beta-1}^{000}] \\ + [A_{\beta+2}(-\rho_b) + (\beta+2)\rho_b^{-1} A_{\beta+1}(-\rho_b) - A_\beta(-\rho_b) - \beta\rho_b^{-1} A_{\beta-1}(-\rho_b)]G \\ + (-1)^\beta [A_{\beta+2}(\rho_b) - (\beta+2)\rho_b^{-1} A_{\beta+1}(\rho_b) - A_\beta(\rho_b) + \beta\rho_b^{-1} A_{\beta-1}(\rho_b)]F , \end{aligned} \quad (4.19)$$

which follows directly from Eq. (4.15) and holds for  $\beta \geq 0$ . The linear combination of the C-functions in (4.19) is chosen so that the coefficients of the functions F

TWO-CENTER INTEGRALS. III

and  $G$  on the right-hand side vanish; this follows from the recurrence relation for the functions  $A_n(x)$ , Eq. (5.7). Making use of Eq. (4.14), we may write then for (4.19)

$$\begin{aligned} \rho_b^{-\beta-2}[D_{-1,\beta+2}^{000} + (\beta+2)D_{-1,\beta+1}^{000}] - \rho_b^{-\beta}[D_{-1,\beta}^{000} + \beta D_{-1,\beta-1}^{000}] \\ = [\partial_b^{\beta+2} + (\beta+2)\rho_b^{-1}\partial_b^{\beta+1} - \partial_b^{\beta} - \beta\rho_b^{-1}\partial_b^{\beta-1}]C_{-1,0}^{000}. \end{aligned} \quad (4.20)$$

The right-hand side of Eq. (4.20) can be further simplified by making use of the general relation

$$\rho_b^{-1}\partial_b^{\beta}\rho_b = \partial_b^{\beta} + \beta\rho_b^{-1}\partial_b^{\beta-1}, \quad (4.21)$$

so that

$$\begin{aligned} \rho_b^{-\beta-2}[D_{-1,\beta+2}^{000} + (\beta+2)D_{-1,\beta+1}^{000}] - \rho_b^{-\beta}[D_{-1,\beta}^{000} + \beta D_{-1,\beta-1}^{000}] \\ = \rho_b^{-1}\partial_b^{\beta}(\partial_b^2 - 1)\rho_b C_{-1,0}^{000}. \end{aligned} \quad (4.22)$$

It is now possible to express the right-hand side of Eq. (4.22) in terms of C-functions with  $\alpha \geq 0$ . First we convert  $(\partial_b^2 - 1)\rho_b C_{-1,0}^{000}$  in the following manner. We insert  $C_{-1,0}^{000}$  as given by Eq. (4.9) and observe that  $(\partial_b - 1)e^{\rho_b} = e^{\rho_b}\partial_b$ ,  $(\partial_b + 1)e^{-\rho_b} = e^{-\rho_b}\partial_b$ , so that

$$\begin{aligned} (\partial_b^2 - 1)\rho_b C_{-1,0}^{000} &= (\partial_b^2 - 1)(-e^{\rho_b}G + e^{-\rho_b}F) \\ &= -(\partial_b + 1)e^{\rho_b}\partial_b G + (\partial_b - 1)e^{-\rho_b}F \\ &= \partial_b(-e^{\rho_b}\partial_b G + e^{-\rho_b}\partial_b F) - e^{\rho_b}\partial_b G - e^{-\rho_b}\partial_b F; \end{aligned}$$

taking  $\partial_b F$  and  $\partial_b G$  from Eq. (4.12), and making use of Eqs. (3.8,10), we find

$$\begin{aligned} (\partial_b^2 - 1)\rho_b C_{-1,0}^{000} &= \partial_b[-2\rho_a(e^{-\rho_a}e^{-\rho_b})/(\rho_a^2 - \rho_b^2)] + 2(\rho_b e^{-\rho_a} - \rho_a e^{-\rho_b})/(\rho_a^2 - \rho_b^2) \\ &= \partial_b \rho_a \rho_b^{-1} C_{00}^{000} + \rho_a \rho_b^{-2} C_{01}^{000} - \rho_b^{-1} C_{10}^{000}; \end{aligned}$$

finally, using Eq. (4.13), this reduces to

$$(\partial_b^2 - 1)\rho_b C_{-1,0}^{000} = 2\rho_a \rho_b^{-2} C_{01}^{000} - \rho_b^{-1} C_{10}^{000}. \quad (4.23)$$

We apply now the operator  $\rho_b^{-1}\partial_b^{\beta}$  to Eq. (4.23), and make use of Eqs. (4.13,21):

$$\begin{aligned}
 \rho_b^{-1} \partial_b^\beta (\partial_b^{2-1}) \rho_b C_{-1,0}^{000} &= 2\rho_a \rho_b^{-1} \partial_b^\beta \rho_b^{-2} C_{01}^{000} - \rho_b^{-1} \partial_b^\beta \rho_b^{-1} C_{10}^{000} \\
 &= 2\rho_a \rho_b^{-1} \partial_b^\beta \rho_b^{-2} C_{01}^{000} - (\partial_b^\beta + \beta \rho_b^{-1} \partial_b^{\beta-1}) \rho_b^{-2} C_{10}^{000} \\
 &= 2\rho_a \rho_b^{-\beta-3} C_{0,\beta+1}^{000} - \rho_b^{-\beta-2} (C_{1\beta}^{000} + \beta C_{1,\beta-1}^{000}) ; \quad (4.24)
 \end{aligned}$$

substituting this result into Eq. (4.22), we obtain the recurrence relation

$$\begin{aligned}
 D_{-1,\beta+2} + (\beta+2)D_{-1,\beta+1} - \rho_b^2 (D_{-1,\beta} + \beta D_{-1,\beta-1}) \\
 = 2\rho_a \rho_b^{-1} C_{0,\beta+1}^{000} - C_{1\beta}^{000} - \beta C_{-1,\beta-1}^{000} . \quad (4.25)
 \end{aligned}$$

In order to calculate the functions  $D_{-1,\beta}^{000}$  from Eq. (4.25), we need, aside from the C-functions on the right-hand side, which were dealt with in Section 3, also the starting functions  $D_{-1,0}^{000}$  and  $D_{-1,1}^{000}$ . The former is given by Eq. (4.18); the latter we obtain by direct application of Eq. (4.14):

$$C_{-1,1}^{000} = \rho_b \partial_b C_{-1,0}^{000} = \rho_b \partial_b \rho_b^{-1} (-e^{\rho_b G} + e^{-\rho_b F}) ,$$

or

$$D_{-1,1}^{000} = -e^{\rho_b G} \partial_b G + e^{-\rho_b F} \partial_b F ;$$

in view of Eqs. (4.12; 3.8,10) this reduces to

$$D_{-1,1}^{000} = \rho_a \rho_b^{-1} C_{00}^{000} . \quad (4.26)$$

The recurrence relation (4.25) enables us to express each D-function in terms of three D-functions with a lower index  $\beta$  and C-functions known from Section 3. However, we can carry out this recurrence scheme in two steps, each step by itself being simpler than Eq. (4.25). Namely if we define a new set of auxiliary functions  $D_\beta(\rho_a, \rho_b)$  by

$$D_\beta = D_{-1,\beta}^{000} + \beta D_{-1,\beta-1}^{000} , \quad (4.27)$$

then we may write for Eq. (4.25)

$$D_{\beta+2} - \rho_b^2 D_\beta = 2\rho_a \rho_b^{-1} C_{0,\beta+1}^{000} - C_{1\beta}^{000} - \beta C_{1,\beta-1}^{000} . \quad (4.28)$$

We can now use Eq. (4.28) as a recurrence relation to calculate the functions  $D_\beta$ . For that purpose we still need the starting functions  $D_0$  and  $D_1$ ; they follow from

TWO-CENTER INTEGRALS. III

Eq. (4.27) for  $\beta = 0$  and  $\beta = 1$ , respectively, and Eqs. (4.18,26), namely

$$\left. \begin{aligned} D_0 &= 0, \\ D_1 &= \rho_a \rho_b^{-1} C_{00}^{000}. \end{aligned} \right\} \quad (4.29)$$

Once the functions  $D_\beta$  are found from Eqs. (4.28,29), we can then use Eq. (4.27) as a recurrence relation to calculate the functions  $D_{-1,\beta}^{000}$ ; no starting D-functions are needed in this case. If desired, we can also use instead of Eq. (4.27) the following explicit expression of D-functions in terms of D-functions:

$$D_{-1,\beta}^{000} = \sum_{k=0}^{\beta} (-1)^{\beta-k} (\beta!/k!) D_k, \quad (4.30)$$

which follows easily from Eq. (4.27).

Which one of the two alternative recurrence schemes is to be used for calculating the functions  $D_{-1,\beta}^{000}$  --the direct scheme of Eqs. (4.18,25,26) or the scheme employing the auxiliary functions  $D_\beta$  --is of course a matter of taste. The first method has the advantage of directness, whereas the second method consists of more, but simpler, steps.

c. Raising of the Upper Indices and Lowering of the Index  $\alpha$

In order to raise the upper indices we can directly use the methods developed in Section 3c, since the derivations in that section are completely independent of whether  $\alpha$  is positive, zero, or negative.

Actually the application of those methods are more economical for  $\alpha < 0$  than for  $\alpha \geq 0$ . Consider for example Eq. (3.11). If  $\alpha \geq 0$  one has first to raise  $\alpha$  (and  $\beta$ ) by two additional units before  $\gamma$  can be raised by one unit. However, if  $\alpha \leq -2$ , the situation is more pleasant: here  $\alpha+2$  corresponds to a previous step on the recurrence ladder which starts with  $\alpha = -1$  and proceeds to  $\alpha = -2, -3, -4, \dots$ ; therefore it is not necessary to make a detour via  $\alpha$ -values which are not actually needed.

The situation with respect to  $\beta$  on the other hand is of course unchanged, and since C-functions with  $\beta = 1$  and  $\gamma+\delta+2\epsilon = 4$  are finally needed, it is necessary to start with the set  $C_{-1,\beta}^{000}$ , where  $\beta = 0, 1, 2, \dots 9$ . This case is indeed simpler than the one for the case  $\alpha \geq 0$ : there we had to start with the set  $C_{\alpha\beta}^{000}$ , where  $\alpha$  and  $\beta$  assumed the values  $0, 1, 2, \dots 9$ .

In Fig. 5 the different pyramids represent different negative values of  $\alpha$ ; due to the restriction (4.1) they become progressively smaller for decreasing  $\alpha$ . The arrows

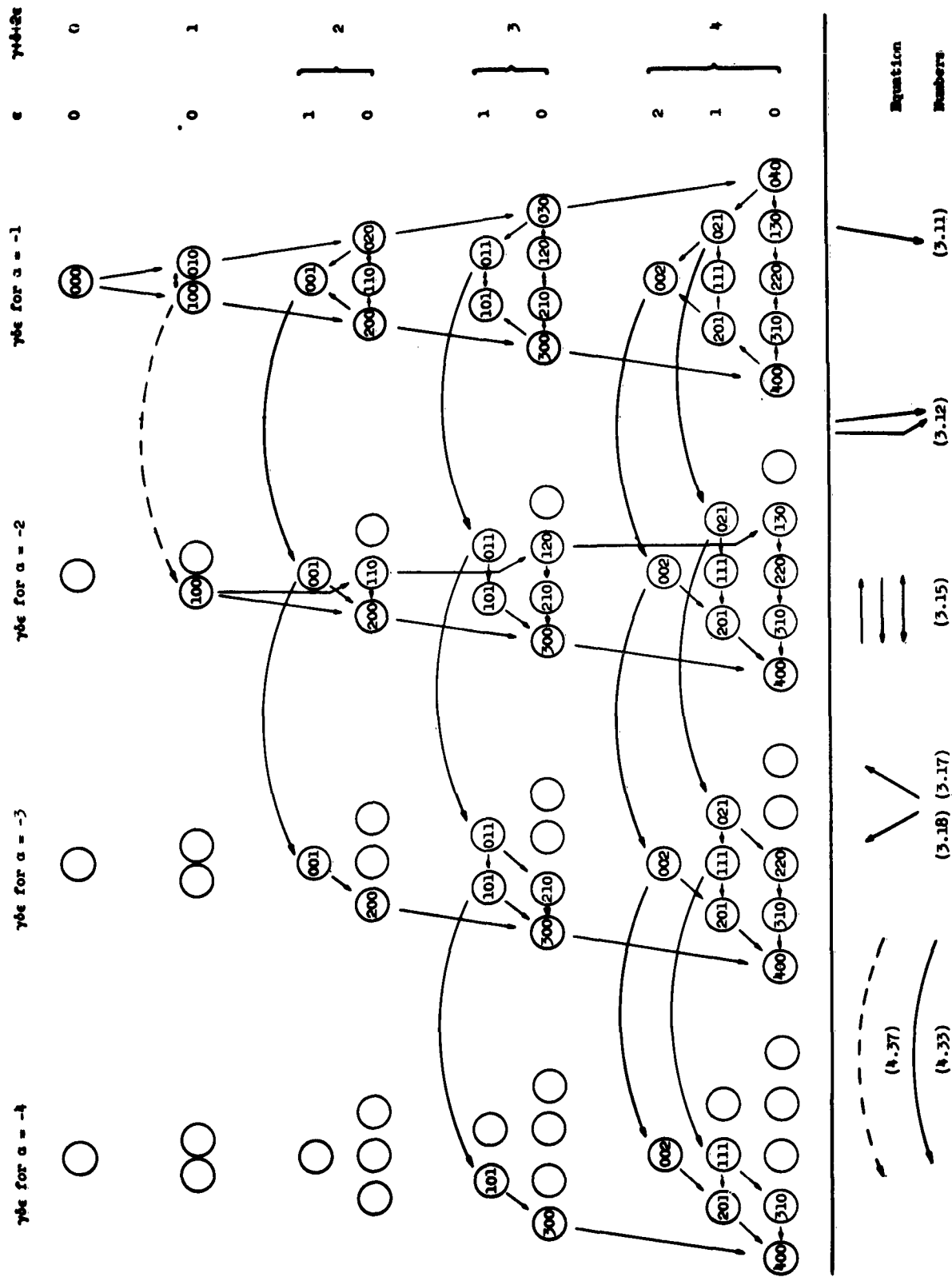


Fig. 5. A Possible Scheme for Lowering the Index  $\alpha$  and Raising the Indices  $\beta$ .

TWO-CENTER INTEGRALS. III

within each pyramid represent applications of the formulas (3.11-19); the interconnections between different pyramids are indicated by curved arrows, corresponding to formulas for lowering  $\alpha$  which we shall now derive.

We start with the case  $\alpha < -1$ ,  $\epsilon \geq 1$ . From the identities

$$(\alpha+1)(\xi+\eta)^\alpha = (\partial/\partial\xi)(\xi+\eta)^{\alpha+1} = (\partial/\partial\eta)(\xi+\eta)^{\alpha+1}, \quad (4.31)$$

we obtain by partial integration with respect to  $\xi$  and  $\eta$

$$\begin{aligned} (\alpha+1)C_{\alpha\beta}^{\gamma\delta\epsilon} &= -(-1)^{\beta+\delta+\epsilon} (\frac{1}{2}\rho_b)^{\alpha+\beta+\gamma+\delta+2\epsilon+1} \int_1^\infty d\xi \int_{-1}^1 d\eta (\xi+\eta)^{\alpha+1} \\ &\times \left\{ \frac{\partial/\partial\xi}{\partial/\partial\eta} \right\} e^{-\rho\xi-\tau\rho\eta} (\xi-\eta)^\beta (1+\xi\eta)^\gamma (1-\xi\eta)^\delta (\xi^2-1)^\epsilon (1-\eta^2)^\epsilon, \end{aligned} \quad (4.32)$$

since the integrated parts vanish for  $\epsilon \geq 1$ . Adding the two Eqs. (4.32) and performing the indicated differentiations, we obtain

$$(\alpha+1)\rho_b C_{\alpha\beta}^{\gamma\delta\epsilon} = \rho_a C_{\alpha+1,\beta}^{\gamma\delta\epsilon} - \gamma C_{\alpha+2,\beta}^{\gamma-1,\delta\epsilon} - \delta C_{\alpha+2,\beta}^{\gamma,\delta-1,\epsilon} - 2\epsilon C_{\alpha+2,\beta}^{\gamma,\delta+1,\epsilon-1}. \quad (4.33)$$

Eq. (4.33) lowers  $\alpha$  if  $\epsilon \geq 1$  and is represented in Fig. 5 by solid curved arrows.

Turning now to the case  $\epsilon = 0$ , we observe first that if  $\gamma \geq 2$  we do not need a direct formula for lowering  $\alpha$ . Namely by virtue of Eq. (3.17) we may write

$$C_{\alpha\beta}^{\gamma\delta 0} = C_{\alpha\beta}^{\gamma-2,\delta 1} + C_{\alpha+2,\beta}^{\gamma-2,\delta 0}, \quad (4.34)$$

and Eq. (4.33) may now be applied to the first term on the right-hand side of Eq. (4.34). Next we note that if  $\epsilon = 0$ ,  $\alpha \leq -3$ , the condition (4.1) yields  $\gamma \geq 2$ . Hence the only case we still have to deal with separately is  $\alpha = -2$ ,  $\epsilon = 0$ ,  $\gamma \leq 1$ ; because of the condition (4.1) this narrows down to  $\gamma = 1$ . We shall deal with this case by deriving a special formula for  $C_{-2,\beta}^{100}$ ; after that the index  $\delta$  can always be raised in single steps by means of Eq. (3.12), or in double steps by means of Eq. (3.18).

We derive first a formula for  $C_{-2,0}^{100}$ . We perform again partial integrations as in the derivation of Eq. (4.33); however, due to  $\epsilon = 0$ , we obtain now additional terms, since the integrated parts do not vanish

$$\left. \begin{aligned} C_{-2,0}^{100} &= \int_{-1}^1 d\eta e^{-\rho-\tau\rho\eta} + \int_1^\infty d\xi \int_{-1}^1 d\eta (\xi+\eta)^{-1} (\partial/\partial\xi) e^{-\rho\xi-\tau\rho\eta} (1+\xi\eta), \\ C_{-2,0}^{100} &= -\int_1^\infty d\xi e^{-\rho\xi} (e^{-\tau\rho} + e^{\tau\rho}) + \int_1^\infty d\xi \int_{-1}^1 d\eta (\xi+\eta)^{-1} (\partial/\partial\eta) e^{-\rho\xi-\tau\rho\eta} (1+\xi\eta). \end{aligned} \right\} \quad (4.35)$$

We add the two Eqs. (4.35), perform the indicated differentiations, and evaluate the single integrals; the result is

$$C_{-2,0}^{100} = -2(\rho_a e^{-\rho_a} e^{-\rho_b}) / (\rho_a^2 - \rho_b^2) - \rho_a \rho_b^{-1} C_{-1,0}^{100} + \rho_b^{-1} C_{00}^{000} ;$$

by virtue of Eqs. (3.8,10) we may write for this

$$C_{-2,0}^{100} = -\rho_a \rho_b^{-1} C_{-1,0}^{100} - \rho_b^{-1} C_{00}^{000} - \rho_b^{-1} C_{01}^{000} + \rho_a \rho_b^{-2} C_{10}^{000} . \quad (4.36)$$

We can now easily proceed to  $C_{-2,\beta}^{100}$  by applying to Eq. (4.36) the operator  $\rho_b^{\beta+1} \partial_b^\beta$ , yielding [see Eqs. (4.13,21)]

$$\rho_b C_{-2,\beta}^{100} = -\rho_a C_{-1,\beta}^{100} - (\beta+1) C_{0\beta}^{000} - C_{0,\beta+1}^{000} + \rho_a \rho_b^{-1} C_{1\beta}^{000} . \quad (4.37)$$

This equation is represented in Fig. 5 by the dashed curved arrow.

Finally we must show that all the C-functions with  $\alpha < 0$  have the form (4.6). Since we saw already that  $C_{-1,\beta}^{000}$  had that form, we only have to show that the form (4.6) is preserved when the upper indices are raised or  $\alpha$  is lowered. These proofs are very simple; as an example we show it for Eq. (4.33) with  $\alpha = -2$ :

$$\rho_b C_{-2,\beta}^{\gamma\delta\epsilon} = -\rho_a C_{-1,\beta}^{\gamma\delta\epsilon} + \gamma C_{0\beta}^{\gamma-1,\delta\epsilon} + \delta C_{0\beta}^{\gamma,\delta-1,\epsilon} + 2\epsilon C_{0\beta}^{\gamma,\delta+1,\epsilon-1} .$$

Now, by assumption, the form (4.6') holds for  $C_{-1,\beta}^{\gamma\delta\epsilon}$ , so that

$$\begin{aligned} \rho_b C_{-2,\beta}^{\gamma\delta\epsilon} &= -\rho_a D_{-1,\beta}^{\gamma\delta\epsilon} + \gamma C_{0\beta}^{\gamma-1,\delta\epsilon} + \delta C_{0\beta}^{\gamma,\delta-1,\epsilon} + 2\epsilon C_{0\beta}^{\gamma,\delta+1,\epsilon-1} \\ &\quad - \rho_a E_{-1,\beta}^{\gamma\delta\epsilon} - \rho_a \bar{E}_{-1,\beta}^{\gamma\delta\epsilon} ; \end{aligned}$$

hence  $C_{-2,\beta}^{\gamma\delta\epsilon}$  also has the form (4.6'), and specifically

$$\begin{aligned} \rho_b D_{-2,\beta}^{\gamma\delta\epsilon} &= -\rho_a D_{-1,\beta}^{\gamma\delta\epsilon} + \gamma C_{0\beta}^{\gamma-1,\delta\epsilon} + \delta C_{0\beta}^{\gamma,\delta-1,\epsilon} + 2\epsilon C_{0\beta}^{\gamma,\delta+1,\epsilon-1} , \\ \rho_b E_{-2,\beta}^{\gamma\delta\epsilon} &= -\rho_a E_{-1,\beta}^{\gamma\delta\epsilon} . \end{aligned}$$

It is also clear now how any one of the recurrence relations (3.11-19; 4.33,37) yields a recurrence relation for the D- and E-functions. Namely such a relation for the D-(E-)functions is obtained from the corresponding relation for the C-functions by changing the C-functions with negative  $\alpha$ 's into D-(E-)functions, and retaining (omitting) the C-functions with non-negative  $\alpha$ 's.

d. The Limiting Cases  $\rho = 0$  and  $\tau = 0$

For the same reason as in Section 3d special formulas have to be given for the functions  $C_{\alpha\beta}^{\gamma\delta\epsilon}$  ( $\alpha < 0$ ) if  $\rho = 0$  or  $\tau = 0$ . They were again derived in two different ways (see below).

TWO-CENTER INTEGRALS. III

Consider first the case  $\rho = 0$ . The first method was the expansion of the exponentials and exponential integrals (see Section 5b) and subsequent passage to the limit  $\rho = 0$  in the general formulas. It should be mentioned that the parts  $D_{\alpha\beta}^{\gamma\delta\epsilon}$  and  $E_{\alpha\beta}^{\gamma\delta\epsilon} F + \bar{E}_{\alpha\beta}^{\gamma\delta\epsilon} G$  each become infinite for  $\rho \rightarrow 0$ ; only their sum remains finite. The second method was the application of Eq. (3.20). It has to be noted that the only condition for the validity of Eq. (3.20) is

$$\alpha + \beta + \gamma + \delta + 2\epsilon \geq 0, \quad (4.38)$$

as Eq. (3.22) shows. Now, since the volume element always contributes the factor  $\xi - \eta$ , we have always  $\beta \geq 1$ , and this fact in conjunction with the condition (4.1) yields

$$\alpha + \beta + \gamma + 2\epsilon \geq 0, \quad (4.39)$$

so that the condition (4.38) is always satisfied and Eq. (3.20) applies also if  $\alpha < 0$ .

In the case  $\tau = 0$  the first method was again the expansion of exponentials and exponential integrals in the general formulas. The second method was as follows: First, by expansion, we calculated  $E_{-1,\beta}^{000} F + \bar{E}_{-1,\beta}^{000} G$  and  $D_1$  for  $\rho_a = \rho_b = \rho$ . Next, we calculated  $D_\beta$  and subsequently  $D_{-1,\beta}$  by means of the recurrence relations (4.27,28) (depending now only on  $\rho$ ). Finally, we calculated  $C_{\alpha\beta}^{\gamma\delta\epsilon}$  using Eqs. (3.11-19) and (4.33,37) (again depending only on  $\rho$ ).

The agreement of the results obtained by the two different methods constituted a further check of the derived formulas. A final check was the agreement found by putting  $\rho = 0$  in the formulas for  $\tau = 0$ , and  $\tau = 0$  in the formulas for  $\rho = 0$ .

By means of the methods described in Section 4b, c, and d, explicit formulas were calculated for the 84 C-functions listed in Table XIIb. They were needed in order to establish the 65 among them appearing in Tables VII and IX. The formulas for the latter are given in Tables XIII, XIV, and XV. In addition, these tables also contain the seven functions  $C_{-1,\beta}^{000}$  ( $\beta = 3,4,5,6,7,8,9$ ). The latter have rather long expressions, and their derivation is lengthy; since they form the "basis" from which all other C-functions with  $\alpha < 0$  are rather easily obtained, their inclusion was considered useful. Formulas for C-functions contained in Table XIIb, but not in Tables XIII, XIV, and XV, can be made available upon demand.

5. THE EXPONENTIAL INTEGRAL AND RELATED FUNCTIONS

a. The Functions  $A_n(x)$ ,  $B_n(x)$

For convenience some properties of the well-known functions<sup>17</sup>  $A_n(x)$ ,  $B_n(x)$  are here collected. They may be defined by the formulas

$$A_n(x) = (-d/dx)^n(e^{-x}/x) = \int_1^{\infty} dt e^{-xt}t^n, \quad (5.1)$$

$$(-1)^{n+1}A_n(-x) = (-d/dx)^n(e^x/x) = \int_{-1}^{\infty} dt e^{-xt}t^n, \quad (5.2)$$

$$B_n(x) = (-d/dx)^n[(e^x - e^{-x})/x] = \int_{-1}^1 dt e^{-xt}t^n, \quad (5.3)$$

whence

$$B_n(x) = (-1)^{n+1}A_n(-x) - A_n(x). \quad (5.4)$$

The definitions of  $A_n(x)$  and  $A_n(-x)$  by means of the integrals are only valid for  $x > 0$ .

From the definitions (5.1-3) follow the recurrence relations

$$A_{n+1}(x) = (-d/dx)A_n(x), \quad (5.5)$$

$$B_{n+1}(x) = (-d/dx)B_n(x), \quad (5.6)$$

$$xA_n(x) = nA_{n-1}(x) + e^{-x}, \quad (5.7)$$

$$xB_n(x) = nB_{n-1}(x) - e^{-x} + (-1)^ne^x, \quad (5.8)$$

and the explicit formulas

$$A_n(x) = (n!/x^{n+1})e^{-x} \sum_{k=0}^n (x^k/k!), \quad (5.9)$$

$$B_n(x) = 2(n!/x^{n+1})[\sinh x \sum_{k=0}^n (x^k/n!) - \cosh x \sum_{k=1}^n (x^k/k!)], \quad (5.10)$$

where  $\sum_k^e$  sums only the terms with even  $k$ , and  $\sum_k^o$  the terms with odd  $k$ .

The functions  $A_n(x)$  of Eq. (5.1) have a simple connection with the  $\Gamma$ -function

$$\Gamma(n+1) = \int_0^{\infty} dt e^{-t}t^n = n! \quad (5.11)$$

and the incomplete  $\Gamma$ -function<sup>18</sup>

<sup>17</sup>See, e.g., (I), Eq. (24) and (II), Eqs. (3.15,18) and (2.27,28).

<sup>18</sup>See, e.g., E. Jahnke and F. Emde, Tables of Functions (Dover: New York, 1945), p. 25.

TWO-CENTER INTEGRALS. III

$$\Gamma(n+1, x) = \int_0^x dt e^{-t} t^n, \quad (5.12)$$

namely:

$$\Gamma(n+1) = \Gamma(n+1, x) + x^{n+1} A_n(x). \quad (5.13)$$

b. The Exponential Integral

The exponential integral  $E_1(z)$  is the analytic function in the complex plane defined by<sup>19</sup>

$$(d/dz)E_1(z) = e^z z^{-1}, \quad (5.14)$$

$$E_1(-\infty+0i) = 0, \quad (5.15)$$

whence

$$E_1(z) = \int_{-\infty}^z d\zeta e^{\zeta} \zeta^{-1}. \quad (5.16)$$

For  $z = 0$  the integral has a logarithmic singularity; therefore the complex plane is slit along the positive real axis from zero to infinity, and the principal value of  $E_1(z)$  is defined by (5.16) if the path of integration from  $(-\infty+0i)$  to  $z$  does not cross the positive real axis. There seems to be no established convention for the definition of the principal value of  $E_1(z)$  on the positive real axis. For the present analysis it is advantageous to let the positive real axis belong to the upper right quarter plane.

Expanding the exponential in (5.16) and integrating term by term one obtains

$$E_1(z) = K + \log z + \sum_{n=1}^{\infty} z^n/n!n, \quad (5.17)$$

since the convergence of the series (5.17) is obvious (the series converges more strongly than the exponential series). The value of the integration constant  $K$  depends on whether  $z$  is located in the upper or lower half of the complex plane; this is due to the fact that in the definition of  $E_1(z)$  it is customary to adopt a cut along the positive real axis, whereas for  $\log z$  one adopts a cut along the negative real axis. It should further be noted that for  $\log z$  the negative real axis belongs by definition to the upper left quarter plane; for this reason it was convenient to include for  $E_1(z)$

<sup>19</sup>See reference 18, p. 1.

the positive real axis in the upper right quarter plane. We shall now evaluate the constant K. From Eq. (5.17) follows

$$K = \lim_{z \rightarrow 0} [Ei(z) - \log z] = \lim_{z \rightarrow 0} \left( \int_{-\infty}^z d\zeta e^{\zeta} \zeta^{-1} - \int_1^z d\zeta \zeta^{-1} \right). \quad (5.18)$$

We adopt the paths of integration indicated in Fig. 6; they comply with the conventions discussed above. We then obtain for the constant K

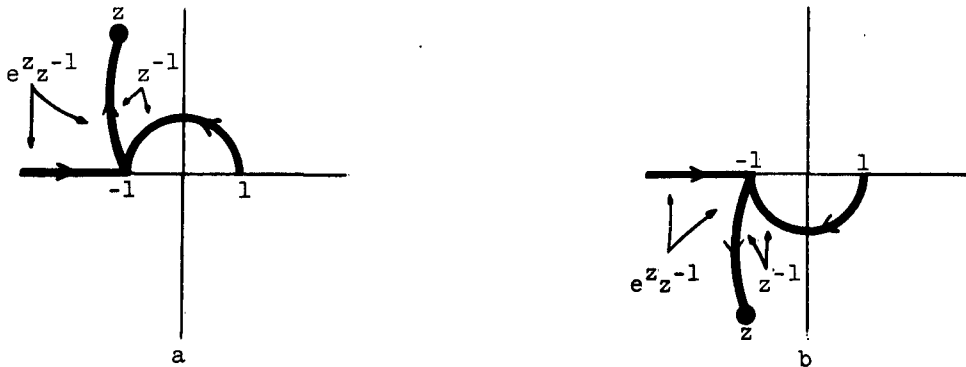


Fig. 6. Paths of integration for the evaluation of K: a)  $\text{Im}(z) \geq 0$ ; b)  $\text{Im}(z) < 0$ .

$$\begin{aligned} K &= \int_{-\infty}^{-1} d\zeta e^{\zeta} \zeta^{-1} + \lim_{z \rightarrow 0} \int_{-1}^z d\zeta (e^{\zeta} - 1) \zeta^{-1} - \int_1^{-1} d\zeta \zeta^{-1} \\ &= - \int_1^{\infty} dt e^{-t} t^{-1} + \int_0^1 dt (1 - e^{-t}) t^{-1} - \int_1^{-1} d\zeta \zeta^{-1}. \end{aligned}$$

The last integral is different according to whether  $\text{Im}(z) \geq 0$  or  $\text{Im}(z) < 0$ , and yields  $\pm \pi i$ , respectively; hence

$$K = \begin{cases} C - \pi i & \text{if } \text{Im}(z) \geq 0, \\ C + \pi i & \text{if } \text{Im}(z) < 0, \end{cases} \quad (5.19)$$

where

$$C = - \int_1^{\infty} dt e^{-t} t^{-1} + \int_0^1 dt (1 - e^{-t}) t^{-1} \quad (5.20)$$

is Euler's constant.

For real  $x$  Eqs. (5.17,19) yield

$$Ei(x) = C + \log|x| + \sum_{n=1}^{\infty} x^n / n!n, \quad x < 0, \quad (5.21)$$

$$Ei(x \pm 0i) = C + \log x + \sum_{n=1}^{\infty} x^n / n!n \mp \pi i, \quad x > 0; \quad (5.21')$$

by definition:

TWO-CENTER INTEGRALS. III

$$Ei(x+0i) = Ei(x) , \quad x > 0 . \quad (5.22)$$

It is now useful to define a new real function  $\overline{Ei}(x)$  by means of

$$\overline{Ei}(x) = \frac{1}{2}[Ei(x+0i) + Ei(x-0i)] ; \quad (5.23)$$

in view of Eqs. (5.21-23) we obtain

$$\overline{Ei}(x) = Ei(x) , \quad x < 0 , \quad (5.24)$$

$$\overline{Ei}(x) = Ei(x) + \pi i , \quad x > 0 , \quad (5.24')$$

and explicitly

$$\overline{Ei}(x) = C + \log|x| + \sum_{n=1}^{\infty} x^n/n!n , \quad (5.25)$$

which holds for positive and negative values of  $x$ .  $\overline{Ei}(x)$  is a function different from  $Ei(x)$ ; it is only defined on the real axis and is not an analytical function in the complex plane. Its importance is based on the fact that it is also given by the integral

$$\overline{Ei}(x) = \int_{-\infty}^x dt e^{t}t^{-1} = - \int_{-x}^{\infty} dt e^{-t}t^{-1} , \quad (5.26)$$

if this integral is interpreted for positive values of  $x$  by its principal value. This is easily verified by integrating  $e^z z^{-1}$  along the path indicated in Fig. 7; this yields

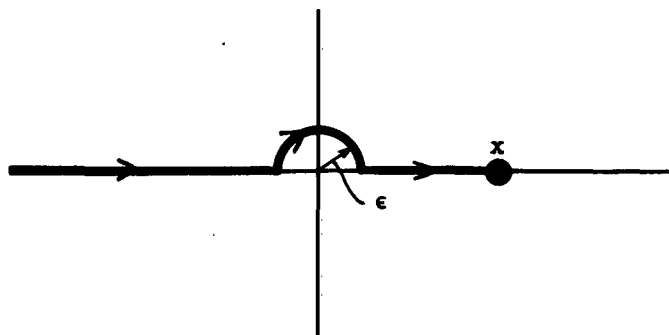


Fig. 7. Path of integration for the relation between  $Ei(x)$  and  $\overline{Ei}(x)$

for  $x > 0$

$$Ei(x) = \lim_{\epsilon \rightarrow 0} \left( \int_{-\infty}^{-\epsilon} dt e^t/t + \int_{\epsilon}^x dt e^t/t \right) - \pi i ,$$

or, because of Eq. (5.24'),

$$\overline{Ei}(x) = \lim_{\epsilon \rightarrow 0} \left( \int_{-\infty}^{-\epsilon} dt e^t/t + \int_{\epsilon}^x dt e^t/t \right) . \quad (5.27)$$

For negative values of  $x$ , Eq. (4.26) is obvious in view of Eqs. (5.16,24).

The exponential integral which occurs in Section 4 actually is the function  $\overline{Ei}(x)$  in all instances. However, since numerical tables<sup>22</sup> mostly use the notation  $Ei(x)$  for the function  $\overline{Ei}(x)$ , we have also written  $Ei(x)$  instead of  $\overline{Ei}(x)$  in Section 4.

c. Connections Between the Functions  $A_n(x)$  and the Exponential Integral

From Eqs. (5.2,14,26) follows

$$\begin{aligned} -(-d/dx)^{n+1} Ei(-x) &= -(-d/dx)^{n+1} \overline{Ei}(-x) \\ &= (-d/dx)^n (e^{-x} x^{-1}) = A_n(x) . \end{aligned} \quad (5.28)$$

Now the generalized exponential integrals  $E_n(x)$  are defined by<sup>20</sup>

$$\left. \begin{aligned} E_0(x) &= e^{-x} x^{-1} , \quad E_1(x) = -Ei(-x) , \\ (n-1)! E_n(x) &= (-x)^{n-1} E_1(x) + e^{-x} \sum_{k=0}^{n-2} (n-2-k)! (-x)^k , \quad n \geq 2 . \end{aligned} \right\} \quad (5.29)$$

From Eqs. (5.29) follows the differential relation

$$(-d/dx) E_n(x) = E_{n-1}(x) , \quad n \geq 1 , \quad (5.30)$$

and the recurrence formula

$$(n-1) E_n(x) = e^{-x} - x E_{n-1}(x) , \quad n \geq 1 ; \quad (5.31)$$

if we eliminate  $E_{n-1}(x)$  from Eqs. (5.30,31) we find the second differential relation

$$(-d/dx)[E_n(x) x^{-n+1}] = e^{-x} x^{-n} , \quad n \geq 0 .^{21} \quad (5.32)$$

<sup>20</sup>See: G. Placzek, "The Functions  $E_n(x)$ ", and J. Lecaine, "Integrals Involving the Functions  $E_n(x)$ ", edited by the National Research Council of Canada, NRC No. 1547 and No. 1553. Our definitions are those used by the Canadian authors.

<sup>21</sup>Although Eq. (5.32) has been established by this derivation only for  $n \geq 1$ , it is easily verified that it still holds for  $n = 0$ .

TWO-CENTER INTEGRALS. III

If Eq. (5.28) is rewritten as

$$A_n(x) = (-d/dx)^{n+1}E_1(x) = (-d/dx)^nE_0(x), \quad (5.33)$$

it becomes apparent that the functions

$$\dots E_n(x) \dots E_2(x), E_1(x), E_0(x) = A_0(x), A_1(x), A_2(x), \dots A_n(x) \dots$$

form one sequence in the sense that the operation  $-d/dx$  applied to any member of the sequence produces the next member to the right.

The relations (5.32) suggest that it should be possible to express the functions  $C_{\alpha\beta}^{\gamma\delta\epsilon}$  for  $\alpha < 0$  by means of the functions  $E_1, E_2, \dots, E_{|\alpha|}$ . Although this was found to be true, this procedure proved to be less simple than the one described in Section 4.

d. Numerical Computation of the Function EI(x)

Several methods are available for the computation of the exponential integral in cases where the available Tables<sup>22</sup> are not sufficient.

- (1) Computation by means of the expansion (5.25). This method is particularly easy for small values of  $|x|$ , but it is also feasible for larger values of  $|x|$ .
- (2) For very large values of  $|x|$  the asymptotic expansion<sup>23</sup>

$$EI(x) = (e^x x^{-1})(1+x^{-1}+2!x^{-2}+3!x^{-3}+ \dots) \quad (5.34)$$

can be used. However it cannot give even 10 significant figures for  $x \leq 20$ .

- (3) A new method of computation was found convenient in conjunction with the functions  $A_n(x)$ . By virtue of Eq. (5.28) one has the Taylor expansion

$$EI(x+h) = EI(x) - \sum_{k=1}^{\infty} (h^k/k!)A_{k-1}(-x), \quad (5.35)$$

which is useful in the intermediate region where the expansion discussed under (1) converges but slowly and the expansion mentioned under (2) does not yield enough significant figures.

This method proved particularly convenient in conjunction with Kotani's

<sup>22</sup>Tables of Sine, Cosine, and Exponential Integral, National Bureau of Standards (N. Y. M. T. P., 1940); Mathematical Tables of the British Association for the Advancement of Science (London, 1931), Vol. 1, p. 31.

<sup>23</sup>See, e.g., E. T. Whittaker and G. N. Watson, Modern Analysis (Cambridge University Press, 1946), p. 150.

tables,<sup>24</sup> which give values of the functions  $E_1(-x)$  and  $A_n(x)$  for  $x$ -values up to 24 in steps of 1.0 or closer. Thus  $\overline{EI}(-x)$  was easily obtained for any argument value  $> 15$ , where no tables exist and where the asymptotic expansion was found to be inadequate. For  $10 < x < 15$  this method was preferred to the use of Everett interpolation in the British Tables,<sup>22</sup> since the available tables of Everett coefficients did not have close enough entries. Finally the method was also used with ease for  $x < 10$  in order to obtain more significant figures than present tables<sup>22</sup> provide.

The computation of  $\overline{EI}(x)$  for  $x > 0$  by means of Eq. (5.35) requires the function  $A_n(-x)$ . By virtue of Eq. (5.4) the latter can be constructed from the functions  $A_n(x)$  and  $B_n(x)$ , which are contained in Kotani's tables.

- (4) Another method for computing exponential integrals has been used by Kotani;<sup>24</sup> namely the expansion

$$-EI[-(x+h)] = -EI(-x) + e^{-x} \sum_{n=0}^{\infty} (-x)^{-n-1} K_n(h), \quad (5.36)$$

where

$$K_n(h) = n! - h^{n+1} A_n(h). \quad (5.37)$$

Eq. (5.37) follows from

$$\begin{aligned} -EI(-x-h) + EI(-x) &= - \int_x^{x+h} dt e^{-t} t^{-1} \\ &= - e^{-x} \int_0^h dt e^{-t} (x+t)^{-1} = e^{-x} \sum_{n=0}^{\infty} (-x)^{-n-1} \int_0^h dt e^{-t} t^n \end{aligned}$$

and Eqs. (5.11,12,13). The functions  $K_n(h)$  defined by Eq. (5.37) satisfy the recurrence relation

$$\left. \begin{aligned} K_n(h) &= nK_{n-1}(h) - h^n e^{-h}, \\ K_0(h) &= 1 - e^{-h}. \end{aligned} \right\} \quad (5.38)$$

- (5) Approximations of the exponential integral by rational functions (quotients of two polynomials) have been given by Hastings.<sup>25</sup>

<sup>24</sup>See (I), Section 5, for a description of these useful tables.

<sup>25</sup>C. Hastings, Approximations in Numerical Analysis (The Rand Corporation, Los Angeles).

TABLE XII  
C-FUNCTIONS WITH FORMULAS ESTABLISHED

(a) C-functions with  $\alpha \geq 0$

$\alpha\beta$	$\gamma\delta\epsilon$
All values in Figure 2	000
All values in Figure 2 above line denoted "1", except cases with $\beta = 0$	100 010
All values in Figure 2 above line denoted "2", except cases with $\beta = 0$	200 110 020 001
All values in Figure 2 above line denoted "3", except cases with $\beta = 0$	300 210 120 030 101 011
All values in Figure 2 above line denoted "4", except cases with $\beta = 0$	400 310 220 130 040 201 111 002

(b) C-functions with  $\alpha < 0$

$\alpha\beta$	$\gamma\delta\epsilon$
$\alpha = -1$ $1 \leq \beta \leq 9$	000
$\alpha = -1$ $1 \leq \beta \leq 2$	010
$\alpha = -1$ $4 \leq \beta \leq 5$	001
$-2 \leq \alpha \leq -1$ $1 \leq \beta \leq 3$	100
$-2 \leq \alpha \leq -1$ $1 \leq \beta \leq 2$	110
$-2 \leq \alpha \leq -1$ $\beta = 1$	120
$-2 \leq \alpha \leq -1$ $\beta = 2$	210 011
$-3 \leq \alpha \leq -1$ $1 \leq \beta \leq 3$	001
$-3 \leq \alpha \leq -1$ $1 \leq \beta \leq 2$	200
$-3 \leq \alpha \leq -1$ $\beta = 1$	210 011 021
$-4 \leq \alpha \leq -1$ $1 \leq \beta \leq 2$	300 101
$-4 \leq \alpha \leq -1$ $\beta = 1$	310 201 111 002

TABLE XIII

EXPLICIT FORMULAS FOR C-FUNCTIONS IN THE CASE  $\rho \neq 0$ ,  $\tau \neq 0$

Note: C-functions with negative  $\alpha$  are obtained from the corresponding D- and E-functions listed in the table according to Eqs. (4.6, 11).

Functions with  $\gamma + \delta + 2\epsilon = 0$

(1)  $\beta, \gamma, \delta\epsilon = 1, 0, 0, 0$ ;  $-1 \leq \alpha \leq 4$

$$D_{-1,1}^{000} = \rho_a^{-1}(\kappa+1)\{-e^{-\rho_a} + e^{-\rho_b}\}$$

$$E_{-1,1}^{000} = -\rho_b^{-1}(1+\rho_b)e^{-\rho_b} = -\rho_b A_1(\rho_b)$$

$$C_{01}^{000} = \rho_b^{-1}(\kappa-1)\{- (\kappa-1)e^{-\rho_a} + [(\kappa-1)-\rho_b]e^{-\rho_b}\}$$

$$C_{11}^{000} = \rho_a^{-1}(\kappa-1)\{- (\kappa-1)[2(\kappa+1)+\rho_a]e^{-\rho_a} + (\kappa+1)[2(\kappa-1)-\rho_b]e^{-\rho_b}\}$$

$$C_{21}^{000} = \rho_b^{-1}(\kappa+1)^{-1}(\kappa-1)^2\{- (\kappa-1)[2(\kappa+1)(3\kappa+2)+4(\kappa+1)\rho_a+\rho_a^2]e^{-\rho_a} + (\kappa+1)[2(\kappa-1)(3\kappa+2)-(2\kappa+1)\rho_b]e^{-\rho_b}\}$$

$$C_{31}^{000} = \rho_a^{-1}(\kappa+1)^{-1}(\kappa-1)^2\{- (\kappa-1)[6(\kappa+1)^2(4\kappa+1)+6(\kappa+1)(3\kappa+2)\rho_a+6(\kappa+1)\rho_a^2+\rho_a^3]e^{-\rho_a} + (\kappa+1)^2[6(\kappa-1)(4\kappa+1)-6\kappa\rho_b]e^{-\rho_b}\}$$

$$C_{41}^{000} = \rho_b^{-1}(\kappa+1)^{-2}(\kappa-1)^3\{- (\kappa-1)[6(\kappa+1)^2(20\kappa^2+16\kappa-1)+24(\kappa+1)^2(4\kappa+1)\rho_a+12(\kappa+1)(3\kappa+2)\rho_a^2+8(\kappa+1)\rho_a^3+\rho_a^4]e^{-\rho_a} + (\kappa+1)^2[6(\kappa-1)(20\kappa^2+16\kappa-1)-6(4\kappa^2+2\kappa-1)\rho_b]e^{-\rho_b}\}$$

(2)  $\beta, \gamma, \delta\epsilon = 2, 0, 0, 0$ ;  $-1 \leq \alpha \leq 4$

$$D_{-1,2}^{000} = \rho_a^{-1}\{- [(\kappa+1)(\kappa-3)-(\kappa-1)\rho_a]e^{-\rho_a} + (\kappa+1)[(\kappa-3)-2\rho_b]e^{-\rho_b}\}$$

$$E_{-1,2}^{000} = \rho_b^{-1}(2+2\rho_b+\rho_b^2)e^{-\rho_b} = \rho_b^2 A_2(\rho_b)$$

$$C_{02}^{000} = \rho_b^{-1}(\kappa-1)\{- (\kappa-1)(2\kappa-1)e^{-\rho_a} + [(\kappa-1)(2\kappa-1)-2(\kappa-1)\rho_b+\rho_b^2]e^{-\rho_b}\}$$

TABLE XIII (continued)

$$\begin{aligned}
C_{12}^{000} &= \rho_a^{-1}(\kappa-1)\{- (\kappa-1)[2(\kappa+1)(3\kappa-2)+(2\kappa-1)\rho_a]e^{-\rho_a} + (\kappa+1)[2(\kappa-1)(3\kappa-2)-4(\kappa-1)\rho_b+\rho_b^2]e^{-\rho_b}\} \\
C_{22}^{000} &= \rho_b^{-1}(\kappa+1)^{-1}(\kappa-1)^2\{- (\kappa-1)[2(\kappa+1)(12\kappa^2-7)+4(\kappa+1)(3\kappa-2)\rho_a+(2\kappa-1)\rho_a^2]e^{-\rho_a} \\
&\quad + (\kappa+1)[2(\kappa-1)(12\kappa^2-7)-4(\kappa-1)(3\kappa+2)\rho_b+(2\kappa+1)\rho_b^2]e^{-\rho_b}\} \\
C_{32}^{000} &= \rho_a^{-1}(\kappa+1)^{-1}(\kappa-1)^2\{- (\kappa-1)[6(\kappa+1)^2(20\kappa^2-8\kappa-7)+6(\kappa+1)(12\kappa^2-7)\rho_a+6(\kappa+1)(3\kappa-2)\rho_a^2+(2\kappa-1)\rho_a^3]e^{-\rho_a} \\
&\quad + (\kappa+1)^2[6(\kappa-1)(20\kappa^2-8\kappa-7)-12(\kappa-1)(4\kappa+1)\rho_b+6\kappa\rho_b^2]e^{-\rho_b}\} \\
C_{42}^{000} &= \rho_b^{-1}(\kappa+1)^{-2}(\kappa-1)^3\{- (\kappa-1)[6(\kappa+1)^2(120\kappa^3+20\kappa^2-92\kappa-13)+24(\kappa+1)^2(20\kappa^2-8\kappa-7)\rho_a+12(\kappa+1)(12\kappa^2-7)\rho_a^2 \\
&\quad +8(\kappa+1)(3\kappa-2)\rho_a^3+(2\kappa-1)\rho_a^4]e^{-\rho_a} + (\kappa+1)^2[6(\kappa-1)(120\kappa^3+20\kappa^2-92\kappa-13)-12(\kappa-1)(20\kappa^2+16\kappa-1)\rho_b \\
&\quad +6(4\kappa^2+2\kappa-1)\rho_b^2]e^{-\rho_b}\} \\
D_{-1,3}^{000} &= \rho_a^{-1}\{- [2(\kappa+1)(\kappa^2-3\kappa+5)-(\kappa-1)(\kappa-3)\rho_a+(\kappa-1)\rho_a^2]e^{-\rho_a} + (\kappa+1)[2(\kappa^2-3\kappa+5)-3(\kappa-3)\rho_b+3\rho_b^2]e^{-\rho_b}\} \\
E_{-1,3}^{000} &= -\rho_b^{-1}(6+6\rho_b+3\rho_b^2+\rho_b^3)e^{-\rho_b} = -\rho_b^3 A_3(\rho_b) \\
C_{03}^{000} &= \rho_b^{-1}(\kappa-1)\{- 6\kappa(\kappa-1)^2e^{-\rho_a} + [6\kappa(\kappa-1)^2-3(\kappa-1)(2\kappa-1)\rho_b+3(\kappa-1)\rho_b^2-\rho_b^3]e^{-\rho_b}\} \\
C_{13}^{000} &= \rho_a^{-1}(\kappa-1)\{- (\kappa-1)^2[6(\kappa+1)(4\kappa-1)+6\kappa\rho_a]e^{-\rho_a} + (\kappa+1)[6(\kappa-1)^2(4\kappa-1)-6(\kappa-1)(3\kappa-2)\rho_b+6(\kappa-1)\rho_b^2-\rho_b^3]e^{-\rho_b}\} \\
C_{23}^{000} &= \rho_b^{-1}(\kappa+1)^{-1}(\kappa-1)^2\{- (\kappa-1)^2[6(\kappa+1)(20\kappa^2+8\kappa-7)+12(\kappa+1)(4\kappa-1)\rho_a+6\kappa\rho_a^2]e^{-\rho_a} \\
&\quad + (\kappa+1)[6(\kappa-1)^2(20\kappa^2+8\kappa-7)-6(\kappa-1)(12\kappa^2-7)\rho_b+6(\kappa-1)(3\kappa+2)\rho_b^2-(2\kappa+1)\rho_b^3]e^{-\rho_b}\} \\
C_{33}^{000} &= 6\rho_a^{-1}(\kappa+1)^{-1}(\kappa-1)^2\{- (\kappa-1)^2[12(\kappa+1)^2(10\kappa^2-3)+3(\kappa+1)(20\kappa^2+8\kappa-7)\rho_a+3(\kappa+1)(4\kappa-1)\rho_a^2+\kappa\rho_a^3]e^{-\rho_a} \\
&\quad + (\kappa+1)^2[12(\kappa-1)^2(10\kappa^2-3)-3(\kappa-1)(20\kappa^2-8\kappa-7)\rho_b+3(\kappa-1)(4\kappa+1)\rho_b^2-\kappa\rho_b^3]e^{-\rho_b}\}
\end{aligned}$$

$$(3) \quad \beta, \gamma, \delta \epsilon = 3, 000; \quad -1 \leq \alpha \leq 3$$

TABLE XIII (continued)

$$(4) \quad \alpha, \gamma \delta \epsilon = -1, 000; \quad 4 \leq \beta \leq 9$$

$$D_{-1,4}^{000} = \rho_a^{-1} (\kappa+1)^{-1} \{- [2(\kappa+1)^2 (3\kappa^3 - 10\kappa^2 + 15\kappa - 20) - (\kappa^2 - 1)(2\kappa^2 - 5\kappa + 11)\rho_a + (\kappa^2 - 1)(\kappa - 5)\rho_a^2 - (\kappa - 1)^2 \rho_a^3] e^{-\rho_a} \\ + (\kappa+1)^2 [2(3\kappa^3 - 10\kappa^2 + 15\kappa - 20) - 8(\kappa^2 - 3\kappa + 5)\rho_b + 6(\kappa - 3)\rho_b^2 - 4\rho_b^3] e^{-\rho_b}\}$$

$$E_{-1,4}^{000} = \rho_b^{-1} (24 + 24\rho_b + 12\rho_b^2 + 4\rho_b^3 + \rho_b^4) e^{-\rho_b} = \rho_b^4 A_4(\rho_b)$$

$$D_{-1,5}^{000} = \rho_a^{-1} (\kappa+1)^{-1} \{- [2(\kappa+1)^2 (12\kappa^4 - 45\kappa^3 + 71\kappa^2 - 75\kappa + 97) - 2(\kappa^2 - 1)(3\kappa^3 - 8\kappa^2 + 11\kappa - 26)\rho_a + 2(\kappa^2 - 1)(\kappa^2 - 4\kappa + 13)\rho_a^2 \\ - (\kappa - 1)^2 (\kappa - 5)\rho_a^3 + (\kappa - 1)^2 \rho_a^4] e^{-\rho_a} + (\kappa+1)^2 [2(12\kappa^4 - 45\kappa^3 + 71\kappa^2 - 75\kappa + 97) - 10(3\kappa^3 - 10\kappa^2 + 15\kappa - 20)\rho_b \\ + 20(\kappa^2 - 3\kappa + 5)\rho_b^2 - 10(\kappa - 3)\rho_b^3 + 5\rho_b^4] e^{-\rho_b}\}$$

$$E_{-1,5}^{000} = -\rho_b^{-1} (120 + 120\rho_b + 60\rho_b^2 + 20\rho_b^3 + 5\rho_b^4 + \rho_b^5) e^{-\rho_b} = -\rho_b^5 A_5(\rho_b)$$

$$D_{-1,6}^{000} = \rho_a^{-1} (\kappa+1)^{-2} \{- [6(\kappa+1)^3 (20\kappa^5 - 84\kappa^4 + 145\kappa^3 - 147\kappa^2 + 135\kappa - 189) - 6(\kappa - 1)(\kappa+1)^2 (4\kappa^4 - 12\kappa^3 + 15\kappa^2 - 18\kappa + 51)\rho_a \\ + 6(\kappa - 1)(\kappa+1)^2 (\kappa^3 - 4\kappa^2 + 9\kappa - 26)\rho_a^2 - (\kappa+1)(\kappa - 1)^2 (2\kappa^2 - 7\kappa + 29)\rho_a^3 + (\kappa+1)(\kappa - 1)^2 (\kappa - 7)\rho_a^4 - (\kappa - 1)^3 \rho_a^5] e^{-\rho_a} \\ + (\kappa+1)^3 [6(20\kappa^5 - 84\kappa^4 + 145\kappa^3 - 147\kappa^2 + 135\kappa - 189) - 12(12\kappa^4 - 45\kappa^3 + 71\kappa^2 - 75\kappa + 97)\rho_b + 30(3\kappa^3 - 10\kappa^2 + 15\kappa - 20)\rho_b^2 \\ - 40(\kappa^2 - 3\kappa + 5)\rho_b^3 + 15(\kappa - 3)\rho_b^4 - 6\rho_b^5] e^{-\rho_b}\}$$

$$E_{-1,6}^{000} = \rho_b^{-1} (720 + 720\rho_b + 360\rho_b^2 + 120\rho_b^3 + 30\rho_b^4 + 6\rho_b^5 + \rho_b^6) e^{-\rho_b} = \rho_b^6 A_6(\rho_b)$$

$$D_{-1,7}^{000} = \rho_a^{-1} (\kappa+1)^{-2} \{- [24(\kappa+1)^3 (30\kappa^6 - 140\kappa^5 + 267\kappa^4 - 280\kappa^3 + 216\kappa^2 - 210\kappa + 327) \\ - 6(\kappa - 1)(\kappa+1)^2 (20\kappa^5 - 68\kappa^4 + 89\kappa^3 - 75\kappa^2 + 111\kappa - 357)\rho_a + 6(\kappa - 1)(\kappa+1)^2 (4\kappa^4 - 17\kappa^3 + 35\kappa^2 - 63\kappa + 181)\rho_a^2 \\ - 2(\kappa+1)(\kappa - 1)^2 (3\kappa^3 - 10\kappa^2 + 23\kappa - 100)\rho_a^3 + 2(\kappa+1)(\kappa - 1)^2 (\kappa^2 - 5\kappa + 25)\rho_a^4 - (\kappa - 1)^3 (\kappa - 7)\rho_a^5 + (\kappa - 1)^3 \rho_a^6] e^{-\rho_a} \\ + (\kappa+1)^3 [24(30\kappa^6 - 140\kappa^5 + 267\kappa^4 - 280\kappa^3 + 216\kappa^2 - 210\kappa + 327) - 42(20\kappa^5 - 68\kappa^4 + 84\kappa^3 + 145\kappa^2 - 147\kappa - 189)\rho_b \\ + 84\kappa^4 + 145\kappa^3 - 147\kappa^2 + 135\kappa - 189]\rho_b\}$$

TABLE XIII (continued)

$$+42(12\kappa^4-45\kappa^3+71\kappa^2-75\kappa+97)\rho_b^2-70(3\kappa^3-10\kappa^2+15\kappa-20)\rho_b^3+70(\kappa^2-3\kappa+5)\rho_b^4-21(\kappa-3)\rho_b^5+7\rho_b^6]e^{-\rho_b}$$

$$E_{-1,7}^{000} = -\rho_b^{-1}(5040+5040\rho_b+2520\rho_b^2+840\rho_b^3+210\rho_b^4+42\rho_b^5+7\rho_b^6+\rho_b^7)e^{-\rho_b} = -\rho_b^7 A_7(\rho_b)$$

$$D_{-1,8}^{000} = \rho_a^{-1}(\kappa+1)^{-3}\{-[24(\kappa+1)^4(210\kappa^7-1080\kappa^6+2275\kappa^5-2556\kappa^4+1820\kappa^3-1308\kappa^2+1575\kappa-2616)-6(\kappa-1)(\kappa+1)^3$$

$$(120\kappa^6-460\kappa^5+664\kappa^4-487\kappa^3+405\kappa^2-873\kappa+2871)]\rho_a+6(\kappa-1)(\kappa+1)^3(20\kappa^5-92\kappa^4+191\kappa^3-285\kappa^2+489\kappa-1443)]\rho_a^2$$

$$-2(\kappa^2-1)^2(12\kappa^4-42\kappa^3+77\kappa^2-172\kappa+797)]\rho_a^3+2(\kappa^2-1)^2(3\kappa^3-14\kappa^2+43\kappa-200)]\rho_a^4-(\kappa+1)(\kappa-1)^3(2\kappa^2-9\kappa+55)]\rho_a^5$$

$$+(\kappa+1)(\kappa-1)^3(\kappa-9)\rho_a^6-(\kappa-1)^4\rho_a^7]e^{-\rho_a} + (\kappa+1)^4[24(210\kappa^7-1080\kappa^6+2275\kappa^5-2556\kappa^4+1820\kappa^3-1308\kappa^2+1575\kappa-2616)$$

$$-192(30\kappa^6-140\kappa^5+267\kappa^4-280\kappa^3+216\kappa^2-210\kappa+327)]\rho_b+168(20\kappa^5-84\kappa^4+145\kappa^3-147\kappa^2+135\kappa-189)]\rho_b^2$$

$$-112(12\kappa^4-45\kappa^3+71\kappa^2-75\kappa+97)]\rho_b^3+140(3\kappa^3-10\kappa^2+15\kappa-20)]\rho_b^4-112(\kappa^2-3\kappa+5)]\rho_b^5+28(\kappa-3)]\rho_b^6-8\rho_b^7]e^{-\rho_b}$$

$$E_{-1,8}^{000} = \rho_b^{-1}(40320+40320\rho_b+20160\rho_b^2+6720\rho_b^3+1680\rho_b^4+336\rho_b^5+56\rho_b^6+8\rho_b^7+\rho_b^8)e^{-\rho_b} = \rho_b^8 A_8(\rho_b)$$

$$D_{-1,9}^{000} = \rho_a^{-1}(\kappa+1)^{-3}\{-[72(\kappa+1)^4(560\kappa^8-3150\kappa^7+7300\kappa^6-8925\kappa^5+6303\kappa^4-3360\kappa^3+3154\kappa^2-4725\kappa+7883)$$

$$-72(\kappa-1)(\kappa+1)^3(70\kappa^7-300\kappa^6+485\kappa^5-358\kappa^4+164\kappa^3-260\kappa^2+681\kappa-2162)]\rho_a$$

$$+72(\kappa-1)(\kappa+1)^3(10\kappa^6-50\kappa^5+109\kappa^4-152\kappa^3+200\kappa^2-358\kappa+1081)]\rho_a^2-6(\kappa^2-1)^2(20\kappa^5-76\kappa^4+131\kappa^3-201\kappa^2+501\kappa-2391)]\rho_a^3$$

$$+6(\kappa^2-1)^2(4\kappa^4-19\kappa^3+49\kappa^2-129\kappa+599)]\rho_a^4-6(\kappa+1)(\kappa-1)^3(\kappa^3-4\kappa^2+13\kappa-82)]\rho_a^5+2(\kappa+1)(\kappa-1)^3(\kappa^2-6\kappa+41)]\rho_a^6$$

$$-(\kappa-1)^4(\kappa-9)\rho_a^7+(\kappa-1)^4\rho_a^8]e^{-\rho_a} + (\kappa+1)^4[72(560\kappa^8-3150\kappa^7+7300\kappa^6-8925\kappa^5+6303\kappa^4-3360\kappa^3+3154\kappa^2-4725\kappa+7883)$$

$$-216(210\kappa^7-1080\kappa^6+2275\kappa^5-2556\kappa^4+1820\kappa^3-1308\kappa^2+1575\kappa-2616)]\rho_b$$

$$+864(30\kappa^6-140\kappa^5+267\kappa^4-280\kappa^3+216\kappa^2-210\kappa+327)]\rho_b^2-504(20\kappa^5-84\kappa^4+145\kappa^3-147\kappa^2+135\kappa-189)]\rho_b^3$$

$$+252(12\kappa^4-45\kappa^3+71\kappa^2-75\kappa+97)]\rho_b^4-252(3\kappa^3-10\kappa^2+15\kappa-20)]\rho_b^5+168(\kappa^2-3\kappa+5)]\rho_b^6-36(\kappa-3)]\rho_b^7+9\rho_b^8]e^{-\rho_b}$$

TABLE XIII (continued)

$$E_{-1,9}^{000} = -\rho_b^{-1}(362880+362880\rho_b+181440\rho_b^2+60480\rho_b^3+15120\rho_b^4+3024\rho_b^5+504\rho_b^6+72\rho_b^7+9\rho_b^8+\rho_b^9)e^{-\rho_b} = -\rho_b^9 A_9(\rho_b)$$

Functions with  $\gamma+\delta+2\epsilon = 1$

$$(5) \quad \beta, \gamma\delta\epsilon = 1, 1, 0, 0; \quad -2 \leq \alpha \leq 3$$

$$D_{-2,1}^{100} = \rho_b^{-2}\{-[(\kappa+5)+(\kappa-1)\rho_a]e^{-\rho_a} + [(\kappa+5)(1+\rho_b)+2\rho_b^2]e^{-\rho_b}\}$$

$$E_{-2,1}^{100} = -\rho_a\rho_b^{-3}(3+3\rho_b+\rho_b^2)e^{-\rho_b} = -\frac{1}{2}\rho_a\rho_b[A_3(\rho_b)-A_1(\rho_b)]$$

$$D_{-1,1}^{100} = \rho_a^{-1}\rho_b^{-1}\{-[(\kappa+1)(\kappa-4)+(\kappa-1)(\kappa-2)\rho_a]e^{-\rho_a} + (\kappa+1)[(\kappa-4)(1+\rho_b)-\rho_b^2]e^{-\rho_b}\}$$

$$E_{-1,1}^{100} = \rho_b^{-2}(3+3\rho_b+\rho_b^2)e^{-\rho_b} = \frac{1}{2}\rho_b^2[A_3(\rho_b)-A_1(\rho_b)]$$

$$C_{01}^{100} = \rho_a^{-2}(\kappa-1)\{- (\kappa-1)[2(\kappa+1)(1+\rho_a)+\rho_a^2]e^{-\rho_a} + (\kappa+1)[2(\kappa-1)(1+\rho_b)-\rho_b^2]e^{-\rho_b}\}$$

$$C_{11}^{100} = \rho_a^{-1}\rho_b^{-1}(\kappa+1)^{-1}(\kappa-1)^2\{- (\kappa-1)[6(\kappa+1)^2(1+\rho_a)+4(\kappa+1)\rho_a^2+\rho_a^3]e^{-\rho_a} + (\kappa+1)^2[6(\kappa-1)(1+\rho_b)-2\rho_b^2]e^{-\rho_b}\}$$

$$C_{21}^{100} = \rho_a^{-2}(\kappa+1)^{-1}(\kappa-1)^2\{- (\kappa-1)[6(\kappa+1)^2(4\kappa+3)(1+\rho_a)+2(\kappa+1)(9\kappa+7)\rho_a^2+6(\kappa+1)\rho_a^3+\rho_a^4]e^{-\rho_a}$$

$$+ (\kappa+1)^2[6(\kappa-1)(4\kappa+3)(1+\rho_b)-2(3\kappa+2)\rho_b^2]e^{-\rho_b}\}$$

$$C_{31}^{100} = \rho_a^{-1}\rho_b^{-1}(\kappa+1)^{-2}(\kappa-1)^3\{- (\kappa-1)[24(\kappa+1)^3(5\kappa+2)(1+\rho_a)+6(\kappa+1)^2(16\kappa+7)\rho_a^2+2(\kappa+1)(18\kappa+13)\rho_a^3+8(\kappa+1)\rho_a^4$$

$$+\rho_a^5]e^{-\rho_a} + (\kappa+1)^3[24(\kappa-1)(5\kappa+2)(1+\rho_b)-6(4\kappa+1)\rho_b^2]e^{-\rho_b}\}$$

$$(6) \quad \beta, \gamma\delta\epsilon = 2, 1, 0, 0; \quad -2 \leq \alpha \leq 3$$

$$D_{-2,2}^{100} = \rho_b^{-2}\{-[(\kappa^2-6\kappa-19)+(\kappa-1)(\kappa-5)\rho_a-(\kappa-1)\rho_a^2]e^{-\rho_a} + [(\kappa^2-6\kappa-19)(1+\rho_b)-2(\kappa+4)\rho_b^2-2\rho_b^3]e^{-\rho_b}\}$$

$$E_{-2,2}^{100} = \rho_a\rho_b^{-3}(12+12\rho_b+5\rho_b^2+\rho_b^3)e^{-\rho_b} = \frac{1}{2}\rho_a\rho_b^2[A_4(\rho_b)-A_2(\rho_b)]$$

$$D_{-1,2}^{100} = \rho_a^{-1}\rho_b^{-1}\{-[2(\kappa+1)(\kappa^2-4\kappa+9)+2(\kappa-1)(\kappa^2-2\kappa+3)\rho_a+(\kappa-1)\rho_a^2]e^{-\rho_a} + (\kappa+1)[2(\kappa^2-4\kappa+9)(1+\rho_b)$$

TABLE XIII (continued)

$$-(2\kappa-7)\rho_b^2 + \rho_b^3]e^{-\rho_b}$$

$$E_{-1,2}^{100} = \rho_b^{-2}(12+12\rho_b+5\rho_b^2+\rho_b^3)e^{-\rho_b} = -\frac{1}{2}\rho_b^3[A_4(\rho_b)-A_2(\rho_b)]$$

$$C_{02}^{100} = \rho_a^{-2}(\kappa-1)\{- (\kappa-1)[2(\kappa+1)(3\kappa-2)(1+\rho_a)+(2\kappa-1)\rho_a^2]e^{-\rho_a} + (\kappa+1)[2(\kappa-1)(3\kappa-2)(1+\rho_b)-(4\kappa-3)\rho_b^2+\rho_b^3]e^{-\rho_b}\}$$

$$C_{12}^{100} = \rho_a^{-1}\rho_b^{-1}(\kappa+1)^{-1}(\kappa-1)^2\{- (\kappa-1)[6(\kappa+1)^2(4\kappa-3)(1+\rho_a)+4(\kappa+1)(3\kappa-2)\rho_a^2+(2\kappa-1)\rho_a^3]e^{-\rho_a}$$

$$+ (\kappa+1)^2[6(\kappa-1)(4\kappa-3)(1+\rho_b)-2(6\kappa-5)\rho_b^2+2\rho_b^3]e^{-\rho_b}\}$$

$$C_{22}^{100} = \rho_a^{-2}(\kappa+1)^{-1}(\kappa-1)^2\{- (\kappa-1)[6(\kappa+1)^2(20\kappa^2-13)(1+\rho_a)+2(\kappa+1)(36\kappa^2+3\kappa-23)\rho_a^2+5(\kappa+1)(3\kappa-2)\rho_a^3+(2\kappa-1)\rho_a^4]e^{-\rho_a}$$

$$+ (\kappa+1)^2[6(\kappa-1)(20\kappa^2-13)(1+\rho_b)-2(24\kappa^2-3\kappa-16)\rho_b^2+2(3\kappa+2)\rho_b^3]e^{-\rho_b}\}$$

$$C_{32}^{100} = \rho_a^{-1}\rho_b^{-1}(\kappa+1)^{-2}(\kappa-1)^3\{- (\kappa-1)[24(\kappa+1)^3(30\kappa^2-10\kappa-13)(1+\rho_a)+6(\kappa+1)^2(80\kappa^2-20\kappa-37)\rho_a^2+2(\kappa+1)(72\kappa^2+3\kappa-44)\rho_a^3$$

$$+8(\kappa+1)(3\kappa-2)\rho_a^4+(2\kappa-1)\rho_a^5]e^{-\rho_a} + (\kappa+1)^3[24(\kappa-1)(30\kappa^2-10\kappa-13)(1+\rho_b)-30(8\kappa^2-4\kappa-3)\rho_b^2+6(4\kappa+1)\rho_b^3]e^{-\rho_b}\}$$

$$(7) \quad B, \gamma \delta \epsilon = 3, 100; \quad -2 \leq \alpha \leq 2$$

$$D_{-2,3}^{100} = \rho_b^{-2}(\kappa+1)^{-1}\{- [2(\kappa+1)(\kappa^3-5\kappa^2+17\kappa+47)+2(\kappa^2-1)(\kappa^2-4\kappa+13)]\rho_a - (\kappa^2-1)(\kappa-8)\rho_a^2+(\kappa-1)^2\rho_a^3]e^{-\rho_a}$$

$$+ (\kappa+1)[2(\kappa^3-5\kappa^2+17\kappa+47)(1+\rho_b)-3(\kappa-7)(\kappa+2)\rho_b^2+(3\kappa+11)\rho_b^3+2\rho_b^4]e^{-\rho_b}\}$$

$$E_{-2,3}^{100} = -\rho_a\rho_b^{-3}(60+60\rho_b+27\rho_b^2+7\rho_b^3+\rho_b^4)e^{-\rho_b} = -\frac{1}{2}\rho_a\rho_b^3[A_5(\rho_b)-A_3(\rho_b)]$$

$$D_{-1,3}^{100} = \rho_a^{-1}\rho_b^{-1}(\kappa+1)^{-1}\{- [2(\kappa+1)^2(3\kappa^3-13\kappa^2+27\kappa+47)+2(\kappa^2-1)(3\kappa^3-7\kappa^2+7\kappa-13)]\rho_a+(\kappa^2-1)(\kappa-8)\rho_a^2-(\kappa-1)^2\rho_a^3]e^{-\rho_a}$$

$$+ (\kappa+1)^2[2(3\kappa^3-13\kappa^2+27\kappa+47)(1+\rho_b)-3(2\kappa^2-7\kappa+14)\rho_b^2+(3\kappa-10)\rho_b^3-\rho_b^4]e^{-\rho_b}\}$$

$$E_{-1,3}^{100} = \rho_b^{-2}(60+60\rho_b+27\rho_b^2+7\rho_b^3+\rho_b^4)e^{-\rho_b} = \frac{1}{2}\rho_b^4[A_5(\rho_b)-A_3(\rho_b)]$$

TABLE XIII (continued)

$$\begin{aligned}
 C_{03}^{100} &= \rho_a^{-2}(\kappa-1)\{- (\kappa-1)^2[6(\kappa+1)(4\kappa-1)(1+p_a)+6\kappa\rho_a^2]e^{-p_a} + (\kappa+1)[6(\kappa-1)^2(4\kappa-1)(1+p_b)-6(\kappa-1)(3\kappa-1)\rho_b^2 \\
 &\quad +2(3\kappa-2)\rho_b^3-\rho_b^4]e^{-p_b}\} \\
 C_{13}^{100} &= 2\rho_a^{-1}\rho_b^{-1}(\kappa+1)^{-1}(\kappa-1)^2\{- (\kappa-1)^2[12(\kappa+1)^2(5\kappa-2)(1+p_a)+6(\kappa+1)(4\kappa-1)\rho_a^2+3\kappa\rho_a^3]e^{-p_a} \\
 &\quad + (\kappa+1)^2[12(\kappa-1)^2(5\kappa-2)(1+p_b)-18(\kappa-1)(2\kappa-1)\rho_b^2+(9\kappa-7)\rho_b^3-\rho_b^4]e^{-p_b}\} \\
 C_{23}^{100} &= 2\rho_a^{-2}(\kappa+1)^{-1}(\kappa-1)^2\{- (\kappa-1)^2[12(\kappa+1)^2(30\kappa^2+10\kappa-13)(1+p_a)+6(\kappa+1)(30\kappa^2+14\kappa-11)\rho_a^2+9(\kappa+1)(4\kappa-1)\rho_a^3 \\
 &\quad +3\kappa\rho_a^4]e^{-p_a} + (\kappa+1)^2[12(\kappa-1)^2(30\kappa^2+10\kappa-13)(1+p_b)-18(\kappa-1)(10\kappa^2+2\kappa-5)\rho_b^2+(36\kappa^2-3\kappa-23)\rho_b^3-(3\kappa+2)\rho_b^4]e^{-p_b}\} \\
 (8) \quad \beta, \gamma\delta\epsilon &= 1, 010; \quad -1 \leq \alpha \leq 4 \\
 D_{-1,1}^{010} &= \rho_a^{-1}\rho_b^{-1}\{- [(\kappa+1)(\kappa-4)+(\kappa-1)(\kappa-2)\rho_a-(\kappa-1)\rho_a^2]e^{-p_a} + (\kappa+1)[(\kappa-4)(1+p_b)-2\rho_b^2]e^{-p_b}\} \\
 E_{-1,1}^{010} &= \rho_b^{-2}(3+3\rho_b+2\rho_b^2+\rho_b^3)e^{-p_b} = \frac{1}{2}\rho_b^2[A_2(\rho_b)+A_1(\rho_b)] \\
 C_{01}^{010} &= \rho_a^{-2}(\kappa+1)\{- 2(\kappa-1)^2(1+p_a)e^{-p_a} + [2(\kappa-1)^2(1+p_b)-2(\kappa-1)\rho_b^2+\rho_b^3]e^{-p_b}\} \\
 C_{11}^{010} &= \rho_a^{-1}\rho_b^{-1}(\kappa-1)\{- (\kappa-1)^2[6(\kappa+1)(1+p_a)+2\rho_a^2]e^{-p_a} + (\kappa+1)[6(\kappa-1)^2(1+p_b)-4(\kappa-1)\rho_b^2+\rho_b^3]e^{-p_b}\} \\
 C_{21}^{010} &= \rho_a^{-2}(\kappa-1)\{- (\kappa-1)^2[6(\kappa+1)(4\kappa+3)(1+p_a)+2(6\kappa+5)\rho_a^2+2\rho_a^3]e^{-p_a} + (\kappa+1)[6(\kappa-1)^2(4\kappa+3)(1+p_b) \\
 &\quad -4(\kappa-1)(3\kappa+2)\rho_b^2+(2\kappa+1)\rho_b^3]e^{-p_b}\} \\
 C_{31}^{010} &= 2\rho_a^{-1}\rho_b^{-1}(\kappa+1)^{-1}(\kappa-1)^2\{- (\kappa-1)^2[12(\kappa+1)^2(5\kappa+2)(1+p_a)+18(\kappa+1)(2\kappa+1)\rho_a^2+(9\kappa+7)\rho_a^3+\rho_a^4]e^{-p_a} \\
 &\quad + (\kappa+1)^2[12(\kappa-1)^2(5\kappa+2)(1+p_b)-6(\kappa-1)(4\kappa+1)\rho_b^2+3\kappa\rho_b^3]e^{-p_b}\} \\
 C_{41}^{010} &= 2\rho_a^{-2}(\kappa+1)^{-1}(\kappa-1)^2\{- (\kappa-1)^2[36(\kappa+1)^2(10\kappa^2+10\kappa+1)(1+p_a)+6(\kappa+1)(40\kappa^2+4\kappa+7)\rho_a^2+6(\kappa+1)(12\kappa+5)\rho_a^3 \\
 &\quad +3(4\kappa+3)\rho_a^4+\rho_a^5]e^{-p_a} + (\kappa+1)^2[36(\kappa-1)^2(10\kappa^2+10\kappa+1)(1+p_b)-6(\kappa-1)(20\kappa^2+16\kappa-1)\rho_b^2+3(4\kappa^2+2\kappa-1)\rho_b^3]e^{-p_b}\}
 \end{aligned}$$

TABLE XIII (continued)

$$(9) \quad \beta, \gamma \delta \epsilon = 2, 010; \quad 0 \leq \alpha \leq 3$$

$$C_{02}^{010} = \rho_a^{-2}(\kappa+1)\{-2(\kappa-1)^2(3\kappa-2)(1+\rho_a)e^{-\rho_a} + [2(\kappa-1)^2(3\kappa-2)(1+\rho_b)-2(\kappa-1)(3\kappa-2)\rho_b^2+3(\kappa-1)\rho_b^3-\rho_b^4]e^{-\rho_b}\}$$

$$C_{12}^{010} = \rho_a^{-1}\rho_b^{-1}(\kappa-1)\{- (\kappa-1)^2[6(\kappa+1)(4\kappa-3)(1+\rho_a)+2(3\kappa-2)\rho_a^2]e^{-\rho_a} + (\kappa+1)[6(\kappa-1)^2(4\kappa-3)(1+\rho_b)-2(\kappa-1)(9\kappa-7)\rho_b^2+6(\kappa-1)\rho_b^3-\rho_b^4]e^{-\rho_b}\}$$

$$C_{22}^{010} = \rho_a^{-2}(\kappa-1)\{- (\kappa-1)^2[6(\kappa+1)(20\kappa^2-13)(1+\rho_a)+2(24\kappa^2+3\kappa-16)\rho_a^2+2(3\kappa-2)\rho_a^3]e^{-\rho_a} + (\kappa+1)[6(\kappa-1)^2(20\kappa^2-13)(1+\rho_b)-2(\kappa-1)(36\kappa^2-3\kappa-23)\rho_b^2+6(\kappa-1)(3\kappa+2)\rho_b^3-(2\kappa+1)\rho_b^4]e^{-\rho_b}\}$$

$$C_{32}^{010} = 2\rho_a^{-1}\rho_b^{-1}(\kappa+1)^{-1}(\kappa-1)^2\{- (\kappa-1)^2[12(\kappa+1)^2(30\kappa^2-10\kappa-13)(1+\rho_a)+18(\kappa+1)(10\kappa^2-2\kappa-5)\rho_a^2+(36\kappa^2+3\kappa-23)\rho_a^3+3(\kappa-2)\rho_a^4]e^{-\rho_a} + (\kappa+1)^2[12(\kappa-1)^2(30\kappa^2-10\kappa-13)(1+\rho_b)-6(\kappa-1)(30\kappa^2-14\kappa-11)\rho_b^2+9(\kappa-1)(4\kappa+1)\rho_b^3-3\kappa\rho_b^4]e^{-\rho_b}\}$$

Functions with  $\gamma+\delta+2\epsilon = 2$

$$(10) \quad \beta, \gamma \delta \epsilon = 1, 200; \quad -3 \leq \alpha \leq 2$$

$$D_{-3,1}^{200} = \rho_a^{-1}\rho_b^{-2}(\kappa-1)^{-1}\{- [2(\kappa+1)(\kappa+14)+2(\kappa-1)(\kappa+4)\rho_a+(\kappa^2-1)\rho_a^2]e^{-\rho_a} + (\kappa+1)[2(\kappa+14)(1+\rho_b)+(\kappa+11)\rho_b^2+2\rho_b^3]e^{-\rho_b}\}$$

$$E_{-3,1}^{200} = -\rho_b^{-3}[\rho_a^2\rho_b^{-2}(15+15\rho_b+6\rho_b^2+\rho_b^3)-(3+3\rho_b+\rho_b^2)]e^{-\rho_b} = -(1/8)\rho_b[\rho_a^2[A_5(\rho_b)-2A_3(\rho_b)+A_1(\rho_b)]]-4[A_3(\rho_b)-A_1(\rho_b)]$$

$$D_{-2,1}^{200} = \rho_b^{-3}(\kappa+1)^{-1}\{- [2(\kappa+1)(\kappa^2-7\kappa-24)+2(\kappa^2-1)(\kappa-6)\rho_a+(\kappa-1)(\kappa^2-4\kappa-1)\rho_a^2]e^{-\rho_a} + (\kappa+1)[2(\kappa^2-7\kappa-24)(1+\rho_b)+(\kappa^2-6\kappa-19)\rho_b^2-(\kappa+3)\rho_b^3]e^{-\rho_b}\}$$

$$E_{-2,1}^{200} = 2\rho_a\rho_b^{-4}(15+15\rho_b+6\rho_b^2+\rho_b^3)e^{-\rho_b} = \frac{1}{4}\rho_a\rho_b^2[A_5(\rho_b)-2A_3(\rho_b)+A_1(\rho_b)]$$

TABLE XIII (continued)

$$D_{-1,1}^{200} = \rho_a^{-3}(\kappa-1)^{-1}\{- [2(\kappa+1)^2(2\kappa^2-9\kappa+22)+2(\kappa^2-1)(2\kappa^2-5\kappa+8)\rho_a+2(\kappa^2-1)(\kappa^2-2\kappa+2)\rho_a^2+(\kappa-1)^3\rho_a^3]e^{-\rho_a} \\ + (\kappa+1)^2[2(2\kappa^2-9\kappa+22)(1+\rho_b)+2(\kappa^2-4\kappa+9)\rho_b^2-(\kappa-3)\rho_b^3]e^{-\rho_b}\}$$

$$E_{-1,1}^{200} = -2\rho_b^{-3}(15+15\rho_b+6\rho_b^2+\rho_b^3)e^{-\rho_b} = -\frac{1}{4}\rho_b^3[A_5(\rho_b)-2A_3(\rho_b)+A_1(\rho_b)]$$

$$C_{01}^{200} = \rho_a^{-2}\rho_b^{-1}(\kappa+1)^{-1}(\kappa-1)\{- (\kappa-1)^2[12(\kappa+1)^2(1+\rho_a)+2(\kappa+1)(3\kappa+4)\rho_a^2+4(\kappa+1)\rho_a^3+\rho_a^4]e^{-\rho_a} \\ + (\kappa+1)^2[12(\kappa-1)^2(1+\rho_b)+2(\kappa-1)(3\kappa-2)\rho_b^2-(2\kappa-1)\rho_b^3]e^{-\rho_b}\}$$

$$C_{11}^{200} = \rho_a^{-3}(\kappa+1)^{-1}(\kappa-1)\{- (\kappa-1)^2[48(\kappa+1)^3(1+\rho_a)+6(\kappa+1)^2(4\kappa+5)\rho_a^2+2(\kappa+1)(9\kappa+8)\rho_a^3+6(\kappa+1)\rho_a^4+\rho_a^5]e^{-\rho_a} \\ + (\kappa+1)^3[48(\kappa-1)^2(1+\rho_b)+6(\kappa-1)(4\kappa-3)\rho_b^2-2(3\kappa-2)\rho_b^3]e^{-\rho_b}\}$$

$$C_{21}^{200} = \rho_a^{-2}\rho_b^{-1}(\kappa+1)^{-2}(\kappa-1)^2\{- (\kappa-1)^2[48(\kappa+1)^3(5\kappa+4)(1+\rho_a)+6(\kappa+1)^2(20\kappa^2+40\kappa+19)\rho_a^2+12(\kappa+1)^2(8\kappa+5)\rho_a^3 \\ +4(\kappa+1)(9\kappa+7)\rho_a^4+8(\kappa+1)\rho_a^5+\rho_a^6]e^{-\rho_a} + (\kappa+1)^3[48(\kappa-1)^2(5\kappa+4)(1+\rho_b)+6(\kappa-1)(20\kappa^2-13)\rho_b^2-2(12\kappa^2-7)\rho_b^3]e^{-\rho_b}\}$$

$$(11) \quad \beta, \gamma \delta \epsilon = 2, 200 ; \quad -3 \leq \alpha \leq 2$$

$$D_{-3,2}^{200} = \rho_a^{-1}\rho_b^{-2}(\kappa-1)^{-1}\{- [2(\kappa+1)(\kappa-16)(\kappa+5)+2(\kappa-1)(\kappa-11)(\kappa+2)\rho_a+(\kappa-1)(\kappa^2-8\kappa-11)\rho_a^2-(\kappa-1)^2\rho_a^3]e^{-\rho_a} \\ + (\kappa+1)[2(\kappa-16)(\kappa+5)(1+\rho_b)+(\kappa^2-10\kappa-69)\rho_b^2-2(\kappa+8)\rho_b^3-2\rho_b^4]e^{-\rho_b}\}$$

$$E_{-3,2}^{200} = \rho_b^{-3}[\rho_a^2\rho_b^{-2}(90+90\rho_b+39\rho_b^2+9\rho_b^3+\rho_b^4)-(12+12\rho_b+5\rho_b^2+\rho_b^3)]e^{-\rho_b} = (1/8)\rho_b^2\{\rho_a^2[A_6(\rho_b)-2A_4(\rho_b)+A_2(\rho_b)] \\ -4[A_4(\rho_b)-A_2(\rho_b)]\}$$

$$D_{-2,2}^{200} = \rho_b^{-3}(\kappa+1)^{-1}\{- [4(\kappa+1)(\kappa^3-6\kappa^2+24\kappa+71)+4(\kappa^2-1)(\kappa^2-5\kappa+19)\rho_a+(\kappa-1)(2\kappa^3-7\kappa^2+22\kappa+19)\rho_a^2+2(\kappa-1)^2\rho_a^3]e^{-\rho_a} \\ + (\kappa+1)[4(\kappa^3-6\kappa^2+24\kappa+71)(1+\rho_b)+(2\kappa^3-11\kappa^2+42\kappa+123)\rho_b^2-2(\kappa-7)(\kappa+2)\rho_b^3+(\kappa+3)\rho_b^4]e^{-\rho_b}\}$$

TABLE XIII (continued)

$$\begin{aligned}
E_{-2,2}^{200} &= -2\rho_a\rho_b^{-4}(90+90\rho_b+39\rho_b^2+9\rho_b^3+\rho_b^4)e^{-\rho_b} = \frac{1}{4}\rho_a\rho_b^3[A_6(\rho_b)-2A_4(\rho_b)+A_2(\rho_b)] \\
D_{-1,2}^{200} &= \rho_a^{-3}(\kappa-1)^{-1}\{-[12(\kappa+1)^2(\kappa^3-5\kappa^2+12\kappa-23)+12(\kappa^2-1)(\kappa^3-3\kappa^2+4\kappa-7)\rho_a+2(\kappa^2-1)(3\kappa^3-8\kappa^2+8\kappa-12)\rho_a^2 \\
&\quad +(\kappa-1)^2(2\kappa^2-3\kappa-1)\rho_a^3]e^{-\rho_a} + (\kappa+1)^2[12(\kappa^3-5\kappa^2+12\kappa-23)(1+\rho_b)+2(3\kappa^3-14\kappa^2+32\kappa-60)\rho_b^2 \\
&\quad -2(2\kappa^2-7\kappa+14)\rho_b^3+(\kappa-3)\rho_b^4]e^{-\rho_b}\} \\
E_{-1,2}^{200} &= 2\rho_b^{-3}(90+90\rho_b+39\rho_b^2+9\rho_b^3+\rho_b^4)e^{-\rho_b} = \frac{1}{4}\rho_b^4[A_6(\rho_b)-2A_4(\rho_b)+A_2(\rho_b)] \\
C_{02}^{200} &= \rho_a^{-2}\rho_b^{-1}(\kappa+1)^{-1}(\kappa-1)\{- (\kappa-1)^2[12(\kappa+1)^2(4\kappa-3)(1+\rho_a)+2(\kappa+1)(12\kappa^2+6\kappa-11)\rho_a^2+4(\kappa+1)(3\kappa-2)\rho_a^3 \\
&\quad + (2\kappa-1)\rho_a^4]e^{-\rho_a} + (\kappa+1)^2[12(\kappa-1)^2(4\kappa-3)(1+\rho_b)+2(\kappa-1)(12\kappa^2-18\kappa+7)\rho_b^2-4(\kappa-1)(3\kappa-1)\rho_b^3+(2\kappa-1)\rho_b^4]e^{-\rho_b}\} \\
C_{12}^{200} &= \rho_a^{-3}(\kappa+1)^{-1}(\kappa-1)\{- (\kappa-1)^2[48(\kappa+1)^3(5\kappa-4)(1+\rho_a)+6(\kappa+1)^2(20\kappa^2+8\kappa-19)\rho_a^2+2(\kappa+1)(36\kappa^2+6\kappa-25)\rho_a^3 \\
&\quad +6(\kappa+1)(3\kappa-2)\rho_a^4+(2\kappa-1)\rho_a^5]e^{-\rho_a} + (\kappa+1)^3[48(\kappa-1)^2(5\kappa-4)(1+\rho_b)+6(\kappa-1)(20\kappa^2-32\kappa+13)\rho_b^2-24(\kappa-1)(2\kappa-1)\rho_b^3 \\
&\quad +2(3\kappa-2)\rho_b^4]e^{-\rho_b}\} \\
C_{22}^{200} &= \rho_a^{-2}\rho_b^{-1}(\kappa+1)^{-1}(\kappa-1)^2\{- (\kappa-1)^2[144(\kappa+1)^3(10\kappa^2-7)(1+\rho_a)+6(\kappa+1)^2(120\kappa^3+140\kappa^2-84\kappa-97)\rho_a^2 \\
&\quad +12(\kappa+1)^2(40\kappa^2-4\kappa-23)\rho_a^3+4(\kappa+1)(36\kappa^2+3\kappa-23)\rho_a^4+8(\kappa+1)(3\kappa-2)\rho_a^5+(2\kappa-1)\rho_a^6]e^{-\rho_a} \\
&\quad + (\kappa+1)^3[144(\kappa-1)^2(10\kappa^2-7)(1+\rho_b)+6(\kappa-1)(120\kappa^3-100\kappa^2-84\kappa+71)\rho_b^2-24(\kappa-1)(10\kappa^2+2\kappa-5)\rho_b^3+2(12\kappa^2-7)\rho_b^4]e^{-\rho_b}\} \\
(12) \quad \beta, \gamma \delta \epsilon &= 3, 200; \quad 0 \leq \alpha \leq 1 \\
C_{03}^{200} &= \rho_a^{-2}\rho_b^{-1}(\kappa+1)^{-1}(\kappa-1)\{- (\kappa-1)^3[48(\kappa+1)^2(5\kappa-2)(1+\rho_a)+6(\kappa+1)(20\kappa^2+16\kappa-9)\rho_a^2+12(\kappa+1)(4\kappa-1)\rho_a^3 \\
&\quad +6\kappa\rho_a^4]e^{-\rho_a} + (\kappa+1)^2[48(\kappa-1)^3(5\kappa-2)(1+\rho_b)+6(\kappa-1)^2(20\kappa^2-24\kappa+7)\rho_b^2-2(\kappa-1)(36\kappa^2-36\kappa+5)\rho_b^3
\end{aligned}$$

TABLE XIII (continued)

$$\begin{aligned}
 & +2(\kappa-1)(9\kappa-2)\rho_b^4 - (2\kappa-1)\rho_b^5]e^{-\rho_b} \\
 C_{13}^{200} & = 2\rho_a^{-3}(\kappa+1)^{-1}(\kappa-1)\{- (\kappa-1)^3[360(\kappa+1)^3(2\kappa-1)(1+\rho_a)+12(\kappa+1)^2(30\kappa^2+20\kappa-17)\rho_a^2+3(\kappa+1)(60\kappa^2+32\kappa-23)\rho_a^3 \\
 & +9(\kappa+1)(4\kappa-1)\rho_a^4+3\kappa\rho_a^5]e^{-\rho_a} + (\kappa+1)^3[360(\kappa-1)^3(2\kappa-1)(1+\rho_b)+12(\kappa-1)^2(30\kappa^2-40\kappa+13)\rho_b^2 \\
 & -3(\kappa-1)(60\kappa^2-72+17)\rho_b^3+3(\kappa-1)(12\kappa-5)\rho_b^4-(3\kappa-2)\rho_b^5]e^{-\rho_b}\} \\
 (13) \quad & \beta, \gamma, \delta \epsilon = 1, 110; \quad -2 \leq \alpha \leq 3 \\
 D_{-2,1}^{110} & = \rho_b^{-3}(\kappa+1)^{-1}\{- [2(\kappa+1)(\kappa^2-7\kappa-24)+2(\kappa^2-1)(\kappa-6)(\rho_a+\frac{1}{2}\rho_a^2)]-(\kappa-1)^2\rho_a^3]e^{-\rho_a} \\
 & + (\kappa+1)[2(\kappa^2-7\kappa-24)(1+\rho_b+\frac{1}{2}\rho_b^2)]-2(\kappa+4)\rho_b^3-2\rho_b^4]e^{-\rho_b}\} \\
 E_{-2,1}^{110} & = \rho_a\rho_b^{-4}(30+30\rho_b+15\rho_b^2+5\rho_b^3+\rho_b^4)e^{-\rho_b} = \frac{1}{4}\rho_a\rho_b^2[A_5(\rho_b)-A_1(\rho_b)] \\
 D_{-1,1}^{110} & = \rho_a^{-3}(\kappa-1)^{-1}\{- [2(\kappa+1)^2(2\kappa^2-9\kappa+22)+2(\kappa^2-1)(2\kappa^2-5\kappa+8)(\rho_a+\frac{1}{2}\rho_a^2)]+(\kappa-1)^2\rho_a^3]e^{-\rho_a} \\
 & + (\kappa+1)^2[2(2\kappa^2-9\kappa+22)(1+\rho_b+\frac{1}{2}\rho_b^2)]-(2\kappa-7)\rho_b^3+\rho_b^4]e^{-\rho_b}\} \\
 E_{-1,1}^{110} & = -\rho_b^{-3}(30+30\rho_b+15\rho_b^2+5\rho_b^3+\rho_b^4)e^{-\rho_b} = -\frac{1}{4}\rho_b^3[A_5(\rho_b)-A_1(\rho_b)] \\
 C_{01}^{110} & = \rho_a^{-2}\rho_b^{-1}(\kappa-1)\{- (\kappa-1)^2[12(\kappa+1)(1+\rho_a+\frac{1}{2}\rho_a^2)+2\rho_a^3]e^{-\rho_a} + (\kappa+1)[12(\kappa-1)^2(1+\rho_b+\frac{1}{2}\rho_b^2)]-(4\kappa-3)\rho_b^3+\rho_b^4]e^{-\rho_b}\} \\
 C_{11}^{110} & = 2\rho_a^{-3}(\kappa-1)\{- (\kappa-1)^2[24(\kappa+1)^2(1+\rho_a+\frac{1}{2}\rho_a^2)]+(6\kappa+5)\rho_a^3+\rho_a^4]e^{-\rho_a} + (\kappa+1)^2[24(\kappa-1)^2(1+\rho_b+\frac{1}{2}\rho_b^2)]-(6\kappa-5)\rho_b^3 \\
 & +\rho_b^4]e^{-\rho_b}\} \\
 C_{21}^{110} & = 2\rho_a^{-2}\rho_b^{-1}(\kappa+1)^{-1}(\kappa-1)^2\{- (\kappa-1)^2[24(\kappa+1)^2(5\kappa+4)(1+\rho_a+\frac{1}{2}\rho_a^2)]+3(\kappa+1)(12\kappa+7)\rho_a^3+(9\kappa+7)\rho_a^4+\rho_a^5]e^{-\rho_a} \\
 & + (\kappa+1)^2[24(\kappa-1)^2(5\kappa+4)(1+\rho_b+\frac{1}{2}\rho_b^2)]-(24\kappa^2-3\kappa-16)\rho_b^3+(3\kappa+2)\rho_b^4]e^{-\rho_b}\}
 \end{aligned}$$

TABLE XIII (continued)

$$\begin{aligned}
C_{31}^{110} &= 2\rho_a^{-3}(\kappa+1)^{-1}(\kappa-1)^2\{- (\kappa-1)^2[360(\kappa+1)^3(2\kappa+1)(1+\rho_a+\frac{1}{2}\rho_a^2)+15(\kappa+1)(16\kappa^2+20\kappa+5)\rho_a^3+3(\kappa+1)(24\kappa+11)\rho_a^4 \\
&\quad +3(4\kappa+3)\rho_a^5+\rho_a^6]e^{-\rho_a} + (\kappa+1)^3[360(\kappa-1)^2(2\kappa+1)(1+\rho_b+\frac{1}{2}\rho_b^2)-15(8\kappa^2-4\kappa-3)\rho_b^3+3(4\kappa+1)\rho_b^4]e^{-\rho_b}\} \\
(14) \quad \beta, \gamma\delta\epsilon &= 2, 110; \quad -2 \leq \alpha \leq 2 \\
D_{-2,2}^{110} &= \rho_b^{-3}(\kappa+1)^{-1}\{- [4(\kappa+1)(\kappa^3-6\kappa^2+24\kappa+71)+4(\kappa^2-1)(\kappa^2-5\kappa+19)(\rho_a+\frac{1}{2}\rho_a^2)-(\kappa-1)^2(\kappa-7)\rho_a^3+(\kappa-1)^2\rho_a^4]e^{-\rho_a} \\
&\quad + (\kappa+1)[4(\kappa^3-6\kappa^2+24\kappa+71)(1+\rho_b+\frac{1}{2}\rho_b^2)-(3\kappa^2-16\kappa-47)\rho_b^3+(3\kappa+11)\rho_b^4+2\rho_b^5]e^{-\rho_b}\} \\
E_{-2,2}^{110} &= -\rho_a\rho_b^{-4}(180+180\rho_b+90\rho_b^2+30\rho_b^3+7\rho_b^4+\rho_b^5)e^{-\rho_b} = -\frac{1}{4}\rho_a\rho_b^3[A_6(\rho_b)-A_2(\rho_b)] \\
D_{-1,2}^{110} &= \rho_a^{-3}(\kappa-1)^{-1}\{- [12(\kappa+1)^2(\kappa^3-5\kappa^2+12\kappa-23)+12(\kappa^2-1)(\kappa^3-3\kappa^2+4\kappa-7)(\rho_a+\frac{1}{2}\rho_a^2)+(\kappa-1)^2(\kappa-7)\rho_a^3-(\kappa-1)^2\rho_a^4]e^{-\rho_a} \\
&\quad + (\kappa+1)^2[12(\kappa^3-5\kappa^2+12\kappa-23)(1+\rho_b+\frac{1}{2}\rho_b^2)-2(3\kappa^2-11\kappa+23)\rho_b^3+(3\kappa-10)\rho_b^4-\rho_b^5]e^{-\rho_b}\} \\
E_{-1,2}^{110} &= \rho_b^{-3}(180+180\rho_b+90\rho_b^2+30\rho_b^3+7\rho_b^4+\rho_b^5)e^{-\rho_b} = \frac{1}{4}\rho_b^4[A_6(\rho_b)-A_2(\rho_b)] \\
C_{02}^{110} &= \rho_a^{-2}\rho_b^{-1}(\kappa-1)\{- (\kappa-1)^2[12(\kappa+1)(4\kappa-3)(1+\rho_a+\frac{1}{2}\rho_a^2)+2(3\kappa-2)\rho_a^3]e^{-\rho_a} \\
&\quad + (\kappa+1)[12(\kappa-1)^2(4\kappa-3)(1+\rho_b+\frac{1}{2}\rho_b^2)-2(\kappa-1)(9\kappa-4)\rho_b^3+2(3\kappa-2)\rho_b^4-\rho_b^5]e^{-\rho_b}\} \\
C_{12}^{110} &= 2\rho_a^{-3}(\kappa-1)\{- (\kappa-1)^2[24(\kappa+1)^2(5\kappa-4)(1+\rho_a+\frac{1}{2}\rho_a^2)+(24\kappa^2+3\kappa-16)\rho_a^3+(3\kappa-2)\rho_a^4]e^{-\rho_a} \\
&\quad + (\kappa+1)^2[24(\kappa-1)^2(5\kappa-4)(1+\rho_b+\frac{1}{2}\rho_b^2)-3(\kappa-1)(12\kappa-7)\rho_b^3+(9\kappa-7)\rho_b^4-\rho_b^5]e^{-\rho_b}\} \\
C_{22}^{110} &= 2\rho_a^{-2}\rho_b^{-1}(\kappa+1)^{-1}(\kappa-1)^2\{- (\kappa-1)^2[72(\kappa+1)^2(10\kappa^2-7)(1+\rho_a+\frac{1}{2}\rho_a^2)+3(\kappa+1)(60\kappa^2-8\kappa-33)\rho_a^3+(36\kappa^2+3\kappa-23)\rho_a^4 \\
&\quad + (3\kappa-2)\rho_a^5]e^{-\rho_a} + (\kappa+1)^2[72(\kappa-1)^2(10\kappa^2-7)(1+\rho_b+\frac{1}{2}\rho_b^2)-3(\kappa-1)(60\kappa^2+8\kappa-33)\rho_b^3+(36\kappa^2-3\kappa-23)\rho_b^4 \\
&\quad - (3\kappa+2)\rho_b^5]e^{-\rho_b}\}
\end{aligned}$$

TABLE XIII (continued)

(15)  $\beta, \gamma\delta\epsilon = 1, 020$ ;  $0 \leq \alpha \leq 3$

$$C_{01}^{020} = \rho_a^{-2} \rho_b^{-1} \{ -(\kappa-1)^3 [12(\kappa+1)(1+\rho_a) + 2(3\kappa+2)\rho_a^2] e^{-\rho_a} + (\kappa+1) [12(\kappa-1)^3 (1+\rho_b) + 2(\kappa-1)^2 (3\kappa-4)\rho_b^2] \}$$

$$- (\kappa-1) (6\kappa-5) \rho_b^3 + 3(\kappa-1) \rho_b^4 - \rho_b^5 e^{-\rho_b} \}$$

$$C_{11}^{020} = \rho_a^{-3} \{ -(\kappa-1)^3 [48(\kappa+1)^2 (1+\rho_a) + 6(\kappa+1) (4\kappa+3) \rho_a^2 + 2(3\kappa+2) \rho_a^3] e^{-\rho_a} + (\kappa+1)^2 [48(\kappa-1)^3 (1+\rho_b) + 6(\kappa-1)^2 (4\kappa-5) \rho_b^2] \}$$

$$- 2(\kappa-1) (9\kappa-8) \rho_b^3 + 6(\kappa-1) \rho_b^4 - \rho_b^5 e^{-\rho_b} \}$$

$$C_{21}^{020} = \rho_a^{-2} \rho_b^{-1} (\kappa-1) \{ -(\kappa-1)^3 [48(\kappa+1)^2 (5\kappa+4) (1+\rho_a) + 6(\kappa+1) (20\kappa^2 + 32\kappa + 13) \rho_a^2 + 24(\kappa+1) (2\kappa+1) \rho_a^3] \}$$

$$+ 2(3\kappa+2) \rho_a^4 e^{-\rho_a} + (\kappa+1)^2 [48(\kappa-1)^3 (5\kappa+4) (1+\rho_b) + 6(\kappa-1)^2 (20\kappa^2 - 8\kappa - 19) \rho_b^2 - 2(\kappa-1) (36\kappa^2 - 6\kappa - 25) \rho_b^3] \}$$

$$+ 6(\kappa-1) (3\kappa+2) \rho_b^4 - (2\kappa+1) \rho_b^5 e^{-\rho_b} \}$$

$$C_{31}^{020} = 2\rho_a^{-3} (\kappa+1)^{-1} (\kappa-1) \{ -(\kappa-1)^3 [360(\kappa+1)^3 (2\kappa+1) (1+\rho_a) + 12(\kappa+1)^2 (30\kappa^2 + 40\kappa + 13) \rho_a^2 + 3(\kappa+1) (60\kappa^2 + 72\kappa + 17) \rho_a^3] \}$$

$$+ 3(\kappa+1) (12\kappa+5) \rho_a^4 + (3\kappa+2) \rho_a^5 e^{-\rho_a} + (\kappa+1)^3 [360(\kappa-1)^3 (2\kappa+1) (1+\rho_b) + 12(\kappa-1)^2 (30\kappa^2 - 20\kappa - 17) \rho_b^2] \}$$

$$- 3(\kappa-1) (60\kappa^2 - 32\kappa - 23) \rho_b^3 + 9(\kappa-1) (4\kappa+1) \rho_b^4 - 3\kappa \rho_b^5 e^{-\rho_b} \}$$

(16)  $\beta, \gamma\delta\epsilon = 1, 001$ ;  $-3 \leq \alpha \leq 3$

$$D_{-3,1}^{001} = 2\rho_a^{-1} \rho_b^{-2} (\kappa-1)^{-1} \{ - [(\kappa+1) (\kappa+14) + (\kappa-1) (\kappa+4) \rho_a + (\kappa-1) \rho_a^2] e^{-\rho_a} + (\kappa+1) [(\kappa+14) (1+\rho_b) + 6\rho_b^2 + \rho_b^3] e^{-\rho_b} \}$$

$$E_{-3,1}^{001} = -\rho_b^{-3} [\rho_a^2 \rho_b^{-2} (15+15\rho_b+6\rho_b^2+\rho_b^3) - (3+3\rho_b+2\rho_b^2+\rho_b^3)] e^{-\rho_b} = -(1/8) \rho_b \{ \rho_a^2 [A_5(\rho_b) - 2A_3(\rho_b) + A_1(\rho_b)] \}$$

$$- 4[A_3(\rho_b) + A_1(\rho_b)] \}$$

$$D_{-2,1}^{001} = 2\rho_b^{-3} \{ - [(\kappa^2 - 7\kappa - 24) + (\kappa-1) (\kappa-6) \rho_a - (\kappa-1) \rho_a^2] e^{-\rho_a} + [(\kappa^2 - 7\kappa - 24) (1+\rho_b) - 2(\kappa+5) \rho_b^2 - 2\rho_b^3] e^{-\rho_b} \}$$

TABLE XIII (continued)

$$\begin{aligned}
E_{-2,1}^{001} &= 2\rho_a\rho_b^{-4}(15+15\rho_b+6\rho_b^2+\rho_b^3)e^{-\rho_b} = \frac{1}{4}\rho_a\rho_b^2[A_5(\rho_b)-2A_3(\rho_b)+A_1(\rho_b)] \\
D_{-1,1}^{001} &= 2\rho_a^{-1}\rho_b^{-2}\{-[(\kappa+1)(2\kappa^2-9\kappa+22)+(\kappa-1)(2\kappa^2-5\kappa+8)\rho_a+(\kappa-1)\rho_a^2]e^{-\rho_a} + (\kappa+1)[(2\kappa^2-9\kappa+22)(1+\rho_b)-2(\kappa-4)\rho_b^2 \\
&\quad +\rho_b^3]e^{-\rho_b}\} \\
E_{-1,1}^{001} &= -2\rho_b^{-3}(15+15\rho_b+6\rho_b^2+\rho_b^3)e^{-\rho_b} = \frac{1}{4}\rho_b^3[A_5(\rho_b)-2A_3(\rho_b)+A_1(\rho_b)] \\
C_{01}^{001} &= 2\rho_a^{-2}\rho_b^{-1}(\kappa-1)\{-(\kappa-1)^2[6(\kappa+1)(1+\rho_a)+2\rho_a^2]e^{-\rho_a} + (\kappa+1)[6(\kappa-1)^2(1+\rho_b)-4(\kappa-1)\rho_b^2+\rho_b^3]e^{-\rho_b}\} \\
C_{11}^{001} &= 4\rho_a^{-3}(\kappa-1)\{-(\kappa-1)^2[12(\kappa+1)^2(1+\rho_a)+6(\kappa+1)\rho_a^2+\rho_a^3]e^{-\rho_a} + (\kappa+1)^2[12(\kappa-1)^2(1+\rho_b)-6(\kappa-1)\rho_b^2+\rho_b^3]e^{-\rho_b}\} \\
C_{21}^{001} &= 4\rho_a^{-2}\rho_b^{-1}(\kappa+1)^{-1}(\kappa-1)^2\{-(\kappa-1)^2[12(\kappa+1)^2(1+\rho_a)+6(\kappa+1)(1+\rho_a)+9(\kappa+1)\rho_a^2+\rho_a^4]e^{-\rho_a} \\
&\quad + (\kappa+1)^2[12(\kappa-1)^2(1+\rho_b)-6(\kappa-1)(4\kappa+3)\rho_b^2+(3\kappa+2)\rho_b^3]e^{-\rho_b}\} \\
C_{31}^{001} &= 4\rho_a^{-3}(\kappa+1)^{-1}(\kappa-1)^2\{-(\kappa-1)^2[180(\kappa+1)^3(2\kappa+1)(1+\rho_a)+12(\kappa+1)^2(20\kappa+11)\rho_a^2+3(\kappa+1)(24\kappa+19)\rho_a^3 \\
&\quad +12(\kappa+1)\rho_a^4+\rho_a^5]e^{-\rho_a} + (\kappa+1)^3[180(\kappa-1)^2(2\kappa+1)(1+\rho_b)-24(\kappa-1)(5\kappa+2)\rho_b^2+3(4\kappa+1)\rho_b^3]e^{-\rho_b}\} \\
(17) \quad \beta, \gamma \delta \epsilon &= 2, 001; \quad -3 \leq \alpha \leq 2 \\
D_{-3,2}^{001} &= 2\rho_a^{-3}(\kappa-1)^{-2}\{-[(\kappa+1)^2(\kappa-16)(\kappa+5)+(\kappa^2-1)(\kappa-11)(\kappa+2)\rho_a-(\kappa^2-1)(2\kappa+7)\rho_a^2-(\kappa-1)^2\rho_a^3]e^{-\rho_a} \\
&\quad + (\kappa+1)^2[(\kappa-16)(\kappa+5)(1+\rho_b)-3(\kappa+12)\rho_b^2-9\rho_b^3-\rho_b^4]e^{-\rho_b}\} \\
E_{-3,2}^{001} &= \rho_b^{-3}[\rho_a^2\rho_b^{-2}(90+90\rho_b+39\rho_b^2+9\rho_b^3+\rho_b^4)-(12+12\rho_b+7\rho_b^2+3\rho_b^3+\rho_b^4)]e^{-\rho_b} \\
&= (1/8)\rho_b^2\{\rho_a^2[A_6(\rho_b)-2A_4(\rho_b)+A_2(\rho_b)]-4[A_4(\rho_b)+A_2(\rho_b)]\} \\
D_{-2,2}^{001} &= 2\rho_b^{-3}(\kappa+1)^{-1}\{-[2(\kappa+1)(\kappa^3-6\kappa^2+24\kappa+71)+2(\kappa^2-1)(\kappa^2-5\kappa+19)\rho_a-(\kappa^2-1)(\kappa-10)\rho_a^2+(\kappa-1)^2\rho_a^3]e^{-\rho_a} \\
&\quad + (\kappa+1)[2(\kappa^3-6\kappa^2+24\kappa+71)(1+\rho_b)-(3\kappa^2-19\kappa-62)\rho_b^2+3(\kappa+5)\rho_b^3+2\rho_b^4]e^{-\rho_b}\}
\end{aligned}$$

TABLE XIII (continued)

$$\begin{aligned}
 E_{-2,2}^{001} &= -2\rho_a\rho_b^{-4}(90+90\rho_b+39\rho_b^2+9\rho_b^3+\rho_b^4)e^{-\rho_b} = -\frac{1}{4}\rho_a\rho_b^3[A_6(\rho_b)-2A_4(\rho_b)+A_2(\rho_b)] \\
 D_{-1,2}^{001} &= 2\rho_a^{-3}(\kappa-1)^{-1}\{-[6(\kappa+1)^2(\kappa^3-5\kappa^2+12\kappa-23)+6(\kappa^2-1)(\kappa^3-3\kappa^2+4\kappa-7)\rho_a+(\kappa^2-1)(\kappa-10)\rho_a^2-(\kappa-1)^2\rho_a^3]e^{-\rho_a} \\
 &\quad +(\kappa+1)^2[6(\kappa^3-5\kappa^2+12\kappa-23)(1+\rho_b)-(6\kappa^2-25\kappa+58)\rho_b^2+3(\kappa-4)\rho_b^3-\rho_b^4]e^{-\rho_b}\} \\
 E_{-1,2}^{001} &= 2\rho_b^{-3}(90+90\rho_b+39\rho_b^2+9\rho_b^3+\rho_b^4)e^{-\rho_b} = \frac{1}{4}\rho_b^4[A_6(\rho_b)-2A_4(\rho_b)+A_2(\rho_b)] \\
 C_{02}^{001} &= 2\rho_a^{-2}\rho_b^{-1}(\kappa-1)\{- (\kappa-1)^2[6(\kappa+1)(4\kappa-3)(1+\rho_a)+2(3\kappa-2)\rho_a^2]e^{-\rho_a} + (\kappa+1)[6(\kappa-1)^2(4\kappa-3)(1+\rho_b)-2(\kappa-1)(9\kappa-7)\rho_b^2 \\
 &\quad +6(\kappa-1)\rho_b^3-\rho_b^4]e^{-\rho_b}\} \\
 C_{12}^{001} &= 4\rho_a^{-3}(\kappa-1)\{- (\kappa-1)^2[12(\kappa+1)^2(5\kappa-4)(1+\rho_a)+6(\kappa+1)(4\kappa-3)\rho_a^2+(3\kappa-2)\rho_a^3]e^{-\rho_a} \\
 &\quad +(\kappa+1)^2[12(\kappa-1)^2(5\kappa-4)(1+\rho_b)-6(\kappa-1)(6\kappa-5)\rho_b^2+9(\kappa-1)\rho_b^3-\rho_b^4]e^{-\rho_b}\} \\
 C_{22}^{001} &= 4\rho_a^{-2}\rho_b^{-1}(\kappa+1)^{-1}(\kappa-1)^2\{- (\kappa-1)^2[36(\kappa+1)^2(10\kappa^2-7)(1+\rho_a)+6(\kappa+1)(30\kappa^2+2\kappa-21)\rho_a^2+9(\kappa+1)(4\kappa-3)\rho_a^3 \\
 &\quad +3(3\kappa-2)\rho_a^4]e^{-\rho_a} + (\kappa+1)^2[36(\kappa-1)^2(10\kappa^2-7)(1+\rho_b)-6(\kappa-1)(30\kappa^2-2\kappa-21)\rho_b^2+9(\kappa-1)(4\kappa+3)\rho_b^3-(3\kappa+2)\rho_b^4]e^{-\rho_b}\} \\
 D_{-4,1}^{300} &= (1/3)\rho_b^{-4}(\kappa^2-1)^{-1}\{- [6(\kappa+1)(3\kappa^2+89\kappa+118)+6(\kappa^2-1)(3\kappa^2+24\kappa+13)\rho_a^2+3(\kappa+1)(\kappa-1)^2\rho_a^3]e^{-\rho_a} \\
 &\quad +(\kappa+1)[6(3\kappa^2+89\kappa+118)(1+\rho_b)+9(\kappa^2+26\kappa+33)\rho_b^2+(3\kappa^2+56\kappa+61)\rho_b^3+4(2\kappa+1)\rho_b^4]e^{-\rho_b}\} \\
 E_{-4,1}^{300} &= -\rho_a\rho_b^{-5}[\rho_a^2\rho_b^{-2}(105+105\rho_b+45\rho_b^2+10\rho_b^3+\rho_b^4)-3(15+15\rho_b+6\rho_b^2+\rho_b^3)]e^{-\rho_b} \\
 &= -(1/48)\rho_a\rho_b^4[\rho_a^2[A_7(\rho_b)-3A_5(\rho_b)+3A_3(\rho_b)-A_1(\rho_b)]-18[A_5(\rho_b)-2A_3(\rho_b)+A_1(\rho_b)]] \\
 D_{-3,1}^{300} &= \rho_a^{-3}\rho_b^{-1}(\kappa-1)^{-2}\{- [6(\kappa+1)^2(\kappa^2-12\kappa-94)+6(\kappa^2-1)(\kappa^2-10\kappa-26)\rho_a+3(\kappa^2-1)(\kappa^2-9\kappa-12)\rho_a^2
 \end{aligned}$$

Functions with  $\gamma+\delta+2\epsilon = 3$

$$(18) \quad \beta, \gamma\delta\epsilon = 1, 300; \quad -4 \leq \alpha \leq 1$$

TABLE XIII (continued)

$$\begin{aligned}
& +(\kappa-1)^2(\kappa^2-5\kappa-2)\rho_a^3 e^{-\rho_a} + (\kappa+1)^2[6(\kappa^2-12\kappa-94)(1+\rho_b)+3(\kappa-16)(\kappa+5)\rho_b^2+(\kappa-13)(\kappa+4)\rho_b^3-(\kappa+5)\rho_b^4]e^{-\rho_b} \\
E_{-3,1}^{300} &= 3\rho_b^{-4}[\rho_a^2\rho_b^{-2}(105+105\rho_b+45\rho_b^2+10\rho_b^3+\rho_b^4)-(15+15\rho_b+6\rho_b^2+\rho_b^3)]e^{-\rho_b} \\
&= (1/16)\rho_b^2\{\rho_a^2[A_7(\rho_b)-3A_5(\rho_b)+3A_3(\rho_b)-A_1(\rho_b)]-6[A_5(\rho_b)-2A_3(\rho_b)+A_1(\rho_b)]\} \\
D_{-2,1}^{300} &= \rho_b^{-4}(\kappa+1)^{-2}\{-[6(\kappa+1)^2(2\kappa^3-13\kappa^2+55\kappa+166)+6(\kappa-1)(\kappa+1)^2(2\kappa^2-11\kappa+4)\rho_a+6(\kappa^2-1)(\kappa^3-4\kappa^2+13\kappa+10)\rho_a^2 \\
&+2(\kappa+1)(\kappa-1)^2(\kappa^2-2\kappa+4)\rho_a^3+(\kappa-1)^4\rho_a^4\}e^{-\rho_a} + (\kappa+1)^2[6(2\kappa^3-13\kappa^2+55\kappa+166)(1+\rho_b)+6(\kappa^3-6\kappa^2+24\kappa+71)\rho_b^2 \\
&+2(\kappa^3-5\kappa^2+17\kappa+47)\rho_b^3-(\kappa^2-4\kappa-9)\rho_b^4]e^{-\rho_b} \\
E_{-2,1}^{300} &= -6\rho_a\rho_b^{-5}(105+105\rho_b+45\rho_b^2+10\rho_b^3+\rho_b^4)e^{-\rho_b} = -(1/8)\rho_a\rho_b^3[A_7(\rho_b)-3A_5(\rho_b)+3A_3(\rho_b)-A_1(\rho_b)] \\
D_{-1,1}^{300} &= \rho_a^{-3}\rho_b^{-1}(\kappa^2-1)^{-1}\{-[6(\kappa+1)^3(6\kappa^3-32\kappa^2+81\kappa-160)+6(\kappa-1)(\kappa+1)^2(6\kappa^3-20\kappa^2+29\kappa-50)\rho_a \\
&+6(\kappa-1)(\kappa+1)^2(3\kappa^3-9\kappa^2+10\kappa-14)\rho_a^2+2(\kappa+1)(\kappa-1)^2(3\kappa^3-\kappa^2-7\kappa+2)\rho_a^3+4(\kappa+1)(\kappa-1)^4\rho_a^4\}e^{-\rho_a} \\
&+ (\kappa+1)^3[6(6\kappa^3-32\kappa^2+81\kappa-160)(1+\rho_b)+18(\kappa^3-5\kappa^2+12\kappa-23)\rho_b^2+2(3\kappa^3-13\kappa^2+27\kappa-47)\rho_b^3-2(\kappa^2-3\kappa+5)\rho_b^4]e^{-\rho_b} \\
E_{-1,1}^{300} &= 6\rho_b^{-4}(105+105\rho_b+45\rho_b^2+10\rho_b^3+\rho_b^4)e^{-\rho_b} = (1/8)\rho_b^4[A_7(\rho_b)-3A_5(\rho_b)+3A_3(\rho_b)-A_1(\rho_b)] \\
C_{01}^{300} &= \rho_a^{-4}(\kappa+1)^{-1}(\kappa-1)^2[144(\kappa+1)^3(1+\rho_a)+18(\kappa+1)^2(4\kappa+5)\rho_a^2+6(\kappa+1)^2(4\kappa+7)\rho_a^3+18(\kappa+1)^2\rho_a^4 \\
&+6(\kappa+1)\rho_a^5+\rho_a^6]e^{-\rho_a} + (\kappa+1)^3[144(\kappa-1)^2(1+\rho_b)+18(\kappa-1)(4\kappa-3)\rho_b^2+6(\kappa-1)(4\kappa-1)\rho_b^3-6\kappa\rho_b^4]e^{-\rho_b} \\
C_{11}^{300} &= \rho_a^{-3}\rho_b^{-1}(\kappa+1)^{-2}(\kappa-1)^2\{- (\kappa-1)^2[720(\kappa+1)^4(1+\rho_a)+72(\kappa+1)^3(5\kappa+6)\rho_a^2+24(\kappa+1)^3(5\kappa+8)\rho_a^3+6(\kappa+1)^2(16\kappa+13)\rho_a^4 \\
&+6(\kappa+1)(6\kappa+5)\rho_a^5+8(\kappa+1)\rho_a^6+\rho_a^7]e^{-\rho_a} + (\kappa+1)^4[720(\kappa-1)^2(1+\rho_b)+72(\kappa-1)(5\kappa-4)\rho_b^2+24(\kappa-1)(5\kappa-2)\rho_b^3 \\
&-6(4\kappa-1)\rho_b^4]e^{-\rho_b}\}
\end{aligned}$$



TABLE XIII (continued)

$$\begin{aligned}
& +6(\kappa-1)(\kappa+1)^2(12\kappa^4-45\kappa^3+65\kappa^2-56\kappa+119)\rho_a^2+2(\kappa+1)(\kappa-1)^2(12\kappa^4-15\kappa^3-19\kappa^2+32\kappa+29)\rho_a^3 \\
& +2(\kappa+1)(\kappa-1)^2(6\kappa^3-16\kappa^2+14\kappa-1)\rho_a^4+(\kappa-1)^4(2\kappa-1)\rho_a^5]e^{-\rho_a} + (\kappa+1)^3[48(3\kappa^4-18\kappa^3+50\kappa^2-93\kappa+163)(1+\rho_b) \\
& +6(12\kappa^4-69\kappa^3+185\kappa^2-336\kappa+583)\rho_b^2+2(12\kappa^4-63\kappa^3+155\kappa^2-264\kappa+445)\rho_b^3-2(6\kappa^3-23\kappa^2+42\kappa-67)\rho_b^4 \\
& +2(\kappa^2-3\kappa+5)\rho_b^5]e^{-\rho_b}
\end{aligned}$$

$$E_{-1,2}^{300} = -6\rho_b^{-4}(840+840\rho_b+375\rho_b^2+95\rho_b^3+14\rho_b^4+\rho_b^5)e^{-\rho_b} = -(1/8)\rho_b^5[A_8(\rho_b)-3A_6(\rho_b)+3A_4(\rho_b)-A_2(\rho_b)]$$

$$C_{02}^{300} = \rho_a^{-4}(\kappa+1)^{-1}(\kappa-1)\{- (\kappa-1)^2[144(\kappa+1)^3(5\kappa-4)(1+\rho_a)+18(\kappa+1)^2(20\kappa^2+8\kappa-19)\rho_a^2+6(\kappa+1)^2(20\kappa^2+16\kappa-25)\rho_a^3$$

$$+18(\kappa+1)(4\kappa^2+\kappa-3)\rho_a^4+6(\kappa+1)(3\kappa-2)\rho_a^5+(2\kappa-1)\rho_a^6+(\kappa+1)^3[144(\kappa-1)^2(5\kappa-4)(1+\rho_b)$$

$$+18(\kappa-1)(20\kappa^2-32\kappa+13)\rho_b^2+6(\kappa-1)(20\kappa^2-24\kappa+7)\rho_b^3-6\kappa(8\kappa-7)\rho_b^4+6\kappa\rho_b^5]e^{-\rho_b}\}$$

$$C_{12}^{300} = \rho_a^{-3}\rho_b^{-1}(\kappa+1)^{-2}(\kappa-1)^2\{- (\kappa-1)^2[720(\kappa+1)^4(6\kappa-5)(1+\rho_a)+72(\kappa+1)^3(30\kappa^2+10\kappa-29)\rho_a^2+24(\kappa+1)^3(30\kappa^2+20\kappa-37)\rho_a^3$$

$$+6(\kappa+1)^2(80\kappa^2+4\kappa-55)\rho_a^4+6(\kappa+1)(24\kappa^2+3\kappa-16)\rho_a^5+8(\kappa+1)(3\kappa-2)\rho_a^6+(2\kappa-1)\rho_a^7]e^{-\rho_a}$$

$$+ (\kappa+1)^4[720(\kappa-1)^2(6\kappa-5)(1+\rho_b)+72(\kappa-1)(30\kappa^2-50\kappa+21)\rho_b^2+24(\kappa-1)(30\kappa^2-40\kappa+13)\rho_b^3-6(40\kappa^2-44\kappa+7)\rho_b^4$$

$$+6(4\kappa-1)\rho_b^5]e^{-\rho_b}\}$$

$$(20) \quad \beta, \gamma, \delta, \epsilon = 1, 2, 10; \quad -3 \leq \alpha \leq 2$$

$$\begin{aligned}
D_{-3,1}^{210} &= \rho_a^{-3}\rho_b^{-1}(\kappa-1)^{-2}\{- [6(\kappa+1)^2(\kappa^2-12\kappa-94)+6(\kappa^2-1)(\kappa^2-10\kappa-26)\rho_a+(\kappa^2-1)(3\kappa^2-29\kappa-64)\rho_a^2+(\kappa-1)^2(\kappa^2-7\kappa-10)\rho_a^3 \\
&\quad -(\kappa+1)(\kappa-1)^2\rho_a^4]e^{-\rho_a} + (\kappa+1)^2[6(\kappa^2-12\kappa-94)(1+\rho_b)+(3\kappa^2-35\kappa-268)\rho_b^2+(\kappa-16)(\kappa+5)\rho_b^3-2(\kappa+8)\rho_b^4-2\rho_b^5]e^{-\rho_b}\}
\end{aligned}$$

$$E_{-3,1}^{210} = \rho_b^{-4}[\rho_a^2\rho_b^{-2}(315+315\rho_b+150\rho_b^2+45\rho_b^3+9\rho_b^4+\rho_b^5)-(45+45\rho_b+21\rho_b^2+6\rho_b^3+\rho_b^4)]e^{-\rho_b}$$

TABLE XIII (continued)

$$\begin{aligned}
 &= (1/16)\rho_b^2 \{A_7(\rho_b) - A_5(\rho_b) - A_3(\rho_b) + A_1(\rho_b)\} - 2[3A_5(\rho_b) - 2A_3(\rho_b) - A_1(\rho_b)]\} \\
 D_{-2,1}^{210} &= \rho_b^{-4} (\kappa+1)^{-1} \{- [6(\kappa+1)(2\kappa^3 - 13\kappa^2 + 55\kappa + 166) + 6(\kappa^2 - 1)(2\kappa^2 - 11\kappa + 44)]\rho_a + 2(\kappa - 1)(3\kappa^3 - 13\kappa^2 + 46\kappa + 54)\rho_a^2 \\
 &\quad + 2(\kappa - 1)^2(\kappa^2 - 3\kappa + 10)\rho_a^3 + 2(\kappa - 1)^2 \rho_a^4 + (\kappa + 1)[6(2\kappa^3 - 13\kappa^2 + 55\kappa + 166)(1 + \rho_b) + 2(3\kappa^3 - 19\kappa^2 + 79\kappa + 237)\rho_b^2 \\
 &\quad + 2(\kappa^3 - 6\kappa^2 + 24\kappa + 71)\rho_b^3 - 2(\kappa - 7)(\kappa + 2)\rho_b^4 + (\kappa + 3)\rho_b^5]e^{-\rho_b}\} \\
 E_{-2,1}^{210} &= -2\rho_a\rho_b^{-5} (315 + 315\rho_b + 150\rho_b^2 + 45\rho_b^3 + 9\rho_b^4 + \rho_b^5)e^{-\rho_b} = -(1/8)\rho_a\rho_b^3 [A_7(\rho_b) - A_5(\rho_b) - A_3(\rho_b) + A_1(\rho_b)] \\
 D_{-1,1}^{210} &= \rho_a^{-3}\rho_b^{-1}(\kappa - 1)^{-1} \{- [6(\kappa + 1)^2(6\kappa^3 - 32\kappa^2 + 81\kappa - 160) + 6(\kappa^2 - 1)(6\kappa^3 - 20\kappa^2 + 29\kappa - 50)]\rho_a + 2(\kappa^2 - 1)(9\kappa^3 - 29\kappa^2 + 39\kappa - 64)\rho_a^2 \\
 &\quad + 2(\kappa - 1)^2(3\kappa^3 - 3\kappa^2 - 2\kappa - 6)\rho_a^3 + 2(\kappa - 1)^2(\kappa - 2)\kappa\rho_a^4 + (\kappa + 1)^2[6(6\kappa^3 - 32\kappa^2 + 81\kappa - 160)(1 + \rho_b) \\
 &\quad + 2(9\kappa^3 - 47\kappa^2 + 117\kappa - 229)\rho_b^2 + 6(\kappa^3 - 5\kappa^2 + 12\kappa - 23)\rho_b^3 - 2(2\kappa^2 - 7\kappa + 14)\rho_b^4 + (\kappa - 3)\rho_b^5]e^{-\rho_b}\} \\
 E_{-1,1}^{210} &= 2\rho_b^{-4} (315 + 315\rho_b + 150\rho_b^2 + 45\rho_b^3 + 9\rho_b^4 + \rho_b^5)e^{-\rho_b} = (1/8)\rho_b^4 [A_7(\rho_b) - A_5(\rho_b) - A_3(\rho_b) + A_1(\rho_b)] \\
 C_{01}^{210} &= \rho_a^{-4} \{- (\kappa - 1)^3 [144(\kappa + 1)^2(1 + \rho_a) + 6(\kappa + 1)(12\kappa + 13)]\rho_a^2 + 6(\kappa + 1)(4\kappa + 5)\rho_a^3 + 2(6\kappa + 5)\rho_a^4 + 2\rho_a^5\}e^{-\rho_a} \\
 &\quad + (\kappa + 1)^2 [144(\kappa - 1)^3(1 + \rho_b) + 6(\kappa - 1)^2(12\kappa - 11)\rho_b^2 + 6(\kappa - 1)^2(4\kappa - 3)\rho_b^3 - 4(\kappa - 1)(3\kappa - 1)\rho_b^4 + (2\kappa - 1)\rho_b^5]e^{-\rho_b}\} \\
 C_{11}^{210} &= 2\rho_a^{-3}\rho_b^{-1}(\kappa + 1)^{-1}(\kappa - 1) \{- (\kappa - 1)^3 [360(\kappa + 1)^3(1 + \rho_a) + 12(\kappa + 1)^2(15\kappa + 16)]\rho_a^2 + 12(\kappa + 1)^2(5\kappa + 6)\rho_a^3 \\
 &\quad + 12(\kappa + 1)(3\kappa + 2)\rho_a^4 + (9\kappa + 7)\rho_a^5 + \rho_a^6\}e^{-\rho_a} + (\kappa + 1)^3 [360(\kappa - 1)^3(1 + \rho_b) + 12(\kappa - 1)^2(15\kappa - 14)]\rho_b^2 \\
 &\quad + 12(\kappa - 1)^2(5\kappa - 4)\rho_b^3 - 12(\kappa - 1)(2\kappa - 1)\rho_b^4 + (3\kappa - 2)\rho_b^5]e^{-\rho_b}\} \\
 C_{21}^{210} &= 2\rho_a^{-4}(\kappa + 1)^{-1}(\kappa - 1) \{- (\kappa - 1)^3 [360(\kappa + 1)^3(6\kappa + 5)(1 + \rho_a) + 12(\kappa + 1)^2(90\kappa^2 + 170\kappa + 79)]\rho_a^2 + 12(\kappa + 1)^2(30\kappa^2 + 60\kappa + 29)\rho_a^3 \\
 &\quad + 12(\kappa + 1)(20\kappa^2 + 28\kappa + 9)\rho_a^4 + 36(\kappa + 1)(2\kappa + 1)\rho_a^5 + 3(4\kappa + 3)\rho_a^6 + \rho_a^7\}e^{-\rho_a} + (\kappa + 1)^3 [360(\kappa - 1)^3(6\kappa + 5)(1 + \rho_b) \\
 &\quad + 12(\kappa - 1)^2(90\kappa^2 - 10\kappa - 71)\rho_b^2 + 36(\kappa - 1)^2(10\kappa^2 - 7)\rho_b^3 - 12(\kappa - 1)(10\kappa^2 + 2\kappa - 5)\rho_b^4 + (12\kappa^2 - 7)\rho_b^5]e^{-\rho_b}\}
 \end{aligned}$$

TABLE XIII (continued)

$$(21) \quad \beta, \gamma \delta \epsilon = 1, 120; \quad -2 \leq \alpha \leq 2$$

$$\begin{aligned}
 D_{-2,1}^{120} &= \rho_b^{-4} (\kappa+1)^{-2} \{- [6(\kappa+1)^2 (2\kappa^3 - 13\kappa^2 + 55\kappa + 166) + 6(\kappa-1)(\kappa+1)^2 (2\kappa^2 - 11\kappa + 44) \rho_a + 2(\kappa^2 - 1)(3\kappa^3 - 14\kappa^2 + 53\kappa + 78) \rho_a^2 \\
 &\quad + 2(\kappa+1)(\kappa-1)^2 (\kappa^2 - 4\kappa + 16) \rho_a^3 - (\kappa-1)^2 (\kappa+1)(\kappa-8) \rho_a^4 + (\kappa-1)^3 \rho_a^5\} e^{-\rho_a} + (\kappa+1)^2 [6(2\kappa^2 - 13\kappa^2 + 55\kappa + 166)(1 + \rho_b) \\
 &\quad + 2(3\kappa^3 - 20\kappa^2 + 86\kappa + 261) \rho_b^2 + 2(\kappa^3 - 7\kappa^2 + 31\kappa + 95) \rho_b^3 - (3\kappa^2 - 17\kappa - 52) \rho_b^4 + (3\kappa + 11) \rho_b^5 + 2\rho_b^6] e^{-\rho_b} \\
 E_{-2,1}^{120} &= -\rho_a \rho_b^{-5} (630 + 630\rho_b + 330\rho_b^2 + 120\rho_b^3 + 33\rho_b^4 + 7\rho_b^5 + \rho_b^6) e^{-\rho_b} = -(1/8) \rho_a \rho_b^3 [A_7(\rho_b) + A_5(\rho_b) - A_3(\rho_b) - A_1(\rho_b)] \\
 D_{-1,1}^{120} &= \rho_a^{-1} \rho_b^{-3} (\kappa+1)^{-2} \{- [6(\kappa+1)^3 (6\kappa^3 - 32\kappa^2 + 81\kappa - 160) + 6(\kappa-1)(\kappa+1)^2 (6\kappa^3 - 20\kappa^2 + 29\kappa - 50) \rho_a \\
 &\quad + 2(\kappa-1)(\kappa+1)^2 (9\kappa^3 - 31\kappa^2 + 48\kappa - 86) \rho_a^2 + 2(\kappa+1)(\kappa-1)^2 (3\kappa^3 - 5\kappa^2 + 3\kappa - 14) \rho_a^3 + (\kappa+1)(\kappa-1)^2 (\kappa-8) \rho_a^4 \\
 &\quad - (\kappa-1)^3 \rho_a^5\} e^{-\rho_a} + (\kappa+1)^3 [6(6\kappa^3 - 32\kappa^2 + 81\kappa - 160)(1 + \rho_b) + 2(9\kappa^3 - 49\kappa^2 + 126\kappa - 251) \rho_b^2 + 2(3\kappa^3 - 17\kappa^2 + 45\kappa - 91) \rho_b^3 \\
 &\quad - (6\kappa^2 - 23\kappa + 50) \rho_b^4 + (3\kappa - 10) \rho_b^5 - \rho_b^6] e^{-\rho_b} \\
 E_{-1,1}^{120} &= \rho_b^{-4} (630 + 630\rho_b + 330\rho_b^2 + 120\rho_b^3 + 33\rho_b^4 + 7\rho_b^5 + \rho_b^6) e^{-\rho_b} = (1/8) \rho_b^4 [A_7(\rho_b) + A_5(\rho_b) - A_3(\rho_b) - A_1(\rho_b)] \\
 C_{01}^{120} &= \rho_a^{-4} \{- (\kappa-1)^3 [144(\kappa+1)^2 (1 + \rho_a) + 6(\kappa+1)(12\kappa + 11) \rho_a^2 + 6(\kappa+1)(4\kappa + 3) \rho_a^3 + 2(3\kappa + 2) \rho_a^4] e^{-\rho_a} \\
 &\quad + (\kappa+1)^2 [144(\kappa-1)^3 (1 + \rho_b) + 6(\kappa-1)^2 (12\kappa - 13) \rho_b^2 + 6(\kappa-1)^2 (4\kappa - 5) \rho_b^3 - 2(\kappa-1)(9\kappa - 5) \rho_b^4 + 2(3\kappa - 2) \rho_b^5 - \rho_b^6] e^{-\rho_b} \\
 C_{11}^{120} &= 2\rho_a^{-3} \rho_b^{-1} (\kappa+1)^{-1} (\kappa-1) \{- (\kappa-1)^3 [360(\kappa+1)^3 (1 + \rho_a) + 12(\kappa+1)^2 (15\kappa + 14) \rho_a^2 + 12(\kappa+1)^2 (5\kappa + 4) \rho_a^3 \\
 &\quad + 12(\kappa+1)(2\kappa + 1) \rho_a^4 + (3\kappa + 2) \rho_a^5] e^{-\rho_a} + (\kappa+1)^3 [360(\kappa-1)^3 (1 + \rho_b) + 12(\kappa-1)^2 (15\kappa - 16) \rho_b^2 + 12(\kappa-1)^2 (5\kappa - 6) \rho_b^3 \\
 &\quad - 12(\kappa-1)(3\kappa - 2) \rho_b^4 + (9\kappa - 7) \rho_b^5 - \rho_b^6] e^{-\rho_b} \\
 C_{21}^{120} &= 2\rho_a^{-4} (\kappa+1)^{-1} (\kappa-1) \{- (\kappa-1)^3 [360(\kappa+1)^3 (6\kappa + 5)(1 + \rho_a) + 12(\kappa+1)^2 (90\kappa^2 + 160\kappa + 71) \rho_a^2 + 12(\kappa+1)^2 (30\kappa^2 + 50\kappa + 21) \rho_a^3 \\
 &\quad + 12(\kappa+1)(15\kappa^2 + 19\kappa + 5) \rho_a^4 + 3(\kappa+1)(12\kappa + 5) \rho_a^5 + (3\kappa + 2) \rho_a^6] e^{-\rho_a} + (\kappa+1)^3 [360(\kappa-1)^3 (6\kappa + 5)(1 + \rho_b)
 \end{aligned}$$

TABLE XIII (continued)

$$+12(\kappa-1)^2(90\kappa^2-20\kappa-79)\rho_b^2+12(\kappa-1)^2(30\kappa^2-10\kappa-29)\rho_b^3-12(\kappa-1)(15\kappa^2+\kappa-9)\rho_b^4+(36\kappa^2-3\kappa-23)\rho_b^5-(3\kappa+2)\rho_b^6]e^{-\rho_b}$$

$$(22) \quad \beta, \gamma \delta \epsilon = 1, 101; \quad -4 \leq \alpha \leq 2$$

$$D_{-4,1}^{101} = (2/3)\rho_b^{-4}(\kappa^2-1)^{-1}\{- [3(\kappa+1)(3\kappa^2+89\kappa+118)+3(\kappa^2-1)(\kappa+9)\rho_a^2+3(\kappa-1)^2\rho_a^3]e^{-\rho_a}$$

$$+ (\kappa+1)[3(3\kappa^2+89\kappa+118)(1+\rho_b)+3(\kappa^2+37\kappa+52)\rho_b^2+2(11\kappa+19)\rho_b^3+(\kappa+5)\rho_b^4]e^{-\rho_b}\}$$

$$E_{-4,1}^{101} = -\rho_a\rho_b^{-5}[\rho_a^2\rho_b^{-2}(105+105\rho_b+45\rho_b^2+10\rho_b^3+\rho_b^4)- (45+45\rho_b+21\rho_b^2+6\rho_b^3+\rho_b^4)]e^{-\rho_b}$$

$$= -(1/48)\rho_a\rho_b^2\{\rho_a^2[A_7(\rho_b)-3A_5(\rho_b)+3A_3(\rho_b)-A_1(\rho_b)]-6[3A_5(\rho_b)-2A_3(\rho_b)-A_1(\rho_b)]\}$$

$$D_{-3,1}^{101} = 2\rho_a^{-3}\rho_b^{-1}(\kappa-1)^{-2}\{- [3(\kappa+1)^2(\kappa^2-12\kappa-94)+3(\kappa^2-1)(\kappa^2-10\kappa-26)\rho_a+(\kappa^2-1)(\kappa^2-11\kappa-20)\rho_a^2-(\kappa-1)^2(\kappa+2)\rho_a^3]e^{-\rho_a}$$

$$+ (\kappa+1)^2[3(\kappa^2-12\kappa-94)(1+\rho_b)+(\kappa^2-14\kappa-122)\rho_b^2-2(\kappa+14)\rho_b^3-3\rho_b^4]e^{-\rho_b}\}$$

$$E_{-3,1}^{101} = \rho_b^{-4}[3\rho_a^2\rho_b^{-2}(105+105\rho_b+45\rho_b^2+10\rho_b^3+\rho_b^4)- (45+45\rho_b+21\rho_b^2+6\rho_b^3+\rho_b^4)]e^{-\rho_b}$$

$$= (1/16)\rho_b^2\{\rho_a^2[A_7(\rho_b)-3A_5(\rho_b)+3A_3(\rho_b)-A_1(\rho_b)]-2[3A_5(\rho_b)-2A_3(\rho_b)-A_1(\rho_b)]\}$$

$$D_{-2,1}^{101} = 2\rho_b^{-4}(\kappa+1)^{-1}\{- [3(\kappa+1)(2\kappa^3-13\kappa^2+55\kappa+166)+3(\kappa^2-1)(2\kappa^2-11\kappa+44)\rho_a+(\kappa-1)(2\kappa^3-9\kappa^2+36\kappa+31)\rho_a^2$$

$$+3(\kappa-1)^2\rho_a^3]e^{-\rho_a} + (\kappa+1)[3(2\kappa^3-13\kappa^2+55\kappa+166)(1+\rho_b)+(2\kappa^3-15\kappa^2+69\kappa+214)\rho_b^2-2(\kappa^2-7\kappa-24)\rho_b^3$$

$$+(\kappa+5)\rho_b^4]e^{-\rho_b}\}$$

$$E_{-2,1}^{101} = -6\rho_a\rho_b^{-5}(105+105\rho_b+45\rho_b^2+10\rho_b^3+\rho_b^4)e^{-\rho_b} = -(1/8)\rho_a\rho_b^3[A_7(\rho_b)-3A_5(\rho_b)+3A_3(\rho_b)-A_1(\rho_b)]$$

$$D_{-1,1}^{101} = 2\rho_a^{-3}\rho_b^{-1}(\kappa-1)^{-1}\{- [3(\kappa+1)^2(6\kappa^3-32\kappa^2+81\kappa-160)+3(\kappa^2-1)(6\kappa^3-20\kappa^2+29\kappa-50)\rho_a+3(\kappa^2-1)(2\kappa^3-6\kappa^2+7\kappa-13)\rho_a^2$$

$$+(\kappa-1)^2(2\kappa^2-4\kappa-1)\rho_a^3]e^{-\rho_a} + (\kappa+1)^2[3(6\kappa^3-32\kappa^2+81\kappa-160)(1+\rho_b)+3(2\kappa^3-12\kappa^2+33\kappa-68)\rho_b^2-2(2\kappa^2-9\kappa+22)\rho_b^3$$

TABLE XIII (continued)

$$\begin{aligned}
& +(\kappa-4)\rho_b^4]e^{-\rho_b} \\
E_{-1,1}^{101} &= 6\rho_b^{-4}(105+105\rho_b^2+45\rho_b^4+10\rho_b^6+\rho_b^8)e^{-\rho_b} = (1/8)\rho_b^4[A_7(\rho_b)-3A_5(\rho_b)+3A_3(\rho_b)-A_1(\rho_b)] \\
C_{01}^{101} &= 4\rho_a^{-4}(\kappa-1)\{- (\kappa-1)^2[36(\kappa+1)^2(1+\rho_a)+6(\kappa+1)(2\kappa+3)\rho_a^2+6(\kappa+1)\rho_a^3+\rho_a^4]e^{-\rho_a} + (\kappa+1)^2[36(\kappa-1)^2(1+\rho_b) \\
& \quad +6(\kappa-1)(2\kappa-3)\rho_b^2-6(\kappa-1)\rho_b^3+\rho_b^4]e^{-\rho_b}\} \\
C_{11}^{101} &= 4\rho_a^{-3}\rho_b^{-1}(\kappa+1)^{-1}(\kappa-1)^2\{- (\kappa-1)^2[180(\kappa+1)^3(1+\rho_a)+12(\kappa+1)^2(5\kappa+8)\rho_a^2+36(\kappa+1)^2\rho_a^3+9(\kappa+1)\rho_a^4+\rho_a^5]e^{-\rho_a} \\
& \quad + (\kappa+1)^3[180(\kappa-1)^2(1+\rho_b)+12(\kappa-1)(5\kappa-7)\rho_b^2-24(\kappa-1)\rho_b^3+3\rho_b^4]e^{-\rho_b}\} \\
C_{21}^{101} &= 4\rho_a^{-4}(\kappa+1)^{-1}(\kappa-1)^2\{- (\kappa-1)^2[180(\kappa+1)^3(6\kappa+5)(1+\rho_a)+36(\kappa+1)^2(10\kappa^2+25\kappa+14)\rho_a^2+12(\kappa+1)^2(20\kappa+17)\rho_a^3 \\
& \quad +9(\kappa+1)(8\kappa+7)\rho_a^4+12(\kappa+1)\rho_a^5+\rho_a^6]e^{-\rho_a} + (\kappa+1)^3[180(\kappa-1)^2(6\kappa+5)(1+\rho_b)+36(\kappa-1)(10\kappa^2-5\kappa-11)\rho_b^2 \\
& \quad -24(\kappa-1)(5\kappa+4)\rho_b^3+3(4\kappa+3)\rho_b^4]e^{-\rho_b}\} \\
(23) \quad \beta, \gamma \delta \epsilon &= 2, 101; \quad -4 \leq \alpha \leq 1 \\
D_{-4,2}^{101} &= (2/3)\rho_b^{-4}(\kappa^2-1)^{-1}\{- [3(\kappa+1)(3\kappa^3-48\kappa^2-763\kappa-872)+3(\kappa^2-1)(3\kappa^2-45\kappa-238)\rho_a+3(\kappa^2-1)(\kappa^2-17\kappa-79)\rho_a^2 \\
& \quad -3(\kappa-1)^2(2\kappa+11)\rho_a^3-3(\kappa-1)^2\rho_a^4]e^{-\rho_a} + (\kappa+1)[3(3\kappa^3-48\kappa^2-763\kappa-872)(1+\rho_b)+3(\kappa^3-19\kappa^2-336\kappa-396)\rho_b^2 \\
& \quad - (9\kappa^2+245\kappa+316)\rho_b^3-4(8\kappa+13)\rho_b^4-(\kappa+5)\rho_b^5]e^{-\rho_b}\} \\
E_{-4,2}^{101} &= \rho_a\rho_b^{-5}[\rho_a^2\rho_b^{-2}(840+840\rho_b+375\rho_b^2+95\rho_b^3+14\rho_b^4+\rho_b^5)-(270+270\rho_b+129\rho_b^2+39\rho_b^3+8\rho_b^4+\rho_b^5)]e^{-\rho_b} \\
& = (1/48)\rho_a\rho_b^2\{\rho_a^2[A_8(\rho_b)-3A_6(\rho_b)+3A_4(\rho_b)-A_2(\rho_b)]-6[3A_6(\rho_b)-2A_4(\rho_b)-A_2(\rho_b)]\} \\
D_{-3,2}^{101} &= 2\rho_a^{-3}\rho_b^{-1}(\kappa-1)^{-2}\{- [3(\kappa+1)^2(2\kappa^3-19\kappa^2+127\kappa+730)+3(\kappa^2-1)(2\kappa^3-15\kappa^2+93\kappa+200)\rho_a \\
& \quad +(\kappa^2-1)(2\kappa^3-16\kappa^2+110\kappa+189)\rho_a^2-(\kappa-1)^2(\kappa^2-15\kappa-25)\rho_a^3+(\kappa-1)^2(\kappa+2)\rho_a^4]e^{-\rho_a}
\end{aligned}$$

TABLE XIII (continued)

$$E_{-3,2}^{101} = -\rho_b^{-4} [3\rho_a^2 \rho_b^{-2} (840+840\rho_b+375\rho_b^2+95\rho_b^3+14\rho_b^4+\rho_b^5) - (270+270\rho_b+129\rho_b^2+39\rho_b^3+8\rho_b^4+\rho_b^5)] e^{-\rho_b} \\ + (\kappa+1)^2 [3(2\kappa^3-19\kappa^2+127\kappa+730)(1+\rho_b) + (2\kappa^3-22\kappa^2+161\kappa+984)\rho_b^2 - (3\kappa^2-34\kappa-254)\rho_b^3 + 3(\kappa+13)\rho_b^4 + 3\rho_b^5] e^{-\rho_b}$$

$$= -(1/16)\rho_b^3 \{ \rho_a^2 [A_8(\rho_b) - 3A_6(\rho_b) + 3A_4(\rho_b) - A_2(\rho_b)] - 2[3A_6(\rho_b) - 2A_4(\rho_b) - A_2(\rho_b)] \}$$

$$D_{-2,2}^{101} = 2\rho_b^{-4} (\kappa+1)^{-1} \{ - [6(\kappa+1)(3\kappa^4-20\kappa^3+70\kappa^2-232\kappa-661) + 6(\kappa^2-1)(3\kappa^3-17\kappa^2+53\kappa-179)] \rho_a \\ + (\kappa-1)(6\kappa^4-28\kappa^3+75\kappa^2-297\kappa-326)\rho_a^2 + 3(\kappa-1)^2(\kappa-14)\rho_a^3 - 3(\kappa-1)^2\rho_a^4 \} e^{-\rho_a}$$

$$+ (\kappa+1) [6(3\kappa^4-20\kappa^3+70\kappa^2-232\kappa-661)(1+\rho_b) + (6\kappa^4-46\kappa^3+177\kappa^2-615\kappa-1772)\rho_b^2 \\ - (6\kappa^3-37\kappa^2+151\kappa+50)\rho_b^3 + (3\kappa^2-20\kappa-67)\rho_b^4 - (\kappa+5)\rho_b^5] e^{-\rho_b}$$

$$E_{-2,2}^{101} = 6\rho_a\rho_b^{-5} (840+840\rho_b+375\rho_b^2+95\rho_b^3+14\rho_b^4+\rho_b^5) e^{-\rho_b} = (1/8)\rho_a\rho_b^4 [A_8(\rho_b) - 3A_6(\rho_b) + 3A_4(\rho_b) - A_2(\rho_b)]$$

$$D_{-1,2}^{101} = 2\rho_a^{-3} \rho_b^{-1} (\kappa-1)^{-1} \{ - [24(\kappa+1)^2(3\kappa^4-18\kappa^3+50\kappa^2-93\kappa+163) + 24(\kappa^2-1)(3\kappa^4-12\kappa^3+20\kappa^2-23\kappa+7)] \rho_a \\ + 3(\kappa^2-1)(8\kappa^4-30\kappa^3+44\kappa^2-43\kappa+116)\rho_a^2 + (\kappa-1)^2(6\kappa^3-16\kappa^2+11\kappa+38)\rho_a^3 + 3(\kappa-1)^2\rho_a^4 \} e^{-\rho_a}$$

$$+ (\kappa+1)^2 [24(3\kappa^4-18\kappa^3+50\kappa^2-93\kappa+163)(1+\rho_b) + 3(8\kappa^4-54\kappa^3+164\kappa^2-323\kappa+580)\rho_b^2 - (18\kappa^3-92\kappa^2+225\kappa-436)\rho_b^3 \\ + 2(3\kappa^2-13\kappa+31)\rho_b^4 - (\kappa-4)\rho_b^5] e^{-\rho_b}$$

$$E_{-1,2}^{101} = -6\rho_b^{-4} (840+840\rho_b+375\rho_b^2+95\rho_b^3+14\rho_b^4+\rho_b^5) e^{-\rho_b} = -(1/8)\rho_b^5 [A_8(\rho_b) - 3A_6(\rho_b) + 3A_4(\rho_b) - A_2(\rho_b)]$$

$$C_{02}^{101} = 4\rho_a^{-4} (\kappa-1) \{ - (\kappa-1)^2 [36(\kappa+1)^2(5\kappa-4)(1+\rho_a) + 6(\kappa+1)(10\kappa^2+6\kappa-11)\rho_a^2 + 6(\kappa+1)(4\kappa-3)\rho_a^3 + (3\kappa-2)\rho_a^4] e^{-\rho_a} \\ + (\kappa+1)^2 [36(\kappa-1)^2(5\kappa-4)(1+\rho_b) + 6(\kappa-1)(10\kappa^2-24\kappa+13)\rho_b^2 - 6(\kappa-1)(6\kappa-5)\rho_b^3 + (9\kappa-8)\rho_b^4 - \rho_b^5] e^{-\rho_b} \}$$

$$C_{12}^{101} = 4\rho_a^{-3} \rho_b^{-1} (\kappa+1)^{-1} (\kappa-1)^2 \{ - (\kappa-1)^2 [180(\kappa+1)^3(6\kappa-5)(1+\rho_a) + 12(\kappa+1)^2(30\kappa^2+20\kappa-37)\rho_a^2 + 36(\kappa+1)^2(5\kappa-4)\rho_a^3$$

TABLE XIII (continued)

$$+9(\kappa+1)(4\kappa-3)\rho_a^4 + (3\kappa-2)\rho_a^5]e^{-\rho_a} + (\kappa+1)^3[180(\kappa-1)^2(6\kappa-5)(1+\rho_b) + 24(\kappa-1)(15\kappa^2-35\kappa+19)\rho_b^2 - 12(\kappa-1)(15\kappa-13)\rho_b^3 + 3(12\kappa-11)\rho_b^4 - 3\rho_b^5]e^{-\rho_b}$$

$$(24) \quad \beta, \gamma \delta \epsilon = 1, 0, 1, 1; \quad -3 \leq \alpha \leq 2$$

$$D_{-3,1}^{011} = 2\rho_a^{-3}\rho_b^{-1}(\kappa-1)^{-2}\{-[3(\kappa+1)^2(\kappa^2-12\kappa-94) + 3(\kappa^2-1)(\kappa^2-10\kappa-26)\rho_a + (\kappa^2-1)(\kappa^2-12\kappa-34)\rho_a^2 - 2(\kappa-1)^2(\kappa+3)\rho_a^3 - (\kappa-1)^2\rho_a^4]e^{-\rho_a} + (\kappa+1)^2[3(\kappa^2-12\kappa-94)(1+\rho_b) + (\kappa^2-15\kappa-136)\rho_b^2 - 3(\kappa+14)\rho_b^3 - 9\rho_b^4 - \rho_b^5]e^{-\rho_b}\}$$

$$E_{-3,1}^{011} = \rho_b^{-4}[\rho_a^2\rho_b^{-2}(315+315\rho_b+150\rho_b^2+45\rho_b^3+9\rho_b^4+\rho_b^5) - (45+45\rho_b+24\rho_b^2+9\rho_b^3+3\rho_b^4+\rho_b^5)e^{-\rho_b} \\ = (1/16)\rho_b^2\{\rho_a^2[A_7(\rho_b)-A_5(\rho_b)-A_3(\rho_b)+A_1(\rho_b)] - 2[3A_5(\rho_b)+2A_3(\rho_b)+3A_1(\rho_b)]\}$$

$$D_{-2,1}^{011} = 2\rho_b^{-4}(\kappa+1)^{-1}\{-[3(\kappa+1)(2\kappa^3-13\kappa^2+55\kappa+166) + 3(\kappa^2-1)(2\kappa^2-11\kappa+44)\rho_a + (\kappa^2-1)(2\kappa^2-12\kappa+55)\rho_a^2 - (\kappa-1)^2(\kappa-9)\rho_a^3 + (\kappa-1)^2\rho_a^4]e^{-\rho_a} + (\kappa+1)[3(2\kappa^3-13\kappa^2+55\kappa+166)(1+\rho_b) + 2(\kappa^3-8\kappa^2+38\kappa+119)\rho_b^2 - 3(\kappa^2-7\kappa-24)\rho_b^3 + 3(\kappa+5)\rho_b^4 + 2\rho_b^5]e^{-\rho_b}\}$$

$$E_{-2,1}^{011} = -2\rho_a\rho_b^{-5}(315+315\rho_b+150\rho_b^2+45\rho_b^3+9\rho_b^4+\rho_b^5)e^{-\rho_b} = -(1/8)\rho_a\rho_b^3[A_7(\rho_b)-A_5(\rho_b)-A_3(\rho_b)+A_1(\rho_b)]$$

$$D_{-1,1}^{011} = 2\rho_a^{-3}\rho_b^{-1}(\kappa-1)^{-1}\{-[3(\kappa+1)^2(6\kappa^3-32\kappa^2+81\kappa-160) + 3(\kappa^2-1)(6\kappa^3-20\kappa^2+29\kappa-50)\rho_a + (\kappa^2-1)(6\kappa^3-20\kappa^2+30\kappa-61)\rho_a^2 + (\kappa-1)^2(\kappa-9)\rho_a^3 - (\kappa-1)^2\rho_a^4]e^{-\rho_a} + (\kappa+1)^2[3(6\kappa^3-32\kappa^2+81\kappa-160)(1+\rho_b) + 2(3\kappa^3-19\kappa^2+54\kappa-113)\rho_b^2 - 3(2\kappa^2-9\kappa+22)\rho_b^3 + 3(\kappa-4)\rho_b^4 - \rho_b^5]e^{-\rho_b}\}$$

$$E_{-1,1}^{011} = 2\rho_b^{-4}(315+315\rho_b+150\rho_b^2+45\rho_b^3+9\rho_b^4+\rho_b^5)e^{-\rho_b} = (1/8)\rho_b^4[A_7(\rho_b)-A_5(\rho_b)-A_3(\rho_b)+A_1(\rho_b)]$$

$$C_{01}^{011} = 2\rho_a^{-4}(\kappa+1)\{- (\kappa-1)^3[72(\kappa+1)(1+\rho_a) + 6(4\kappa+5)\rho_a^2 + 6\rho_a^3]e^{-\rho_a} + (\kappa+1)[72(\kappa-1)^3(1+\rho_b) + 6(\kappa-1)^2(4\kappa-7)\rho_b^2 - 18(\kappa-1)^2\rho_b^3 + 6(\kappa-1)\rho_b^4 - \rho_b^5]e^{-\rho_b}\}$$

TABLE XIII (continued)

$$C_{11}^{011} = 4\rho_a^{-3}\rho_b^{-1}(\kappa-1)\{- (\kappa-1)^3[180(\kappa+1)^2(1+\rho_a)+12(\kappa+1)(5\kappa+7)\rho_a^2+24(\kappa+1)\rho_a^3+3\rho_a^4]e^{-\rho_a} + (\kappa+1)^2[180(\kappa-1)^3(1+\rho_b)+12(\kappa-1)^2(5\kappa-8)\rho_b^2-36(\kappa-1)\rho_b^3+9(\kappa-1)\rho_b^4-\rho_b^5]e^{-\rho_b}\}$$

$$C_{21}^{011} = 4\rho_a^{-4}(\kappa-1)\{- (\kappa-1)^3[180(\kappa+1)^2(6\kappa+5)(1+\rho_a)+24(\kappa+1)(15\kappa^2+35\kappa+19)\rho_a^2+12(\kappa+1)(15\kappa+13)\rho_a^3+3(12\kappa+11)\rho_a^4 +3\rho_a^5]e^{-\rho_a} + (\kappa+1)^2[180(\kappa-1)^3(6\kappa+5)(1+\rho_b)+12(\kappa-1)^2(30\kappa^2-20\kappa-37)\rho_b^2-36(\kappa-1)^2(5\kappa+4)\rho_b^3 +9(\kappa-1)(4\kappa+3)\rho_b^4-(3\kappa+2)\rho_b^5]e^{-\rho_b}\}$$

Functions with  $\gamma+6+2\epsilon = 4$

$$(25) \quad \beta, \gamma\delta\epsilon = 1, 310; \quad -4 \leq \alpha \leq 1$$

$$D_{-4,1}^{310} = (1/3)\rho_b^{-5}(\kappa^2-1)^{-1}\{- [72(\kappa+1)(\kappa^3-17\kappa^2-284\kappa-330)+72(\kappa^2-1)(\kappa^2-16\kappa-90)\rho_a+6(\kappa-1)(6\kappa^3-87\kappa^2-547\kappa-422)\rho_a^2 +6(\kappa-1)^2(2\kappa^2-25\kappa-68)\rho_a^3+3(\kappa-1)^2(\kappa^2-11\kappa-18)\rho_a^4-3(\kappa-1)^3\rho_a^5]e^{-\rho_a} + (\kappa+1)[72(\kappa^3-17\kappa^2-284\kappa-330)(1+\rho_b) +6(6\kappa^3-99\kappa^2-1615\kappa-1862)\rho_b^2+6(2\kappa^3-31\kappa^2-479\kappa-542)\rho_b^3+3(\kappa^3-14\kappa^2-195\kappa-212)\rho_b^4-2(3\kappa^2+41\kappa+40)\rho_b^5 -4(2\kappa+1)\rho_b^6]e^{-\rho_b}\}$$

$$E_{-4,1}^{310} = \rho_a\rho_b^{-6}[\rho_a^2\rho_b^{-2}(3780+3780\rho_b+1785\rho_b^2+525\rho_b^3+105\rho_b^4+14\rho_b^5+\rho_b^6)-3(420+420\rho_b+195\rho_b^2+55\rho_b^3+10\rho_b^4+\rho_b^5)]e^{-\rho_b} = (1/96)\rho_a\rho_b^2\{\rho_a^2[A_9(\rho_b)-2A_7(\rho_b)+2A_5(\rho_b)-A_1(\rho_b)]-12[2A_7(\rho_b)-3A_5(\rho_b)+A_1(\rho_b)]\}$$

$$D_{-3,1}^{310} = \rho_a^{-1}\rho_b^{-4}(\kappa^2-1)^{-1}\{- [24(\kappa+1)^2(2\kappa^3-20\kappa^2+139\kappa+824)+24(\kappa^2-1)(2\kappa^3-16\kappa^2+103\kappa+226)\rho_a +6(\kappa^2-1)(4\kappa^3-31\kappa^2+194\kappa+358)\rho_a^2+2(\kappa-1)^2(4\kappa^3-21\kappa^2+120\kappa+170)\rho_a^3+(\kappa-1)^2(2\kappa^3-9\kappa^2+45\kappa+46)\rho_a^4+3(\kappa-1)^3\rho_a^5]e^{-\rho_a} +(\kappa+1)^2[24(2\kappa^3-20\kappa^2+139\kappa+824)(1+\rho_b)+6(4\kappa^3-39\kappa^2+266\kappa+1554)\rho_b^2+2(4\kappa^3-37\kappa^2+242\kappa+1366)\rho_b^3 +2(2\kappa^3-17\kappa^2+103\kappa+542)\rho_b^4-(2\kappa^2-15\kappa-71)\rho_b^5+(\kappa+5)\rho_b^6]e^{-\rho_b}\}$$

TABLE XIII (continued)

$$\begin{aligned}
E_{-3,1}^{310} &= -3\rho_b^{-5}[\rho_a^2\rho_b^{-2}(3780+3780\rho_b+1785\rho_b^2+525\rho_b^3+105\rho_b^4+14\rho_b^5+\rho_b^6)-(420+420\rho_b+195\rho_b^2+55\rho_b^3+10\rho_b^4+\rho_b^5)]e^{-\rho_b} \\
&= -(1/32)\rho_b^3[\rho_a^2[A_9(\rho_b)-2A_7(\rho_b)+2A_3(\rho_b)-A_1(\rho_b)]-4[2A_7(\rho_b)-3A_5(\rho_b)+A_1(\rho_b)]] \\
D_{-2,1}^{310} &= \rho_b^{-5}(\kappa+1)^{-2}\{-[72(\kappa+1)^2(2\kappa^4-14\kappa^3+51\kappa^2-173\kappa-496)+72(\kappa-1)(\kappa+1)^2(2\kappa^3-12\kappa^2+39\kappa-134)]\rho_a \\
&\quad +6(\kappa^2-1)(12\kappa^4-58\kappa^3+149\kappa^2-515\kappa-638)\rho_a^2+6(\kappa+1)(\kappa-1)^2(4\kappa^3-14\kappa^2+27\kappa-108)\rho_a^3+6(\kappa+1)(\kappa-1)^2(\kappa^3-3\kappa^2+4\kappa-16)\rho_a^4 \\
&\quad +2(\kappa-1)^3(\kappa^2-2\kappa-2)\rho_a^5\}e^{-\rho_a} + (\kappa+1)^2[72(2\kappa^4-14\kappa^3+51\kappa^2-173\kappa-496)(1+\rho_b)+6(12\kappa^4-82\kappa^3+293\kappa^2-983\kappa-2810)\rho_b^2 \\
&\quad +6(4\kappa^4-26\kappa^3+89\kappa^2-291\kappa-826)\rho_b^3+6(\kappa^4-6\kappa^3+19\kappa^2-59\kappa-165)\rho_b^4-(4\kappa^3-17\kappa^2+50\kappa+131)\rho_b^5+(\kappa^2-4\kappa-9)\rho_b^6]e^{-\rho_b} \\
E_{-2,1}^{310} &= 6\rho_a\rho_b^{-6}(3780+3780\rho_b+1785\rho_b^2+525\rho_b^3+105\rho_b^4+14\rho_b^5+\rho_b^6)e^{-\rho_b} = (1/16)\rho_a\rho_b^4[A_9(\rho_b)-2A_7(\rho_b)+2A_3(\rho_b)-A_1(\rho_b)] \\
D_{-1,1}^{310} &= 2\rho_a^{-5}(\kappa-1)^{-2}\{-[36(\kappa+1)^3(8\kappa^4-50\kappa^3+144\kappa^2-275\kappa+488)+36(\kappa-1)(\kappa+1)^2(8\kappa^4-34\kappa^3+60\kappa^2-71\kappa+142)]\rho_a \\
&\quad +3(\kappa-1)(\kappa+1)^2(48\kappa^4-198\kappa^3+328\kappa^2-345\kappa+692)\rho_a^2+3(\kappa+1)(\kappa-1)^2(16\kappa^4-30\kappa^3-4\kappa^2+23\kappa+86)\rho_a^3 \\
&\quad +3(\kappa+1)^2(\kappa-1)^2(4\kappa^3-10\kappa^2+4\kappa+9)\rho_a^4+(\kappa-1)^3(6\kappa^3-7\kappa^2-4\kappa+8)\rho_a^5+(\kappa-1)^5\rho_a^6\}e^{-\rho_a} \\
&\quad +(\kappa+1)^3[36(8\kappa^4-50\kappa^3+144\kappa^2-275\kappa+488)(1+\rho_b)+3(48\kappa^4-294\kappa^3+832\kappa^2-1569\kappa+2768)\rho_b^2 \\
&\quad +3(16\kappa^4-94\kappa^3+256\kappa^2-469\kappa+816)\rho_b^3+3(4\kappa^4-22\kappa^3+56\kappa^2-97\kappa+164)\rho_b^4-(6\kappa^3-23\kappa^2+42\kappa-67)\rho_b^5+(\kappa^2-3\kappa+5)\rho_b^6]e^{-\rho_b} \\
E_{-1,1}^{310} &= -6\rho_b^{-5}(3780+3780\rho_b+1785\rho_b^2+525\rho_b^3+105\rho_b^4+14\rho_b^5+\rho_b^6)e^{-\rho_b} = -(1/16)\rho_b^5[A_9(\rho_b)-2A_7(\rho_b)+2A_3(\rho_b)-A_1(\rho_b)] \\
C_{01}^{310} &= 2\rho_a^{-4}\rho_b^{-1}(\kappa+1)^{-1}(\kappa-1)\{- (\kappa-1)^3[1440(\kappa+1)^3(1+\rho_a)+72(\kappa+1)^2(10\kappa+11)\rho_a^2+24(\kappa+1)^2(10\kappa+13)\rho_a^3 \\
&\quad +12(\kappa+1)^2(5\kappa+8)\rho_a^4+9(\kappa+1)(4\kappa+3)\rho_a^5+(9\kappa+7)\rho_a^6+\rho_a^7\}e^{-\rho_a} + (\kappa+1)^3[1440(\kappa-1)^3(1+\rho_b)+72(\kappa-1)^2(10\kappa-9)\rho_b^2 \\
&\quad +24(\kappa-1)^2(10\kappa-7)\rho_b^3+12(\kappa-1)^2(5\kappa-2)\rho_b^4-3\kappa(8\kappa-7)\rho_b^5+3\kappa\rho_b^6]e^{-\rho_b}
\end{aligned}$$

TABLE XIII (continued)

$$\begin{aligned}
 C_{11}^{310} = & 2\rho_a^{-5}(\kappa+1)^{-1}(\kappa-1)\{- (\kappa-1)^3[8640(\kappa+1)^4(1+\rho_a)+360(\kappa+1)^3(12\kappa+13)\rho_a^2+360(\kappa+1)^3(4\kappa+5)\rho_a^3+180(\kappa+1)^3(2\kappa+3)\rho_a^4 \\
 & +3(\kappa+1)(80\kappa^2+124\kappa+47)\rho_a^5+3(\kappa+1)(24\kappa+13)\rho_a^6+3(4\kappa+3)\rho_a^7+\rho_a^8\}e^{-\rho_a} + (\kappa+1)^4[8640(\kappa-1)^3(1+\rho_b) \\
 & +360(\kappa-1)^2(12\kappa-11)\rho_b^2+360(\kappa-1)^2(4\kappa-3)\rho_b^3+180(\kappa-1)^2(2\kappa-1)\rho_b^4-3(40\kappa^2-44\kappa+7)\rho_b^5+3(4\kappa-1)\rho_b^6]e^{-\rho_b}
 \end{aligned}$$

(26)  $\beta, \gamma\delta\epsilon = 1, 220$ ;  $0 \leq \alpha \leq 1$

$$\begin{aligned}
 C_{01}^{220} = & 2\rho_a^{-4}\rho_b^{-1}(\kappa+1)^{-1}\{- (\kappa-1)^4[1440(\kappa+1)^3(1+\rho_a+\frac{1}{2}\rho_a^2+(1/6)\rho_a^3)+3(\kappa+1)(20\kappa^2+40\kappa+19)\rho_a^4+12(\kappa+1)(2\kappa+1)\rho_a^5 \\
 & +(3\kappa+2)\rho_a^6]e^{-\rho_a} + (\kappa+1)^3[1440(\kappa-1)^4(1+\rho_b+\frac{1}{2}\rho_b^2+(1/6)\rho_b^3)+3(\kappa-1)^2(20\kappa^2-40\kappa+19)\rho_b^4-3(\kappa-1)(12\kappa^2-14\kappa+3)\rho_b^5 \\
 & +(\kappa-1)(9\kappa-2)\rho_b^6-\frac{1}{2}(2\kappa-1)\rho_b^7]e^{-\rho_b}
 \end{aligned}$$

$$\begin{aligned}
 C_{11}^{220} = & 2\rho_a^{-5}(\kappa+1)^{-1}\{- (\kappa-1)^4[8640(\kappa+1)^4(1+\rho_a+\frac{1}{2}\rho_a^2+(1/6)\rho_a^3)+12(\kappa+1)^2(30\kappa^2+60\kappa+29)\rho_a^4+3(\kappa+1)(60\kappa^2+80\kappa+23)\rho_a^5 \\
 & +3(\kappa+1)(12\kappa+5)\rho_a^6+(3\kappa+2)\rho_a^7]e^{-\rho_a} + (\kappa+1)^4[8640(\kappa-1)^4(1+\rho_b+\frac{1}{2}\rho_b^2+(1/6)\rho_b^3)+12(\kappa-1)^2(30\kappa^2-60\kappa+29)\rho_b^4 \\
 & -3(\kappa-1)(60\kappa^2-80\kappa+23)\rho_b^5+3(\kappa-1)(12\kappa-5)\rho_b^6-(3\kappa-2)\rho_b^7]e^{-\rho_b}
 \end{aligned}$$

(27)  $\beta, \gamma\delta\epsilon = 1, 201$ ;  $-4 \leq \alpha \leq 1$

$$\begin{aligned}
 D_{-4,1}^{201} = & (2/3)\rho_b^{-5}(\kappa^2-1)^{-1}\{- [36(\kappa+1)(\kappa^3-17\kappa^2-284\kappa-330)+36(\kappa^2-1)(\kappa^2-16\kappa-90)\rho_a+3(\kappa-1)(5\kappa^3-76\kappa^2-441\kappa-328)\rho_a^2 \\
 & +3(\kappa-1)^2(\kappa^2-15\kappa-42)\rho_a^3-3(\kappa-1)^2(\kappa+3)\rho_a^4]e^{-\rho_a} + (\kappa+1)[36(\kappa^3-17\kappa^2-284\kappa-330)(1+\rho_b) \\
 & +3(5\kappa^3-88\kappa^2-1509\kappa-1768)\rho_b^2+3(\kappa^3-20\kappa^2-373\kappa-448)\rho_b^3-6(\kappa^2+26\kappa+33)\rho_b^4-2(5\kappa+7)\rho_b^5]e^{-\rho_b} \\
 E_{-4,1}^{201} = & 2\rho_a\rho_b^{-6}[2\rho_a^2\rho_b^{-2}(945+945\rho_b+420\rho_b^2+105\rho_b^3+15\rho_b^4+\rho_b^5)-(630+630\rho_b+285\rho_b^2+75\rho_b^3+12\rho_b^4+\rho_b^5)]e^{-\rho_b} \\
 = & (1/96)\rho_a\rho_b^2\{\rho_a^2[A_9(\rho_b)-4A_7(\rho_b)+6A_5(\rho_b)-4A_3(\rho_b)+A_1(\rho_b)]-24[A_7(\rho_b)-2A_5(\rho_b)+A_3(\rho_b)]\}
 \end{aligned}$$

TABLE XIII (continued)

$$\begin{aligned}
D_{-3,1}^{201} &= 2\rho_a^{-1}\rho_b^{-4}(\kappa^2-1)^{-1}\{-[12(\kappa+1)^2(2\kappa^3-20\kappa^2+139\kappa+824)+12(\kappa^2-1)(2\kappa^3-16\kappa^2+103\kappa+226)\rho_a \\
&\quad +(\kappa^2-1)(10\kappa^3-79\kappa^2+515\kappa+814)\rho_a^2+(\kappa-1)^2(2\kappa^3-11\kappa^2+77\kappa+100)\rho_a^3+(\kappa-1)^2(5\kappa+7)\rho_a^4\}e^{-\rho_a} \\
&\quad +(\kappa+1)^2\{12(2\kappa^3-20\kappa^2+139\kappa+824)(1+\rho_b)+(10\kappa^3-103\kappa^2+731\kappa+402)\rho_b^2+(2\kappa^3-23\kappa^2+175\kappa+1106)\rho_b^3 \\
&\quad -2(\kappa-16)(\kappa+5)\rho_b^4+(\kappa+11)\rho_b^5\}e^{-\rho_b} \\
E_{-3,1}^{201} &= -2\rho_b^{-5}\{6\rho_a^2\rho_b^{-2}(945+945\rho_b+420\rho_b^2+105\rho_b^3+15\rho_b^4+\rho_b^5)-(630+630\rho_b+285\rho_b^2+75\rho_b^3+12\rho_b^4+\rho_b^5)\}e^{-\rho_b} \\
&= -(1/32)\rho_b^3\{\rho_a^2[A_9(\rho_b)-4A_7(\rho_b)+6A_5(\rho_b)+A_1(\rho_b)]-8[A_7(\rho_b)-2A_5(\rho_b)+A_3(\rho_b)]\} \\
D_{-2,1}^{201} &= 2\rho_b^{-5}(\kappa+1)^{-2}\{-36(\kappa+1)^2(2\kappa^4-14\kappa^3+51\kappa^2-173\kappa-496)+36(\kappa-1)(\kappa+1)^2(2\kappa^3-12\kappa^2+39\kappa-134)\rho_a \\
&\quad +6(\kappa^2-1)(5\kappa^4-24\kappa^3+62\kappa^2-226\kappa-237)\rho_a^2+6(\kappa+1)(\kappa-1)^2(\kappa^3-3\kappa^2+5\kappa-31)\rho_a^3+2(\kappa-1)^2(\kappa^3-3\kappa^2-3\kappa-7)\rho_a^4\}e^{-\rho_a} \\
&\quad +(\kappa+1)^2\{36(2\kappa^4-14\kappa^3+51\kappa^2-173\kappa-496)(1+\rho_b)+6(5\kappa^4-36\kappa^3+134\kappa^2-460\kappa-1323)\rho_b^2+6(\kappa^4-8\kappa^3+32\kappa^2-114\kappa-331)\rho_b^3 \\
&\quad -4(\kappa^3-6\kappa^2+24\kappa+71)\rho_b^4+(\kappa^2-6\kappa-19)\rho_b^5\}e^{-\rho_b} \\
E_{-2,1}^{201} &= 24\rho_a\rho_b^{-6}(945+945\rho_b+420\rho_b^2+105\rho_b^3+15\rho_b^4+\rho_b^5)e^{-\rho_b} = (1/16)\rho_a\rho_b^4[A_9(\rho_b)-4A_7(\rho_b)+6A_5(\rho_b)+A_1(\rho_b)] \\
D_{-1,1}^{201} &= 4\rho_a^{-5}(\kappa-1)^{-2}\{-[18(\kappa+1)^3(8\kappa^4-50\kappa^3+144\kappa^2-275\kappa+488)+18(\kappa-1)(\kappa+1)^2(8\kappa^4-34\kappa^3+60\kappa^2-71\kappa+142)\rho_a \\
&\quad +6(\kappa-1)(\kappa+1)^2(10\kappa^4-40\kappa^3+62\kappa^2-58\kappa+131)\rho_a^2+6(\kappa+1)^2(\kappa-1)^2(2\kappa^3-4\kappa^2-2\kappa+11)\rho_a^3+6\kappa(\kappa+1)(\kappa-1)^2(\kappa^2-3\kappa+3)\rho_a^4 \\
&\quad +(\kappa-1)^5\rho_a^5\}e^{-\rho_a} +(\kappa+1)^3\{18(8\kappa^4-50\kappa^3+144\kappa^2-275\kappa+488)(1+\rho_b)+12(5\kappa^4-32\kappa^3+94\kappa^2-182\kappa+325)\rho_b^2 \\
&\quad +6(2\kappa^4-14\kappa^3+44\kappa^2-89\kappa+162)\rho_b^3-6(\kappa^3-5\kappa^2+12\kappa-23)\rho_b^4+(\kappa^2-4\kappa+9)\rho_b^5\}e^{-\rho_b} \\
E_{-1,1}^{201} &= -24\rho_b^{-5}(945+945\rho_b+420\rho_b^2+105\rho_b^3+15\rho_b^4+\rho_b^5)e^{-\rho_b} = -(1/16)\rho_b^5[A_9(\rho_b)-4A_7(\rho_b)+6A_5(\rho_b)+A_1(\rho_b)]
\end{aligned}$$

TABLE XIII (continued)

$$C_{01}^{201} = 4\rho_a^{-4}\rho_b^{-1}(\kappa+1)^{-1}(\kappa-1)\{- (\kappa-1)^3[720(\kappa+1)^3(1+\rho_a)+12(\kappa+1)^2(25\kappa+32)\rho_a^2+12(\kappa+1)^2(5\kappa+12)\rho_a^3+6(\kappa+1)(6\kappa+7)\rho_a^4 \\ +9(\kappa+1)\rho_a^5+\rho_a^6]e^{-\rho_a} + (\kappa+1)^3[720(\kappa-1)^3(1+\rho_b)+12(\kappa-1)^2(25\kappa-28)\rho_b^2+12(\kappa-1)^2(5\kappa-8)\rho_b^3-6(\kappa-1)(4\kappa-3)\rho_b^4 \\ + (3\kappa-2)\rho_b^5]e^{-\rho_b}\}$$

$$C_{11}^{201} = 4\rho_a^{-5}(\kappa+1)^{-1}(\kappa-1)\{- (\kappa-1)^3[4320(\kappa+1)^4(1+\rho_a)+180(\kappa+1)^3(10\kappa+13)\rho_a^2+180(\kappa+1)^3(2\kappa+5)\rho_a^3+12(\kappa+1)^2(20\kappa+23)\rho_a^4 \\ +3(\kappa+1)(24\kappa+23)\rho_a^5+12(\kappa+1)\rho_a^6+\rho_a^7]e^{-\rho_a} + (\kappa+1)^4[4320(\kappa-1)^3(1+\rho_b)+180(\kappa-1)^2(10\kappa-11)\rho_b^2 \\ +180(\kappa-1)^2(2\kappa-3)\rho_b^3-24(\kappa-1)(5\kappa-4)\rho_b^4+3(4\kappa-3)\rho_b^5]e^{-\rho_b}\}$$

$$(28) \quad \beta, \gamma, \delta \epsilon = 1, 1, 1, 1; \quad -4 \leq \alpha \leq 1$$

$$D_{-4,1}^{111} = (2/3)\rho_b^{-5}(\kappa+1)^{-2}(\kappa-1)^{-1}\{- [36(\kappa+1)^2(\kappa^3-17\kappa^2-284\kappa-330)+36(\kappa-1)(\kappa+1)^2(\kappa^2-16\kappa-90)\rho_a \\ +3(\kappa-1)(\kappa+1)^2(5\kappa^2-84\kappa-446)\rho_a^2+3(\kappa+1)(\kappa-1)^2(\kappa^2-18\kappa-74)\rho_a^3-6(\kappa+1)(\kappa-1)^3(\kappa+6)\rho_a^4-3(\kappa-1)^3\rho_a^5]e^{-\rho_a} \\ + (\kappa+1)^2[36(\kappa^3-17\kappa^2-284\kappa-330)(1+\rho_b)+3(5\kappa^3-91\kappa^2-1598\kappa-1886)\rho_b^2+3(\kappa^3-23\kappa^2-462\kappa-566)\rho_b^3 \\ -3(3\kappa^2+89\kappa+118)\rho_b^4-4(8\kappa+13)\rho_b^5-(\kappa+5)\rho_b^6]e^{-\rho_b}\}$$

$$E_{-4,1}^{111} = \rho_a\rho_b^{-6}[\rho_a^2\rho_b^{-2}(3780+3780\rho_b+1785\rho_b^2+525\rho_b^3+105\rho_b^4+14\rho_b^5+\rho_b^6) \\ -(1260+1260\rho_b+615\rho_b^2+195\rho_b^3+45\rho_b^4+8\rho_b^5+\rho_b^6)]e^{-\rho_b} = (1/96)\rho_a\rho_b^2\{\rho_a^2[A_9(\rho_b)-2A_7(\rho_b)+2A_5(\rho_b)-A_1(\rho_b)] \\ -12[2A_7(\rho_b)-A_5(\rho_b)-A_1(\rho_b)]\}$$

$$D_{-3,1}^{111} = 2\rho_a^{-5}(\kappa-1)^{-3}\{- [12(\kappa+1)^3(2\kappa^3-20\kappa^2+139\kappa+824)+12(\kappa-1)(\kappa+1)^2(2\kappa^3-16\kappa^2+103\kappa+226)\rho_a \\ +(\kappa-1)(\kappa+1)^2(10\kappa^3-82\kappa^2+551\kappa+1096)\rho_a^2+(\kappa+1)(\kappa-1)^2(2\kappa^3-14\kappa^2+107\kappa+178)\rho_a^3-(\kappa+1)(\kappa-1)^2(\kappa^2-16\kappa-27)\rho_a^4\}$$

TABLE XIII (continued)

$$+(\kappa-1)^3(\kappa+2)\rho_a^5 e^{-\rho_a} + (\kappa+1)^3[12(2\kappa^3-20\kappa^2+139\kappa+824)(1+\rho_b) + (10\kappa^3-106\kappa^2+767\kappa+4684)\rho_b^2 + (2\kappa^3-26\kappa^2+211\kappa+1388)\rho_b^3 - 3(\kappa^2-12\kappa-94)\rho_b^4 + 3(\kappa+13)\rho_b^5 + 3\rho_b^6]e^{-\rho_b}$$

$$\begin{aligned} E_{-3,1}^{111} &= -\rho_b^{-5}[3\rho_a^2\rho_b^{-2}(3780+3780\rho_b+1785\rho_b^2+525\rho_b^3+105\rho_b^4+14\rho_b^5+\rho_b^6) \\ &\quad - (1260+1260\rho_b+615\rho_b^2+195\rho_b^3+45\rho_b^4+8\rho_b^5+\rho_b^6)]e^{-\rho_b} = -(1/32)\rho_b^3[\rho_a^2[A_9(\rho_b)-2A_7(\rho_b)+2A_3(\rho_b)-A_1(\rho_b)] \\ &\quad - 4[2A_7(\rho_b)-A_5(\rho_b)-A_1(\rho_b)]] \end{aligned}$$

$$D_{-2,1}^{111} = 2\rho_b^{-5}(\kappa+1)^{-2}\{-[36(\kappa+1)^2(2\kappa^4-14\kappa^3+51\kappa^2-173\kappa-496)+36(\kappa-1)(\kappa+1)^2(2\kappa^3-12\kappa^2+39\kappa-134)\rho_a \\ + 3(\kappa^2-1)(10\kappa^4-50\kappa^3+137\kappa^2-507\kappa-640)\rho_a^2+3(\kappa+1)(\kappa-1)^2(2\kappa^3-8\kappa^2+21\kappa-106)\rho_a^3+3(\kappa+1)(\kappa-1)^2(\kappa-15)\rho_a^4$$

$$-3(\kappa-1)^3\rho_a^5]e^{-\rho_a} + (\kappa+1)^2[36(2\kappa^4-14\kappa^3+51\kappa^2-173\kappa-496)(1+\rho_b)+3(10\kappa^4-74\kappa^3+281\kappa^2-975\kappa-2812)\rho_b^2 \\ + 3(2\kappa^4-18\kappa^3+77\kappa^2-283\kappa-828)\rho_b^3-3(2\kappa^3-13\kappa^2+55\kappa+166)\rho_b^4+(3\kappa^2-20\kappa-67)\rho_b^5-(\kappa+5)\rho_b^6]e^{-\rho_b}$$

$$E_{-2,1}^{111} = 6\rho_a\rho_b^{-6}(3780+3780\rho_b+1785\rho_b^2+525\rho_b^3+105\rho_b^4+14\rho_b^5+\rho_b^6)e^{-\rho_b} = (1/16)\rho_a\rho_b^4[A_9(\rho_b)-2A_7(\rho_b)+2A_3(\rho_b)-A_1(\rho_b)]$$

$$D_{-1,1}^{111} = 2\rho_a^{-5}(\kappa-1)^{-2}\{-[36(\kappa+1)^3(8\kappa^4-50\kappa^3+144\kappa^2-275\kappa+488)+36(\kappa-1)(\kappa+1)^2(8\kappa^4-34\kappa^3+60\kappa^2-71\kappa+142)\rho_a \\ + 3(\kappa-1)(\kappa+1)^2(40\kappa^4-166\kappa^3+280\kappa^2-313\kappa+684)\rho_a^2+3(\kappa+1)(\kappa-1)^2(8\kappa^4-14\kappa^3-4\kappa^2+7\kappa+94)\rho_a^3$$

$$+ 3(\kappa+1)^2(\kappa-1)^2(2\kappa^2-8\kappa+13)\rho_a^4+3(\kappa-1)^3\rho_a^5]e^{-\rho_a} + (\kappa+1)^3[36(8\kappa^4-50\kappa^3+144\kappa^2-275\kappa+488)(1+\rho_b) \\ + 3(40\kappa^4-262\kappa^3+784\kappa^2-1537\kappa+2760)\rho_b^2+3(8\kappa^4-62\kappa^3+208\kappa^2-437\kappa+808)\rho_b^3-3(6\kappa^3-32\kappa^2+81\kappa-160)\rho_b^4 \\ + 2(3\kappa^2-13\kappa+31)\rho_b^5-(\kappa-4)\rho_b^6]e^{-\rho_b}$$

$$E_{-1,1}^{111} = -6\rho_b^{-5}(3780+3780\rho_b+1785\rho_b^2+525\rho_b^3+105\rho_b^4+14\rho_b^5+\rho_b^6)e^{-\rho_b} = -(1/16)\rho_b^5[A_9(\rho_b)-2A_7(\rho_b)+2A_3(\rho_b)-A_1(\rho_b)]$$

TABLE XIII (continued)

$$C_{01}^{111} = 4\rho_a^{-4}\rho_b^{-1}(\kappa-1)\{- (\kappa-1)^3[720(\kappa+1)^2(1+\rho_a)+12(\kappa+1)(25\kappa+29)\rho_a^2+12(\kappa+1)(5\kappa+9)\rho_a^3+24(\kappa+1)\rho_a^4+3\rho_a^5]e^{-\rho_a} \\ + (\kappa+1)^2[720(\kappa-1)^3(1+\rho_b)+12(\kappa-1)^2(25\kappa-31)\rho_b^2+12(\kappa-1)^2(5\kappa-11)\rho_b^3-36(\kappa-1)^2\rho_b^4+(9\kappa-8)\rho_b^5-\rho_b^6]e^{-\rho_b}\}$$

$$C_{11}^{111} = 12\rho_a^{-5}(\kappa-1)\{- (\kappa-1)^3[1440(\kappa+1)^3(1+\rho_a)+120(\kappa+1)^2(5\kappa+6)\rho_a^2+120(\kappa+1)^2(\kappa+2)\rho_a^3+60(\kappa+1)^2\rho_a^4 \\ + (12\kappa+11)\rho_a^5+\rho_a^6]e^{-\rho_a} + (\kappa+1)^3[1440(\kappa-1)^3(1+\rho_b)+120(\kappa-1)^2(5\kappa-6)\rho_b^2+120(\kappa-1)^2(\kappa-2)\rho_b^3-60(\kappa-1)^2\rho_b^4 \\ + (12\kappa-11)\rho_b^5-\rho_b^6]e^{-\rho_b}\}$$

$$(29) \quad \beta, \gamma \delta \epsilon = 1, 002; \quad -4 \leq \alpha \leq 1$$

$$D_{-4,1}^{002} = (8/3)\rho_b^{-5}(\kappa^2-1)^{-1}\{- [9(\kappa+1)(\kappa^3-17\kappa^2-284\kappa-330)+9(\kappa^2-1)(\kappa^2-16\kappa-90)\rho_a+3(\kappa^2-1)(\kappa^2-18\kappa-88)\rho_a^2 \\ -6(\kappa-1)^2(\kappa+6)\rho_a^3-3(\kappa-1)^2\rho_a^4+\rho_a^5 + (\kappa+1)[9(\kappa^3-17\kappa^2-284\kappa-330)(1+\rho_b)+3(\kappa^3-20\kappa^2-373\kappa-448)\rho_b^2 \\ -3(3\kappa^2+89\kappa+118)\rho_b^3-3(11\kappa+19)\rho_b^4-(\kappa+5)\rho_b^5]e^{-\rho_b}\}$$

$$E_{-4,1}^{002} = 4\rho_a\rho_b^{-6}[\rho_a^2\rho_b^{-2}(945+945\rho_b+420\rho_b^2+105\rho_b^3+15\rho_b^4+\rho_b^5)-(315+315\rho_b+150\rho_b^2+45\rho_b^3+9\rho_b^4+\rho_b^5)]e^{-\rho_b} \\ = (1/96)\rho_a\rho_b^2\{ \rho_a^2[A_9(\rho_b)-4A_7(\rho_b)+6A_5(\rho_b)-4A_3(\rho_b)+A_1(\rho_b)]-24[A_7(\rho_b)-A_5(\rho_b)-A_3(\rho_b)+A_1(\rho_b)] \}$$

$$D_{-3,1}^{002} = 8\rho_a^{-1}\rho_b^{-4}(\kappa^2-1)^{-1}\{- [3(\kappa+1)^2(2\kappa^3-20\kappa^2+139\kappa+824)+3(\kappa^2-1)(2\kappa^3-16\kappa^2+103\kappa+226)\rho_a \\ + (\kappa^2-1)(2\kappa^3-17\kappa^2+121\kappa+209)\rho_a^2-(\kappa-1)^2(\kappa^2-16\kappa-27)\rho_a^3+(\kappa-1)^2(\kappa+2)\rho_a^4]e^{-\rho_a} \\ + (\kappa+1)^2[3(2\kappa^3-20\kappa^2+139\kappa+824)(1+\rho_b)+(2\kappa^3-23\kappa^2+175\kappa+1106)\rho_b^2-3(\kappa^2-12\kappa-94)\rho_b^3+3(\kappa+14)\rho_b^4+3\rho_b^5]e^{-\rho_b}\}$$

$$E_{-3,1}^{002} = -4\rho_b^{-5}[3\rho_a^2\rho_b^{-2}(945+945\rho_b+420\rho_b^2+105\rho_b^3+15\rho_b^4+\rho_b^5)-(315+315\rho_b+150\rho_b^2+45\rho_b^3+9\rho_b^4+\rho_b^5)]e^{-\rho_b} \\ = -(1/32)\rho_b^3\{ \rho_a^2[A_9(\rho_b)-4A_7(\rho_b)+6A_5(\rho_b)-4A_3(\rho_b)+A_1(\rho_b)]-8[A_7(\rho_b)-A_5(\rho_b)-A_3(\rho_b)+A_1(\rho_b)] \}$$

TABLE XIII (continued)

$$\begin{aligned}
D_{-2,1}^{002} &= 8\rho_b^{-5}(\kappa+1)^{-1}\{-[9(\kappa+1)(2\kappa^4-14\kappa^3+51\kappa^2-173\kappa-496)+9(\kappa^2-1)(2\kappa^3-12\kappa^2+39\kappa-134)]\rho_a \\
&\quad +3(\kappa-1)(2\kappa^4-10\kappa^3+28\kappa^2-111\kappa-119)\rho_a^2+3(\kappa-1)^2(\kappa-15)\rho_a^3-3(\kappa-1)^2\rho_a^4\}e^{-\rho_a} \\
&\quad +(\kappa+1)[9(2\kappa^4-14\kappa^3+51\kappa^2-173\kappa-496)(1+\rho_b)+6(\kappa^4-8\kappa^3+32\kappa^2-114\kappa-331)\rho_b^2-3(2\kappa^3-13\kappa^2+55\kappa+166)\rho_b^3 \\
&\quad +3(\kappa^2-7\kappa-24)\rho_b^4-(\kappa+5)\rho_b^5]e^{-\rho_b} \\
E_{-2,1}^{002} &= 24\rho_a\rho_b^{-6}(945+945\rho_b+420\rho_b^2+105\rho_b^3+15\rho_b^4+\rho_b^5)e^{-\rho_b} = (1/16)\rho_a\rho_b^4[A_9(\rho_b)-4A_7(\rho_b)+6A_5(\rho_b)-4A_3(\rho_b)+A_1(\rho_b)] \\
D_{-1,1}^{002} &= 8\rho_a^{-1}\rho_b^{-4}(\kappa+1)^{-1}\{-[9(\kappa+1)^2(8\kappa^4-50\kappa^3+144\kappa^2-275\kappa+488)+9(\kappa-1)(\kappa+1)(8\kappa^4-34\kappa^3+60\kappa^2-71\kappa+142)]\rho_a \\
&\quad +3(\kappa^2-1)(8\kappa^4-32\kappa^3+50\kappa^2-50\kappa+129)\rho_a^2+3(\kappa-1)^2(\kappa+1)(2\kappa^2-8\kappa+13)\rho_a^3+3(\kappa-1)^2\rho_a^4\}e^{-\rho_a} \\
&\quad +(\kappa+1)^2[9(8\kappa^4-50\kappa^3+144\kappa^2-275\kappa+488)(1+\rho_b)+12(2\kappa^4-14\kappa^3+44\kappa^2-89\kappa+162)\rho_b^2-3(6\kappa^3-32\kappa^2+81\kappa-160)\rho_b^3 \\
&\quad +3(2\kappa^2-9\kappa+22)\rho_b^4-(\kappa-4)\rho_b^5]e^{-\rho_b} \\
E_{-1,1}^{002} &= -24\rho_b^{-5}(945+945\rho_b+420\rho_b^2+105\rho_b^3+15\rho_b^4+\rho_b^5)e^{-\rho_b} = -(1/16)\rho_b^5[A_9(\rho_b)-4A_7(\rho_b)+6A_5(\rho_b)-4A_3(\rho_b)+A_1(\rho_b)] \\
C_{01}^{002} &= 16\rho_a^{-4}\rho_b^{-1}\rho_b^{-1}\{- (\kappa-1)^3[180(\kappa+1)^2(1+\rho_a)+12(\kappa+1)(5\kappa+7)\rho_a^2+24(\kappa+1)\rho_a^3+3\rho_a^4]e^{-\rho_a} \\
&\quad +(\kappa+1)^2[180(\kappa-1)^3(1+\rho_b)+12(\kappa-1)^2(5\kappa-8)\rho_b^2-36(\kappa-1)^2\rho_b^3+9(\kappa-1)\rho_b^4-\rho_b^5]e^{-\rho_b}\} \\
C_{11}^{002} &= 48\rho_a^{-5}(\kappa-1)\{- (\kappa-1)^3[360(\kappa+1)^3(1+\rho_a)+60(\kappa+1)^2(2\kappa+3)\rho_a^2+60(\kappa+1)^2\rho_a^3+12(\kappa+1)\rho_a^4+\rho_a^5]e^{-\rho_a} \\
&\quad +(\kappa+1)^3[360(\kappa-1)^3(1+\rho_b)+60(\kappa-1)^2(2\kappa-3)\rho_b^2-60(\kappa-1)^2\rho_b^3+12(\kappa-1)\rho_b^4-\rho_b^5]e^{-\rho_b}\}
\end{aligned}$$

TABLE XIV

EXPLICIT FORMULAS FOR C-FUNCTIONS IN THE CASE  $\rho \neq 0$ ,  $\tau = 0$

Note: C-functions with negative  $\alpha$  are obtained from the corresponding D- and E-functions listed in the table according to Eqs. (4.6,11).

Functions with  $\gamma + \delta + 2\epsilon = 0$

(1)  $\beta, \gamma\delta\epsilon = 1,000$  ;  $-1 \leq \alpha \leq 4$

$$D_{-1,1}^{000} = e^{-\rho}$$

$$E_{-1,1}^{000} = -\rho^{-1}(1+\rho)e^{-\rho}$$

$$C_{01}^{000} = -[(1/2)+(1/2)\rho]e^{-\rho}$$

$$C_{11}^{000} = -[(1/2)+(1/2)\rho+(1/6)\rho^2]e^{-\rho}$$

$$C_{21}^{000} = -[(3/4)+(3/4)\rho+(1/3)\rho^2+(1/12)\rho^3]e^{-\rho}$$

$$C_{31}^{000} = -[(3/2)+(3/2)\rho+(3/4)\rho^2+(1/4)\rho^3+(1/20)\rho^4]e^{-\rho}$$

$$C_{41}^{000} = -[(15/4)+(15/4)\rho+2\rho^2+(3/4)\rho^3+(1/5)\rho^4+(1/30)\rho^5]e^{-\rho}$$

(2)  $\beta, \gamma\delta\epsilon = 2,000$  ;  $-1 \leq \alpha \leq 4$

$$D_{-1,2}^{000} = -[(7/2)+(3/2)\rho]e^{-\rho}$$

$$E_{-1,2}^{000} = \rho^{-1}(2+2\rho+\rho^2)e^{-\rho}$$

$$C_{02}^{000} = [(1/2)+(1/2)\rho+(1/3)\rho^2]e^{-\rho}$$

$$C_{12}^{000} = [(3/4)+(3/4)\rho+(1/3)\rho^2+(1/12)\rho^3]e^{-\rho}$$

$$C_{22}^{000} = [(3/2)+(3/2)\rho+(2/3)\rho^2+(1/6)\rho^3+(1/30)\rho^4]e^{-\rho}$$

$$C_{32}^{000} = [(15/4)+(15/4)\rho+(7/4)\rho^2+(1/2)\rho^3+(1/10)\rho^4+(1/60)\rho^5]e^{-\rho}$$

$$C_{42}^{000} = [(45/4)+(45/4)\rho+(11/2)\rho^2+(7/4)\rho^3+(2/5)\rho^4+(1/15)\rho^5+(1/105)\rho^6]e^{-\rho}$$

(3)  $\beta, \gamma\delta\epsilon = 3,000$  ;  $-1 \leq \alpha \leq 3$

$$D_{-1,3}^{000} = [(23/2)+(11/2)\rho+(11/6)\rho^2]e^{-\rho}$$

$$E_{-1,3}^{000} = -\rho^{-1}(6+6\rho+3\rho^2+\rho^3)e^{-\rho}$$

## TWO-CENTER INTEGRALS. III

TABLE XIV (continued)

$$C_{03}^{000} = -[(3/4)+(3/4)\rho+(1/2)\rho^2+(1/4)\rho^3]e^{-\rho}$$

$$C_{13}^{000} = -[(3/2)+(3/2)\rho+(3/4)\rho^2+(1/4)\rho^3+(1/20)\rho^4]e^{-\rho}$$

$$C_{23}^{000} = -[(15/4)+(15/4)\rho+(7/4)\rho^2+(1/2)\rho^3+(1/10)\rho^4+(1/60)\rho^5]e^{-\rho}$$

$$C_{33}^{000} = -[(45/4)+(45/4)\rho+(21/4)\rho^2+(3/2)\rho^3+(3/10)\rho^4+(1/20)\rho^5+(1/140)\rho^6]e^{-\rho}$$

$$(4) \quad \alpha, \gamma \delta \epsilon = -1,000 ; \quad 4 \leq \beta \leq 9$$

$$D_{-1,4}^{000} = -[(189/4)+(93/4)\rho+(59/6)\rho^2+(25/12)\rho^3]e^{-\rho}$$

$$E_{-1,4}^{000} = \rho^{-1}(24+24\rho+12\rho^2+4\rho^3+\rho^4)e^{-\rho}$$

$$D_{-1,5}^{000} = [(477/2)+(237/2)\rho+(623/12)\rho^2+(149/12)\rho^3+(137/60)\rho^4]e^{-\rho}$$

$$E_{-1,5}^{000} = -\rho^{-1}(120+120\rho+60\rho^2+20\rho^3+5\rho^4+\rho^5)e^{-\rho}$$

$$D_{-1,6}^{000} = [(5745/4)+(2865/4)\rho+(1267/4)\rho^2+78\rho^3+(86/5)\rho^4+(49/20)\rho^5]e^{-\rho}$$

$$E_{-1,6}^{000} = \rho^{-1}(720+720\rho+360\rho^2+120\rho^3+30\rho^4+6\rho^5+\rho^6)e^{-\rho}$$

$$D_{-1,7}^{000} = [(40275/4)+(20115/4)\rho+(8923/4)\rho^2+(1109/2)\rho^3+(1259/10)\rho^4+(403/20)\rho^5 \\ + (363/140)\rho^6]e^{-\rho}$$

$$E_{-1,7}^{000} = -\rho^{-1}(5040+5040\rho+2520\rho^2+840\rho^3+210\rho^4+42\rho^5+7\rho^6+\rho^7)e^{-\rho}$$

$$D_{-1,8}^{000} = -[(644805/8)+(322245/8)\rho+(71555/4)\rho^2+(35695/8)\rho^3+(20429/20)\rho^4+(3359/20)\rho^5 \\ + (1767/70)\rho^6+(761/280)\rho^7]e^{-\rho}$$

$$E_{-1,8}^{000} = \rho^{-1}(40320+40320\rho+20160\rho^2+6720\rho^3+1680\rho^4+336\rho^5+56\rho^6+8\rho^7+\rho^8)e^{-\rho}$$

$$D_{-1,9}^{000} = [(1451205/2)+(725445/2)\rho+(1289265/8)\rho^2+(322005/8)\rho^3+(369627/40)\rho^4 \\ + (15323/10)\rho^5+(33101/140)\rho^6+(7969/280)\rho^7+(7129/2520)\rho^8]e^{-\rho}$$

$$E_{-1,9}^{000} = -\rho^{-1}(362880+362880\rho+181440\rho^2+60480\rho^3+15120\rho^4+3024\rho^5+504\rho^6+72\rho^7+9\rho^8+\rho^9)e^{-\rho}$$

RUEDEBERG, ROTHAAAN, AND JAUNZEMIS

TABLE XIV (continued)

Functions with  $\gamma + \delta + 2\epsilon = 1$

(5)  $\beta, \gamma\delta\epsilon = 1, 100$  ;  $-2 \leq \alpha \leq 3$

$$D_{-2,1}^{100} = \rho^{-1}(6+3\rho)e^{-\rho}$$

$$E_{-2,1}^{100} = -\rho^{-2}(3+3\rho+\rho^2)e^{-\rho}$$

$$D_{-1,1}^{100} = -\rho^{-1}[6+3\rho+(1/2)\rho^2]e^{-\rho}$$

$$E_{-1,1}^{100} = \rho^{-2}(3+3\rho+\rho^2)e^{-\rho}$$

$$C_{01}^{100} = -[(1/6)\rho+(1/6)\rho^2]e^{-\rho}$$

$$C_{11}^{100} = -[(1/4)\rho+(1/4)\rho^2+(1/12)\rho^3]e^{-\rho}$$

$$C_{21}^{100} = -[(1/2)\rho+(1/2)\rho^2+(13/60)\rho^3+(1/20)\rho^4]e^{-\rho}$$

$$C_{31}^{100} = -[(5/4)\rho+(5/4)\rho^2+(3/5)\rho^3+(11/60)\rho^4+(1/30)\rho^5]e^{-\rho}$$

(6)  $\beta, \gamma\delta\epsilon = 2, 100$  ;  $-2 \leq \alpha \leq 3$

$$D_{-2,2}^{100} = -\rho^{-1}[24+12\rho+(7/2)\rho^2]e^{-\rho}$$

$$E_{-2,2}^{100} = \rho^{-2}(12+12\rho+5\rho^2+\rho^3)e^{-\rho}$$

$$D_{-1,2}^{100} = \rho^{-1}[24+12\rho+(10/3)\rho^2+(1/3)\rho^3]e^{-\rho}$$

$$E_{-1,2}^{100} = -\rho^{-2}(12+12\rho+5\rho^2+\rho^3)e^{-\rho}$$

$$C_{02}^{100} = [(1/12)\rho+(1/12)\rho^2+(1/12)\rho^3]e^{-\rho}$$

$$C_{12}^{100} = [(1/4)\rho+(1/4)\rho^2+(7/60)\rho^3+(1/30)\rho^4]e^{-\rho}$$

$$C_{22}^{100} = [(3/4)\rho+(3/4)\rho^2+(1/3)\rho^3+(1/12)\rho^4+(1/60)\rho^5]e^{-\rho}$$

$$C_{32}^{100} = [(5/2)\rho+(5/2)\rho^2+(23/20)\rho^3+(19/60)\rho^4+(5/84)\rho^5+(1/105)\rho^6]e^{-\rho}$$

(7)  $\beta, \gamma\delta\epsilon = 3, 100$  ;  $-2 \leq \alpha \leq 2$

$$D_{-2,3}^{100} = \rho^{-1}[120+60\rho+(125/6)\rho^2+(23/6)\rho^3]e^{-\rho}$$

$$E_{-2,3}^{100} = -\rho^{-2}(60+60\rho+27\rho^2+7\rho^3+\rho^4)e^{-\rho}$$

## TWO-CENTER INTEGRALS. III

TABLE XIV (continued)

$$D_{-1,3}^{100} = -\rho^{-1}[120+60\rho+(247/12)\rho^2+(43/12)\rho^3+(1/4)\rho^4]e^{-\rho}$$

$$E_{-1,3}^{100} = \rho^{-2}(60+60\rho+27\rho^2+7\rho^3+\rho^4)e^{-\rho}$$

$$C_{03}^{100} = -[(1/20)\rho^3+(1/20)\rho^4]e^{-\rho}$$

$$C_{13}^{100} = -[(1/4)\rho+(1/4)\rho^2+(3/20)\rho^3+(1/15)\rho^4+(1/60)\rho^5]e^{-\rho}$$

$$C_{23}^{100} = -[(5/4)\rho+(5/4)\rho^2+(3/5)\rho^3+(11/60)\rho^4+(17/420)\rho^5+(1/140)\rho^6]e^{-\rho}$$

$$(8) \quad \beta, \gamma\delta\epsilon = 1,010 ; \quad -1 \leq \alpha \leq 4$$

$$D_{-1,1}^{010} = -\rho^{-1}[6+3\rho+(3/2)\rho^2]e^{-\rho}$$

$$E_{-1,1}^{010} = \rho^{-2}(3+3\rho+2\rho^2+\rho^3)e^{-\rho}$$

$$C_{01}^{010} = [(1/3)\rho+(1/3)\rho^2]e^{-\rho}$$

$$C_{11}^{010} = [(1/4)\rho+(1/4)\rho^2+(1/12)\rho^3]e^{-\rho}$$

$$C_{21}^{010} = [(1/4)\rho+(1/4)\rho^2+(7/60)\rho^3+(1/30)\rho^4]e^{-\rho}$$

$$C_{31}^{010} = [(1/4)\rho+(1/4)\rho^2+(3/20)\rho^3+(1/15)\rho^4+(1/60)\rho^5]e^{-\rho}$$

$$C_{41}^{010} = [(1/10)\rho^3+(1/10)\rho^4+(3/70)\rho^5+(1/105)\rho^6]e^{-\rho}$$

$$(9) \quad \beta, \gamma\delta\epsilon = 2,010 ; \quad 0 \leq \alpha \leq 3$$

$$C_{02}^{010} = -[(5/12)\rho+(5/12)\rho^2+(1/4)\rho^3]e^{-\rho}$$

$$C_{12}^{010} = -[(1/2)\rho+(1/2)\rho^2+(13/60)\rho^3+(1/20)\rho^4]e^{-\rho}$$

$$C_{22}^{010} = -[(3/4)\rho+(3/4)\rho^2+(1/3)\rho^3+(1/12)\rho^4+(1/60)\rho^5]e^{-\rho}$$

$$C_{32}^{010} = -[(5/4)\rho+(5/4)\rho^2+(3/5)\rho^3+(11/60)\rho^4+(17/420)\rho^5+(1/140)\rho^6]e^{-\rho}$$

Functions with  $\gamma+\delta+2\epsilon = 2$

$$(10) \quad \beta, \gamma\delta\epsilon = 1,200 ; \quad -3 \leq \alpha \leq 2$$

$$D_{-3,1}^{200} = \rho^{-2}(24+12\rho+3\rho^2)e^{-\rho}$$

$$E_{-3,1}^{200} = -\rho^{-3}(12+12\rho+5\rho^2+\rho^3)e^{-\rho}$$

RUEDENBERG, ROTHAN, AND JAUNZEMIS

TABLE XIV (continued)

$$D_{-2,1}^{200} = -\rho^{-2}[60+30\rho+(15/2)\rho^2+(1/2)\rho^3]e^{-\rho}$$

$$E_{-2,1}^{200} = 2\rho^{-3}(15+15\rho+6\rho^2+\rho^3)e^{-\rho}$$

$$D_{-1,1}^{200} = \rho^{-2}[60+30\rho+(43/6)\rho^2+(1/6)\rho^3-(1/6)\rho^4]e^{-\rho}$$

$$E_{-1,1}^{200} = -2\rho^{-3}(15+15\rho+6\rho^2+\rho^3)e^{-\rho}$$

$$C_{01}^{200} = -[(1/4)+(1/4)\rho+(1/6)\rho^2+(1/12)\rho^3]e^{-\rho}$$

$$C_{11}^{200} = -[(1/2)+(1/2)\rho+(7/20)\rho^2+(11/60)\rho^3+(1/20)\rho^4]e^{-\rho}$$

$$C_{21}^{200} = -[(5/4)+(5/4)\rho+(9/10)\rho^2+(29/60)\rho^3+(1/6)\rho^4+(1/30)\rho^5]e^{-\rho}$$

$$(11) \quad \beta, \gamma \delta \epsilon = 2, 200 ; \quad -3 \leq \alpha \leq 2$$

$$D_{-3,2}^{200} = -\rho^{-2}[156+78\rho+(49/2)\rho^2+(7/2)\rho^3]e^{-\rho}$$

$$E_{-3,2}^{200} = \rho^{-3}(78+78\rho+34\rho^2+8\rho^3+\rho^4)e^{-\rho}$$

$$D_{-2,2}^{200} = \rho^{-2}[360+180\rho+(337/6)\rho^2+(49/6)\rho^3+(1/3)\rho^4]e^{-\rho}$$

$$E_{-2,2}^{200} = -2\rho^{-3}(90+90\rho+39\rho^2+9\rho^3+\rho^4)e^{-\rho}$$

$$D_{-1,2}^{200} = -\rho^{-2}[360+180\rho+(223/4)\rho^2+(31/4)\rho^3+(1/6)\rho^4-(1/12)\rho^5]e^{-\rho}$$

$$E_{-1,2}^{200} = 2\rho^{-3}(90+90\rho+39\rho^2+9\rho^3+\rho^4)e^{-\rho}$$

$$C_{02}^{200} = [(1/2)+(1/2)\rho+(7/30)\rho^2+(1/15)\rho^3+(1/30)\rho^4]e^{-\rho}$$

$$C_{12}^{200} = [(5/4)+(5/4)\rho+(13/20)\rho^2+(7/30)\rho^3+(1/15)\rho^4+(1/60)\rho^5]e^{-\rho}$$

$$C_{22}^{200} = [(15/4)+(15/4)\rho+(21/10)\rho^2+(17/20)\rho^3+(53/210)\rho^4+(11/210)\rho^5+(1/105)\rho^6]e^{-\rho}$$

$$(12) \quad \beta, \gamma \delta \epsilon = 3, 200 ; \quad 0 \leq \alpha \leq 1$$

$$C_{03}^{200} = -[(5/4)+(5/4)\rho+(11/20)\rho^2+(2/15)\rho^3+(1/30)\rho^4+(1/60)\rho^5]e^{-\rho}$$

$$C_{13}^{200} = -[(15/4)+(15/4)\rho+(7/4)\rho^2+(1/2)\rho^3+(4/35)\rho^4+(13/420)\rho^5+(1/140)\rho^6]e^{-\rho}$$

## TWO-CENTER INTEGRALS. III

TABLE XIV (continued)

(13)  $\beta, \gamma \delta \epsilon = 1, 110 ; -2 \leq \alpha \leq 3$

$$D_{-2,1}^{110} = -\rho^{-2}[60+30\rho+(27/2)\rho^2+(7/2)\rho^3]e^{-\rho}$$

$$E_{-2,1}^{110} = \rho^{-3}(30+30\rho+15\rho^2+5\rho^3+\rho^4)e^{-\rho}$$

$$D_{-1,1}^{110} = \rho^{-2}[60+30\rho+(79/6)\rho^2+(19/6)\rho^3+(1/3)\rho^4]e^{-\rho}$$

$$E_{-1,1}^{110} = -\rho^{-3}(30+30\rho+15\rho^2+5\rho^3+\rho^4)e^{-\rho}$$

$$C_{01}^{110} = -[(1/4)+(1/4)\rho-(1/12)\rho^3]e^{-\rho}$$

$$C_{11}^{110} = -[(1/2)+(1/2)\rho+(1/10)\rho^2-(1/15)\rho^3-(1/30)\rho^4]e^{-\rho}$$

$$C_{21}^{110} = -[(5/4)+(5/4)\rho+(2/5)\rho^2-(1/60)\rho^3-(1/20)\rho^4-(1/60)\rho^5]e^{-\rho}$$

$$C_{31}^{110} = -[(15/4)+(15/4)\rho+(3/2)\rho^2+(1/4)\rho^3-(1/28)\rho^4-(1/28)\rho^5-(1/105)\rho^6]e^{-\rho}$$

(14)  $\beta, \gamma \delta \epsilon = 2, 110 ; -2 \leq \alpha \leq 2$

$$D_{-2,2}^{110} = \rho^{-2}[360+180\rho+(481/6)\rho^2+(121/6)\rho^3+(23/6)\rho^4]e^{-\rho}$$

$$E_{-2,2}^{110} = -\rho^{-3}(180+180\rho+90\rho^2+30\rho^3+7\rho^4+\rho^5)e^{-\rho}$$

$$D_{-1,2}^{110} = -\rho^{-2}[360+180\rho+(319/4)\rho^2+(79/4)\rho^3+(7/2)\rho^4+(1/4)\rho^5]e^{-\rho}$$

$$E_{-1,2}^{110} = \rho^{-3}(180+180\rho+90\rho^2+30\rho^3+7\rho^4+\rho^5)e^{-\rho}$$

$$C_{02}^{110} = [(1/2)+(1/2)\rho+(3/20)\rho^2-(1/60)\rho^3-(1/20)\rho^4]e^{-\rho}$$

$$C_{12}^{110} = [(5/4)+(5/4)\rho+(2/5)\rho^2-(1/60)\rho^3-(1/20)\rho^4-(1/60)\rho^5]e^{-\rho}$$

$$C_{22}^{110} = [(15/4)+(15/4)\rho+(27/20)\rho^2+(1/10)\rho^3-(17/210)\rho^4-(13/420)\rho^5-(1/140)\rho^6]e^{-\rho}$$

(15)  $\beta, \gamma \delta \epsilon = 1, 020 ; 0 \leq \alpha \leq 3$

$$C_{01}^{020} = -[(1/4)+(1/4)\rho+(1/3)\rho^2+(1/4)\rho^3]e^{-\rho}$$

$$C_{11}^{020} = -[(1/2)+(1/2)\rho+(7/20)\rho^2+(11/60)\rho^3+(1/20)\rho^4]e^{-\rho}$$

$$C_{21}^{020} = -[(5/4)+(5/4)\rho+(13/20)\rho^2+(7/20)\rho^3+(1/15)\rho^4+(1/60)\rho^5]e^{-\rho}$$

$$C_{31}^{020} = -[(15/4)+(15/4)\rho+(7/4)\rho^2+(1/2)\rho^3+(4/35)\rho^4+(13/420)\rho^5+(1/140)\rho^6]e^{-\rho}$$

RUEDENBERG, ROOTHAAN, AND JAUNZEMIS

TABLE XIV (continued)

(16)  $\beta, \gamma \delta \epsilon = 1,001$  ;  $-3 \leq \alpha \leq 3$

$$D_{-3,1}^{001} = \rho^{-2}(24+12\rho+2\rho^2)e^{-\rho}$$

$$E_{-3,1}^{001} = -4\rho^{-3}(3+3\rho+\rho^2)e^{-\rho}$$

$$D_{-2,1}^{001} = -\rho^{-2}(60+30\rho+7\rho^2)e^{-\rho}$$

$$E_{-2,1}^{001} = 2\rho^{-3}(15+15\rho+6\rho^2+\rho^3)e^{-\rho}$$

$$D_{-1,1}^{001} = \rho^{-2}[60+30\rho+(23/3)\rho^2+(2/3)\rho^3]e^{-\rho}$$

$$E_{-1,1}^{001} = -2\rho^{-3}(15+15\rho+6\rho^2+\rho^3)e^{-\rho}$$

$$C_{01}^{001} = [(1/2)+(1/2)\rho+(1/6)\rho^2]e^{-\rho}$$

$$C_{11}^{001} = [1+\rho+(2/5)\rho^2+(1/15)\rho^3]e^{-\rho}$$

$$C_{21}^{001} = [(5/2)+(5/2)\rho+(11/10)\rho^2+(4/15)\rho^3+(1/30)\rho^4]e^{-\rho}$$

$$C_{31}^{001} = [(15/2)+(15/2)\rho+(7/2)\rho^2+\rho^3+(13/70)\rho^4+(2/105)\rho^5]e^{-\rho}$$

(17)  $\beta, \gamma \delta \epsilon = 2,001$  ;  $-3 \leq \alpha \leq 2$

$$D_{-3,2}^{001} = -\rho^{-2}(156+78\rho+21\rho^2+2\rho^3)e^{-\rho}$$

$$E_{-3,2}^{001} = 2\rho^{-3}(39+39\rho+16\rho^2+3\rho^3)e^{-\rho}$$

$$D_{-2,2}^{001} = \rho^{-2}[360+180\rho+(167/3)\rho^2+(23/3)\rho^3]e^{-\rho}$$

$$E_{-2,2}^{001} = -2\rho^{-3}(90+90\rho+39\rho^2+9\rho^3+\rho^4)e^{-\rho}$$

$$D_{-1,2}^{001} = -\rho^{-2}[360+180\rho+(113/2)\rho^2+(17/2)\rho^3+(1/2)\rho^4]e^{-\rho}$$

$$E_{-1,2}^{001} = 2\rho^{-3}(90+90\rho+39\rho^2+9\rho^3+\rho^4)e^{-\rho}$$

$$C_{02}^{001} = -[1+\rho+(13/30)\rho^2+(1/10)\rho^3]e^{-\rho}$$

$$C_{12}^{001} = -[(5/2)+(5/2)\rho+(11/10)\rho^2+(4/15)\rho^3+(1/30)\rho^4]e^{-\rho}$$

$$C_{22}^{001} = -[(15/2)+(15/2)\rho+(17/5)\rho^2+(9/10)\rho^3+(31/210)\rho^4+(1/70)\rho^5]e^{-\rho}$$

## TWO-CENTER INTEGRALS. III

TABLE XIV (continued)

Functions with  $\gamma+\delta+2\epsilon = 3$ (18)  $\beta, \gamma\delta\epsilon = 1, 300$  ;  $-4 \leq \alpha \leq 1$ 

$$D_{-4,1}^{300} = \rho^{-3}[120+60\rho+(62/3)\rho^2+(11/3)\rho^3]e^{-\rho}$$

$$E_{-4,1}^{300} = -\rho^{-4}(60+60\rho+27\rho^2+7\rho^3+\rho^4)e^{-\rho}$$

$$D_{-3,1}^{300} = -\rho^{-3}[540+270\rho+84\rho^2+12\rho^3+(1/2)\rho^4]e^{-\rho}$$

$$E_{-3,1}^{300} = 3\rho^{-4}(90+90\rho+39\rho^2+9\rho^3+\rho^4)e^{-\rho}$$

$$D_{-2,1}^{300} = \rho^{-3}[1260+630\rho+190\rho^2+25\rho^3+(1/2)\rho^4-(1/6)\rho^5]e^{-\rho}$$

$$E_{-2,1}^{300} = -6\rho^{-4}(105+105\rho+45\rho^2+10\rho^3+\rho^4)e^{-\rho}$$

$$D_{-1,1}^{300} = -\rho^{-3}[1260+630\rho+190\rho^2+25\rho^3+(3/4)\rho^4+(1/12)\rho^5+(1/12)\rho^6]e^{-\rho}$$

$$E_{-1,1}^{300} = 6\rho^{-4}(105+105\rho+45\rho^2+10\rho^3+\rho^4)e^{-\rho}$$

$$C_{01}^{300} = -[(3/10)\rho+(3/10)\rho^2+(3/20)\rho^3+(1/20)\rho^4]e^{-\rho}$$

$$C_{11}^{300} = -[(3/4)\rho+(3/4)\rho^2+(2/5)\rho^3+(3/20)\rho^4+(1/30)\rho^5]e^{-\rho}$$

(19)  $\beta, \gamma\delta\epsilon = 2, 300$  ;  $-4 \leq \alpha \leq 1$ 

$$D_{-4,2}^{300} = -\rho^{-3}[1140+570\rho+(598/3)\rho^2+(109/3)\rho^3+(25/6)\rho^4]e^{-\rho}$$

$$E_{-4,2}^{300} = \rho^{-4}(570+570\rho+258\rho^2+68\rho^3+11\rho^4+\rho^5)e^{-\rho}$$

$$D_{-3,2}^{300} = \rho^{-3}[4500+2250\rho+766\rho^2+133\rho^3+13\rho^4+(1/3)\rho^5]e^{-\rho}$$

$$E_{-3,2}^{300} = -3\rho^{-4}(750+750\rho+336\rho^2+86\rho^3+13\rho^4+\rho^5)e^{-\rho}$$

$$D_{-2,2}^{300} = -\rho^{-3}[10080+5040\rho+1700\rho^2+290\rho^3+(107/4)\rho^4+(5/12)\rho^5-(1/12)\rho^6]e^{-\rho}$$

$$E_{-2,2}^{300} = 6\rho^{-4}(840+840\rho+375\rho^2+95\rho^3+14\rho^4+\rho^5)e^{-\rho}$$

$$D_{-1,2}^{300} = \rho^{-3}[10080+5040\rho+1700\rho^2+290\rho^3+(539/20)\rho^4+(37/60)\rho^5+(1/60)\rho^6+(1/30)\rho^7]e^{-\rho}$$

$$E_{-1,2}^{300} = -6\rho^{-4}(840+840\rho+375\rho^2+95\rho^3+14\rho^4+\rho^5)e^{-\rho}$$

$$C_{02}^{300} = [(9/20)\rho+(9/20)\rho^2+(1/5)\rho^3+(1/20)\rho^4+(1/60)\rho^5]e^{-\rho}$$

TABLE XIV (continued)

$$C_{12}^{300} = [(3/2)\rho + (3/2)\rho^2 + (99/140)\rho^3 + (29/140)\rho^4 + (19/420)\rho^5 + (1/105)\rho^6]e^{-\rho}$$

$$(20) \quad \beta, \gamma \delta \epsilon = 1, 210 ; \quad -3 \leq \alpha \leq 2$$

$$D_{-3,1}^{210} = -\rho^{-3}[540 + 270\rho + 108\rho^2 + 24\rho^3 + (7/2)\rho^4]e^{-\rho}$$

$$E_{-3,1}^{210} = \rho^{-4}(270 + 270\rho + 129\rho^2 + 39\rho^3 + 8\rho^4 + \rho^5)e^{-\rho}$$

$$D_{-2,1}^{210} = \rho^{-3}[1260 + 630\rho + 250\rho^2 + 55\rho^3 + 8\rho^4 + (1/3)\rho^5]e^{-\rho}$$

$$E_{-2,1}^{210} = -2\rho^{-4}(315 + 315\rho + 150\rho^2 + 45\rho^3 + 9\rho^4 + \rho^5)e^{-\rho}$$

$$D_{-1,1}^{210} = -\rho^{-3}[1260 + 630\rho + 250\rho^2 + 55\rho^3 + (95/12)\rho^4 + (1/4)\rho^5 - (1/12)\rho^6]e^{-\rho}$$

$$E_{-1,1}^{210} = 2\rho^{-4}(315 + 315\rho + 150\rho^2 + 45\rho^3 + 9\rho^4 + \rho^5)e^{-\rho}$$

$$C_{01}^{210} = -[(1/20)\rho + (1/20)\rho^2 - (1/60)\rho^3 - (1/30)\rho^4]e^{-\rho}$$

$$C_{11}^{210} = -[(1/4)\rho + (1/4)\rho^2 + (1/20)\rho^3 - (1/30)\rho^4 - (1/60)\rho^5]e^{-\rho}$$

$$C_{21}^{210} = -[\rho + \rho^2 + (12/35)\rho^3 + (1/105)\rho^4 - (1/35)\rho^5 - (1/105)\rho^6]e^{-\rho}$$

$$(21) \quad \beta, \gamma \delta \epsilon = 1, 120 ; \quad -2 \leq \alpha \leq 2$$

$$D_{-2,1}^{120} = \rho^{-3}[1260 + 630\rho + 310\rho^2 + 85\rho^3 + (43/2)\rho^4 + (23/6)\rho^5]e^{-\rho}$$

$$E_{-2,1}^{120} = -\rho^{-4}(630 + 630\rho + 330\rho^2 + 120\rho^3 + 33\rho^4 + 7\rho^5 + \rho^6)e^{-\rho}$$

$$D_{-1,1}^{120} = -\rho^{-3}[1260 + 630\rho + 310\rho^2 + 85\rho^3 + (253/12)\rho^4 + (41/12)\rho^5 + (1/4)\rho^6]e^{-\rho}$$

$$E_{-1,1}^{120} = \rho^{-4}(630 + 630\rho + 330\rho^2 + 120\rho^3 + 33\rho^4 + 7\rho^5 + \rho^6)e^{-\rho}$$

$$C_{01}^{120} = [(1/5)\rho + (1/5)\rho^2 + (1/60)\rho^3 - (1/20)\rho^4]e^{-\rho}$$

$$C_{11}^{120} = [(1/4)\rho + (1/4)\rho^2 + (1/20)\rho^3 - (1/30)\rho^4 - (1/60)\rho^5]e^{-\rho}$$

$$C_{21}^{120} = [(1/4)\rho + (1/4)\rho^2 + (2/35)\rho^3 - (11/420)\rho^4 - (3/140)\rho^5 - (1/140)\rho^6]e^{-\rho}$$

## TWO-CENTER INTEGRALS. III

TABLE XIV (continued)

$$(22) \quad \beta, \gamma \delta \epsilon = 1, 101 ; \quad -4 \leq \alpha \leq 2$$

$$D_{-4,1}^{101} = \rho^{-3} [120 + 60\rho + (44/3)\rho^2 + (2/3)\rho^3] e^{-\rho}$$

$$E_{-4,1}^{101} = -4\rho^{-4} (15 + 15\rho + 6\rho^2 + \rho^3) e^{-\rho}$$

$$D_{-3,1}^{101} = -\rho^{-3} (540 + 270\rho + 78\rho^2 + 9\rho^3) e^{-\rho}$$

$$E_{-3,1}^{101} = 2\rho^{-4} (135 + 135\rho + 57\rho^2 + 12\rho^3 + \rho^4) e^{-\rho}$$

$$D_{-2,1}^{101} = \rho^{-3} [1260 + 630\rho + 190\rho^2 + 25\rho^3 + (2/3)\rho^4] e^{-\rho}$$

$$E_{-2,1}^{101} = -6\rho^{-4} (105 + 105\rho + 45\rho^2 + 10\rho^3 + \rho^4) e^{-\rho}$$

$$D_{-1,1}^{101} = -\rho^{-3} [1260 + 630\rho + 190\rho^2 + 25\rho^3 + (1/2)\rho^4 - (1/6)\rho^5] e^{-\rho}$$

$$E_{-1,1}^{101} = 6\rho^{-4} (105 + 105\rho + 45\rho^2 + 10\rho^3 + \rho^4) e^{-\rho}$$

$$C_{01}^{101} = [(1/5)\rho + (1/5)\rho^2 + (1/15)\rho^3] e^{-\rho}$$

$$C_{11}^{101} = [(1/2)\rho + (1/2)\rho^2 + (1/5)\rho^3 + (1/30)\rho^4] e^{-\rho}$$

$$C_{21}^{101} = [(3/2)\rho + (3/2)\rho^2 + (23/35)\rho^3 + (11/70)\rho^4 + (2/105)\rho^5] e^{-\rho}$$

$$(23) \quad \beta, \gamma \delta \epsilon = 2, 101 ; \quad -4 \leq \alpha \leq 1$$

$$D_{-4,2}^{101} = -\rho^{-3} [1140 + 570\rho + 526\rho^2 + (73/3)\rho^3 + (2/3)\rho^4] e^{-\rho}$$

$$E_{-4,2}^{101} = 2\rho^{-4} (285 + 285\rho + 123\rho^2 + 28\rho^3 + 3\rho^4) e^{-\rho}$$

$$D_{-3,2}^{101} = \rho^{-3} [4500 + 2250\rho + 742\rho^2 + 121\rho^3 + (29/3)\rho^4] e^{-\rho}$$

$$E_{-3,2}^{101} = -2\rho^{-4} (1125 + 1125\rho + 498\rho^2 + 123\rho^3 + 17\rho^4 + \rho^5) e^{-\rho}$$

$$D_{-2,2}^{101} = -\rho^{-3} [10080 + 5040\rho + 1700\rho^2 + 290\rho^3 + (161/6)\rho^4 + (1/2)\rho^5] e^{-\rho}$$

$$E_{-2,2}^{101} = 6\rho^{-4} (840 + 840\rho + 375\rho^2 + 95\rho^3 + 14\rho^4 + \rho^5) e^{-\rho}$$

$$D_{-1,2}^{101} = \rho^{-3} [10080 + 5040\rho + 1700\rho^2 + 290\rho^3 + (267/10)\rho^4 + (11/30)\rho^5 - (1/10)\rho^6] e^{-\rho}$$

$$E_{-1,2}^{101} = -6\rho^{-4} (840 + 840\rho + 375\rho^2 + 95\rho^3 + 14\rho^4 + \rho^5) e^{-\rho}$$

TABLE XIV (continued)

$$C_{02}^{101} = -[(3/10)\rho + (3/10)\rho^2 + (2/15)\rho^3 + (1/30)\rho^4]e^{-\rho}$$

$$C_{12}^{101} = -[\rho + \rho^2 + (31/70)\rho^3 + (23/210)\rho^4 + (1/70)\rho^5]e^{-\rho}$$

$$(24) \quad \beta, \gamma\delta\epsilon = 1, 011 ; \quad -3 \leq \alpha \leq 2$$

$$D_{-3,1}^{011} = -\rho^{-3}[540 + 270\rho + 102\rho^2 + 21\rho^3 + 2\rho^4]e^{-\rho}$$

$$E_{-3,1}^{011} = 6\rho^{-4}(45 + 45\rho + 21\rho^2 + 6\rho^3 + \rho^4)e^{-\rho}$$

$$D_{-2,1}^{011} = \rho^{-3}[1260 + 630\rho + 250\rho^2 + 55\rho^3 + (23/3)\rho^4]e^{-\rho}$$

$$E_{-2,1}^{011} = -2\rho^{-4}(315 + 315\rho + 150\rho^2 + 45\rho^3 + 9\rho^4 + \rho^5)e^{-\rho}$$

$$D_{-1,1}^{011} = -\rho^{-3}[1260 + 630\rho + 250\rho^2 + 55\rho^3 + (49/6)\rho^4 + (1/2)\rho^5]e^{-\rho}$$

$$E_{-1,1}^{011} = 2\rho^{-4}(315 + 315\rho + 150\rho^2 + 45\rho^3 + 9\rho^4 + \rho^5)e^{-\rho}$$

$$C_{01}^{011} = -[(3/10)\rho + (3/10)\rho^2 + (1/10)\rho^3]e^{-\rho}$$

$$C_{11}^{011} = -[(1/2)\rho + (1/2)\rho^2 + (1/5)\rho^3 + (1/30)\rho^4]e^{-\rho}$$

$$C_{21}^{011} = -[\rho + \rho^2 + (31/70)\rho^3 + (23/210)\rho^4 + (1/70)\rho^5]e^{-\rho}$$

Functions with  $\gamma + \delta + 2\epsilon = 4$

$$(25) \quad \beta, \gamma\delta\epsilon = 1, 310 ; \quad -4 \leq \alpha \leq 1$$

$$D_{-4,1}^{310} = -\rho^{-4}[5040 + 2520\rho + 1000\rho^2 + 220\rho^3 + (227/6)\rho^4 + (25/6)\rho^5]e^{-\rho}$$

$$E_{-4,1}^{310} = \rho^{-5}(2520 + 2520\rho + 1200\rho^2 + 360\rho^3 + 75\rho^4 + 11\rho^5 + \rho^6)e^{-\rho}$$

$$D_{-3,1}^{310} = \rho^{-4}[20160 + 10080\rho + 3940\rho^2 + 850\rho^3 + (275/2)\rho^4 + (77/6)\rho^5 + (1/3)\rho^6]e^{-\rho}$$

$$E_{-3,1}^{310} = -3\rho^{-5}(3360 + 3360\rho + 1590\rho^2 + 470\rho^3 + 95\rho^4 + 13\rho^5 + \rho^6)e^{-\rho}$$

$$D_{-2,1}^{310} = -\rho^{-4}[45360 + 22680\rho + 8820\rho^2 + 1890\rho^3 + (1199/4)\rho^4 + (107/4)\rho^5 + (1/2)\rho^6 - (1/12)\rho^7]e^{-\rho}$$

$$E_{-2,1}^{310} = 6\rho^{-5}(3780 + 3780\rho + 1785\rho^2 + 525\rho^3 + 105\rho^4 + 14\rho^5 + \rho^6)e^{-\rho}$$

$$D_{-1,1}^{310} = \rho^{-4}[45360 + 22680\rho + 8820\rho^2 + 1890\rho^3 + (2993/10)\rho^4 + (263/10)\rho^5 + (2/5)\rho^6 - (1/30)\rho^7 + (1/30)\rho^8]e^{-\rho}$$

TWO-CENTER INTEGRALS. III

TABLE XIV (continued)

$$E_{-1,1}^{310} = -6\rho^{-5}(3780+3780\rho+1785\rho^2+525\rho^3+105\rho^4+14\rho^5+\rho^6)e^{-\rho}$$

$$C_{01}^{310} = -[(3/4)+(3/4)\rho+(3/10)\rho^2+(1/20)\rho^3-(1/60)\rho^4-(1/60)\rho^5]e^{-\rho}$$

$$C_{11}^{310} = -[(9/4)+(9/4)\rho+(15/14)\rho^2+(9/28)\rho^3+(1/28)\rho^4-(3/140)\rho^5-(1/105)\rho^6]e^{-\rho}$$

$$(26) \quad \beta, \gamma \delta \epsilon = 1, 220 ; \quad 0 \leq \alpha \leq 1$$

$$C_{01}^{220} = -[(3/4)+(3/4)\rho+(1/4)\rho^2+(1/60)\rho^5]e^{-\rho}$$

$$C_{11}^{220} = -[(9/4)+(9/4)\rho+(23/28)\rho^2+(1/14)\rho^3-(1/70)\rho^4+(1/84)\rho^5+(1/140)\rho^6]e^{-\rho}$$

$$(27) \quad \beta, \gamma \delta \epsilon = 1, 201 ; \quad -4 \leq \alpha \leq 1$$

$$D_{-4,1}^{201} = -\rho^{-4}[5040+2520\rho+820\rho^2+130\rho^3+(29/3)\rho^4]e^{-\rho}$$

$$E_{-4,1}^{201} = 2\rho^{-5}(1260+1260\rho+555\rho^2+135\rho^3+18\rho^4+\rho^5)e^{-\rho}$$

$$D_{-3,1}^{201} = \rho^{-4}[20160+10080\rho+3340\rho^2+550\rho^3+(139/3)\rho^4+(2/3)\rho^5]e^{-\rho}$$

$$E_{-3,1}^{201} = -2\rho^{-5}(5040+5040\rho+2235\rho^2+555\rho^3+78\rho^4+5\rho^5)e^{-\rho}$$

$$D_{-2,1}^{201} = -\rho^{-4}[45360+22680\rho+7560\rho^2+1260\rho^3+(219/2)\rho^4+(3/2)\rho^5-(1/6)\rho^6]e^{-\rho}$$

$$E_{-2,1}^{201} = 24\rho^{-5}(945+945\rho+420\rho^2+105\rho^3+15\rho^4+\rho^5)e^{-\rho}$$

$$D_{-1,1}^{201} = \rho^{-4}[45360+22680\rho+7560\rho^2+1260\rho^3+(549/5)\rho^4+(9/5)\rho^5+(1/15)\rho^7]e^{-\rho}$$

$$E_{-1,1}^{201} = -24\rho^{-5}(945+945\rho+420\rho^2+105\rho^3+15\rho^4+\rho^5)e^{-\rho}$$

$$C_{01}^{201} = [(1/2)+(1/2)\rho+(3/10)\rho^2+(2/15)\rho^3+(1/30)\rho^4]e^{-\rho}$$

$$C_{11}^{201} = [(3/2)+(3/2)\rho+(13/14)\rho^2+(3/7)\rho^3+(9/70)\rho^4+(2/105)\rho^5]e^{-\rho}$$

$$(28) \quad \beta, \gamma \delta \epsilon = 1, 111 ; \quad -4 \leq \alpha \leq 1$$

$$D_{-4,1}^{111} = -\rho^{-4}[5040+2520\rho+940\rho^2+190\rho^3+(73/3)\rho^4+(2/3)\rho^5]e^{-\rho}$$

$$E_{-4,1}^{111} = 6\rho^{-5}(420+420\rho+195\rho^2+55\rho^3+10\rho^4+\rho^5)e^{-\rho}$$

$$D_{-3,1}^{111} = \rho^{-4}[20160+10080\rho+3880\rho^2+820\rho^3+(373/3)\rho^4+(29/3)\rho^5]e^{-\rho}$$

RUEDENBERG, ROOTHAAN, AND JAUNZEMIS

TABLE XIV (continued)

$$E_{-3,1}^{111} = -2\rho^{-5}(5040+5040\rho+2370\rho^2+690\rho^3+135\rho^4+17\rho^5+\rho^6)e^{-\rho}$$

$$D_{-2,1}^{111} = -\rho^{-4}[45360+22680\rho+8820\rho^2+1890\rho^3+(599/2)\rho^4+(53/2)\rho^5+(1/2)\rho^6]e^{-\rho}$$

$$E_{-2,1}^{111} = 6\rho^{-5}(3780+3780\rho+1785\rho^2+525\rho^3+105\rho^4+14\rho^5+\rho^6)e^{-\rho}$$

$$D_{-1,1}^{111} = \rho^{-4}[45360+22680\rho+8820\rho^2+1890\rho^3+(1499/5)\rho^4+(134/5)\rho^5+(1/2)\rho^6-(1/10)\rho^7]e^{-\rho}$$

$$E_{-1,1}^{111} = -6\rho^{-5}(3780+3780\rho+1785\rho^2+525\rho^3+105\rho^4+14\rho^5+\rho^6)e^{-\rho}$$

$$C_{01}^{111} = [(1/2)+(1/2)\rho+(1/10)\rho^2-(1/15)\rho^3-(1/30)\rho^4]e^{-\rho}$$

$$C_{11}^{111} = [(3/2)+(3/2)\rho+(3/7)\rho^2-(1/14)\rho^3-(1/14)\rho^4-(1/70)\rho^5]e^{-\rho}$$

$$(29) \quad \beta, \gamma \delta \epsilon = 1,002 ; \quad -4 \leq \alpha \leq 1$$

$$D_{-4,1}^{002} = -\rho^{-4}[5040+2520\rho+760\rho^2+100\rho^3+(8/3)\rho^4]e^{-\rho}$$

$$E_{-4,1}^{002} = 24\rho^{-5}(105+105\rho+45\rho^2+10\rho^3+\rho^4)e^{-\rho}$$

$$D_{-3,1}^{002} = \rho^{-4}[20160+10080\rho+3280\rho^2+520\rho^3+(116/3)\rho^4]e^{-\rho}$$

$$E_{-3,1}^{002} = -8\rho^{-5}(1260+1260\rho+555\rho^2+135\rho^3+18\rho^4+\rho^5)e^{-\rho}$$

$$D_{-2,1}^{002} = -\rho^{-4}(45360+22680+7560\rho^2+1260\rho^3+110\rho^4+2\rho^5)e^{-\rho}$$

$$E_{-2,1}^{002} = 24\rho^{-5}(945+945\rho+420\rho^2+105\rho^3+15\rho^4+\rho^5)e^{-\rho}$$

$$D_{-1,1}^{002} = \rho^{-4}[45360+22680\rho+7560\rho^2+1260\rho^3+(544/5)\rho^4+(4/5)\rho^5-(2/5)\rho^6]e^{-\rho}$$

$$E_{-1,1}^{002} = -24\rho^{-5}(945+945\rho+420\rho^2+105\rho^3+15\rho^4+\rho^5)e^{-\rho}$$

$$C_{01}^{002} = -[2+2\rho+(4/5)\rho^2+(2/15)\rho^3]e^{-\rho}$$

$$C_{11}^{002} = -[6+6\rho+(18/7)\rho^2+(4/7)\rho^3+(2/35)\rho^4]e^{-\rho}$$

TWO-CENTER INTEGRALS. III

TABLE XV

EXPLICIT FORMULAS FOR C-FUNCTIONS IN THE CASE  $\rho = 0$ ,  $\tau \neq 0$

Functions with  $\gamma + \delta + 2\epsilon = 0$

(1)  $\beta, \gamma\delta\epsilon = 1, 0, 0$  ;  $-1 \leq \alpha \leq 4$

$$\begin{array}{lll} c_{-1,1}^{000} = -(1-\tau) & c_{01}^{000} = -(1/2)(1-\tau)^2 & c_{11}^{000} = -(1/2)(1-\tau)^3 \\ c_{21}^{000} = -(3/4)(1-\tau)^4 & c_{31}^{000} = -(3/2)(1-\tau)^5 & c_{41}^{000} = -(15/4)(1-\tau)^6 \end{array}$$

(2)  $\beta, \gamma\delta\epsilon = 2, 0, 0$  ;  $-1 \leq \alpha \leq 4$

$$\begin{array}{lll} c_{-1,2}^{000} = (1/2)(1-\tau)^2 & c_{02}^{000} = (1/2)(1-\tau)^3 & c_{12}^{000} = (3/4)(1-\tau)^4 \\ c_{22}^{000} = (3/2)(1-\tau)^5 & c_{32}^{000} = (15/4)(1-\tau)^6 & c_{42}^{000} = (45/4)(1-\tau)^7 \end{array}$$

(3)  $\beta, \gamma\delta\epsilon = 3, 0, 0$  ;  $-1 \leq \alpha \leq 3$

$$\begin{array}{lll} c_{-1,3}^{000} = -(1/2)(1-\tau)^3 & c_{03}^{000} = -(3/4)(1-\tau)^4 & c_{13}^{000} = -(3/2)(1-\tau)^5 \\ c_{23}^{000} = -(15/4)(1-\tau)^6 & c_{33}^{000} = -(45/4)(1-\tau)^7 & \end{array}$$

(4)  $\alpha, \gamma\delta\epsilon = -1, 0, 0$  ;  $4 \leq \beta \leq 9$

$$\begin{array}{lll} c_{-1,4}^{000} = (3/4)(1-\tau)^4 & c_{-1,5}^{000} = -(3/2)(1-\tau)^5 & c_{-1,6}^{000} = (15/4)(1-\tau)^6 \\ c_{-1,7}^{000} = -(45/4)(1-\tau)^7 & c_{-1,8}^{000} = (315/8)(1-\tau)^8 & c_{-1,9}^{000} = -(315/2)(1-\tau)^9 \end{array}$$

Functions with  $\gamma + \delta + 2\epsilon = 1$

All these C-functions vanish for  $\rho = 0$

Functions with  $\gamma + \delta + 2\epsilon = 2$

(10)  $\beta, \gamma\delta\epsilon = 1, 2, 0$  ;  $-3 \leq \alpha \leq 2$

$$\begin{array}{lll} c_{-3,1}^{200} = -(1/3)(1-\tau) & c_{-2,1}^{200} = -(1/6)(1-\tau)^2 & c_{-1,1}^{200} = -(1/6)(1-\tau)^3 \\ c_{01}^{200} = -(1/4)(1-\tau)^4 & c_{11}^{200} = -(1/2)(1-\tau)^5 & c_{21}^{200} = -(5/4)(1-\tau)^6 \end{array}$$

(11)  $\beta, \gamma\delta\epsilon = 2, 2, 0$  ;  $-3 \leq \alpha \leq 2$

$$\begin{array}{lll} c_{-3,2}^{200} = (1/6)(1-\tau)^2 & c_{-2,2}^{200} = (1/6)(1-\tau)^3 & c_{-1,2}^{200} = (1/4)(1-\tau)^4 \\ c_{02}^{200} = (1/2)(1-\tau)^5 & c_{12}^{200} = (5/4)(1-\tau)^6 & c_{22}^{200} = (15/4)(1-\tau)^7 \end{array}$$

RUEDENBERG, ROOTHAAN, AND JAUNZEMIS

TABLE XV (continued)

(12)  $\beta, \gamma \delta \epsilon = 3, 200 ; 1 \leq \alpha \leq 2$

$$c_{03}^{200} = -(5/4)(1-\tau)^6$$

$$c_{13}^{200} = -(15/4)(1-\tau)^7$$

(13)  $\beta, \gamma \delta \epsilon = 1, 110 ; -2 \leq \alpha \leq 3$

$$c_{-2,1}^{110} = -(1/6)(1-\tau)^2$$

$$c_{-1,1}^{110} = -(1/6)(1-\tau)^3$$

$$c_{01}^{110} = -(1/4)(1-\tau)^4$$

$$c_{11}^{110} = -(1/2)(1-\tau)^5$$

$$c_{21}^{110} = -(5/4)(1-\tau)^6$$

$$c_{31}^{110} = -(15/4)(1-\tau)^7$$

(14)  $\beta, \gamma \delta \epsilon = 2, 110 ; -2 \leq \alpha \leq 2$

$$c_{-2,2}^{110} = (1/6)(1-\tau)^3$$

$$c_{-1,2}^{110} = (1/4)(1-\tau)^4$$

$$c_{02}^{110} = (1/2)(1-\tau)^5$$

$$c_{12}^{110} = (5/4)(1-\tau)^6$$

$$c_{22}^{110} = (15/4)(1-\tau)^7$$

(15)  $\beta, \gamma \delta \epsilon = 1, 020 ; 0 \leq \alpha \leq 3$

$$c_{01}^{020} = -(1/4)(1-\tau)^4$$

$$c_{11}^{020} = -(1/2)(1-\tau)^5$$

$$c_{21}^{020} = -(5/4)(1-\tau)^6$$

$$c_{31}^{020} = -(15/4)(1-\tau)^7$$

(16)  $\beta, \gamma \delta \epsilon = 1, 001 ; -3 \leq \alpha \leq 3$

$$c_{-3,1}^{001} = (2/3)(1-\tau)$$

$$c_{-2,1}^{001} = (1/3)(1-\tau)^2$$

$$c_{-1,1}^{001} = (1/3)(1-\tau)^3$$

$$c_{01}^{001} = (1/2)(1-\tau)^4$$

$$c_{11}^{001} = (1-\tau)^5$$

$$c_{21}^{001} = (5/2)(1-\tau)^6$$

$$c_{31}^{001} = (15/2)(1-\tau)^7$$

(17)  $\beta, \gamma \delta \epsilon = 2, 001 ; -3 \leq \alpha \leq 2$

$$c_{-3,2}^{001} = -(1/3)(1-\tau)^2$$

$$c_{-2,2}^{001} = -(1/3)(1-\tau)^3$$

$$c_{-1,2}^{001} = -(1/2)(1-\tau)^4$$

$$c_{02}^{001} = -(1-\tau)^5$$

$$c_{12}^{001} = -(5/2)(1-\tau)^6$$

$$c_{22}^{001} = -(15/2)(1-\tau)^7$$

TWO-CENTER INTEGRALS. III

TABLE XV (continued)

Functions with  $\gamma+\delta+2\epsilon = 3$

All these C-functions vanish for  $\rho = 0$

Functions with  $\gamma+\delta+2\epsilon = 4$

(25)  $\beta, \gamma\delta\epsilon = 1, 310$  ;  $-4 \leq \alpha \leq 1$

$$\begin{aligned} C_{-4,1}^{310} &= -(1/10)(1-\tau)^2 & C_{-3,1}^{310} &= -(1/10)(1-\tau)^3 & C_{-2,1}^{310} &= -(3/20)(1-\tau)^4 \\ C_{-1,1}^{310} &= -(3/10)(1-\tau)^5 & C_{01}^{310} &= -(3/4)(1-\tau)^6 & C_{11}^{310} &= -(9/4)(1-\tau)^7 \end{aligned}$$

(26)  $\beta, \gamma\delta\epsilon = 1, 220$  ;  $0 \leq \alpha \leq 1$

$$C_{01}^{220} = -(3/4)(1-\tau)^6 \quad C_{11}^{220} = -(9/4)(1-\tau)^7$$

(27)  $\beta, \gamma\delta\epsilon = 1, 201$  ;  $-4 \leq \alpha \leq 1$

$$\begin{aligned} C_{-4,1}^{201} &= (1/15)(1-\tau)^2 & C_{-3,1}^{201} &= (1/15)(1-\tau)^3 & C_{-2,1}^{201} &= (1/10)(1-\tau)^4 \\ C_{-1,1}^{201} &= (1/5)(1-\tau)^5 & C_{01}^{201} &= (1/2)(1-\tau)^6 & C_{11}^{201} &= (3/2)(1-\tau)^7 \end{aligned}$$

(28)  $\beta, \gamma\delta\epsilon = 1, 111$  ;  $-4 \leq \alpha \leq 1$

$$\begin{aligned} C_{-4,1}^{111} &= (1/15)(1-\tau)^2 & C_{-3,1}^{111} &= (1/15)(1-\tau)^3 & C_{-2,1}^{111} &= (1/10)(1-\tau)^4 \\ C_{-1,1}^{111} &= (1/5)(1-\tau)^5 & C_{01}^{111} &= (1/2)(1-\tau)^6 & C_{11}^{111} &= (3/2)(1-\tau)^7 \end{aligned}$$

(29)  $\beta, \gamma\delta\epsilon = 1, 002$  ;  $-4 \leq \alpha \leq 1$

$$\begin{aligned} C_{-4,1}^{002} &= -(4/15)(1-\tau)^2 & C_{-3,1}^{002} &= -(4/15)(1-\tau)^3 & C_{-2,1}^{002} &= -(2/5)(1-\tau)^4 \\ C_{-1,1}^{002} &= -(4/5)(1-\tau)^5 & C_{01}^{002} &= -2(1-\tau)^6 & C_{11}^{002} &= -6(1-\tau)^7 \end{aligned}$$

## LITERATURE ON HYBRID INTEGRALS

The existing publications on the hybrid integrals can be divided into four groups according to the integration methods employed.<sup>26</sup>

First Group:

- (1) N. Rosen, Phys. Rev. **38**, 255 (1931).  
 $[ns_a ns_b | ns_b ns_b]$  in terms of  $A_n(2\rho)$ ,  $B_n(2\tau\rho)$ .
- (2) W. H. Furry and J. H. Bartlett, Jr., Phys. Rev. **38**, 1615 (1931), and **39**, 210 (1932).  
 $[2s_a 2s_a | 2s_a 2s_b]$  in terms of  $A_n(\rho)$ ;  $[2s_a 2p\sigma_a | 2s_a 2s_b]$ ,  $[2s_a 2s_a | 2s_a 2p\sigma_b]$ ,  
 $[2s_a 2s_a | 2p\sigma_a 2p\sigma_b]$ ,  $[2s_a 2p\sigma_a | 2s_a 2p\sigma_b]$ ,  $[2p\sigma_a 2p\sigma_a | 2s_a 2s_b]$ ,  $[2s_a 2s_a | 2p\pi_a 2p\pi_b]$ ,  
 $[2p\pi_a 2s_a | 2s_a 2p\pi_b]$ ,  $[2p\pi_a 2p\pi_a | 2s_a 2s_b]$ , for  $\tau = 0$  in terms of auxiliary functions with numerical tables for the latter.

- (3) J. O. Hirschfelder and J. W. Linnett, J. Chem. Phys. **18**, 130 (1950).

$[1s_a 1s_a | 2s_a 2s_b]$ ,  $[1s_a 2p\sigma_a | 1s_a 2p\sigma_b]$ , for  $\tau = 0$  in terms of auxiliary functions.

The method employed by these authors was developed by Rosen and Bartlett. The early work on hybrid integrals is not very extensive, presumably because in the Heitler-London theory of the covalent bond hybrid integrals do not occur. They appear only if ionic structures are taken into account, and for this reason some authors call them "ionic integrals".

Second Group:

- (4) A. L. Sklar and R. H. Lyddane, J. Chem. Phys. **7**, 374 (1939).

$[2p\pi_a 2p\pi_b | 2p\pi_b 2p\pi_b]$  for  $\tau = 0$  in terms of auxiliary functions.

- (5) R. G. Parr and B. L. Crawford, Jr., J. Chem. Phys. **16**, 1049 (1948).

$[2p\pi_a 2p\pi_b | 2p\pi_b 2p\pi_b]$ ,  $[2p\pi_a 2p\pi_b | 2p\bar{\pi}_b 2p\bar{\pi}_b]$ ,  $[2p\pi_a 2p\bar{\pi}_b | 2p\pi_b 2p\bar{\pi}_b]$  for  $\tau = 0$  in terms of auxiliary functions.

- (6) E. Srocco and O. Salvetti, Ric. Sci. **21**, 1629 (1951).

$[2p\pi_a 2p\pi_a | 2p\pi_a 2p\pi_b]$  for  $\tau \neq 0$ .

- (7) R. O. Brennan and J. F. Mulligan, J. Chem. Phys. **20**, 1635 (1952).

All integrals  $[\chi_a' \chi_a'' | \chi_a \chi_b]$  between orbitals with quantum number 2 have been evaluated in an explicit form, under the additional assumption that  $\chi_a$ ,  $\chi_a'$ ,  $\chi_a''$  have the same orbital exponent (in general different from the orbital exponent of  $\chi_b$ ), i.e.,  $\bar{\rho}_a = \rho_a \neq \rho_b$  in our notation.

The procedure here employed was first developed by Sklar and Lyddane and then improved

<sup>26</sup>These four methods are all different from the one developed in this paper.

TWO-CENTER INTEGRALS. III

by other authors. Brennan and Mulligan make a systematic investigation of the limited class of integrals mentioned above.

Third Group:

- (8) M. Kotani, A. Amemiya, and T. Simose, Proc. Phys. Math. Soc. Japan 20, Extra No. 1 (1938), and 22, Extra No. 1 (1940).

(a)  $[2s_a 2s_a | 2s_a 2s_b], [2p\pi_a 2s_a | 2p\pi_a 2s_b]$  for  $\bar{\rho}_a = \rho_a = \rho_b$ .

(b)  $[2s_a 1s_b | 1s_b 1s_b], [2p\sigma_a 1s_b | 1s_b 1s_b], [2s_a 2s_a | 2s_a 1s_b], [2p\sigma_a 2p\sigma_a | 2s_a 1s_b],$   
 $[2s_a 2p\sigma_a | 2s_a 1s_b], [2p\pi_a 2p\pi_a | 2s_a 1s_b], [2p\pi_a 2p\pi_a | 2p\sigma_a 1s_b], [2s_a 2s_a | 2p\sigma_a 1s_b],$   
 $[2s_a 2p\sigma_a | 2p\sigma_a 1s_b], [2p\sigma_a 2p\sigma_a | 2p\sigma_a 1s_b], [2s_a 2p\pi_a | 2p\pi_a 1s_b], [2p\sigma_a 2p\pi_a | 2p\pi_a 1s_b]$   
 for  $\bar{\rho}_a = \rho_a \neq \rho_b$ .

All in terms of auxiliary functions. Numerical tables for the latter in 20, Extra No. 1 (1938); numerical tables of integrals in 22, Extra No. 1 (1940).

- (9) H. Kopineck, Z. Naturforsch. 5a, 420 (1950), 6a, 177 (1951).

All integrals  $[\chi_a' \chi_a'' | \chi_a \chi_b]$  between orbitals with quantum number 2, with the additional assumption that  $\chi_a', \chi_a'', \chi_a, \chi_b$  all have the same orbital exponent, i.e.,  $\bar{\rho}_a = \rho_b$  in our notation.

The integrals are expressed in terms of auxiliary functions; tables are given for the integrals.

- (10) G. Araki and W. Watari, Progr. Theor. Phys. 6, 961 (1951).

Although being prepared independently, this paper covers the same material as Kopineck's paper (regarding hybrid integrals). The integrals are tabulated for closer steps of the argument and with more significant figures. There are serious discrepancies between the tables of (9) and (10).

- (11) T. Murai and G. Araki, Progr. Theor. Phys. 8, 615 (1952).

They give five Hybrid Integrals for several argument values which include cases with  $\rho_a = \bar{\rho}_a \neq \rho_b$  and  $\rho_a = \rho_b \neq \bar{\rho}_a$ .

This method was developed by the Japanese authors, on whose results also Kopineck's papers are based. This group of papers contains the largest amount of numerical tables yet made. Work in this direction is presently continuing in Japan.<sup>27</sup>

Fourth Group:

- (12) M. P. Barnett and C. A. Coulson, Philos. Trans. A243, 221 (1951).

<sup>27</sup>See Progress Report No. 1 (October, 1952) of the Japanese Research Group for the Study of Atomic and Molecular Structure.

RUEDENBERG, ROTHAN, AND JAUNZEMIS

All hybrid integrals for  $n = 1, 2$  in terms of generalized exponential integrals and half-integral-order Bessel functions of imaginary argument.

(13) S. O. Lundqvist and P.-O. Löwdin, Ark. Fys. 3, 147 (1951).

Outline of a method applicable to all hybrid integrals.

These authors are primarily interested in developing an integration method applicable to all molecular integrals, and apply it then to the hybrid integrals. Coulson and Barnett proceed more by means of an analytical investigation; Löwdin relies more on numerical integration methods.

---

FREE-ELECTRON NETWORK MODEL FOR CONJUGATED SYSTEMS. II. NUMERICAL CALCULATIONS<sup>†‡</sup>

[THIS TECHNICAL REPORT, 1952-53, Part One, 58]

CORRIGENDA

Charles W. Scherr  
Laboratory of Molecular Structure and Spectra  
Department of Physics  
The University of Chicago  
Chicago 37, Illinois

P. 60: The text immediately following Eq. (1) reading: "there exist solutions ..." to the end of the paragraph is incorrect. It should read: "there exist an infinity of solutions which may be found from the considerations of I, Sections 2d and 2e. The symmetries of these higher levels are reproduced in the same fashion as the energy levels of nonalternant molecules."

P. 75, Table II: Under the row heading "n-polyenes",  $(n + 1)/2$  should be corrected to  $2/(n + 1)$ .

P. 83: The next to last line of Eq. (A.2) should read: " $\phi(1,12) - 2\cos\kappa\phi(1) + \phi(2) = 0$ ".

P. 86: Immediately following Eq. (A.9a), the text should read: "Hence,  $0.1799 = \phi(1) = a_1 \cos(3\kappa/2) = 0.5488a_1 \dots$ ".

---

<sup>†</sup>This work was assisted in part by the Office of Naval Research under Task Order IX of Contract N6ori-20 with The University of Chicago.

<sup>‡</sup>These Corrigenda apply only to the version of the article appearing in THIS TECHNICAL REPORT, 1952-53, Part One, and not to that appearing in J. Chem. Phys. 21, 1582 (1953).

STUDIES OF ATOMIC SELF-CONSISTENT FIELDS. I. CALCULATION OF SLATER FUNCTIONS<sup>†</sup>

Per-Olov Löwdin<sup>‡</sup>  
Laboratory of Molecular Structure and Spectra  
Department of Physics  
The University of Chicago  
Chicago 37, Illinois

ABSTRACT

A refined technique is described for approximating the numerically given radial part of atomic wave functions associated with self-consistent fields with exchange by means of Slater's analytical functions obtained by replacing each exponential in a hydrogen-like wave function by the sum of one, two, three, or more exponentials. Exponents and coefficients of these exponentials are calculated for the  $3p$ -function of  $Cl^-$ , corresponding to an accuracy of 0.0015 for the normalized radial part, and, with slightly less accuracy, for all the functions of two closed-shell ions,  $F^-$  (without exchange) and  $Na^+$ , and for some neutral first-row atoms,  $C(^1D)$ ,  $N(^2P)$ , and  $O(^1S)$ . The interpolation problem is discussed, and a new interpolation rule for the coefficients is stated, which gives excellent agreement (0.001) in the examples chosen, namely the  $1s$ -functions of the He-like ions and the  $2p$ -functions of  $Na^+$ ,  $Mg^{+2}$ , and  $Si^{+4}$ .

---

IN THE QUANTUM-MECHANICAL treatment of many-electron atoms, the total antisymmetric wave functions describing the different atomic states are usually approximated by the sum of one, two, three or more determinants<sup>1</sup> of one-electron wave functions, each being a product of an atomic orbital (AO) and a spin function. The atomic orbitals are determined from the basic Schrödinger equation for the atom by means of the variation principle<sup>2</sup> as products of radial parts and spherical harmonics, and the best expressions for the former are obtained numerically by step-by-step integration of the Hartree-Fock equations by using the self-consistent-field technique developed by Hartree.<sup>3</sup>

---

<sup>†</sup>This work was assisted in part by the Office of Naval Research under Task Order IX of Contract N6ori-20 with The University of Chicago, in part by the Swedish Natural Science Research Council, and in part by the Elizabeth Thompson Science Fund.

<sup>‡</sup>Permanent address: Institute for Mechanics and Mathematical Physics, University of Uppsala, Uppsala, Sweden.

<sup>1</sup>J. C. Slater, *Phys. Rev.* **34**, 1293 (1929).

<sup>2</sup>J. C. Slater, *Phys. Rev.* **35**, 210 (1930), and V. Fock, *Z. Physik* **61**, 126 (1930).

<sup>3</sup>For an excellent survey of this field, see D. R. Hartree, *Rep. Prog. Phys.* **11**, 113 (1946).

## ATOMIC SELF-CONSISTENT FIELDS. I

For some purposes, it has been found desirable to use also analytic forms of these atomic orbitals. Here we will not discuss the question whether it is better to base applications of the atomic theory on the analytical wave functions rather than on the numerical tables. It has often been said that the analytic expressions would be better for use, e.g., in the theory of molecules and crystals, but our experience is that it is often just as convenient to use numerical computations as analytical calculations and that many times the former are simpler and quicker. However, considering the fact that many physicists are more accustomed to analytical work than to numerical computations, we think that both methods should be developed simultaneously without giving priority to anyone of them. This series of papers will be devoted to a study of the atomic self-consistent fields with exchange, and various problems will be discussed both from the analytical and the numerical points of view.

Analytic expressions for the radial wave functions can be derived in two ways, either directly by fixing parameters in given analytic functions, for instance, of the hydrogen-like type by means of the variation principle as described by Zener<sup>4</sup> and others,<sup>5</sup> or indirectly by approximating the numerically given Hartree-Fock functions in some way analytically, as was proposed by Slater.<sup>6</sup> Except for the simplest cases, the former method leads to rather formidable calculations, whereas the latter is simple but based on the assumption that the self-consistent-field functions are given in advance. An investigation of the accuracy of these analytic atomic orbitals shows that the Zener and Morse-Young-Haurwitz functions<sup>4,5</sup> containing only a few exponentials represent rather poor approximations of the self-consistent fields<sup>7</sup> and hence also of the true charge distributions,<sup>8</sup> and that the deviations are appreciable, particularly at

<sup>4</sup>V. Guillemin and C. Zener, Z. Physik **61**, 199 (1930); C. Zener, Phys. Rev. **36**, 51 (1930); J. C. Slater, Phys. Rev. **36**, 57 (1930).

<sup>5</sup>Extensive tables have been given by Morse, Young, and Haurwitz, Phys. Rev. **48**, 948 (1935); for improvements and corrections, see also L. Goldberg and A. M. Clogston, Phys. Rev. **56**, 696 (1939), and W. E. Duncanson and C. A. Coulson, Proc. Roy. Soc. (Edinburgh) **62**, 37 (1944).

<sup>6</sup>J. C. Slater, Phys. Rev. **42**, 33 (1932); F. W. Brown, Phys. Rev. **44**, 214 (1933).

<sup>7</sup>Only in a few cases have Zener-type functions been used as starting functions for self-consistent-field calculations; see, e.g., V. Fock and M. J. Petrashen, Physik. Z. Sowjetunion **6**, 368 (1934); **8**, 359 (1935).

<sup>8</sup>H. Bethe, Z. Physik **55**, 431 (1929); **57**, 815 (1929), has given a survey of different approximations of the charge distribution of He and He-like ions in comparison to the "true" distributions given by Hylleraas.

large distances. The last fact is of essential importance in the theory of molecules and crystals, and the simplest way of obtaining good analytical orbitals for applications in this field seems therefore to be to use Slater's approach.<sup>6</sup> Part I of this series of papers will be devoted to a study of a refinement of Slater's method, giving analytic atomic wave functions with almost the same accuracy as the numerical functions themselves.

### I. CALCULATION OF SLATER-FUNCTIONS

An atomic orbital with the quantum numbers  $n, l, m$  is the product of a radial wave function  $f_{nl}(r)/r$  and a normalized spherical harmonic  $Y_{lm}(\theta, \varphi)$ . The best expressions for the functions  $f_{nl}(r)$  are now given numerically for many atoms and ions by Hartree and Hartree, Fock, and others.<sup>3</sup> In order to express  $f_{nl}(r)$  analytically, we will now slightly generalize Slater's original idea<sup>9</sup> and try to approximate these tables by functions obtained by replacing each exponential in the corresponding hydrogen-like functions by a sum of one, two, three or more exponentials. For the lowest functions, this gives the following expansions:

$$\begin{aligned}
 f_{1s}(r) &= r \sum_k A_k \exp(-a_k r) , \\
 f_{2s}(r) &= r \sum_k A_k \exp(-a_k r) - r^2 \sum_k B_k \exp(-b_k r) , \\
 f_{2p}(r) &= r^2 \sum_k B_k \exp(-b_k r) , \\
 f_{3s}(r) &= r \sum_k A_k \exp(-a_k r) - r^2 \sum_k B_k \exp(-b_k r) + r^3 \sum_k C_k \exp(-c_k r) , \\
 f_{3p}(r) &= r^2 \sum_k B_k \exp(-b_k r) - r^3 \sum_k C_k \exp(-c_k r) , \\
 &\dots \text{ etc.}
 \end{aligned} \tag{1}$$

where the exponents  $a_k, b_k, \dots$  and the coefficients  $A_k, B_k, \dots$  may be different for each orbital. We will here determine the values of these parameters by a numerical method, which is a simple development of the graphical method described by Slater.<sup>6</sup>

The exponentials involved in the expansions (1) may be calculated by means of a method of successive approximations<sup>10</sup> going inwards from  $r \approx \infty$  to  $r = 0$ . The

<sup>9</sup>According to Slater (reference 6) only the exponential multiplied with the highest power in  $r$  should eventually be replaced by a sum of exponentials, but our generalization is obvious.

<sup>10</sup>A preliminary report of this method was given at the Shelter Island Conference, 1951.

ATOMIC SELF-CONSISTENT FIELDS. I

computations are based on the fact that in the outer region ( $r \approx \infty$ ) only a single exponential is important, in the next inner region two terms are important, in the following region three terms, etc. The numerically given function  $f(r)$ , divided by the highest power  $r^p$  of  $r$  according to (1), is considered in equidistant points; a quotient series is then formed for the outer region by successive divisions, and from this series a trial exponential function is determined as a geometrical series. This function is now subtracted from  $f(r)/r^p$ , and the difference is investigated in the next inner region, where a new quotient series is formed, giving a new trial exponential function. This second function is now subtracted from  $f(r)/r^p$ , and the outer region is considered a second time with a still better result for the first term, etc. In most cases, this process is quite straightforward, and special care must be taken only in regions where the power of  $r$  has to be changed according to (1).

We note that here the quotient series have taken the place of Slater's logarithmic graphs. The success of the method depends partly on the fact that these quotient series and the trial exponentials, i.e., the geometrical series, can be computed so quickly by means of the modern electric desk machines.

A few words may be said about the fixing of the first trial functions for each region. It is easily seen that if a function  $g_n$  is the sum of two geometric series,

$$g_n = ak_1^n + bk_2^n, \quad (2)$$

of which the first is dominating, then the quotient  $g_{n+1}/g_n$  is slowly varying according to the formula

$$g_{n+1}/g_n = k_1 - (b/a)(k_1 - k_2)(k_2/k_1)^n + \dots \quad (3)$$

From the quotient series, considered in a region where  $g_n$  still has enough significant figures, it is therefore possible to get an approximate value of  $k_1$  and estimates of  $k_2$  and  $bk_2^n/ak_1^n$ , of which the latter are usually too rough to be of real value for determining an initial term  $ak_1^n$  somewhere in the first geometrical series. After fixing a suitable value of  $k_1$ , we form instead the auxiliary function

$$h_n = k_1 g_n - g_{n+1} \approx bk_2^n (k_1 - k_2) \quad (4)$$

and its quotient series  $h_{n+1}/h_n$ , from which we get a much better estimate of  $k_2$ ,  $bk_2^n$ , and finally of  $ak_1^n = g_n - bk_2^n$ . After choosing a specific initial term of the first geometric series, we can then form our first trial exponential by repeated

## LÖWDIN

TABLE I.

Survey of the maximum errors in different intervals in the analytic SCF-functions for  $\text{Rb}^+$  (without exchange) given by Slater (reference 6) as an example of the accuracy of his graphical method.

r-interval	Maximum error in units of $10^{-3}$		
	$\text{Rb}^+_{2s}$	$\text{Rb}^+_{3s}$	$\text{Rb}^+_{3p}$
0.00	14	-41	-9
0.04	-30	$\pm 17$	-46
0.20	-15	$\pm 28$	14
0.50	2	25	-31
1.00		14	5

multiplication with constant factors, different for the various interval lengths. The method of successive approximations, as described above, is now started.

The accuracy of the analytic self-consistent-field (SCF) functions obtained by Slater's graphical method may be illustrated by his own example for  $\text{Rb}^+$  in Table I; even if the maximum error is of the order  $45 \times 10^{-3}$ , the approximation is certainly good for many applications. The analytic SCF-functions, calculated from Slater's exponents<sup>6</sup> for other atoms of the periodic system, have also errors of about the same order of magnitude. In treating F,  $\text{F}^-$ , and Ne, Brown<sup>6</sup> reports errors of the order  $20 \times 10^{-3}$ .

In our investigation of the alkali chlorides,<sup>11</sup> we needed the  $3p$ -function of  $\text{Cl}^-$  with exchange, given numerically by Hartree and Hartree,<sup>12</sup> with a very high accuracy, and most of the technique described in this paper was actually developed for the investigation of this function. Our final result is given in Table II, and, by using

TABLE II.

Exponents and coefficients in an analytic SCF-function of the form (1) for  $\text{Cl}^-(3p)$  with exchange (reference 12). Maximum error =  $1.5 \times 10^{-3}$ .

AO	k =	1			2			3			
		1	2	3	1	2	3	1	2	3	
$\text{Cl}^-(3p)$	$b_k$	4.2435	8.4758	22.314	$c_k$	0.92426	1.6658	2.9859			
	$B_k$	9.0441	26.493	2.49	$C_k$	0.07099	1.3955	8.4236			

<sup>11</sup>P.-O. Löwdin, A Theoretical Investigation into Some Properties of Ionic Crystals (Almqvist and Wiksells, Uppsala, 1948), thesis.

<sup>12</sup>D. R. Hartree and W. Hartree, Proc. Roy. Soc. (London) **A156**, 45 (1936).

ATOMIC SELF-CONSISTENT FIELDS. I

six exponentials (three in the C-group and three in the B-group), we could obtain a fit as good as  $1.5 \times 10^{-3}$ , i.e., the analytic SCF-function has about the same accuracy as the numerical function itself. With slightly less accuracy, we treated then two other

TABLE III.

Exponents and coefficients in analytic SCF-functions of the form (1) for  $F^-$  without exchange (reference 13) and for  $Na^+$  with exchange according to Fock and Petrashen (reference 14). For maximum errors, see Table IV.

AO	k =	1	2	k =	1	2	3	4
$F^-(1s)$	$a_k$	8.1890	12.187					
	$A_k$	40.285	9.5770					
$F^-(2s)$	$a_k$	7.1485	...	$b_k$	1.6465	2.7178	4.1211	...
	$A_k$	11.755	...	$B_k$	1.3054	8.7816	6.6845	...
$F^-(2p)$				$b_k$	0.64417	1.4357	3.0759	5.9696
				$B_k$	0.080948	1.3016	8.6449	7.0549
$Na^+(1s)$	$a_k$	8.1093	11.577					
	$A_k$	12.835	57.640					
$Na^+(2s)$	$a_k$	9.1285	...	$b_k$	2.3650	3.9031	...	
	$A_k$	16.895	...	$B_k$	3.6178	25.462	...	
$Na^+(2p)$				$b_k$	2.3718	3.8934	6.5076	
				$B_k$	5.1958	14.024	18.128	

TABLE IV.

Maximum errors of the analytic SCF-functions for  $F^-$  and  $Na^+$  in Table III, in units of  $10^{-3}$ .

r-interval	$F^-_{1s}$	$F^-_{2s}$	$F^-_{2p}$	r-interval	$Na^+_{1s}$	$Na^+_{2s}$	$Na^+_{2p}$
0.00	1	8	0	0.0	±7	3	-5
0.08	-1	±10	1	0.2	8	±1	-1
0.3	-1	-10	-5	0.4	-3	±2	2
0.6	1	4	±1	1.0		2	-1
1.2		-1	-1	2.0		±1	0
3.0		0	±1				
6.0		0	1				
10.0			-1				

LÖWDIN

closed-shell ions in the same way, namely,  $F^-$  without exchange<sup>13</sup> and  $Na^+$  with exchange.<sup>14</sup> The results in a somewhat improved form are condensed in Table III and the maximum errors for different intervals in Table IV. In tabulating the errors, we are always giving the quantity  $(f_{\text{analytical}} - f_{\text{numerical}})$  for the normalized functions in units of  $10^{-3}$ .

In the theory of molecules, some first-row atoms are of particular importance, and we have therefore tried to obtain analytic SCF-functions for neutral carbon ( $^1D$ -state), neutral nitrogen ( $^2P$ -state), and neutral oxygen ( $^1S$ -state), all given numerically with

TABLE V.

Exponents and coefficients in analytic SCF-functions of the form (1) for neutral carbon (reference 15),  $^1D$  ( $\beta = 0.04$ ), for neutral nitrogen (reference 15),  $^2P$  state ( $\beta = 0$ ), and for neutral oxygen (reference 15),  $^1S$  state ( $\beta = 0$ ), all with exchange. For maximum errors, see Table VI.

State	AO	k =	1	2	k =	1	2	3
$^1D$	C(1s)	$a_k$	4.9840	7.0411				
		$A_k$	14.881	12.811				
	C(2s)	$a_k$	3.9471	...	$b_k$	1.4784	2.8493	7.7990
		$A_k$	5.9095	...	$B_k$	2.5829	5.2230	4.5676
	C(2p)				$b_k$	1.0789	2.1444	5.9216
					$B_k$	0.87935	3.3336	2.1226
$^2P$	N(1s)	$a_k$	6.2736	10.920				
		$A_k$	28.744	6.8632				
	N(2s)	$a_k$	4.1749	...	$b_k$	1.7123	3.4424	8.8037
		$A_k$	7.8400	...	$B_k$	3.5175	11.832	8.4171
	N(2p)				$b_k$	1.2210	2.4466	5.6236
					$B_k$	1.0755	5.2350	3.4611
$^1S$	O(1s)	$a_k$	7.2052	12.523				
		$A_k$	35.267	8.6933				
	O(2s)	$a_k$	5.9096	...	$b_k$	1.9764	3.6744	13.931
		$A_k$	9.8450	...	$B_k$	4.9049	11.246	5.5364
	O(2p)				$b_k$	1.3632	2.7487	5.9169
					$B_k$	1.3284	7.3218	6.0887

<sup>13</sup>D. R. Hartree, Proc. Roy. Soc. (London) A151, 96 (1935).

<sup>14</sup>V. Fock and M. Petrashen, Physik. Z. Sowjetunion 6, 368 (1934). The slightly improved tables for  $Na^+$  given by D. R. Hartree and W. Hartree, Proc. Roy. Soc. (London) A193, 299 (1948), were not available in Uppsala at the time of these first calculations.

## ATOMIC SELF-CONSISTENT FIELDS. I

exchange by different authors.<sup>15</sup> The results are condensed in Table V, and the maximum errors are given in Table VI. We note that all the functions in Tables III and V are of orthodox Slater-type,<sup>6</sup> having only their highest-power exponential developed in a sum. The accuracy is essentially higher than in Slater's original functions, but this improvement is gained by adding at least one more exponential, which will again increase the work in the applications.

As was already pointed out by Slater,<sup>6</sup> all these expansions are not uniquely determined at all, and the exponents and the coefficients may vary over considerable ranges. A drastic example of this phenomenon is obtained by comparing our 2p-function for carbon (<sup>1</sup>D) in Table V with the 2p-function in Table VII given previously by Mulliken and others;<sup>16</sup> it is impossible to see directly that these functions with essentially different parameters approximate the same numerical function, but this is actually the case. The respective errors may be found in Table VI, and a closer

TABLE VI.

Maximum errors of the analytic SCF-functions for C, N, and O given in Tables V and VII, in units of  $10^{-3}$ .

r- inter- val	<sup>1</sup> D				r- inter- val	<sup>2</sup> P			<sup>1</sup> S			<sup>3</sup> P O <sub>2p</sub>
	C <sub>1s</sub>	C <sub>2s</sub>	C <sub>2p</sub>	Mulliken C <sub>2p</sub>		N <sub>1s</sub>	N <sub>2s</sub>	N <sub>2p</sub>	O <sub>1s</sub>	O <sub>2s</sub>	O <sub>2p</sub>	
0.0					0.0							
0.2	6	4	3	-3	0.04	8	-2	0	12	-1	0	0
0.8	±3	8	±3	12	0.2	8	-2	1	10	1	3	±1
2.4	3	-4	3	±8	0.5	±4	2	2	±4	-12	4	±1
4.0	0	-4	±1	±3	1.2	±2	±4	±3	±2	±6	±3	-6
8.0		4	-2	2	4.0	-1	±6	±3	-1	-9	±2	±6
			-2	2	7.0		2	1		2	-3	±2
								-1			-1	0

<sup>15</sup>C: A. Jucys, Proc. Roy. Soc. (London) **A173**, 59 (1939). N: D. R. Hartree and W. Hartree, Proc. Roy. Soc. (London) **A193**, 299 (1948). O: Hartree, Hartree, and Swirles, Trans. Roy. Soc. (London) **A238**, 229 (1939).

<sup>16</sup>Mulliken, Rieke, Orloff, and Orloff, J. Chem. Phys. **17**, 1248 (1949); the function in their Eq. (76) is transformed to our form (1).

LÖWDIN

investigation shows that the two error functions have opposite signs almost everywhere. In general, the order of magnitude and the sign of the errors will determine how much the different parameters in the functions (1) may vary.

The different states of a specific electronic configuration of an atom (or ion) may be characterized by Slater's<sup>17</sup> parameter  $\beta$ , and Hartree and others<sup>15</sup> have found by experience that the corresponding radial functions  $f_{nl}(r)$  vary almost linearly in this parameter. In order to investigate whether this simple linearity in  $\beta$  could be transferred, e.g., to the coefficients in the analytic SCF-functions, we have treated neutral oxygen in two of its states, namely the <sup>1</sup>S-state ( $\beta = 0$ ) and the <sup>3</sup>P-state ( $\beta = -0.6$ ). As may be seen from a comparison between Tables V and VII, the preliminary result was negative, and the problem is therefore still under investigation.

TABLE VII.

Exponents and coefficients in an analytic 2p-function of the form (1) for the <sup>3</sup>P-state of neutral oxygen (reference 15), and in Mulliken's (reference 16) 2p-function for the <sup>1</sup>D-state of neutral carbon (reference 15).

State	AO	k =	1	2	3
<sup>3</sup> P	O(2p)	$b_k$	1.4107	2.8500	6.5935
		$B_k$	1.4384	8.3557	4.7562
<sup>1</sup> D	C(2p)	$b_k$	0.898	1.416	2.694
		$B_k$	0.2727	1.427	3.576
Mulliken:					

II. INTERPOLATION OF SLATER-FUNCTIONS

The purpose of the original Slater-functions<sup>6</sup> was not only to describe numerically given SCF-functions analytically, but even to permit interpolations to atoms for which these self-consistent fields had not yet been prepared. This interpolation was based on the rule that the exponents should vary linearly for similar electron configurations and different atomic numbers. The coefficients in the last group were interpolated by means of an auxiliary "intermediate" exponent, also varying linearly, which gave the ratio between the coefficients; the absolute values were then determined by the normality and orthogonality conditions.

The interpolation problem can, of course, be treated rigorously by investigating

<sup>17</sup>J. C. Slater, Phys. Rev. 34, 1293 (1929).

the effect of variations of the atomic number  $Z$  in the basic Hartree-Fock equations,<sup>18</sup> but, with the present mathematical methods, the error margins seem to be too large to render really useful results. For the moment, it seems therefore to be better to work intuitively by using the hypothesis that the SCF-functions are closely analogous to the hydrogen-like functions, but that they just have more general exponents replacing the atomic number  $Z$ . The interpolation rule for the exponents seems very plausible from this point of view,<sup>19</sup> but, in order to obtain full accuracy also in the interpolated functions, we must modify the interpolation rule for the coefficients.

Let us consider the simplest SCF-functions, namely the  $1s$ -functions of the He-like ions, which we will express in the following form:

$$f_{1s}(r) = A_1 r \exp(-a_1 r) + A_2 r \exp(-a_2 r) . \quad (4a)$$

The numerical functions for  $Li^+(Z = 3)$  and  $C^{+4}(Z = 6)$  are given by Fock and Petrashen<sup>20</sup> and by Jucys,<sup>15</sup> respectively, and the corresponding values of our parameters in (4a) are condensed in Table VIII; the maximum errors are in both cases below  $1.0 \times 10^{-3}$ . By using these data, we will then try to make interpolations and extrapolations in the series of the He-like ions.

The exponents  $a_1$  and  $a_2$  are easily determined as linear functions of  $Z$  from the fixed values for  $Z = 3$  and  $Z = 6$ . For the coefficients  $A_1$  and  $A_2$ , the normalization condition for  $f_{1s}$  gives one relation, but, in order to carry out the interpolation, we need one more equation for them. However, we note that, for a pure hydrogen-like  $1s$ -function, we would have the relations

$$f_{1s}(r) = 2Z^{3/2} r \exp(-Zr), \quad [f_{1s}(r)/2r]_{r=0}^{2/3} = Z , \quad (5)$$

and, according to our analogy rule, the last relation indicates that, also for the SCF-functions, the quantity

$$K_{1s} = [f_{1s}(r)/2r]_{r=0}^{2/3} \quad (6)$$

<sup>18</sup>Compare also D. R. Hartree and W. Hartree, Proc. Roy. Soc. (London) **A166**, 450 (1938), and reference 3.

<sup>19</sup>Compare also the exponents in the analytic wave functions for Be-like atoms and ions, calculated directly from the variational principle by V. Fock and M. Petrashen, Physik. Z. Sowjetunion **8**, 359 (1935), Table IV.

<sup>20</sup>V. Fock and M. Petrashen, Physik. Z. Sowjetunion **8**, 547 (1935).

## LÖWDIN

TABLE VIII.

Analytic SCF-functions of the form (1) for  $\text{Li}^+(1s)$  and for  $\text{C}^{+4}(1s)$ ; the maximum error is below  $1.0 \times 10^{-3}$ .

AO	k =	1	2
$\text{Li}^+(1s)$	$a_k$	2.4346	4.4250
	$A_k$	6.6641	2.5618
$\text{C}^{+4}(1s)$	$a_k$	5.4523	9.5935
	$A_k$	23.919	4.0324

will vary linearly with  $Z$ . We have tested this rule on some numerical SCF-functions calculated by Hartree and others,<sup>3</sup> and the results in Table IX show that the "linearity rule" holds with excellent accuracy. Similar quantities  $K_{2s}$ ,  $K_{2p}$ ,  $K_{3s}$ , ... may be constructed also for the  $2s$ -,  $2p$ -,  $3s$ -, ... functions, and a closer investigation shows that they are approximately linear in  $Z$ , too. Complete results also for the higher functions will be given in a later paper in this series. We note that all these quantities are important in the calculations of self-consistent fields with exchange, since they characterize the behavior of the normalized wave functions in the neighborhood of the point  $r = 0$ .

TABLE IX.

The auxiliary quantity  $K_{1s} = (f_{1s}(r)/2r)_{r=0}^{2/3}$  for some  $1s$ -functions belonging to self-consistent fields with exchange.<sup>3</sup>

Z	Atom	$K_{1s}$	Z	Atom	$K_{1s}$
6	C	5.760	17	$\text{Cl}^-$	16.70
7	N	6.757	18	Ar	17.69
8	O	7.751	19	$\text{K}^+$	18.70
			20	$\text{Ca}^{+2}$	19.69
11	$\text{Na}^+$	10.73			
14	$\text{Si}^{+4}$	13.73			

If the  $K_{1s}$ -rule is applied also to the He-series, we get a second relation for the coefficients  $A_1$  and  $A_2$ , which then may be determined. The results of the interpolation are condensed in Table X, and it may be of some interest to test its accuracy. The  $1s$ -function for  $\text{Be}^{+2}$  is numerically given by Hartree and Hartree,<sup>21</sup> and a comparison

<sup>21</sup>D. R. Hartree and W. Hartree, Proc. Roy. Soc. (London) **A149**, 210 (1935).

## ATOMIC SELF-CONSISTENT FIELDS. I

TABLE X.

Interpolated and extrapolated SCF-functions of the form (1) for some He-like ions, obtained by using the linearity of the quantity  $K_{1s}$ . The star \* indicates the given quantities, taken from Table. VIII.

Z	Atom	$K_{1s}$	$a_1$	$a_2$	$A_1$	$A_2$
1	H <sup>-</sup>	0.7505	0.4228	0.9794	0.30025	1.0001
2	He	1.7608	1.4287	2.7022	2.7626	1.9104
3	Li <sup>+</sup>	2.7711*	2.4346*	4.4250*	6.6641*	2.5618*
4	Be <sup>+2</sup>	3.7814	3.4405	6.1478	11.601	3.1057
5	B <sup>+3</sup>	4.7917	4.4464	7.8706	17.387	3.5909
6	C <sup>+4</sup>	5.8021*	5.4523*	9.5935*	23.919*	4.0324*
7	N <sup>+5</sup>	6.8124	6.4582	11.316	31.101	4.4604
8	O <sup>+6</sup>	7.8227	7.4641	13.039	38.897	4.8621
Difference:		1.0103	1.0059	1.7228		

shows that our analytic function reproduces the numerical table with full accuracy. We may suppose that the same will be true also for B<sup>+3</sup>. In the extrapolations, the accuracy can certainly not be so high, but we note that our analytic function will give the same charge distribution for He as was once numerically given by Hartree.<sup>22</sup> Even for H<sup>-</sup> our analytic function is comparatively good, since it gives a much better fit to Hylleraas's charge distribution<sup>8</sup> than the best hydrogen-like wave function.

The calculations involved in the application of the  $K_{1s}$ -rule are somewhat clumsy, and we have therefore tried to derive a simpler interpolation rule for the coefficients, which could be generalized also to functions containing more exponentials. Using the analogy principle, we will make the assumption that each coefficient  $A_k$  as a function of Z has the form

$$A_k(Z) = \kappa_k \{a_k(Z)\}^{p_k}, \quad (7)$$

where the parameters  $\kappa_k$  and  $p_k$  are independent of Z. This means that  $\log_{10} A_k$  is a linear function of  $\log_{10} a_k$ :

$$\log_{10} A_k(Z) = \log_{10} \kappa_k + p_k \log_{10} a_k(Z), \quad (8)$$

and the coefficients  $A_k$  are therefore easily determined, e.g., by using divided differences. However, these preliminary values of the coefficients  $A_k$  are usually not representing a function which is fully normalized, and, in the last step of the

<sup>22</sup>D. R. Hartree, Proc. Cambridge Phil. Soc. 24, 111 (1928).

LÖWDIN

interpolation, they should therefore be given revised values by using the normalization condition.

The results of the application of the rule (8) to the He-series are given in Table XI, and we note that, for the interpolated ions  $\text{Be}^{+2}$  and  $\text{B}^{+3}$ , the coefficients are practically the same as in Table X.

TABLE XI.

Coefficients in interpolated and extrapolated SCF-functions for some He-like ions. The exponents are the same as in Table X, but, this time, the coefficients are obtained by using the simple rule (8). The star \* indicates given quantities, taken from Table VIII.

Z	Atom	Unnormalized coefficients		Normalized coefficients	
		$A_1$	$A_2$	$A_1$	$A_2$
1	$\text{H}^-$	0.41560	1.0585	0.3385	0.8622
2	He	2.8631	1.9269	2.7772	1.8691
3	$\text{Li}^+$	6.6641*	2.5618*	6.6641	2.5618
4	$\text{Be}^{+2}$	11.529	3.1064	11.593	3.1236
5	$\text{B}^{+3}$	17.312	3.5905	17.382	3.6049
6	$\text{C}^{+4}$	23.919*	4.0324*	23.919	4.0324
7	$\text{N}^{+5}$	31.281	4.4422	31.117	4.4189
8	$\text{O}^{+6}$	39.349	4.8271	38.930	4.7759
		$\kappa = 1.6265$	1.0713		
		$p = 1.5850$	0.5862		

The interpolation rule (8) may be directly generalized also to the other groups of coefficients (B, C, ...). As another example, let us consider the 2p-functions of some Ne-like ions. The functions for  $\text{Na}^+(Z = 11)$  and  $\text{Si}^{+4}(Z = 14)$  are numerically given by Hartree and others,<sup>23</sup> and our parameters for the corresponding analytic functions (1) are listed in Table XII and the maximum error (0.002) in Table XIII. From these fixed data, the interpolations for  $\text{Mg}^{+2}(Z = 12)$  and  $\text{Al}^{+3}(Z = 13)$  were carried out by using the simple rule (8) and the normalization condition. Our analytic 2p-function for  $\text{Mg}^{+2}$  may be checked against the SCF-function given numerically by Yost,<sup>24</sup> which is

<sup>23</sup>Na<sup>+</sup>: D. R. Hartree and W. Hartree, Proc. Roy. Soc. (London) **A193**, 299 (1948).

Si<sup>+4</sup>: Hartree, Hartree, and Manning, Phys. Rev. **60**, 857 (1941).

<sup>24</sup>W. J. Yost, Phys. Rev. **58**, 557 (1940).

ATOMIC SELF-CONSISTENT FIELDS. I

TABLE XII.

Analytic SCF-functions for  $\text{Na}^+(2p)$  and  $\text{Si}^{+4}(2p)$  with exchange calculated from the numerical tables (reference 23), and interpolated functions for  $\text{Mg}^{+2}(2p)$  and  $\text{Al}^{+3}(2p)$  with the coefficients determined by the simple rule (8). For maximum errors, see Table XIII.

Z	Atom	$b_1$	$b_2$	$b_3$	Unnormalized coefficients			Normalized coefficients		
					$B_1$	$B_2$	$B_3$	$B_1$	$B_2$	$B_3$
11	$\text{Na}^+$	2.1880	3.7288	6.8864				3.6164	15.660	18.729
12	$\text{Mg}^{+2}$	2.7226	4.4808	7.9907	6.9728	22.590	21.156	7.0360	22.795	21.348
13	$\text{Al}^{+3}$	3.2572	5.2327	9.0950	11.952	30.781	23.524	12.043	31.016	23.704
14	$\text{Si}^{+4}$	3.7918	5.9847	10.1993				18.870	40.231	25.840
	Diff:	0.5346	0.7520	1.1043						
					$\kappa = 0.34400$	1.1348	3.8533			
					$p = 3.0046$	1.9943	0.81944			

almost fully reproduced with an error below 0.0016; it is somewhat surprising that the error in the interpolated function is even lower than in one of the fixed functions ( $\text{Na}^+$ ), see Table XIII.

The net result of our investigation seems to be that it is possible to interpolate analytic SCF-functions with about the same accuracy as in the fixed functions by using Slater's rule for the exponents and the simple rule (8) and the normalization condition for the coefficients. The results already obtained are somewhat encouraging, and further work on this problem is now in progress.

TABLE XIII.

Maximum errors of the analytic SCF-functions given in Table XII in units of  $10^{-3}$ ; note that  $\text{Mg}^{+2}$  is interpolated between  $\text{Na}^+$  and  $\text{Si}^{+4}$ .

r-interval	$\text{Na}^+_{2p}$	$\text{Mg}^{+2}_{2p}$	$\text{Si}^{+4}_{2p}$
0			
0.04	-0.6	-0.7	-0.9
0.20	2.0	1.6	1.1
0.50	-2.1	-1.3	0.7
1.2	2.1	$\pm 1.1$	-0.9
4.0	-2.1	$\pm 1.4$	-0.8
6.0	-0.6	$\pm 0.4$	

## ATOMIC SELF-CONSISTENT FIELDS. I

TABLE XII.

Analytic SCF-functions for  $\text{Na}^+(2p)$  and  $\text{Si}^{+4}(2p)$  with exchange calculated from the numerical tables (reference 23), and interpolated functions for  $\text{Mg}^{+2}(2p)$  and  $\text{Al}^{+3}(2p)$  with the coefficients determined by the simple rule (8). For maximum errors, see Table XIII.

Z	Atom	$b_1$	$b_2$	$b_3$	Unnormalized coefficients			Normalized coefficients		
					$B_1$	$B_2$	$B_3$	$B_1$	$B_2$	$B_3$
11	$\text{Na}^+$	2.1880	3.7288	6.8864				3.6164	15.660	18.729
12	$\text{Mg}^{+2}$	2.7226	4.4808	7.9907	6.9728	22.590	21.156	7.0360	22.795	21.348
13	$\text{Al}^{+3}$	3.2572	5.2327	9.0950	11.952	30.781	23.524	12.043	31.016	23.704
14	$\text{Si}^{+4}$	3.7918	5.9847	10.1993				18.870	40.231	25.840
Diff:		0.5346	0.7520	1.1043						
					$\kappa = 0.34400$	1.1348	3.8533			
					$p = 3.0046$	1.9943	0.81944			

almost fully reproduced with an error below 0.0016; it is somewhat surprising that the error in the interpolated function is even lower than in one of the fixed functions ( $\text{Na}^+$ ), see Table XIII.

The net result of our investigation seems to be that it is possible to interpolate analytic SCF-functions with about the same accuracy as in the fixed functions by using Slater's rule for the exponents and the simple rule (8) and the normalization condition for the coefficients. The results already obtained are somewhat encouraging, and further work on this problem is now in progress.

TABLE XIII.

Maximum errors of the analytic SCF-functions given in Table XII in units of  $10^{-3}$ ; note that  $\text{Mg}^{+2}$  is interpolated between  $\text{Na}^+$  and  $\text{Si}^{+4}$ .

r-interval	$\text{Na}^+_{2p}$	$\text{Mg}^{+2}_{2p}$	$\text{Si}^{+4}_{2p}$
0			
0.04	-0.6	-0.7	-0.9
0.20	2.0	1.6	1.1
0.50	-2.1	-1.3	0.7
1.2	2.1	$\pm 1.1$	-0.9
4.0	-2.1	$\pm 1.4$	-0.8
6.0	-0.6	$\pm 0.4$	

## LÖWDIN

### CONCLUSIONS

In the theory of molecules and crystals, which is based on the use of atomic orbitals in one or other form, the SCF-functions take a selected and most important place, since they represent the best one-electron AO which are available. The problem of calculating analytic SCF-functions has become particularly important during the last few years, since most of the extensive molecular tables under preparation in Chicago under Mulliken, in Oxford under Coulson, and in Tokyo under Kotani, are based on the use of single exponential functions.<sup>25</sup> In order to make all these tables applicable even to the best atomic orbitals, it would be desirable to have the exponents and the coefficients in the analytic functions (1) calculated for all self-consistent-fields which are numerically available, and to carry out interpolations to atoms which have not yet been treated by the Hartree-Fock technique.<sup>26</sup> In addition to the best fits, it would also be of interest to have fairly accurate analytic SCF-functions containing as few exponentials as possible.

By the generalized Slater method described in this paper, it is possible to calculate analytic SCF-functions from the numerically given tables with any desired accuracy, but, even if the technique is simple, the computations are still time-consuming and rather tedious. It is felt that, if the periodic system should be investigated on a large-scale basis in order to obtain analytic SCF-functions having errors of the order of magnitude (0.001-0.002) exemplified in Tables II, VIII, and XIII, then it would be worthwhile to re-examine the basic method for further improvements, if possible. Work on this program is now in progress, and the results will be reported in a later paper in this series.

The author is greatly indebted to Fil. Mag. L. F. Ljungström, Uppsala, who kindly assisted in the computations on the sodium and the fluorine ions when this work was started, to the Swedish Natural Science Research Council for a grant, which made these calculations possible, and to Professor I. Waller for many forms of valuable support.

The work on the first-row atoms was started on the initiative of Professor R. S. Mulliken, Chicago, and I would like to express my sincere gratitude to him for many valuable discussions and for the great hospitality I enjoyed during my stay in Chicago.

---

<sup>25</sup>Molecular tables for particular atoms may also be prepared directly from the numerically given SCF-functions; see, e.g., reference 11, Method I.

<sup>26</sup>It seems probable that the interpolated analytic functions would give very good initial functions for self-consistent-field calculations.

ATOMIC SELF-CONSISTENT FIELDS. I

I would also like to thank Mr. Tracy J. Kinyon for his valuable assistance in carrying out the calculations on neutral carbon, nitrogen, and oxygen.

Finally, I would like to thank Fl. Kand. K. Appel, leader of our computational group, for his skilful cooperation in performing the computations in connection with the interpolation problem, the Elizabeth Thompson Science Fund for financial aid, and Professor J. C. Slater for his kind interest and valuable support of my work.

---

ON THE USE OF A SINGLE SCALE FACTOR IN ATOMIC WAVE FUNCTIONS. I\*

Charles W. Scherr  
Laboratory of Molecular Structure and Spectra  
Department of Physics  
The University of Chicago  
Chicago 37, Illinois

ABSTRACT

Single scale factors are determined for converting 1s, 2s, and 2p self-consistent field orbitals of atoms in the first row of the periodic table into one another. Several simple relationships are found which allow predictions for fluorine and neon.

I. INTRODUCTION

RECENTLY there has been a recognition<sup>1</sup> of a desirability of using SCF (self-consistent field) atomic orbitals rather than the Slater atomic orbitals in problems on molecular structure. Most of the LCAO MO (linear combination of atomic orbitals molecular orbitals) method has been pursued through the use of Slater orbitals; but decidedly different results may be expected from the use of SCF orbitals, as shown, for example, by calculations of overlap integrals.

Any SCF orbital  $\chi_{A,S}$  is of the form  $R_{A,S}(r)F(\theta,\phi)$ , where A and S refer to the atom and the state, respectively. By introducing a scale factor  $\lambda_{AB,ST}$  one can expect to predict  $\chi_{B,T}$ , the SCF orbital of atom B in state T from  $\chi_{A,S}$  by an approximation  $\chi_{B,T} \approx (\lambda_{AB,ST})^{\frac{1}{2}} R_{A,S}(\lambda_{AB,ST}r)F(\theta,\phi)$ . Since the radial part may be approximated<sup>2</sup> by a sum,

$$R_{A,S,n,\ell} \approx \sum_{k=\ell}^{n-1} a_k r^k e^{-\zeta_k r}, \quad (1)$$

in which the last term is dominant, then

$$\lambda_{AB,ST} \approx \zeta_{n-1,B} / \zeta_{n-1,A}. \quad (2)$$

\*This work was assisted (in part) by the Office of Naval Research under Task Order IX of contract N6ori-20 with The University of Chicago.

<sup>1</sup>See for example R. S. Mulliken, *J. Phys. Chem.* **56**, 295 (1952), particularly p. 300.

<sup>2</sup>J. C. Slater, *Phys. Rev.* **42**, 33 (1932).

## SINGLE SCALE FACTOR IN ATOMIC WAVEFUNCTIONS. I

The  $a_k$ 's and the  $\zeta_k$ 's (orbital exponents)<sup>3</sup> depend on the particular orbital, atom, and (to a small extent) electronic state.

Some early workers<sup>4</sup> on SCF calculations used a scale factor to obtain their first approximations from previously treated atoms, which were nearby in the same row of the periodic table. Brown, Bartlett, and Dunn<sup>5</sup> noted that the reciprocals of the radii at the maxima of the SCF radial wavefunctions were nearly linear in the atomic number, and used the ratios of these reciprocals as scale factors. Hartree<sup>6</sup> has discussed the use of a scale factor, and introduced the idea expressed in Eq. (2).

The present paper is a result of a systematic investigation of the use of a single scale factor in the exact SCF wavefunctions with exchange for atoms of the first row of the periodic table. The SCF wavefunctions are the "best" wavefunctions arising from the variational method with the use of antisymmetrized spinorbital-product wavefunctions.

There is a characterizing coefficient used extensively in this paper which it is best to discuss here.  $R_{A,S}(r)$  depends on  $S$ ; but by Slater's theory of complex spectra,<sup>7</sup>  $E_S = E_C + \beta_S F^2$ , where  $F^2$  is an energy integral and  $E_C$  is a configuration energy, hence  $R_{A,S}(r) = R_A(r, \beta_S)$  for any given configuration. For example the  $^3P$  ground state of carbon has  $\beta = -5/25$ , and the  $^1D$  and  $^1S$  states have  $\beta = +1/25$  and  $+10/25$ , respectively.

## II. PROCEDURE

We have

$$\int_0^{\infty} \lambda_{AB,ST} R_{A,S}^2(\lambda_{AB,ST} r) r^2 dr = \int_0^{\infty} R_{B,T}(r) r^2 dr = 1,$$

where the symbols have all been defined in Section I. Further,

$$\lambda_{AC,ST} = \lambda_{AB,SU} \lambda_{BC,UT}, \quad (3)$$

<sup>3</sup>This term was introduced by C. C. J. Roothaan and K. Ruedenberg. It is the effective nuclear charge divided by the principal quantum number.

<sup>4</sup>Arnot and McLauchland, Proc. Roy. Soc. **146A**, 662 (1934); Manning and Millman, Phys. Rev. **49**, 848 (1936).

<sup>5</sup>Brown, Bartlett, and Dunn, Phys. Rev. **44**, 296 (1933).

<sup>6</sup>D. R. Hartree, Repts. Progr. in Phys., 113 (1946-1947)

<sup>7</sup>J. C. Slater, Phys. Rev. **34**, 1293 (1929).

### SCHERR

where  $\chi_{B,U}$  is any orbital.

Numerically tabulated SCF with exchange  $rR(r)$  functions from the literature<sup>8-11</sup> for the various  $s^2p^n$  states of each of the atoms carbon, nitrogen, oxygen, and neon were approximated by scaling from tabulated SCF with exchange  $rR(r)$  data for the  $s^2p^3$  states of carbon.<sup>8</sup> Various  $\lambda$ -values were tried in each case until that one was found which, for a particular scaling, minimized

$$2 \int_0^{\infty} |(\delta R)_{B,T}| r^2 dr . \quad (4)$$

This procedure may be compared with the usual<sup>12</sup> least squares treatment of problems of similar type, namely the minimization of

$$2 \int_0^{\infty} (\delta R)_{B,T} r^2 dr . \quad (4a)$$

In integrals 4 and 4a,  $R_{B,T}$  is the correct numerical SCF function for the radial part of the orbital that is being approximated.  $\delta R$  is defined as the difference between the correct tabular value of  $R_{B,T}$  and the approximation. The integrals were evaluated by numerical integration.

### III. RESULTS

The best values of the scale factors, determined by the above procedure, are tabulated in Tables I, II, and III. The "criterion error" reported is the magnitude of the minimized integral (4). These criterion errors can be used as measures of the relative errors involved, for different atoms and states, in the best computed orbitals of any one kind obtained by scaling with a single scale factor from an initial SCF tabulation. The published SCF data are accurate to  $\pm 0.002$  unit. This degree of unreliability would correspond to a criterion error of about 0.0035 to 0.0040 for the 2s and 2p orbitals.

<sup>8</sup>A. Jucys, Proc. Roy. Soc. **173A**, 59 (1939); also see J. Phys. USSR, **49** (1947).

<sup>9</sup>Hartree and Hartree, Proc. Roy. Soc. **193A**, 299 (1948).

<sup>10</sup>Hartree, Hartree, and Swirles, Philos. Trans. **238A**, 229 (1939).

<sup>11</sup>D. R. Hartree, private communication of tentative results (first iteration) by Miss B. H. Worsley for the 2p neon orbitals, and of estimations by Hartree for the 1s and 2s neon orbitals.

<sup>12</sup>The original purpose of the work was the estimation of two-center overlap integrals, and integral (4) seems better for this purpose than integral (4a). The two minimizations give scale factors that agree in the second decimal.

TABLE I.  
THE 2p SCALE FACTORS FOR SCALING FROM CARBON<sup>a</sup> SCF ORBITALS.

To		Carbon s <sup>2</sup> p <sup>2</sup>		Nitrogen s <sup>2</sup> p <sup>3</sup>		Oxygen s <sup>2</sup> p <sup>4</sup>		Neon s <sup>2</sup> p <sup>6</sup>		
2p in:	1s	1D	3P	2P	2D	4S	1S	1D	3P	
From	10	1	-5	0	-6	-15	0	-9	-15	-30
2p in: 25B:										
carbon s <sup>2</sup> p <sup>2</sup>	1	(1.041) <sup>b</sup>	1.062 <sub>5</sub>	(1.257)	1.277	(1.301)	1.474	1.495	(1.506)	...
carbon s <sup>2</sup> p <sup>2</sup>	0.962 <sub>5</sub>	1	1.021 <sub>5</sub>	1.207 <sub>5</sub>	1.224	1.249	1.416	1.433 <sub>5</sub>	1.446	1.87
carbon s <sup>2</sup> p <sup>2</sup>	(0.938)	0.977	1	(1.180)	(1.196)	1.218	1.384	(1.400)	1.414	...
Corresponding "criterion errors"										
carbon s <sup>2</sup> p <sup>2</sup>	0	(0.038)	0.0567	(0.020)	0.029	(0.048)	0.0066	0.0143	(0.029)	...
carbon s <sup>2</sup> p <sup>2</sup>	0.0386	0	0.0204	0.0188	0.0080	0.0101	0.0350	0.0232	0.0162	0.0193
carbon s <sup>2</sup> p <sup>2</sup>	(0.058)	0.0233	0	(0.041)	(0.030)	0.0115	~0.058	(0.049)	0.0389	...

<sup>a</sup>Also 2p nitrogen scaled to 3p oxygen,  $\lambda = 1.195$ , criterion error, -0.0037; 1D oxygen scaled to 3p oxygen,  $\lambda = 1.008_5$ , criterion error, -0.0064.

<sup>b</sup>The values in parentheses are the mean values of estimates made by one or more methods, for example, by the use of Eq. (3).

SCHERR

TABLE II. THE 2s SCALE FACTORS FOR

		Beryllium		Carbon		
		$s^2$	$s^2$	$s^2$	$p^2$	$p^2$
To	2s in:	$1s$	$1s$	$1D$	$3P$	
From	25 $\beta$ :	0	10	1		-5
carbon	$1s$	...	1	(0.994) <sup>a</sup>		0.990
carbon	$1D$	0.594	1.006	1		0.996
carbon	$3P$	...	(1.010)	(1.004 <sub>5</sub> )		1
Corresponding						
carbon	$1s$	...	0	(0.0026)		0.0067
carbon	$1D$	0.0176	0.0026	0		0.0028
carbon	$3P$	...	0.0060	(0.0028)		0

<sup>a</sup>The values in parentheses are the mean values of estimates made by one or

<sup>b</sup>The whole spread of criterion error here is too small to make estimates

TABLE III.

THE 1s SCALE FACTORS FOR SCALING FROM CARBON SCF ORBITALS.

To	Beryllium	Carbon	Nitrogen	Oxygen	Neon
From carbon	0.645 <sub>5</sub>	1	1.172	1.349	1.697 <sub>5</sub>
Corresponding "criterion errors"					
From carbon	0.0082	0	0.0023	0.0048	0.0003 <sub>3</sub>

SINGLE SCALE FACTOR IN ATOMIC WAVEFUNCTIONS. I

SCALING FROM CARBON SCF ORBITALS.

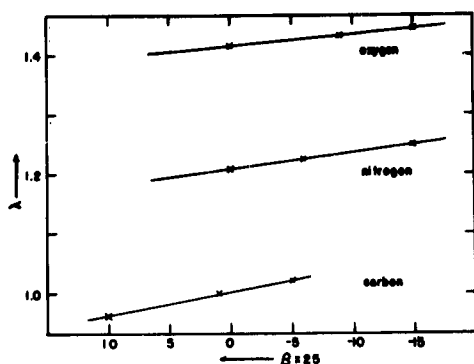
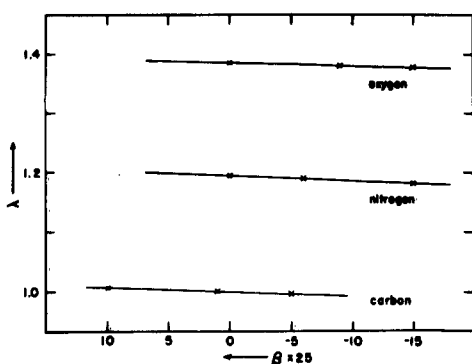
Nitrogen $s^2p^3$			Oxygen $s^2p^4$			Neon $s^2p^6$
$2p$	$2d$	$4s$	$1s$	$1d$	$3p$	$1s$
0	-6	-15	0	-9	-15	-30
1.185 <sub>5</sub>	(1.181)	1.176 <sub>5</sub>	1.377 <sub>5</sub>	(1.374)	1.371 <sub>5</sub>	...
1.194	1.189	1.183	1.385 <sub>5</sub>	1.382	1.378	1.766
1.199 <sub>5</sub>	(1.193)	1.187 <sub>5</sub>	1.393 <sub>5</sub>	(1.388)	1.383 <sub>5</sub>	...
"criterion errors"						
0.0075	(0.0090)	0.0102	0.0095	... <sup>b</sup>	~0.0112	...
0.0060	0.0070	0.0099	0.0100	~0.0094	0.0095	0.0144
0.0079	(0.0040)	0.0065	0.0102	... <sup>b</sup>	0.0094	...

more methods, for example, by the use of Eq. (3).

meaningful.

IV. DISCUSSION

For 2s or 2p scaling from carbon to either oxygen or nitrogen, the scale factors are nearly linear in  $\beta$ . For carbon scaled to carbon the linearity is slightly less good. In Jucys' SCF calculations of carbon, the tabulated values of  $rR(r)$  for the 2s and 2p orbitals in the  $1D$  state were found to be in agreement, to the accuracy of the calculation, with the results of an interpolation linear in  $\beta$ , at any given  $r$  value, between the tabulated values for the  $3P$  and  $1S$  states. Hartree and the others in subsequent SCF calculations on nitrogen and oxygen assumed the validity of corresponding relations for these atoms; the wavefunction of  $2D$  state of nitrogen was assumed to be linearly spaced with respect to  $\beta$  between those of  $2P$  and  $4S$  states; likewise the  $1D$

Fig. 1.  $\lambda_{2p}(N, \beta: 6, 1)$ Fig. 2.  $\lambda_{2s}(N, \beta: 6, 1)$ 

state of oxygen between the  $1s$  and  $3p$  states, and consequently only the last pairs in each case were calculated by them.

Surprisingly enough, the riterion error does not increase as the scaling goes to atoms more remote in the periodic table from carbon. This result may allow one to make safely "long distance" scalings for use as first approximations in SCF calculations. Regularities in the behavior of the riterion error indicate that a scaling to the  $2p$  state of fluorine from the  $1d$  of carbon should have a riterion error of about 0.018, but that scaling to the  $2p$  state of boron should have a large riterion error.

An interesting characteristic of the  $\lambda$ -values, evident if one compares Figures 1 and 2, is that  $\partial\lambda/\partial\beta$  has opposite signs for the  $2p$  and  $2s$  orbitals. This may be

the result of the influence of the inner loop of the  $2s$  orbital which, relatively speaking, requires a much smaller  $\lambda$  than the outer loop, as can be seen from Table IV.

The considerable success of a single scale factor in estimating one SCF orbital from another must reflect a close mathematical similarity between the SCF wavefunctions of the various atoms. The accuracy of such estimates could be increased several fold by using two or more scale factors; for example, in a  $2p$  or  $1s$  orbital these could be one scale factor for a radius less than, and another for a radius greater than, the radius at the maximum of  $rR(r)$ ; and in a  $2s$  orbital, one scale factor for each loop.

In several of the investigated cases any  $\lambda$ -value within an appreciable range gave a satisfactory scaling; that is, the minima of integral (4) were broad. Almost all of these broad minima occurred in scalings with large riterion errors.

#### V. GENERAL FORMULAS

The near linearity of the scale factors with respect to  $\beta$  allows simple formulas to be written for the scale factors of the first row atoms. We use the symbol

SINGLE SCALE FACTOR IN ATOMIC WAVEFUNCTIONS. I

TABLE IV.

A COMPARISON OF  $\lambda$  WITH THE USE OF THE RATIO OF THE RECIPROCAL  
OF THE RADII AT MAXIMA IN THE WAVEFUNCTION FOR SCALE FACTORS.

Carbon scaled to	Method	$\lambda$ for the 1s orbitals	$\lambda$ for the 2s orbitals		$\lambda$ for the 2p orbitals
			Inner max <sup>a</sup>	Outer max <sup>a</sup>	
nitrogen	by reciprocals	1.183	1.148	1.184	1.230
nitrogen	calculated here	1.172	1.176-99 <sup>b</sup>		1.180-1.301
oxygen	by reciprocals	1.356	1.308	1.414	1.482
oxygen	calculated here	1.349	1.371-93		1.384-1.506
neon	by reciprocals	1.680	1.661	1.768	1.963
neon	calculated here	1.697 <sub>5</sub>	1.766		1.87

<sup>a</sup>This refers only to the reciprocal method.

<sup>b</sup>The numbers in this, and the next column, under the row heading "calculated here", are the complete spread of scale factors found for each atom as calculated here. Since the maxima of the SCF functions of the same orbital for the various states of the same atom coincide, there are no "spreads" for the "reciprocal" rows.

$\lambda(N, \beta; 6, 1)$  to mean the scale factor for scaling from  $s^2 p^2 \ ^1D$  carbon to the  $s^2 p^{N-4}$  state, characterized by  $\beta$ , for the atom of atomic number  $N$ . The formulas<sup>13</sup> are:

$$\lambda_{2p}(N, \beta; 6, 1) = 1.002 + 0.207(N-6) - 0.0983(0.707)^{N-6} \beta, \quad (5)$$

$$\lambda_{2s}(N, \beta; 6, 1) = 0.999 + 0.194(N-6) + 0.0025(13-N)\beta, \quad (6)$$

$$\lambda_{1s}(N; 6) = 1 + 0.174(N-6). \quad (7)$$

Scale factors for scalings from other than  $\ ^1D$  carbon, can be obtained by the use of Eq. (3). The scale factors calculated from these formulas, for scaling from the  $\ ^1D$  state of carbon to certain states of boron, fluorine, and neon atoms, are presented in Table V.

<sup>13</sup>Because of the tentative nature of the neon data, and of the probability that Hartree estimated the 1s and 2s neon orbitals on a basis similar to ours, these formulae were not adjusted to fit the neon data. The neon data are however reproduced by the equations.

SCHERR

TABLE V.

SOME CALCULATED SCALE FACTORS FOR SCALING FROM  $1D$  STATE OF CARBON.

Atom Orbital	Boron $s^2p^2$ $2p$	Fluorine $s^2p^5$ $2p$	Neon $s^2p^6$ $1s$
2p	...	1.651	1.860
2s	...	1.573	1.766
1s	0.826	1.522	1.696

VI. A COMPARISON OF SCALE FACTORS FROM VARIOUS SOURCES

Slater<sup>14</sup> has given a recipe for orbital exponents<sup>3</sup> to be used in conjunction with his well-known and very useful orbitals. This recipe may be compared directly with our scale factors by means of Eq. (2). It requires for the coefficient of (N-6) in Eq. (5) and Eq. (6), the value 0.2 and in Eq. (7), the value 0.1754. The results of the present and the following paper of this series indicate that these rather arbitrary choices of Slater were remarkably good. This, of course, is no new conclusion.

TABLE VI.

A COMPARISON OF  $\lambda$  WITH THE SCALE FACTORS CONSTRUCTED FROM THE CALCULATIONS OF DUNCANSON AND COULSON (REFERENCE 15).

Atom	State	Scale factor for scaling from $s^2p^2 \ 3P$ carbon for the:					
		1s orbital		2s orbital		2p orbital	
		Reference 15	$\lambda$	Reference 15	$\lambda$	Reference 15	$\lambda$
L1	$2s$	0.473	(0.478) <sup>a</sup>	0.398	(0.419)	...	...
Be	$1s$	0.648	0.646	0.593	(0.597)	...	...
B	$2p$	0.824	(0.826)	0.800	(0.809)	0.769	(0.777)
N	$4s$	1.174	1.172	1.192	1.188	1.224	1.218
O	$3p$	1.350	1.349	1.385	1.384	1.423	1.414
F	$2p$	1.524	(1.522)	1.580	(1.580)	1.634	(1.613)
Ne	$1s$	1.700	1.698	1.776	(1.774)	1.846	(1.827)

<sup>a</sup>The values in parentheses have been estimated either by the use of Tables I, II, or by the use of Eqs. (5), (6), (7) in conjunction with Eq. (3).

<sup>14</sup>J.C. Slater, Phys. Rev. **36**, 57 (1930), and C. Zener, Phys. Rev. **36**, 51 (1930).

## SINGLE SCALE FACTOR IN ATOMIC WAVEFUNCTIONS. I

Duncanson and Coulson<sup>15</sup> have calculated orbital exponents for approximate SCF wavefunctions. As might be expected (see Table VI), our results are in good agreement with the scale factors constructed from their data.

A comparison of our scale factors with those constructed from the ratios of the reciprocals of the radii at maxima in the wavefunctions is given in Table IV, where the method can be seen to give fairly good scale factors.

### VII. ACKNOWLEDGMENT

I wish to express my indebtedness to Professor R. S. Mulliken for suggesting this investigation and for many helpful discussions; and also Professor C. C. J. Roothaan for some valuable constructive criticism.

---

---

<sup>15</sup>Duncanson and Coulson, Proc. Roy. Soc. Edinburgh **62A**, 37 (1944).

ON THE USE OF A SINGLE SCALE FACTOR IN ATOMIC WAVE FUNCTIONS.

II. APPLICATION TO OVERLAP INTEGRALS\*

Charles W. Scherr  
Laboratory of Molecular Structure and Spectra  
Department of Physics  
The University of Chicago  
Chicago 37, Illinois

ABSTRACT

A method of estimation of two-center homopolar overlap integrals between SCF atomic orbitals, due to Mulliken, has been tested and verified.

THE CALCULATION of two-center overlap integrals from numerically tabulated SCF (self-consistent field) functions is somewhat laborious, and even with the use of analytical fits to the SCF functions, when available, the calculation is still rather lengthy. It is the purpose of this paper to demonstrate the applicability of a simple method of making estimates of homopolar two-center SCF overlap integrals. This method is applicable to the various atom pairs which can be constructed from any particular row of the periodic table, when exact calculations are available for the SCF overlap integrals of one of those pairs.

The method of estimation used in the present paper has been proposed<sup>1</sup> and used<sup>2</sup> by Mulliken. The idea of the method is that two-center overlap integrals are about the same for all the homopolar atom pairs of the same row of the periodic table, for the same orbitals, for any particular  $\rho$ -value, where  $\rho = \zeta R$  and  $\zeta$  is the Slater orbital exponent<sup>3</sup> of the atom, and  $R$  is the internuclear distance in atomic units.<sup>4</sup>

Analytical fits using three to five term linear combinations of Slater-type

---

\*This work was assisted (in part) by the office of Naval Research under Task Order IX of Contract N6ori-20 with The University of Chicago.

<sup>1</sup>R. S. Mulliken, *J. Am. Chem. Soc.* **72**, 4493 (1950).

<sup>2</sup>R. S. Mulliken, *J. Phys. Chem.* **56**, 295 (1952), footnote 42.

<sup>3</sup>See reference 6, footnote 3.

<sup>4</sup>The extension to heteropolar atom pairs should be complicated. If the ratio of the  $\zeta$ -values were near unity, e.g., in NO, it would seem reasonable to use a mean  $\rho$ -value,  $\rho = \frac{1}{2}(\zeta_A + \zeta_B)R$ , where  $\zeta_A$  and  $\zeta_B$  are the orbital exponents on the two atoms.

SINGLE SCALE FACTOR IN ATOMIC WAVEFUNCTIONS. II

orbitals to the "SCF with exchange" numerically tabulated functions for the  $rR(r)$  (radial part of the wave function) of the 1s, 2s, and 2p orbitals of the various states of each of the atoms of carbon, nitrogen, and oxygen, among others, were determined by Löwdin.<sup>5</sup> On the basis of the criterion of accuracy used in the first paper of the present series, these fits give a criterion error of less than 0.0050.<sup>6</sup> As a test of Mulliken's method of estimation of SCF overlap integrals, the present author computed the exact SCF overlap integrals for the nitrogen and oxygen molecules at their equilibrium internuclear distances, from Löwdin's fits for nitrogen and oxygen atoms, and compared them with the same integrals which were computed from the  $^1D$  carbon fit at a  $\rho$ -value corresponding to that of the exact calculations on the nitrogen or oxygen molecules. This  $\rho$ -value depends, of course, on the  $\zeta$ 's (orbital exponents)<sup>3</sup> assigned to the atoms. The exact carbon-carbon bond calculations are tabulated in Table I.

TABLE I.

OVERLAP INTEGRALS FOR THE CARBON-CARBON BOND

These overlap integrals were calculated by the author for the carbon-carbon bond using Löwdin's analytical fits, using three- to five-term linear combinations of Slater-type orbitals, for the 2s and 2p SCF orbitals as computed for the  $s^2p^2$ ,  $^1D$  state of carbon. The  $r$  values are the internuclear separations in atomic units at which the integrals were calculated, and  $\rho^{\text{Slater}} = 1.625r$  is the corresponding two-quantum  $\rho$ . The  $S$  are the overlap integrals, the subscripts referring to the orbitals 1s, 2s,  $\sigma(2p\sigma)$ , and  $\pi(2p\pi)$ . For brevity  $S_{\pi,\pi}$  is written  $S_{\pi}$ , etc. These values may be compared with the corresponding values in Table 6 of reference 8, which were calculated from the Rieke fit.

r au	2-quantum $\rho^{\text{Slater}}$	$S_{\pi}$	$S_{\sigma}$	$S_{2s}$	$S_{2s,\sigma}$	$S_{1s,\sigma}$	$S_{1s,2s}$
2.07	3.36	...	0.085	...	...	...	...
2.27	3.69	0.425	0.148	0.511	0.504	0.121	0.070
2.29	3.72	...	0.152	...	...	...	...
2.49	4.04	0.373	0.193	0.455	0.485	0.100	0.056
2.70	4.39	0.327	0.225	...	...	...	...
2.91	4.73	0.287	0.247	0.357	0.429	0.069	0.035
3.20	5.20	0.238	0.260	0.292	0.384	0.055	0.026
3.32	5.39 <sub>5</sub>	0.219	0.264	...	...	...	...

<sup>5</sup>P.-O. Löwdin, Phys. Rev. **90**, 120 (1953).

<sup>6</sup>C. W. Scherr, J. Chem. Phys. **21**, 1237 (1953), and THIS TECHNICAL REPORT, 1952-53, Part Two. A criterion error of 0.0050 is very close to the error of the SCF calculations

TABLE II. OVERLAP INTEGRAL CALCULATIONS FOR NITROGEN AND OXYGEN BONDS

The row marked "SCF" gives values of the two-center overlap integrals of nitrogen and oxygen molecules calculated from Löwdin's analytical fit for the SCF data of the atoms in the states indicated. The row marked "Slater" gives values of the integrals for the carbon-carbon bond at a  $\rho$ -value found from the Slater  $\zeta$ -values,  $\rho = \zeta R_e$ .  $R_e$  is the experimental equilibrium distance (2.075au for the nitrogen molecule and 2.29au for the oxygen molecule). The row marked " $\lambda$ " is similar to the "Slater" row except that the  $\zeta$ -values from the first paper of the present series are used. The row marked "Rieke" is a similar type estimation using Slater  $\zeta$ -values and carbon-carbon bond overlap integral values from the tables of Mulliken (reference 8).

Integral	$S_{\pi}$		$S_{\sigma}$		$S_{2s}$		$S_{2s,\sigma}$		$S_{1s,\sigma}$		$S_{1s,2s}$	
Molecule	N <sub>2</sub>	O <sub>2</sub>	N <sub>2</sub>	O <sub>2</sub>	N <sub>2</sub>	O <sub>2</sub>	N <sub>2</sub>	O <sub>2</sub>	N <sub>2</sub>	O <sub>2</sub>	N <sub>2</sub>	O <sub>2</sub>
State of the atoms	2p	1s	2p	1s	2p	1s	2p	1s	2p	1s	2p	1s
"SCF"	0.372	0.241	0.185	0.241	0.463	0.300	0.482	0.388	0.099	0.058	0.056	0.028
"Slater"	0.373	0.238	0.193	0.260	0.455	0.292	0.485	0.384	0.100	0.055	0.056	0.026
" $\lambda$ "	0.371	0.232	0.195	0.261	0.460	0.299	0.486	0.383	0.098	0.054	0.056	0.027
"Rieke"	0.375	0.242	0.185	0.252	0.449	0.282	0.493	0.390	...	...	...	...

## SINGLE SCALE FACTOR IN ATOMIC WAVEFUNCTIONS. II

Table II presents a comparison of the exact calculations on the nitrogen and oxygen molecules along with estimations of the same integrals (made from interpolations into Table I) based on  $\zeta$ -values (1) from the Slater recipe<sup>7</sup> and (2) from the formulas of the first paper of the present series. Both estimations are quite satisfactory, and there is little to choose between the two recipes for the  $\zeta$ 's on the basis of these calculations. However, the formulas of the first paper of the present series are more versatile in that they can be adapted without any additional trouble to valence states, or indeed any hypothetical states of the atoms; they also take into account the differences in  $\zeta$ -values of the 2s and 2p orbitals.

The row of Table II marked "Rieke" presents estimations derived from the tables of carbon-carbon bond SCF overlap integrals given by Mulliken<sup>8</sup> which are based on an analytical fit made by Mrs. Rieke<sup>9</sup> from the carbon SCF data. This fit gives a criterion error of 0.0189.<sup>6</sup> The  $\zeta$ -recipe used is that of Slater. The results so obtained show that, although the fit is not so accurate as Löwdin's, nevertheless good estimations of overlap integrals can be made from those tables, which are therefore very convenient to use for this purpose.

---

themselves. A criterion error of 0.0189 implies a reproduction of the SCF functions to about  $\pm 0.010$  units.

<sup>7</sup>J. C. Slater, Phys. Rev. **36**, 57 (1930); C. Zener, Phys. Rev. **36**, 51 (1930). The Slater  $\zeta$ -values are conveniently summarized in Table I of reference 9.

<sup>8</sup>R. S. Mulliken, J. Chem. Phys. **19**, 900 (1951), Tables 6 and 9.

<sup>9</sup>Mulliken, Reike, Orloff, and Orloff, J. Chem. Phys. **17**, 1248 (1949), Sec. Vb.

## HYPERCONJUGATION IN $C_6H_7^+$ AND OTHER HYDROCARBON IONS<sup>†‡</sup>

Norbert Muller\*  
Oxford University  
Oxford, England

Lucy W. Pickett\* and R. S. Mulliken<sup>o</sup>  
Laboratory of Molecular Structure and Spectra  
Department of Physics  
The University of Chicago  
Chicago 37, Illinois

IN CERTAIN REACTIONS of strong acids with aromatic hydrocarbons, conjugate acids of the latter can be formed.<sup>1</sup> Simplest is  $C_6H_7^+$ , which may be called benzenium ion. Using the LCAO MO method, we have calculated energy levels, charge distribution, bond orders, and resonance energy of this ion.

Benzenium ion may be considered the simplest prototype of the probable reaction intermediates in electrophilic substitution reactions of aromatic hydrocarbons. Previous calculations<sup>2</sup> on such intermediates neglected hyperconjugation.

We treat the ion as if it had six  $\pi$  electrons, in orbitals made by combining the six  $2p\pi_C$  AO's and a quasi- $\pi$  orbital ( $1s_H - 1s_H$ ) on the  $H_2$  pseudo-atom (see Figure 1).

The resulting secular determinant contains diagonal elements  $x_i = \alpha_i - E$ ,  $\alpha_i = \int \psi_i H \psi_i d\tau$ , and off-diagonal elements  $\beta_{ij} + \frac{1}{2}S_{ij}(x_i + x_j)$ , where  $\beta_{ij} = \int \psi_i H \psi_j d\tau - \frac{1}{2}S_{ij}(\alpha_i + \alpha_j)$ , and  $S_{ij}$  is the overlap integral  $\int \psi_i \psi_j d\tau$ .

We first set  $x_i = x_0$  for all carbon atoms, and  $x_H = x_0 + \delta\beta_0$ , with  $S_{CC} = 0.25$ ,

---

<sup>†</sup>This work was assisted in part by the Office of Naval Research under Task Order IX of Contract N6ori-20 with The University of Chicago.

<sup>\*</sup>The computations on  $C_6H_7^+$  were begun in this Laboratory in the summer of 1951 and continued at Mount Holyoke by L.W.P., and were extended by N.M. in 1953.

<sup>\*</sup>National Research Council Postdoctorate Fellow at Oxford University, 1952-1953.

<sup>\*</sup>Usual and present address: Department of Chemistry, Mount Holyoke College, South Hadley, Massachusetts.

<sup>o</sup>Fulbright Scholar at Oxford University, 1952-1953.

<sup>1</sup>M. Kilpatrick and F. E. Luborsky, *J. Am. Chem. Soc.* **75**, 577 (1953), and references to McCaulay and Lien, H. C. Brown, and others given there.

<sup>2</sup>G. W. Wheland, *J. Am. Chem. Soc.* **64**, 900 (1942), and others. See in particular V. Gold, *J. Chem. Soc.*, 2184 (1952).

HYPERCONJUGATION IN  $C_6H_7^+$  AND OTHER HYDROCARBON IONS

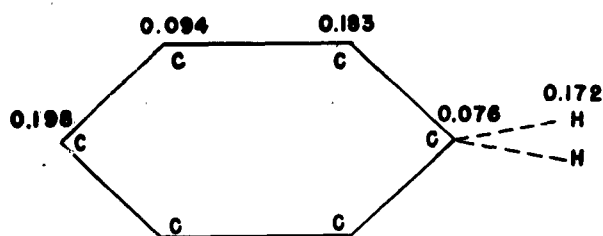


Fig. 1. Diagram of  $C_6H_7^+$  showing charge distribution of  $\delta = 0$ ,  $\omega = 2$ .

$S_{CH} = 0.512$ , and  $\beta_{CH} = 2\beta_{CC}$ .<sup>3</sup> We tried several  $\delta$  values from  $-0.5$  to  $+0.5$ .<sup>4</sup> In further calculations with  $\delta = 0$ , we made the  $\beta$ 's and the  $S$ 's self-consistent with the calculated bond orders and corresponding distances, assuming  $\beta$  proportional to  $S$ .<sup>3</sup> Finally, we allowed for the effect on the  $\alpha$ -values of the uneven computed

distribution of charge among the several atoms by replacing each  $\alpha_i$  by  $\alpha_i + \omega\beta_0q_i$  and repeating the computations until self-consistency was reached. Here  $q_i$  is the charge on the  $i$ th atom, calculated from the appropriately normalized coefficients of the occupied MO's. Trial values of 2 and 4 for  $\omega$  were used.

The hyperconjugation energy is the difference between the energy thus computed and that similarly computed for the conventional model,<sup>2</sup> consisting here of four  $\pi$  electrons on five carbon atoms, plus an "inert"  $CH_2$  group. For  $\delta = 0$ , the computed hyperconjugation energy varies from  $0.288\beta_0$ , or about 17kcal, if  $\omega = 0$ , to  $0.456\beta_0$ , or about 27kcal, if  $\omega = 4$ .<sup>5</sup> It is larger for  $\delta < 0$  and smaller for  $\delta > 0$ ; empirically, it is fairly sure that  $\delta < 0$ , perhaps about  $-0.5$ .<sup>4</sup>

Calculations now in progress indicate that  $\omega$  is about 1.5; they involve the application of procedures like that described above to the ethyl, isopropyl, and t-butyl and allyl free radicals and their positive ions, where the observed stabilization energies<sup>6</sup> become comprehensible if an  $\omega$  of this magnitude is introduced.

The computations predict two electronic transitions in or near the visible for  $C_6H_7^+$ , a moderately strong one at longer and a strong one at shorter wavelengths. Unpublished new experimental work by C. Reid at Chicago on the toluenium and xylenium ion

<sup>3</sup>a. Mulliken and Rieke, *J. Am. Chem. Soc.* **63**, 1770 (1941), and b. Mulliken and Roothaan, *Chem. Rev.* **41**, 219 (1947).

<sup>4</sup>In reference 3,  $\delta$  values between 0 and +1 were used; but on the basis of empirical evidence Coulson and Crawford (in press) assume  $\delta < 0$ , probably about  $-0.5$ .

<sup>5</sup>These values are reduced by about 7kcal by compressional energy corrections, but considerably raised by the use of  $\delta = -0.5$ . These points will be discussed in more detail in a paper in preparation.

<sup>6</sup>Franklin and Lumpkin, *J. Chem. Phys.* **20**, 745 (1952); J. Halpern, *J. Chem. Phys.* **20**, 744 (1952).

spectra shows a strong transition in the violet, with evidence of further absorption in the ultraviolet.

From the present calculations and from computations and observations on alkyl radicals and ions, it appears that in hyperconjugated systems containing an odd number of centers bearing  $\pi$  or quasi- $\pi$  electrons, the hyperconjugation energy is of a larger order of magnitude than in similar systems containing an even number of such centers.<sup>7</sup> It should be noted especially that these results are reproduced theoretically using the same parameters<sup>3,4</sup> in the two cases.

---

---

<sup>7</sup>Twisted ethylene (see reference 3b) containing two independent three- $\pi$ -center hyperconjugated systems, also has large hyperconjugation energy.

## n- $\pi$ EMISSION SPECTRA<sup>†</sup>

C. Reid<sup>‡</sup>  
Laboratory of Molecular Structure and Spectra  
Department of Physics  
The University of Chicago  
Chicago 37, Illinois

MOLECULES containing a heteroatom (O, N, S, etc.) with an "unshared pair" of electrons adjacent to a conjugated system usually show light absorption to longer wavelengths than do the corresponding conjugated molecules with no heteroatom.

This absorption has been attributed to "n- $\pi$ " transitions in which one of the unshared pair electrons is excited into the lowest unfilled level of the conjugated system.<sup>1,2,3</sup>

Most such molecules also show phosphorescence, of lifetime ranging from ca.  $10^{-3}$  seconds for aromatic ketones to several seconds for pyridine. Phosphorescences of this kind have been attributed variously as due to singlet n- $\pi$  transitions (formaldehyde<sup>4</sup>), triplet n- $\pi$  transitions (formaldehyde,<sup>5</sup> pyridine,<sup>2,3</sup> etc.), and triplet  $\pi$ - $\pi$  transitions (pyridine<sup>6</sup>). It is not always possible unambiguously to decide between these possibilities. The following argument clears up some of the difficulties.

Elementary MO considerations show that the singlet-triplet separation =  $2\int\psi_n H \psi_\pi d\tau$  where  $\psi_n$  and  $\psi_\pi$  are the one-electron n and  $\pi$  orbital wavefunctions respectively. We can expect this integral to be very small for two reasons. First, the amount of spatial overlap between these two orbitals is small, particularly if the conjugated system is an extended one. Second, symmetry considerations suggest that the integral should be zero, any positive part being balanced by an equal negative contribution.

<sup>†</sup>This work was assisted by the Office of Ordnance Research under Project TB2-0001(505) of Contract DA-11-022-ORD-1002 with The University of Chicago.

<sup>‡</sup>On leave of absence from The University of British Columbia, Vancouver, B. C., Canada.

<sup>1</sup>H. L. McMurray and R. S. Mulliken, Proc. Nat. Acad. Sci., Wash. **26**, 312 (1940).

<sup>2</sup>M. Kasha, Disc. Faraday Soc. No. 9, 14 (1950).

<sup>3</sup>C. Reid, J. Chem. Phys. **18**, 1673 (1950).

<sup>4</sup>P. J. Dyne, J. Chem. Phys. **20**, 811 (1952), and references contained therein.

<sup>5</sup>A. D. Walsh, J. Chem. Phys. **20**, 1502 (1952).

<sup>6</sup>J. H. Rush and H. Sponer, J. Chem. Phys. **20**, 1847 (1952).

Triplet transitions are often observed in emission only, the corresponding absorption being too weak to observe. This emission is thus well to the red of the longest wavelength (allowed) absorption. However the above argument suggests that in the case of  $n-\pi$  transitions,  $T \rightarrow S$  emission should be much closer to the corresponding singlet absorption. Using as a guide an average S-T separation for  $\pi-\pi$  transitions of  $6-7,000\text{cm}^{-1}$ , and assuming that the splitting will decrease in  $n-\pi$  transitions in about the same ratio that the intensities of these transitions bear to those of  $\pi-\pi$  transitions (about .02), we can expect that only a hundred  $\text{cm}^{-1}$  or so will separate singlet absorption and triplet emission.

This allows us to say at once that the observed long-lived phosphorescence of pyridine at  $27,000\text{cm}^{-1}$  (nearest appreciable absorption  $\approx 36,000\text{cm}^{-1}$ ) is not  $n-\pi$  as has been suggested,<sup>2,3</sup> but  $\pi-\pi$ .

The correctness of this argument has been confirmed in this Laboratory by a comparison of the emission spectrum of pyridine in a rigid glass (EPA) with that of pyridine in concentrated sulphuric acid. For an  $n-\pi$  transition the emission should be much weakened or absent, since the  $n$ -electrons are no longer excitable at such low energy. In fact, the emission is not only present but enhanced, by a factor of about 10 in intensity. Accordingly it is certainly  $\pi-\pi$ , as was suggested tentatively by Spomer and Rush.<sup>6</sup>

Using the above picture, it is also possible to explain why the lifetimes of the emitting states of aldehydes and ketones are about 100-1,000 times longer (ca.  $10^{-3}$  seconds) than is calculated from the extinction coefficient of what looks like the corresponding absorption band ( $\epsilon \approx 200$ ). It is also possible to explain the conflicting results of the detailed analysis of the long-wave absorption and emission of formaldehyde.<sup>4,5</sup> The explanation suggests that the emission is not homogeneous, but comes partly from the  $n-\pi$  singlet and partly from the triplet state. Experiments to confirm or disprove the correctness of this explanation are under way.

## THE AROMATIC CARBONIUM IONS<sup>†</sup>

C. Reid<sup>‡</sup>

Laboratory of Molecular Structure and Spectra  
Department of Physics  
The University of Chicago  
Chicago 37, Illinois

### ABSTRACT

The spectra of a number of aromatic hydrocarbons dissolved in liquid hydrogen fluoride containing boron trifluoride have been examined. Two kinds of absorption bands have been observed and are attributed (1) to the aromatic carbonium ions  $RH^+$  and (2) to the complexes  $R:BF_3$ . The carbonium ions are subdivided into two groups with spectra centered at about  $4,000\text{\AA}$  and  $4,800\text{\AA}$  respectively, and a tentative explanation for these is put forward.

Photochemical changes have also been observed on irradiation of some of the polycyclic carbonium ions and are discussed.

### INTRODUCTION

THE FACT that the more basic, polynuclear hydrocarbons dissolve in strong sulphuric acid, and that even the less basic ones, benzene, toluene, *etc.*, will dissolve in anhydrous hydrofluoric acid, in the presence of boron trifluoride, is well-known.<sup>1,2</sup> Differences in basicity have been used as a mode of separation of these hydrocarbons.<sup>2</sup>

Nevertheless, data on the "carbonium ions" which are formed, it is thought by the addition of a proton to the hydrocarbon--which thus acts as a base--are very scanty, although some spectra of sulphuric-acid solutions of the more basic hydrocarbons have been published.<sup>3</sup> The experimental work here described shows that in fact the phenomena occurring in  $HF-BF_3$  solutions are quite involved, addition compounds of  $BF_3$  and hydrocarbon sometimes forming as well as the carbonium ion, which may itself react to

---

<sup>†</sup>This work was assisted by the Office of Ordnance Research under Project TB2-0001 (505) of Contract DA-11-022-ORD-1002 with The University of Chicago.

<sup>‡</sup>On leave of absence from The University of British Columbia, Vancouver, B. C., Canada, which is presently the correct address.

<sup>1</sup>M. Kilpatrick and F. E. Luborsky, *J. Am. Chem. Soc.* **75**, 577 (1953), and references given there.

<sup>2</sup>D. A. McCaulay, B. H. Shoemaker, and A. P. Lien, *Ind. Eng. Chem.* **42**, 2103 (1950).

<sup>3</sup>V. Gold and F. L. Tye, *J. Chem. Soc.*, 2172 (1952), and references therein.

form further products.

## EXPERIMENTAL

### Absorption

Anhydrous HF (Mathieson C. P.) and dry boron trifluoride (from the same source) were distilled through teflon tubes into the absorption cell. For quantitative measurements a 1cm teflon cell with thin quartz windows was used in a specially constructed dewar vessel (Figure 1). At the temperatures used ( $-80^{\circ}$ ) in this phase of the work,

quartz is not attacked appreciably by the acid mixture, and windows may be used fifteen to twenty times before clouding becomes noticeable. Attempts to use thin teflon windows were not successful. With this arrangement, a Beckman model DU spectrophotometer was used.

For some phases of the investigation, the point-by-point spectrophotometer was unsuitable, and instead a Hilger E<sub>2</sub> spectrograph was used. The advantages were: (1) photographs could be taken only a few seconds after adding the hydrocarbon to the HF-BF<sub>3</sub> mixture; (2) in cases where higher temperatures were required (e.g., for benzene, which at  $-80^{\circ}$  crystallizes almost completely from the BF<sub>3</sub>-HF solution), the absorption cell could be kept several feet from the optical system to avoid attack by hydrogen fluoride vapor. Accurate absorption coefficients were not obtained by this method, however.

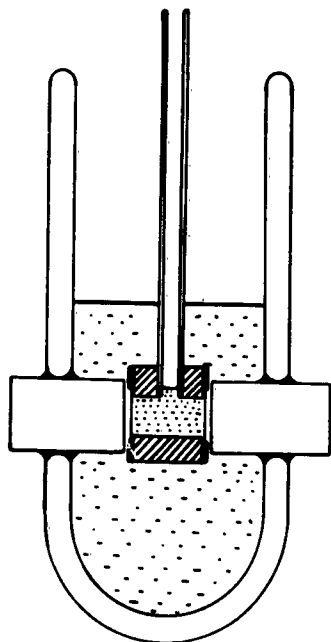


Fig. 1. Low-temperature absorption apparatus. The shaded body of the cell is made of teflon. The space between the double windows is evacuated.

### Emission

Low-temperature emission spectra were taken of frozen systems at  $-180^{\circ}$ . These systems were not the usual solid glasses used in emission work but crystalline masses of HF containing the carbonium ions as impurities. Since solid HF is a molecular rather than an ionic crystal, however, with absorption only at much higher energies than in the range studied, it is not surprising that the absorption spectra observed are in general obviously those of the same species which absorbs in the liquid systems. Most of the emission spectra were short-lived species. In a few cases a mechanical phosphoroscope was used to separate a short-lived from a long-lived component. Loss of light by scattering in the crystalline mass was considerable, but

## AROMATIC CARBONIUM IONS

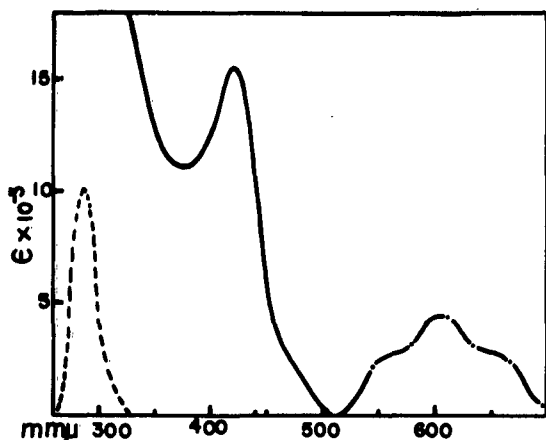


Fig. 2. Spectrum of the benzene - HF-BF<sub>3</sub> system.

- - - C<sub>6</sub>H<sub>6</sub>·BF<sub>3</sub> complex absorption
- C<sub>6</sub>H<sub>7</sub><sup>+</sup> absorption
- ..... C<sub>6</sub>H<sub>7</sub><sup>+</sup> fluorescence emission

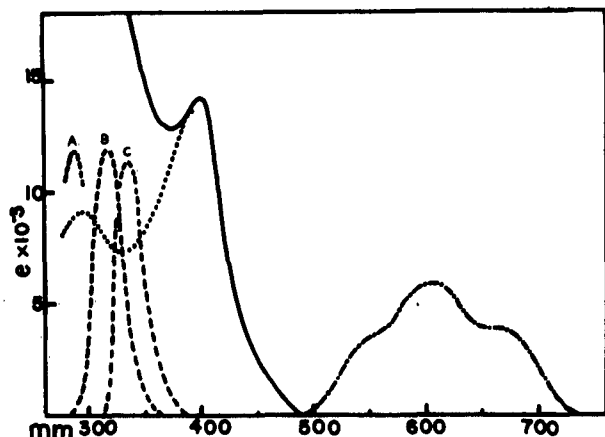


Fig. 3. Spectrum of the toluene - HF-BF<sub>3</sub> system.

- - - Curve B, C<sub>7</sub>H<sub>8</sub>·BF<sub>3</sub> complex absorption
- { Curve A, C<sub>6</sub>H<sub>6</sub>·BF<sub>3</sub> } for comparison
- { Curve C, o-xylene·BF<sub>3</sub> }
- Absorption curve after 5 minutes at -20°C showing the C<sub>7</sub>H<sub>9</sub><sup>+</sup> peak
- ..... Absorption curve after 30 minutes at -20°C
- ..... Fluorescence emission spectrum of final solution

emitted light intensities were still high enough for photographs to be taken in one to five minutes, using a 1,500-watt high-pressure mercury arc as illuminating source.

### RESULTS AND DISCUSSIONS

Curves showing some typical spectra are shown in Figures 2-9. The outstanding features are the following.

- (1) The ions examined divide themselves clearly into two groups: (a) those whose "long-wave" absorption is close to 4,000Å; this group includes all the monocyclic hydrocarbons, naphthalene, and anthracene; (b) those whose long-wave absorption is at considerably lower energies, usually in the neighborhood of 4,800-5,000Å, but not quite so sharply delineated as group (a); this group includes phenanthrene, naphthacene, pyrene, fluoranthene, etc.

It must be emphasized that the position of the "carbonium ion" band is not directly related to the position of the absorption spectrum of the parent hydrocarbon. Thus we find phenanthrene, itself absorbing at slightly shorter wavelengths than anthracene, with a carbonium-ion absorption at much longer wavelengths. Similarly, naphthacene, chrysene, and pyrene all have carbonium-ion absorption in approximately the same region, although, of the parent

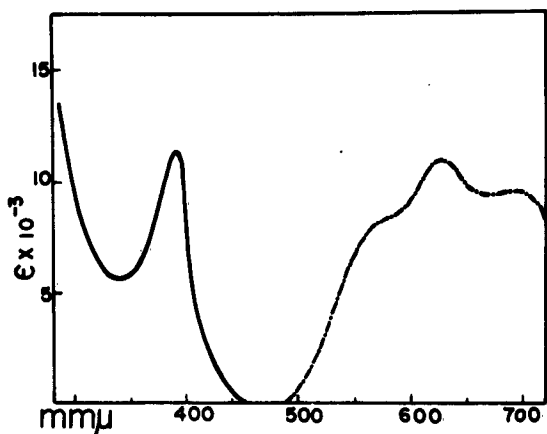


Fig. 4. Spectrum of the naphthalene - HF-BF<sub>3</sub> system.

— C<sub>10</sub>H<sub>9</sub><sup>+</sup> absorption  
 - - - C<sub>10</sub>H<sub>9</sub><sup>+</sup> fluorescence emission

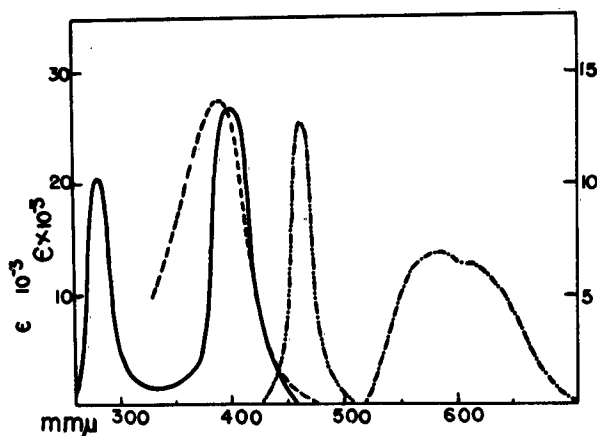


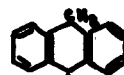
Fig. 5. Comparison of the mesitylene and hexaethyl benzene spectra in HF-BF<sub>3</sub>. The left-hand ordinate is for hexaethyl benzene, that on the right for mesitylene.

- - - mesitylene·H<sup>+</sup> absorption  
 - - - - mesitylene·H<sup>+</sup> fluorescence emission  
 — hexaethyl benzene·H<sup>+</sup> absorption  
 - - - - hexaethyl benzene·H<sup>+</sup> fluorescence emission

hydrocarbons, naphthalene absorbs at considerably longer wavelengths than do the other two.

There is no very obvious relationship between the structure of the parent molecule and the position of the absorption maximum of the carbonium ion. If we adopt the usually accepted geometrical structure for the carbonium ion, in which the proton forms a normal CH<sub>2</sub> group (which then "hyperconjugates" with the rest of the ring<sup>4</sup>), the most likely explanation seems to be that the "4,000Å" group of carbonium ions are those for which only one ring of the hydrocarbon is strongly involved, while in the 4,800-5,000Å group more than one ring is strongly involved.

This idea for instance explains very well why anthracene long-wavelength carbonium-ion absorption is almost identical with that of benzene. (Here also see Gold and Tye,<sup>3</sup> whose spectrum of the anthracene carbonium ion in strong sulphuric acid is similar to that obtained here in hydrofluoric acid.) The 9-10 positions of anthracene are so much more susceptible to attack by electropositive reagents that we may safely assume that the carbonium ion has the structure



(as also assumed by Gold and Tye).<sup>3</sup> This means that the anthracene

<sup>4</sup>L. W. Pickett, N. Müller, and R. S. Mulliken, *J. Chem. Phys.* **21**, 1400 (1953); *J. Am. Chem. Soc.* **76**, 000 (1954).

## AROMATIC CARBONIUM IONS

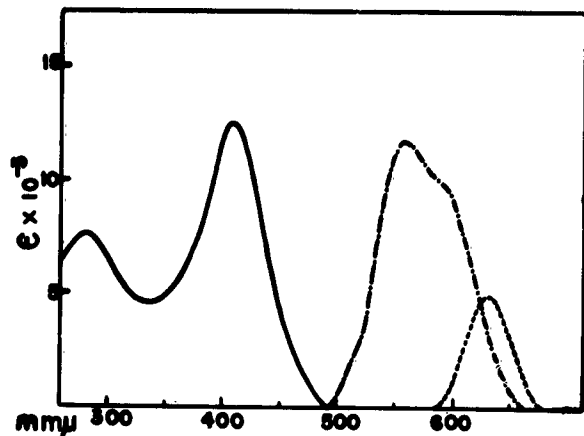


Fig. 6. Spectrum of the anthracene - HF-BF<sub>3</sub> system.  
 — C<sub>14</sub>H<sub>11</sub><sup>+</sup> ion absorption  
 - - - fluorescence emission (short-lived)  
 - . - phosphorescence emission (long-lived)

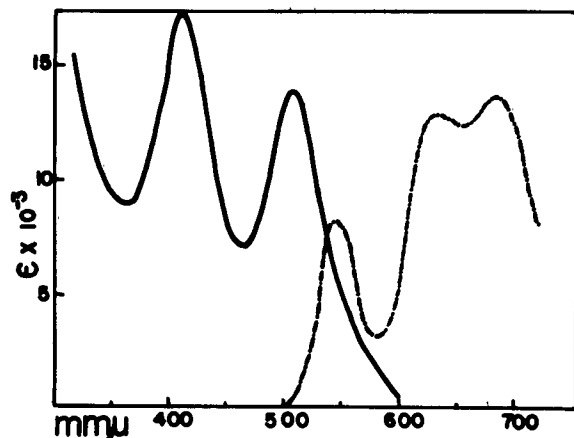


Fig. 7. Spectrum of the phenanthrene - HF-BF<sub>3</sub> system.  
 — C<sub>14</sub>H<sub>11</sub><sup>+</sup> ion absorption  
 - - - C<sub>14</sub>H<sub>11</sub><sup>+</sup> ion fluorescence emission

about 2.5 times as strong as the former.

To explain the long wavelength absorption of the phenanthrene carbonium ion, we must assume that in it--and in all the larger polycyclics--strong migration of positive charge into rings other than that attacked by the proton must occur.

<sup>5</sup>M. G. Evans, *Trans. Faraday Soc.* **42**, 101 (1946).

bonds are to some extent "frozen" into a particular structure much in the way that they were visualized as frozen in quinoid compounds by Evans,<sup>5</sup> and the probability of the positive charge migrating into the end rings is low, *i.e.*, the "carbonium-ion" structure is essentially confined to the middle ring. The fact that for naphthalene and anthracene the positive charge remains largely localized in the ring first attacked is substantiated by the substitution reactions of these molecules. Thus for monosubstituted naphthalenes, when the substituent is one attracting electrons, we find that a second (electrophilic) substituent goes into the second ring, and at a rate similar to that of monosubstitution in benzene. It follows that the deactivation is localized in the ring first attacked, and that the positive charge can therefore be considered as largely localized on this ring.

In the case of the benzene carbonium ion, the observed spectrum (Figure 2) is in fairly satisfactory agreement with the theoretical prediction<sup>4</sup> that this ion should show two strong peaks near 4,000Å and 3,200Å respectively, with the latter

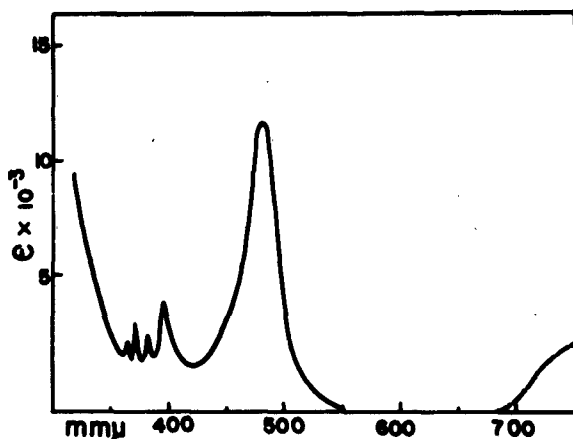


Fig. 8. Spectrum of the naphthacene - HF-BF<sub>3</sub> system.  
 — C<sub>16</sub>H<sub>13</sub><sup>+</sup> ion absorption  
 - - - Fluorescence emission of system

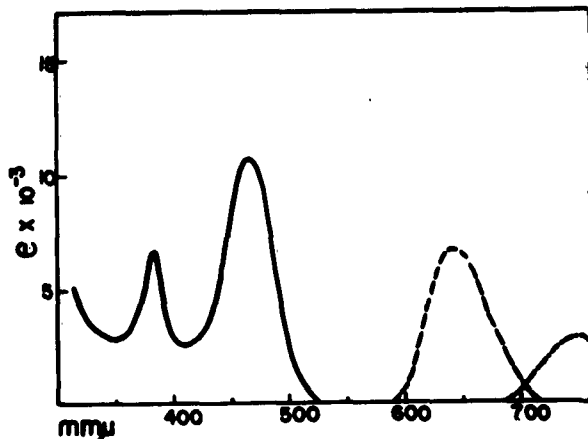


Fig. 9. Spectrum of the pyrene - HF-BF<sub>3</sub> system.  
 — C<sub>16</sub>H<sub>11</sub><sup>+</sup> ion initial absorption  
 - - - Fluorescence emission spectrum of system  
 - - - New absorption band appearing after irradiation

Neglecting hyperconjugation effects, this means that the conjugated system increases from 5 centers + 4 electrons to 9 centers + 8 electrons or 13 centers + 12 electrons, according to whether two or three rings are involved. A simple free-electron calculation suggests that the observed shifts fit the two-ring much better than the three-ring picture.

(2) In the case of the weakest bases (benzene, toluene, etc.), at the low temperatures used, the appearance of the characteristic carbonium ion peak at 4,000Å is not the first observation. Instead, the solution at first remains colorless, but examination of the absorption spectrum shows an intense peak in the ultraviolet at 3,180Å for toluene and at 2,840Å for benzene. These peaks are certainly not simply due to a solvent shift of the hydrocarbon bands, which themselves may be seen weakly at shorter wavelengths. It seems certain that these new bands are charge-transfer spectra<sup>6</sup> due to the presence of molecular complexes such as C<sub>6</sub>H<sub>6</sub>:BF<sub>3</sub> and C<sub>7</sub>H<sub>8</sub>:BF<sub>3</sub>. Highly allowed optical transitions lying in approximately the region where these bands were observed are then expected, to states approximately described as C<sub>6</sub>H<sub>6</sub><sup>+</sup>·B<sup>-</sup>F<sub>3</sub> and C<sub>7</sub>H<sub>8</sub><sup>+</sup>·B<sup>-</sup>F<sub>3</sub>. The differences in position of the benzene, toluene, and xylene bands (about 3,000cm<sup>-1</sup>) are in good agreement with what would be expected from their differences in ionization potential.<sup>7</sup>

<sup>6</sup>R. S. Mulliken, *J. Am. Chem. Soc.* **74**, 811 (1952).

<sup>7</sup>H. McConnell, J. S. Ham, and J. R. Platt, *J. Chem. Phys.* **21**, 66 (1953); S. M. Hastings,

## AROMATIC CARBONIUM IONS

Warming of the colorless solutions to above about  $-20^{\circ}\text{C}$  results in the rapid development of color due to the appearance of the characteristic carbonium-ion absorption at  $4,000\text{\AA}$ . Even at  $-70^{\circ}\text{C}$  in the case of xylene the appearance of color takes only a minute or two.

(3) Most of the systems investigated are not stable for an indefinite period even after the carbonium ion has formed. Quite early in the investigation it was found that absorption bands appeared erratically in the red and infrared and bore no consistent relationship to the main absorption around  $4,000\text{\AA}$ . Some insight into what such phenomena may involve is provided by the case of pyrene (Figure 9).

Solution of pyrene in  $\text{HF-BF}_3$  leads to the immediate production of a yellow-orange solution with a sharp absorption band just below  $5,000\text{\AA}$ . It is found, however, that the emission is far to the red of this, and further that irradiation leads to a change in color, the solution rapidly becoming a clear green and remaining thus when irradiation is discontinued. Reinvestigation of the absorption spectrum after irradiation shows a new absorption band with obvious mirror relationship to the emission.

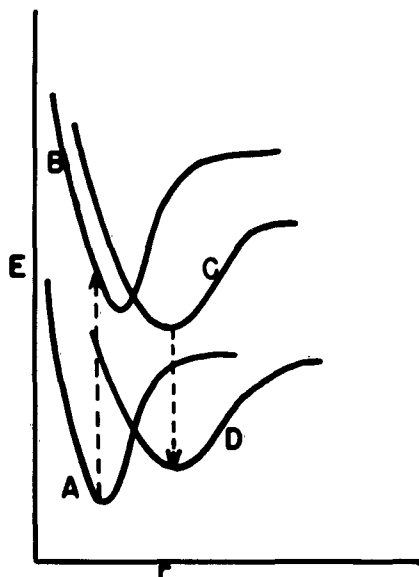


Fig. 10. Possible potential curves for pyrene carbonium-ion system.

- A. Initial carbonium ion
- B. Excited state of same
- C. Curve onto which system moves in upper-state tautomerism
- D. Ground state of photoproduct

It appears therefore that the first formed carbonium ion after excitation undergoes tautomerism or perhaps chemical reaction in the excited state, the new species then emitting and persisting in the ground state.

Schematically such a process can be visualized on the basis of the potential curves shown in Figure 10. Curves A and B then represent the ground- and excited-state potential curves of the originally formed carbonium ion, and C and D those of the new species, tautomerism being effected by a radiationless transition from curve B to curve C. Since the green end-product does not revert to the original carbonium ion again there must be a considerable barrier between states A and D. A similar wide separation between absorption and emission, and

J. L. Franklin, J. C. Schiller, and F. A. Matsen, *J. Am. Chem. Soc.* **75**, 2900 (1953).

ready photodecomposition is found for the naphthalene carbonium ion.

(4) Some ambiguity is present in the case of hexaethyl benzene. The  $\text{BF}_3$ -hydrocarbon complex and the carbonium ion may in this case be expected to absorb in approximately the same region of the spectrum. The observed absorption peak is very sharp, and so is the corresponding emission. The bands are certainly different in appearance from the usual "carbonium-ion" bands, and it is tentatively suggested that they are in fact charge-transfer bands. If this is so, the non-appearance of the "carbonium" band must be attributed to a greater stability of the charge-transfer complex, which perhaps is itself not a good enough donor to form a carbonium ion. This different behavior may be due to the steric effect of the bulky ethyl groups which probably result in some buckling of the aromatic ring.

(5) Finally it is noteworthy that of all the hydrocarbon carbonium ions examined, only that of anthracene showed a long-lived (presumably triplet) phosphorescence spectrum. Although perhaps coincidental, it is remarkable that anthracene is the one hydrocarbon which itself shows so little phosphorescence that the position of its lowest triplet level is in debate.<sup>8</sup>

If it is granted as reasonable that the triplet levels like the singlets will shift to the red in the carbonium ion, the position of the carbonium-ion triplet (5,800Å) is evidence in favor of the assignment of the anthracene triplet<sup>8</sup> at 5,200Å rather than at 6,900Å.

#### ACKNOWLEDGEMENTS

The author wishes to take this opportunity to thank Professor R. S. Mulliken for the invitation to Chicago which made this work possible and for many helpful discussions. Thanks are also due to The University of British Columbia for granting special leave of absence and to many members of the Chicago group for hospitality and stimulating conversations.

---

<sup>8</sup>C. Reid, J. Chem. Phys. **20**, 1214 (1952).

LOW-TEMPERATURE ABSORPTION SPECTRA OF SELECTED  
OLEFINS IN THE FARTHER ULTRAVIOLET REGION<sup>†‡</sup>

W. J. Potts, Jr.<sup>\*o</sup>  
Laboratory of Molecular Structure and Spectra  
Department of Physics  
The University of Chicago  
Chicago 37, Illinois

INTRODUCTION

THERE HAS LONG been a great interest in the far ultraviolet absorption spectra of ethylenes, for these molecules are the simplest of all  $\pi$ -electronic systems. The ultraviolet absorption work of E. Carr, L. Pickett, and co-workers<sup>1,2,3,4</sup> on several olefins in solution and vapor phases, and the work of Price and Tutte<sup>5</sup> in the vapor phase has given much information about the double bond. Platt, Klevens, and Price<sup>6</sup> give extinction coefficients in the farther ultraviolet region of a few olefins, from work in n-heptane solution. A rather complete bibliography of the literature on ethylenes is given by Platt and Klevens.<sup>7</sup>

The above authors (especially those in references 3 and 5) have shown that the magnitude of the red shift with increasing alkyl substitution of the N  $\rightarrow$  V transition

---

<sup>†</sup>This work was assisted in part by the Office of Ordnance Research under Project TB2-0001(505) of Contract DA-11-022-ORD-1002 with The University of Chicago.

<sup>‡</sup>This paper is essentially an extract version of Part II of a doctoral dissertation [Low-Temperature Spectroscopy in the Farther Ultraviolet Region, Chicago: March, 1953] submitted to the Faculty of the Division of the Physical Sciences, The University of Chicago.

<sup>\*</sup>AEC Predoctoral Fellow, 1950-52.

<sup>o</sup>Present address: Spectroscopy Department, The Dow Chemical Company, Midland, Michigan.

<sup>1</sup>E. Carr and M. Walker, J. Chem. Phys. **4**, 751 (1936).

<sup>2</sup>E. Carr and G. Walter, J. Chem. Phys. **4**, 756 (1936).

<sup>3</sup>E. Carr and H. Stücklen, J. Chem. Phys. **4**, 760 (1936).

<sup>4</sup>Pickett, Muntz, and McPherson, J. Am. Chem. Soc. **73**, 4862 (1951).

<sup>5</sup>W. C. Price and W. T. Tutte, Proc. Roy. Soc. (London) **A174**, 207 (1940).

<sup>6</sup>Platt, Klevens, and Price, J. Chem. Phys. **17**, 466 (1949).

<sup>7</sup>J. R. Platt and H. B. Klevens, Rev. Mod. Phys. **16**, 182 (1944).

## POTTS

(the strong, allowed transition near  $1,800\text{\AA}$ ) depends primarily on the number of alkyl substituents, and only to a lesser extent upon the size and position of substituents.

Extensive theoretical investigations by R. S. Mulliken<sup>8,9,10</sup> have to a great measure correlated and explained the existing data. Mulliken and Roothaan<sup>10</sup> have made MO calculations which predict semi-quantitatively the potential energy (vs. twist about the double bond) curves of ethylene in its ground and excited electronic states.

The present research was undertaken to compare the ultraviolet absorption spectra of four alkyl-substituted ethylenes--tetramethylethylene, trimethylethylene, cyclohexene, and hexene-1--in solution at room temperature ( $298^{\circ}\text{K}$ ) and in a rigid hydrocarbon glass at liquid-nitrogen temperature ( $77^{\circ}\text{K}$ ), and to see what effect, if any, low temperature might have on the spectra, which are presumably sensitive to twist about the double bond. It was also hoped that the well-known effect of producing sharper spectra at low temperature would be achieved, and thereby locate the  $\text{N} \rightarrow \text{T}$  (absorption to the triplet state) transition.

## EXPERIMENTAL

### Materials

The four olefins measured were National Bureau of Standards samples, with the following maximum impurities: tetramethylethylene (540-5S),  $0.10 \pm 0.05$  mole %; trimethylethylene (286-5S),  $0.06 \pm 0.04$  mole %; cyclohexene (522-5S),  $0.023 \pm 0.02$  mole %; and hexene-1 (519-5S),  $0.14 \pm 0.08$  mole %. These compounds were used without further purification. All measurements on any compound were run the same day the sealed tube was opened, the solutions being made up and measurements taken as rapidly as physically possible. This was done because the rate at which the solutions of these compounds became impure when exposed to the air (presumably due to peroxide formation) is excessive, particularly in the case of hexene-1.

### Methods

The room-temperature data above  $2,200\text{\AA}$  were obtained in 3-methylpentane solution with a Beckman model DU quartz spectrophotometer, using 1cm quartz cells. The data below  $2,200\text{\AA}$  were obtained with a Cario-Schmitt-Ott vacuum fluorite spectrograph, using

---

<sup>8</sup>R. S. Mulliken, Phys. Rev. **41**, 751 (1932).

<sup>9</sup>R. S. Mulliken, Rev. Mod. Phys. **14**, 265 (1942).

<sup>10</sup>R. S. Mulliken and C. C. J. Roothaan, Chem. Rev. **41**, 219 (1947).

## LOW-TEMPERATURE FAR UV SPECTRA OF OLEFINS

techniques similar to those of Jacobs and Platt.<sup>11</sup> A 1cm cell was used, except in the farthest ultraviolet region (below 1,850Å), where a .13mm cell was employed. The solvent was a mixture of 3-methylpentane and isopentane.

All the low-temperature data were obtained in a rigid hydrocarbon glass: the mixture of six parts isopentane and one part 3-methylpentane as discussed by Potts.<sup>12</sup> The apparatus and techniques used are those described elsewhere by Potts.<sup>12</sup>

### Errors

As has been discussed by Potts,<sup>12</sup> errors of reciprocity failure of emulsions, spectrophotometer errors, inaccuracies of sample preparation, etc., are small compared to the error of variance of the optical density of the solvents and glasses in this farther ultraviolet region. An index of error is provided by the closeness of agreement with Beer's law as solutions of different concentration were used. (All solutions were in steps of factors of five in concentration.) The maximum error of extinction coefficient is somewhat more than 15% at the far ultraviolet end, becoming progressively better toward the nearer ultraviolet, being about 10% at 2,000Å, 5% at 2,500Å. In the regions of the spectra where data from the Beckman spectrophotometer overlap with data from the vacuum fluorite spectrograph, the agreement is generally quite good.

### Agreement of Room-temperature Data with Previous Work

For solution data above 2,200Å the agreement is generally good. Tetramethylethylene and trimethylethylene data are in essential agreement with those of Carr.<sup>1,2</sup> Disagreement of their data on hexene-1 with the present data is perhaps because the very pure NBS standard samples were not available at the time of their work. The solution data on tetramethylethylene and hexene-1 obtained by Stevenson,<sup>13</sup> using NBS standard samples, agree very closely with the present work.

The data below 2,200Å of vapor-phase investigations of Carr and Stücklen<sup>3</sup> and of Price and Tutte<sup>5</sup> are qualitative. The sharper bands superimposed upon the N → V transition observed by these authors are not found in the present (solution) work, which is explained below. Otherwise, the data seem in approximate agreement.

The data of Pickett et al.<sup>4</sup> on cyclohexene in the vapor phase, using an NBS sample, shows general agreement with the present solution data, although a shoulder on the red

<sup>11</sup>L. E. Jacobs and J. R. Platt, J. Chem. Phys. **16**, 1137 (1948).

<sup>12</sup>W. J. Potts, Jr., J. Chem. Phys. **20**, 809 (1952); **21**, 191 (1953).

<sup>13</sup>D. P. Stevenson, Shell Development Company, private communication.

side of the  $N \rightarrow V$  transition seems better resolved in their work. This is perhaps due to the expected difference in resolution between vapor and solution spectra. The cyclohexene solution data of Platt *et al.*<sup>6</sup> are in general agreement with the present work, but show a much higher absorption on the "tail" of the  $N \rightarrow V$  absorption than the present work. This again may be due to the fact the NBS standard samples were not used in their work, for the present author has noted a rather extreme difficulty in keeping this compound "spectroscopically" pure.

Far ultraviolet solution data of Platt *et al.*<sup>6</sup> on octene-1 agrees rather poorly with the present work on hexene-1, whose spectra presumably should be quite similar. Their extinction coefficient of the  $N \rightarrow V$  transition is considerably higher (50% or so) than the present work, and they indicate a much sharper peak to the band than the present work. This disagreement is difficult to explain, as the techniques used in obtaining these data were identical. Critical examination of both sets of data seems to indicate that the present  $\epsilon_{\max}$  is probably too low, while that of Platt *et al.* is perhaps somewhat high.

## RESULTS

### Absorption Data

Figures 1-4 give the room-temperature (dashed curve) and low-temperature (solid curve) absorption spectra from  $2,500\text{\AA}$  to  $1,700\text{\AA}$  of tetramethylethylene, trimethylethylene, cyclohexene, and hexene-1, respectively.  $\log_{10}\epsilon_m$  (molar extinction coefficient) obtained from measured optical density, cell length, and known concentration by the usual relation  $\epsilon l c = -\log_{10}(I/I_0) = \text{O.D.}$  ( $l$  in cm,  $c$  in moles/liter), is plotted

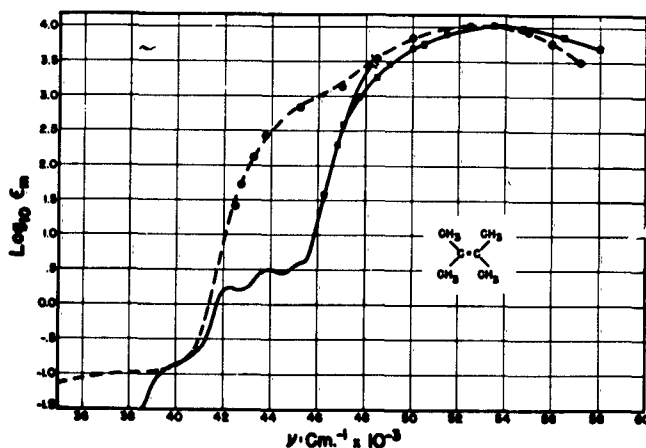


Fig. 1. Absorption spectrum of tetramethylethylene.

against the frequency in wave numbers.

When the rigid glass is employed, it is necessary to correct the concentration values for the 22% contraction of the glass in cooling.

Table I gives the frequency of the absorption maximum, corresponding peak molar extinction coefficient, and estimated oscillator strength (room temperature only) of the rather broad, allowed  $N \rightarrow V$  transition for the various olefins

LOW-TEMPERATURE FAR UV SPECTRA OF OLEFINS

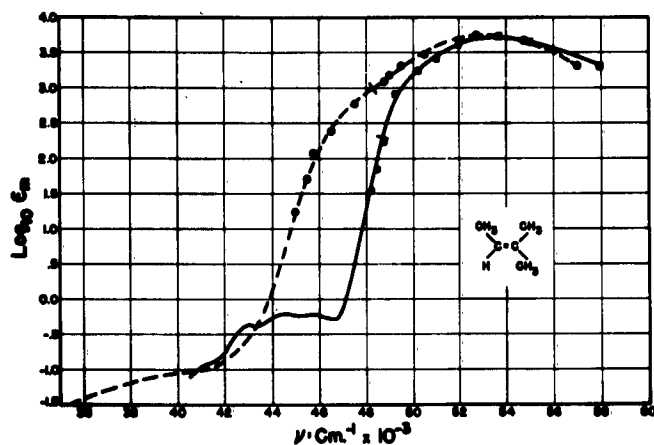


Fig. 2. Absorption spectrum of trimethylethylene.

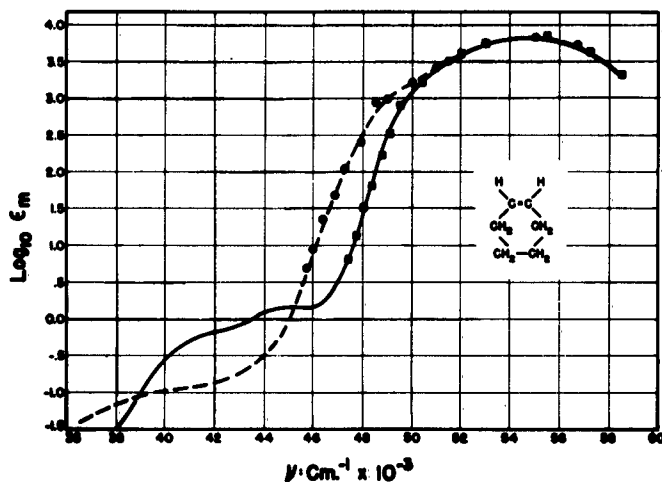


Fig. 3. Absorption spectrum of cyclohexene.

studied here. There is an uncertainty of about  $500\text{cm}^{-1}$  in the position of the absorption peaks because of the broadness of these peaks. The shift toward the red is seen to depend primarily on the number of alkyl substitutes at both temperatures.

Normally, in going from solution to a rigid glass medium a red shift of the absorption peak is observed, because of the greatly increased refractive index of the medium. That a blue shift of the absorption peak is observed in olefins is accounted for below.

It was thought inadvisable to calculate the oscillator strengths<sup>14</sup> of the  $N \rightarrow V$  transitions at low temperature, because the limit of the experimental technique was  $1,700\text{\AA}$ , and it seems probable that the broad  $N \rightarrow V$  transition extends to yet shorter wavelengths.<sup>3,5</sup>

There are not sufficient data in the present work to calculate accurately the oscillator strengths at room temperature, but these values were estimated by extra-

polating the present data to higher frequencies, using the qualitative results of Price and Tutte<sup>5</sup> as a guide. Their data on propene-1 are used to extrapolate hexene-1, for presumably these compounds should have very similar absorption spectra.<sup>3,9</sup>

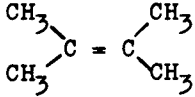
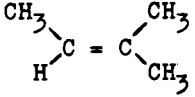
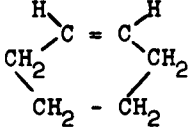
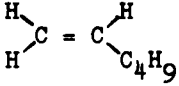
There are some weak bands appearing in the region  $40,000\text{--}48,000\text{cm}^{-1}$ <sup>15</sup> which are masked at room temperature by the strong shoulder on the red side of the  $N \rightarrow V$  absorption, but which are seen at low temperatures. A possible explanation--that their

<sup>14</sup>f-number, or oscillator strength, is defined as:  $f = 10^3(\log_{10}e)\frac{mc^2}{\pi e^2 N} \int \epsilon_\nu d\nu = 4.32 \times 10^{-9} \int \epsilon_\nu d\nu$ , where  $\nu$  is in  $\text{cm}^{-1}$ ,  $\epsilon_\nu$  is molar extinction coefficient.

<sup>15</sup>P. G. Wilkinson and H. L. Johnson, *J. Chem. Phys.* **18**, 190 (1950).

TABLE I.

## POSITIONS OF THE N → V TRANSITIONS IN OLEFINS

Structural Formula	Tetramethyl-ethylene		Trimethyl-ethylene		Cyclohexene		Hexene-1	
								
Temperature	298°K	77°K	298°K	77°K	298°K	77°K	298°K	77°K
$\nu_{\max}$ of N → V transition $\pm 500\text{cm}^{-1}$	52,250	53,750	53,000	54,000	54,750	55,500	56,000	56,500
$\epsilon_{\max}$	10,000 $\pm 700$	10,500 $\pm 900$	5,800 $\pm 700$	5,600 $\pm 900$	6,800 $\pm 700$	6,800 $\pm 900$	6,300 $\pm 700$	5,400 $\pm 900$
Red shift from $\nu_{\max}$ of ethylene (61,400 $\text{cm}^{-1}$ ) (See refs. 5 and 15)	9,150		8,400		6,700		5,400	
Low-temperature blue shift, $\text{cm}^{-1}$		1,500		1,000		750		500
f-number	.45 $\pm$ .10		.34 $\pm$ .09		.38 $\pm$ .09		.29 $\pm$ .08	

existence is due to a ground-state-to-triplet (N → T) transition (and not to trace impurities!)--is discussed below. The "centers" of the transitions, average molar extinction coefficient, and oscillator strengths of these transitions are given in Table II. The vibrational separation (?) is tabulated where it is sufficiently

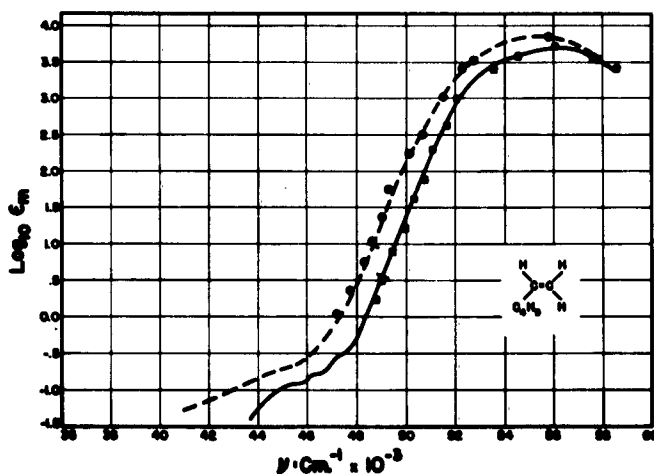


Fig. 4. Absorption spectrum of hexene-1.

resolved.

Most curious is the low-temperature spectrum of cyclohexene in the region 40,000-45,000 $\text{cm}^{-1}$ . The low-temperature absorption is pronouncedly greater than the absorption at room temperature. That this surprising effect is probably real was indicated by showing that the room-temperature absorption is reproduced within experimental error upon warming up the identical solutions used

LOW-TEMPERATURE FAR UV SPECTRA OF OLEFINS

TABLE II.  
POSITIONS OF THE N → T (?) TRANSITIONS IN OLEFINS

	Tetramethyl-ethylene	Trimethyl-ethylene	Cyclohexene	Hexene-1
"Center" of of N → T transition	43,800cm <sup>-1</sup>	44,200cm <sup>-1</sup>	44,000cm <sup>-1</sup>	46,400cm <sup>-1</sup>
Average ε	2.5±.5	.6±.1	1.0±.2	.2±.1
f-number	4.2±1.0 x 10 <sup>-5</sup>	1.0±.5 x 10 <sup>-5</sup>	2.7±.8 x 10 <sup>-5</sup>	.26±.1 x 10 <sup>-5</sup>
Vibrational separation	1,400±100cm <sup>-1</sup>	1,400±100cm <sup>-1</sup>		

for the low-temperature determinations.

Three molecules are obvious by their omission from this study, namely, the three dimethylethylenes: cis- and trans- butene-2, and 2-methylpropene. Their absorption-spectra curves would be expected to be about midway between trimethylethylene and hexene-1.<sup>2,3</sup> (Hexene-1 should have essentially the same ultraviolet spectrum as propene;<sup>3</sup> it was chosen only for convenience of physical properties.)

Ethylene, of course, should also be included in this study. However, new experimental techniques are necessary before a gas can be studied by the low-temperature methods used in this work.

In Figure 5 the low-temperature absorption curves of all four compounds are plotted together for comparison.

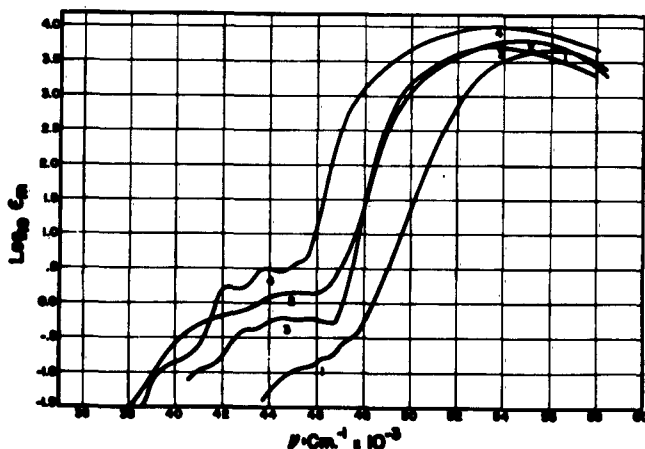


Fig. 5. Low-temperature spectra compared. Schmitt-Ott fluorite spectrograph was made

Search for Phosphorescence

Observation of olefin phosphorescence (T → N long-lived emission) would lend strong support to the singlet-triplet<sup>16</sup> (N → T) assignment given the weaker bands in the 40-48,000cm region. Hence a search for phosphorescence was made, using the methods described elsewhere by Potts.<sup>12</sup> In this setup, the slit of the Cario-

<sup>16</sup>It has been quite firmly established that phosphorescence in electronic systems is due to the lowest-triplet-to-ground-singlet emission. (See reference 17.)

## POTTS

very wide (lmm), and the very fast Eastman SWR plates were used, so that the weakest radiations could be detected. With this arrangement it was possible to record the notably weak phosphorescence of benzene<sup>17</sup> with only 15 minutes' exposure time.

Tetramethylethylene was chosen for this study because of its higher absorption less farther in the ultraviolet. No phosphorescence was observed. An explanation for its non-appearance is given below.

The phosphorescences of chloro-ethylenes reported by Kasha<sup>17,18</sup> must be regarded as erroneous because their reported lifetimes are much too long. Phosphorescence of these compounds (if it exists at all!--see discussion below) would be very short-lived, for the only selection rule forbidding the transition in chloro-ethylenes is the singlet-triplet intercombination rule, and chloro-substitution tends to break down this very rule.<sup>19</sup>

## DISCUSSION

As noted above, the larger the number of alkyl substituents about the double bond, the lower is the energy (longer the wavelength) of the N → V transition peak. This effect, due to increasing hyperconjugation<sup>9,20</sup> and/or increased inductive transfer of charge towards the double bond from the more electro-positive alkyl groups with increasing alkyl substitution,<sup>5</sup> has been dealt with at length by other authors<sup>3,5,9</sup> and hence will not be discussed further here.

In the vapor absorption spectra of Carr and Stücklen<sup>3</sup> and of Price and Tutte<sup>5</sup> several sharp bands appear superimposed on the broad N → V absorption. These bands have been interpreted as belonging to a Rydberg-type transition<sup>5,9,21</sup> called N → R in the notation of Mulliken.<sup>9</sup> No such bands were observed in the present work.

The explanation of their non-appearance (if they are truly Rydberg-type transitions) lies in the fact that one would not expect such spectral states to be observed in a condensed medium (solution or low-temperature glass) because the large-sized Rydberg orbitals would probably be strongly perturbed by closely neighboring solvent molecules. When these bands have been observed by other authors it has always been in

<sup>17</sup>G. N. Lewis and M. Kasha, J. Am. Chem. Soc. **66**, 2100 (1944).

<sup>18</sup>M. Kasha, Chem. Rev. **41**, 401 (1947).

<sup>19</sup>D. S. McClure, J. Chem. Phys. **17**, 905 (1949).

<sup>20</sup>Mulliken, Rieke, and Brown, J. Am. Chem. Soc. **63**, 41 (1941).

<sup>21</sup>E. Carr and H. Stücklen, J. Chem. Phys. **7**, 631 (1939).

## LOW-TEMPERATURE FAR UV SPECTRA OF OLEFINS

the vapor phase at low pressures.

### Shape of the $N \rightarrow V$ Absorption Curve at Low Temperature

It is noticed that in each compound there is a shoulder in the absorption curve of greater or smaller size on the red side of the  $N \rightarrow V$  transition. The width of this shoulder decreases as one goes from tetramethylethylene, the most substituted ethylene, to hexene-1, the least substituted. For an explanation of these phenomena, we refer to Mulliken and Roothaan's picture<sup>10</sup> of the potential energy of the various electronic states of ethylene as a function of twist about the double bond. An adaptation of their figure is shown in Figure 6.

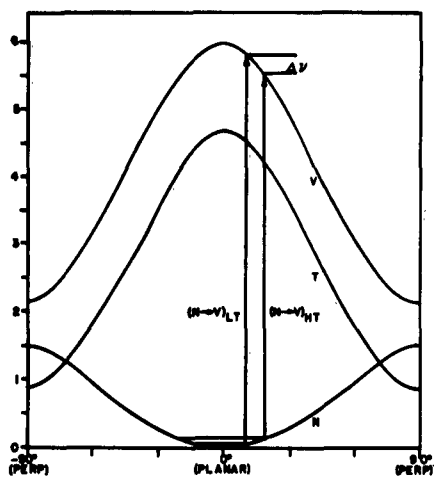


Fig. 6. The potential energy of the electronic states of ethylene as a function of twist about the double bond. Energy is in wave numbers. The vertical arrows represent the  $N \rightarrow V$  transitions.

The curves represent the potential energy as a function of angle of twist,  $\theta$ , about the double bond of ethylene for the normal (ground singlet) state,  $N$ , the first excited singlet  $\pi$ -electronic state,  $V$ , and its corresponding triplet state,  $T$ . They are drawn to the qualitative scale indicated by the LCAO MO calculations of Mulliken and Roothaan,<sup>10</sup> as corrected by the author to correspond with the corrected assignment of the twisting frequency of Arnett and Crawford.<sup>22</sup>

From Figure 6, it is seen that the ground state has its minimum energy in the planar form, while the planar form gives maximum energy for the excited states. That is, the slopes of the ground- and excited-state curves are of opposite sign.

Thus, in an  $N \rightarrow V$  spectral transition, the more the molecule is twisted, the less the energy required for the transition, and hence the longer the wavelength of the absorption. The fact that absorption sets in at longer wavelength at room temperature than at low temperature [ $(N \rightarrow V)_{HT}$  and  $(N \rightarrow V)_{LT}$  in Figure 6] must indicate that the low-temperature conditions restrict the amount of twist either in the upper ( $V$ ) state or in the ground ( $N$ ) state, or both.

From the corrected assignment of the twisting frequency in the ground ( $N$ )

<sup>22</sup>R. L. Arnett and B. L. Crawford, *J. Chem. Phys.* **18**, 118 (1950). These authors give  $\nu_4 = 1027\text{cm}^{-1}$ , where the older value was  $825\text{cm}^{-1}$ .

POTTS

electronic state of ethylene<sup>22</sup> one calculates  $k_\gamma = 2.71 \times 10^4$  wave numbers/radian for the force constant, which allows  $11.1^\circ$  twist in the ground level and  $19.3^\circ$  twist in the first vibrational level ( $1,027\text{cm}^{-1}$ ), using  $V = \frac{1}{2}k_\gamma\theta^2$ , where  $V$  is potential energy in  $\text{cm}^{-1}$ . From Figure 6 it is seen that a vertical (Franck-Condon allowed) transition from the most twisted configuration of the first excited vibrational level in the ground electronic state [labelled  $(N \rightarrow V)_{\text{HT}}$  in the figure] is of lower energy by some 3-4,000  $\text{cm}^{-1}$  than a corresponding transition from the lowest vibrational level [ $(N \rightarrow V)_{\text{LT}}$ ], most of this energy being due to the steepness of the upper (V) state potential curve. However, statistics allow only 0.7% of the molecules in the first vibrational level at room temperature, and hence a low-temperature medium would not be expected to have much effect upon the absorption-spectra curve of ethylene compared to the spectra at room temperature.

The values of the twisting frequencies of alkyl-substituted ethylenes are still in doubt,<sup>23</sup> and only estimates of their values may be made. In the case of tetramethylethylene, which has the same symmetry properties as ethylene, if the force constant of twist ( $k_\gamma$ ) is the same as in ethylene, the energy of the first vibrational level of twist is calculated to be  $264\text{cm}^{-1}$ . The corresponding maximum twist angles are  $9.8^\circ$  for the first excited level of twist,  $5.7^\circ$  for the ground level. Application of statistics shows that 28% of the molecules will be in the first excited vibrational level of twist at room temperature.

The assumption that the force constant of tetramethylethylene will be the same as ethylene is, of course, a poor one. Examination of a Fischer-Hirschfelder atom model of tetramethylethylene indicates that the van der Waals radii of the H atoms on the methyl groups would actually overlap considerably in the planar configuration if free rotation of methyl groups could take place. This must be regarded as a rather strong repulsion by the methyl groups, which would tend to force the molecule into a more twisted configuration. This in turn would tend to decrease the force constant of twist about the double bond, and thus make the ground-state potential curve (N) somewhat flatter than pictured in Figure 6. On the other hand, the repulsion of methyl groups in tetramethylethylene will tend to steepen the potential curve for the upper (V) electronic state, particularly in the region of planarity.

An additional effect of the low-temperature rigid glass may result from the increased viscosity of the surroundings at low temperature. This increased viscosity

<sup>23</sup>N. Sheppard and G. B. B. M. Sutherland, Proc. Roy. Soc. (London) A196, 195 (1949).

## LOW-TEMPERATURE FAR UV SPECTRA OF OLEFINS

would make the energy of rotation about the double bond somewhat greater, which would slightly steepen the ground-state (N) potential curve, slightly flatten the excited-state (V) curve at low temperature (compared to the curves of the same molecule at room temperature). This effect should be small, however, in view of the high value of the twisting force constant for the ground state and the yet higher force constant for the excited state (at least a factor of 3 greater, probably more in the more highly substituted ethylenes).

Less highly substituted ethylenes (mono-, di-, tri-) should have values somewhere between ethylene and tetramethylethylene for the above effects, i.e., force constant of twist, twist vibrational energy separation, % population of the first vibrational level, viscosity-dependent resistance to twist. These effects all operate in the same direction: the more alkyl substituents, the greater the "twisted population" at room temperature compared to low temperature.

Thus, from these considerations it seems reasonable to suppose that the larger the number of alkyl substituents, the more likely will be the N → V transition between the twisted states of the substituted ethylene at room temperature, as compared to low temperature. That is, with increased alkyl substitution, one observes a lower frequency (energy) for the onset of absorption at room temperature compared to the onset of absorption at low temperature. This accounts in a satisfactory manner for the increasing width of the "red shoulder" on the N → V absorption curve with increasing alkyl substitution, which disappears at low temperature. (This "red shoulder" effect is, of course, a separate effect from the red shift of the absorption peak with increased alkyl substitution.)

In Figure 7 are plotted together for purposes of comparison potential curves for the ground (N) and excited singlet (V) states of ethylene (solid), and the probable curves for tetramethylethylene (dashed). Also shown are the N → V transitions from the zeroth and first levels of twist vibration. In comparing them, one must bear in mind that at room temperature the first vibrational level of ethylene will be very sparingly (.7%) populated, while in tetramethylethylene the first vibrational level will be strongly (at least 28%) populated. [The absolute heights of the upper (V) state curves are drawn as if the peaks of the N → V transitions of these molecules coincided, but of course they do not; however this is immaterial to the present discussion.]

Cyclohexene is a somewhat different case from the other olefins considered here in that it is a ring structure. Comparison of the N → V absorption curves at room and

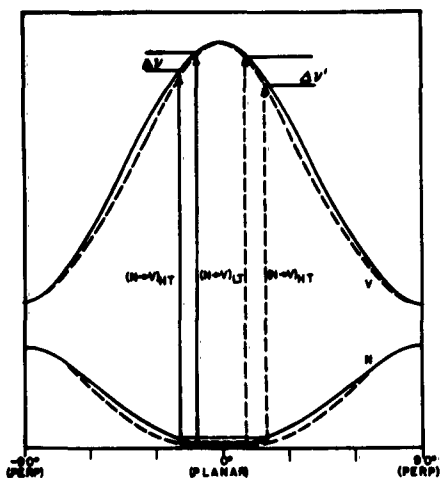


Fig. 7. Potential curves of ethylene (solid) and probable curves of tetramethylethylene (dashed) compared.

low temperatures indicate that, insofar as the "red shoulder" on the  $N \rightarrow V$  transition is concerned, it behaves essentially like a dialkyl ethylene. Apparently the shape of the complete  $N \rightarrow V$  absorption curve (including data below  $1,700\text{\AA}$ ) is quite different from that of a cis-olefin,<sup>3,4</sup> which Platt *et al.*<sup>6</sup> consider to be due to a permanent twist of the double bond. But references cited by them and the more recent work of Beckett, Freeman, and Pitzer<sup>24</sup> indicate that there is no such permanent twist of the double bond in cyclohexene. The effect of the structure of cyclohexene on its ultraviolet absorption spectra will be considered below in more detail in the discussion of the triplet state.

#### The Triplet State of Olefins

When the red shoulder of the  $N \rightarrow V$  transition is "removed" at low temperature, a weaker band is revealed in the region  $40\text{--}48,000\text{cm}^{-1}$ . These bands presumably are the ground-to-triplet ( $N \rightarrow T$ ) transitions, and are so assigned for the following reasons.

Reference to Figure 5 shows a certain regularity to these transitions, if we neglect cyclohexene for the moment. This regular trend closely parallels that of the position of the singlet ( $N \rightarrow V$ ) peaks, suggesting that the two transitions may be related. The singlet-triplet separation of the excited states is approximately constant throughout the compounds, and is about the amount predicted by Mulliken.<sup>9,10</sup> Reference to Tables I and II shows that the trend of both  $\epsilon$  and oscillator strength is qualitatively the same for both the  $N \rightarrow V$  and  $N \rightarrow T$  transitions. The values and oscillator strengths of the  $N \rightarrow T$  transitions are within the range of what could be expected for a singlet-triplet transition between  $\pi$ -electronic states corresponding to an allowed singlet-singlet transition in olefins.<sup>19</sup>

There is the possibility that the bands observed in the  $40\text{--}48,000\text{cm}^{-1}$  region are due to impurities. Olefins are difficult to keep "spectroscopically" pure; however, it is felt that the source of materials and experimental precautions used in obtaining these data were sufficiently good to render impurities unlikely.

<sup>24</sup>Beckett, Freeman, and Pitzer, *J. Am. Chem. Soc.* **70**, 4227 (1948).

## LOW-TEMPERATURE FAR UV SPECTRA OF OLEFINS

Upon exposure to air these compounds begin to show increased absorption in just this "triplet" region, but this is exactly the region wherein one expects formation of impurities to be most noticeable: at higher frequencies any impurity would be masked by the already great absorption of the pure compound itself, while at lower frequencies the expected impurities (oxygen containing compounds) would have small absorption themselves.<sup>7,25</sup>

In the molecules where they are resolved, vibration peak separations of  $1,400\text{cm}^{-1}$  appear in the  $N \rightarrow T$  transition. This is approximately the  $C = C$  stretch frequency. That these should be observed in the  $N \rightarrow T$  transition and not in the  $N \rightarrow V$  transition is unexplained.

If these bands in the region  $40-48,000\text{cm}^{-1}$  are then truly the  $N \rightarrow T$  transitions, there is one point a bit more difficult to explain. Their  $\epsilon$  values and oscillator strengths increase by a factor of 20 in going from the least substituted ethylene (hexene-1) to the most substituted (tetramethylethylene), while the corresponding values of the  $N \rightarrow V$  transition increase by only a factor of two. This must mean that the singlet-triplet selection rule is being strongly affected by the presence of the alkyl groups, and this can apparently happen in two ways.

It is known from phosphorescence studies of other  $\pi$ -electronic systems, notably aromatics, that the intrinsic phosphorescence lifetime of a molecule is markedly decreased when substituents are added,<sup>19</sup> particularly if these substituents are heavier atoms. This shortening of phosphorescence lifetime is due to the partial breakdown of the singlet-triplet intercombination rule, whose breakdown is presumably the result of increased spin-orbit ( $j-j$ ) coupling at the expense of L-S coupling. The breakdown of the singlet-triplet selection rule, then, will also increase the light absorption from the ground (singlet) state to the excited triplet state.

As the effect is currently interpreted a substituent as small in atomic number as a methyl group should have little effect on the spin-orbit coupling. However, extrapolation of data from heavier atoms to lighter atoms shows that the effect of a methyl group while small is yet finite.<sup>26</sup> McClure,<sup>19</sup> although he finds no essential difference between phosphorescence lifetime of toluene and benzene, does find shorter lifetimes for phenol and aniline than for benzene, and he attributes the phenomenon to

<sup>25</sup>H. Sponer and E. Teller, Rev. Mod. Phys. **13**, 76 (1941).

<sup>26</sup>M. Kasha, Disc. Faraday Soc. **9**, 14 (1950).

POTTS

this atomic number effect. Other workers in this laboratory<sup>27</sup> have found that the reverse process of phosphorescence in benzene, namely absorption of light from the ground state to the lowest excited triplet state, is twice as strong in toluene as in benzene, while the corresponding singlet absorption remains little changed in intensity. Now with ethylene it is possible to add more methyl groups per  $\pi$ -electron than with benzene. Hence it is conceivable that several alkyl substitutions<sup>28</sup> will cause an "atomic number" effect on the singlet-triplet selection rule in olefins.

Another possible effect of increasing alkyl substitution upon ethylene  $N \rightarrow T$  absorption is that of a steric effect at low temperature. In its 22% contraction, the rigid-glass medium may distort the molecule. Presumably the olefin having the greater number of alkyl groups about the double bond would be more subject to such distortion, because of its larger "area." Under such distortion there might be a tendency to enhance the unpaired (or triplet) character of the  $\pi$ -electrons in the ground (N) state, and thus make the  $N \rightarrow T$  transition more allowed. The distortion perhaps most likely to do so is twist,<sup>9,29</sup> but if the molecule were to be "frozen" in a twisted state, then the "red shoulder" of the  $N \rightarrow V$  transition would not disappear at low temperature. Further, the twist distortion at low temperatures seems unlikely in view of the large force constant of twist, as has been noted above. Perhaps some other distortion, such as bending of the C = C plane [force constant less than one-half of twist<sup>30</sup>], could produce some unpaired character in the  $\pi$ -electrons.

Perhaps the correct choice between these two possible explanations for the rapid increase of the  $N \rightarrow T$  transition with increasing substitution could be found by examining the absorption spectra of the various fluoro-substituted ethylenes at low temperatures. If one observed a weak transition analogous to the  $N \rightarrow T$  transition studied here, which increased strongly in intensity with increasing fluoro-substitution, the first explanation (that of increased spin-orbit coupling with increasing substitution) would be strengthened; fluorine atoms are too small to cause much steric effect, as the second explanation requires.

<sup>27</sup>J. S. Ham, unpublished data.

<sup>28</sup>As to whether the shortening of phosphorescence lifetimes in aromatic compounds is additive as more of the same substituents are added, McClure's data are inconclusive (see reference 19).

<sup>29</sup>H. McConnell, *J. Chem. Phys.* **20**, 1043 (1952).

<sup>30</sup>G. Herzberg, *Infrared and Raman Spectra of Polyatomic Molecules*, page 184.

## LOW-TEMPERATURE FAR UV SPECTRA OF OLEFINS

Another point about the present  $N \rightarrow T$  transition assignment to be discussed is the "red shoulder" effect for this transition. The potential curve of the excited triplet state (T) is of the same general shape as the excited singlet (V) state (Figure 6). Hence, the same arguments about a red shoulder at higher temperatures that obtain for the  $N \rightarrow V$  transition apply for the  $N \rightarrow T$  transition. This shoulder can be seen at room temperature in Figures 1, 2, and 4. (The "main part" of the  $N \rightarrow T$  transition at room temperature is hidden by the red shoulder of the  $N \rightarrow V$  transition, except in the case of hexene-1. In hexene-1 the "main part" of the  $N \rightarrow T$  transition appears at room temperature because it is only partly hidden by the narrower shoulder of the  $N \rightarrow V$  transition.)

### Phosphorescence and the Triplet State

Observation of a comparatively long-lived light emission (phosphorescence), which is now well established as triplet-singlet emission<sup>17,18,19,26</sup> ( $T \rightarrow N$  in the present discussion), might confirm the present  $N \rightarrow T$  assignment. As mentioned above, no such phosphorescence was observed in tetramethylethylene. If the statement above, that a low-temperature glass does not appreciably affect the potential curves (N, V, or T), is correct, the non-appearance of phosphorescence is easily explained. For as the molecules get into the triplet state, they could rapidly lose vibrational energy to the surroundings as they cascaded down through vibrational levels of the triplet state, eventually reaching the excited triplet (T) and ground singlet (N) crossover point, at  $\theta \approx 60^\circ$  (see Figure 6). Here they become singlet states, and cascade through the ground state vibrational levels back to zero energy. This radiationless process would be far more rapid than a triplet-singlet ( $T \rightarrow N$ ) emission.<sup>18</sup> Thus, no longer-lived (phosphorescent) emission would be observed.

### Cyclohexene

Cyclohexene is a somewhat different case from the other olefins already discussed. Superimposed upon the double-bond twisting potential will be certain strain potentials resulting from the fact that it is a six-membered ring structure. As the infrared frequency assignments are still in doubt, no attempt will be made to go into the finer details of cyclohexene structure; however, certain general statements may be made which, it is hoped, will be sufficient to explain the absorption spectrum.

It is expected that steric forces of the ring will have little effect upon the energy of C - C twist in its region of planarity. This is expected from the high

## POTTS

energy of C = C twist, about 1.3kcal/deg (as estimated from Arnett and Crawford's value in ethylene<sup>22</sup>), and the comparatively small strain energy of the entire ring, about 1.6kcal.<sup>24</sup> That is, the 1.6kcal of strain will be taken up by distortions other than the high-energy twist distortion. The only change in the region of double-bond planarity might be a small tendency toward flattening the ground-state (N) curve near planarity. Of course, for the region of large angle of twist ( $\theta > 45^\circ$ , say) the potential curve would be greatly altered, because it would require breaking a C - C bond. Presumably, this higher twisted region is not of importance in the present discussion.

At low temperature, negligible change (compared to room temperature) in the V and T state potential curves is expected in the region of planarity, as in the case of non-cyclic olefins, and for the same reason--namely, that energy of C = C twist is too great. Nor is much change anticipated in the ground-state (N) twist-potential curve in going to low temperature, except some small steepening of the curve which is due to contraction of the surroundings.

From this reasoning the behavior of the N  $\rightarrow$  V transition should in principle be just like the other olefins at room and low temperatures, and this is what is observed: a red shoulder on the N  $\rightarrow$  V absorption, disappearing at low temperature.

In cyclohexene the behavior of the weaker transition at  $43,000\text{cm}^{-1}$  (presumably the N  $\rightarrow$  T absorption) is quite different from that of the other olefins in that its absorption is greatly increased at low temperature. Although it may be coincidental, it is interesting to note that the oscillator strength of this transition, compared to the other olefins, follows the same trend as the oscillator strength of the N  $\rightarrow$  V transition. This gives additional support to its assignment as the N  $\rightarrow$  T transition.

If this is indeed the N  $\rightarrow$  T transition, the only possible explanation for its abnormally high intensity at low temperature is that the singlet-triplet selection rule is violated to a greater extent than would be expected. Recalling the sensitivity of this selection rule to alkyl substitution (as with the other olefins) it would be expected that the N  $\rightarrow$  T absorption for cyclohexene would be about the same as for cis-butene-2, which, as mentioned, should be about midway between mono- and tri-substituted ethylene. The additional effect on the selection rule in cyclohexene must then be due to its ring character.

As pointed out, the ring structure should not have any great effect on twist of the double bond in the region of planarity ( $\theta < 15^\circ$ , say), for the energy of twist is too large. Further, if the N  $\rightarrow$  T transition were enhanced because the molecule was

## LOW-TEMPERATURE FAR UV SPECTRA OF OLEFINS

somehow "frozen" into a twisted state at low temperature, then the  $N \rightarrow V$  transition would probably not show much disappearance of a red shoulder at low temperature.

What is proposed to explain the abnormal intensity at low temperature of the  $N \rightarrow T$  transition in cyclohexene is that the contraction of the rigid surroundings at low temperature tend to put some additional strain on the cyclohexene ring, which is to some extent taken up by an out-of-plane bending of the  $C = C$  plane. By analogy with ethylene, the force constant of this bending is sensibly lower (less than half) than the force constant of twist,<sup>30</sup> and hence a bending of the  $C = C$  plane produced by contraction of surroundings is more energetically feasible than a twisting of the double bond.

As has been noted, the singlet-triplet selection rule is sensitive to perturbation of the molecule. Thus, such an out-of-plane bending of the double bond could quite possibly decrease the bonding nature of the  $\pi$ -electrons by tending to localize them on the separate carbon atoms and by decreasing their overlap. This, in turn, would enhance their unpaired character. This tendency toward unpairing of the  $\pi$ -electrons mixes a certain triplet character into the ground-state wavefunction.<sup>29</sup> Thus, a transition from such a state to a triplet state becomes less strongly forbidden.

That such an "extra" enhancement of the  $N \rightarrow T$  absorption is not encountered in the other olefins is explained by the fact that they are not cyclic. It is presumed that the bending of the double bond in cyclohexene is the unique result of the force of contracting rigid surroundings upon a ring structure.

This explanation is to be regarded only as rather tentative. Little more can be said at the present time until such effects are investigated more thoroughly, both experimentally and theoretically.

### SUMMARY

A "red shoulder" on the  $N \rightarrow V$  absorption curve of olefins, observed at room temperature, but not at low temperature, is shown to result from the fact that the potential curve for twist about the double bond in the ground and excited states have slopes of opposite sign. The weaker absorption in the region  $40-48,000\text{cm}^{-1}$  is assigned to the  $N \rightarrow T$  absorption on the basis of its analogy to the  $N \rightarrow V$  transition in position, extinction coefficient, and oscillator strength, and to the sensitivity of the singlet-triplet selection rule to perturbations of the molecule.

LOW-TEMPERATURE ABSORPTION SPECTRA OF BENZENE, TOLUENE,  
AND PARA-XYLENE IN THE FARTHER ULTRAVIOLET REGION<sup>†\*</sup>

W. J. Potts, Jr.<sup>\*o</sup>  
Laboratory of Molecular Structure and Spectra  
Department of Physics  
The University of Chicago  
Chicago 37, Illinois

INTRODUCTION

PERHAPS no polyatomic molecule has been investigated spectroscopically as extensively as has benzene. In spite of the vast amount of literature on this subject, comparatively few investigations have been made of the shorter wavelength transitions (below 2,200Å) of benzene, and of these only a very few have given absolute extinction coefficients.

The nearer ultraviolet absorption bands of benzene (at 2,600Å, assigned to the  $^1A_{1g} \rightarrow ^1B_{2u}$  transition by most authors) have such extensive literature that only a few selected references will be cited here. The nearer ultraviolet absorption spectra of benzene and several alkyl benzenes have been systematically investigated in hydrocarbon solution,<sup>1</sup> in the vapor state,<sup>2</sup> in the crystalline state at low temperature,<sup>3</sup> and in rigid-glassy media at low temperature.<sup>4</sup> While the low-temperature spectra of the 2,600Å transitions of benzene and alkyl benzenes are very much sharper than the room-temperature solution spectra, the low-temperature method still cannot compete with

<sup>†</sup>This work was assisted in part by the Office of Ordnance Research under Project TB2-0001(505) of Contract DA-11-022-ORD-1002 with The University of Chicago.

<sup>\*</sup>This paper is essentially an extract version of Part III of a doctoral dissertation [Low-Temperature Spectroscopy in the Farther Ultraviolet Region, Chicago: March, 1953] submitted to the Faculty of the Division of the Physical Sciences, The University of Chicago.

<sup>\*</sup>AEC Predoctoral Fellow, 1950-52.

<sup>o</sup>Present address: Spectroscopy Department, The Dow Chemical Company, Midland, Michigan.

<sup>1</sup>Catalog of Ultraviolet Spectrograms, American Petroleum Institute, Project 44 (1945-1950).

<sup>2</sup>H. Sponer, J. Chem. Phys. **8**, 705 (1940).

<sup>3</sup>A. Kronenberger, Z. Phys. **63**, 494 (1930).

<sup>4</sup>E. Clar, Spectrochim. Acta **4**, 116 (1950).

## LOW-TEMPERATURE FAR UV SPECTRA OF BENZENE, TOLUENE, AND PARA-XYLENE

vapor spectra in resolution of these bands. Hence, vapor spectra have been used for the complete analysis of the 2,600Å transitions of benzene<sup>5</sup> and the analogous transitions of substituted benzenes.<sup>6</sup>

In the farther ultraviolet region, the spectral data on benzene and substituted benzenes become far scarcer. The far ultraviolet vapor spectrum of benzene has been obtained qualitatively by Carr and Stücklen,<sup>7</sup> and, along with that of toluene and the xylenes, by Price and others.<sup>8,9</sup> The vapor spectrum of benzene has been obtained quantitatively by Pickett and co-workers,<sup>10</sup> and by Romand and Vodar.<sup>11</sup>

The absorption spectra of benzene, toluene, and the xylenes have been obtained quantitatively in n-heptane solution by Platt and Klevens in the region 2,200-1,700Å.<sup>12</sup> Their work shows nearly as much resolution of structure as most of the aforementioned vapor work. In their work, as in the vapor absorption spectra, the strong transitions of benzene and the alkyl benzenes at about 1,850Å are quite diffuse.

Romand and Vodar<sup>11</sup> have obtained the far ultraviolet spectrum of benzene in the crystalline state at liquid-nitrogen temperature, but their work shows decidedly less sharpening of the spectrum than either their own vapor spectrum or the room-temperature solution spectra of Platt and Klevens.<sup>12</sup>

The present research was undertaken to see if use of rigid glasses at low temperature would give increased resolution in the diffuse transitions in the farther ultraviolet region of benzene and alkyl benzene absorption spectra. The results are most encouraging and show that these far ultraviolet transitions in aromatics do indeed have sharp structure. The absolute extinction coefficients and positions of several vibrational bands have been obtained for the farther ultraviolet (2,200-1,700Å region) spectral transitions of benzene, toluene, and para-xylene both at room temperature and at low temperature. Generally, much more vibrational structure is seen at low temperature.

<sup>5</sup>Sponer, Nordheim, Sklar, and Teller, *J. Chem. Phys.* **7**, 207 (1939).

<sup>6</sup>H. Sponer, *Rev. Mod. Phys.* **14**, 224 (1942).

<sup>7</sup>E. Carr and H. Stücklen, *J. Chem. Phys.* **6**, 645 (1938).

<sup>8</sup>W. C. Price and W. D. Walsh, *Proc. Roy. Soc. A191*, 22 (1947).

<sup>9</sup>Hammond, Price, Teegan, and Walsh, *Disc. Faraday Soc.* **9**, 53 (1950).

<sup>10</sup>Pickett, Muntz, and McPherson, *J. Am. Chem. Soc.* **73**, 4862 (1951).

<sup>11</sup>J. Romand and B. Vodar, *C. R. Acad. Sci., Paris* **233**, 930 (1951).

<sup>12</sup>J. R. Platt and H. B. Klevens, *Chem. Rev.* **41**, 301 (1947).

## POTTS

### EXPERIMENTAL

#### Materials

Benzene and toluene used in this research were Merck Reagent Grade chemicals; para-xylene was Eastman "White Label" grade, m.p. 13°C. Each was purified by several recrystallizations from itself, then distilled from sodium wire to remove any possible condensed water from the crystallization process. Although this method gives a product of extremely high purity,<sup>13</sup> the problem of impurities in this research is small, for only regions of intense absorption ( $\epsilon > 5,000$ ) were being investigated. The only trouble that might arise in this respect would be small amounts of ortho- and meta-xylenes in the para-xylene. The original melting point of the source of para-xylene and its method of purification however assure against it.

#### Method

The spectra at room temperature were obtained in a mixture of isopentane and 3-methylpentane by the same methods used by Platt and Klevens<sup>12</sup> and described elsewhere.<sup>14</sup> The liquid-nitrogen temperature spectra were obtained by the methods described elsewhere by Potts.<sup>15</sup> For both series of spectra the Cario-Schmitt-Ott vacuum fluorite spectrograph was employed, and Ilford Q1 plates were used.

#### Errors

The errors in these methods have been discussed elsewhere by Potts<sup>15,16</sup> and are believed to be about 8% in molar extinction coefficient at 2,200Å, increasing to somewhat greater than 15% at 1,700Å, the limit of the present techniques. Samples of different concentrations gave results consistent within these errors. However, the error may well be higher than estimated in the region at the "blue" end of the first absorption (2,100Å transition) which is being overlapped by the beginning of a region of stronger absorption (1,850Å transition), where it is difficult to pick a solution of favorable concentration. Also, the errors in the room-temperature data at the extreme end of the region investigated (1,730Å) are probably quite high, as the solvents are rapidly cutting off here at room temperature.

---

<sup>13</sup>G. N. Lewis and M. Kasha, *J. Am. Chem. Soc.* **66**, 2100 (1944).

<sup>14</sup>L. E. Jacobs and J. R. Platt, *J. Chem. Phys.* **16**, 1137 (1948).

<sup>15</sup>W. J. Potts, Jr., *J. Chem. Phys.* **20**, 809 (1952), **21**, 191 (1953).

<sup>16</sup>W. J. Potts, Jr., "Low-Temperature Absorption Spectra of Selected Olefins in the Farther Ultraviolet Region", THIS TECHNICAL REPORT, 1952-53, Part Two.

## LOW-TEMPERATURE FAR UV SPECTRA OF BENZENE, TOLUENE, AND PARA-XYLENE

### Agreement with Other Authors

The room-temperature data presented here are essentially a repetition of the work of Platt and Klevens<sup>12</sup> and generally agree fairly well with their results. Other workers in this laboratory have independently verified many of these values of extinction coefficient.<sup>17</sup> However, the present data differ from those of Platt and Klevens in two instances: (a) the present work shows no weak transition at 1,730Å in toluene, which Platt and Klevens observed and have interpreted in a later paper<sup>18</sup> as being analogous to a  ${}^1A_{1g} \rightarrow {}^1E_{2g}$  transition in benzene; (b) the transition in para-xylene at 2,200Å shows a somewhat lower extinction in the present work than in that of Platt and Klevens. These discrepancies will be discussed in detail below.

The present work shows none of the very sharp Rydberg bands superimposed upon the strong 1,850Å transition in any of these compounds which have been observed in the vapor spectra of Carr and Stücklen,<sup>7</sup> Price *et al.*,<sup>8,9</sup> and Pickett *et al.*<sup>10</sup> This is presumably to be expected when spectra are obtained in condensed phases, however, because of the large size of the Rydberg orbitals, which would become strongly perturbed by closely neighboring molecules.

The value of peak extinction coefficient of the benzene 1,850Å transition at room temperature obtained here, and agreeing with Platt and Klevens<sup>12</sup> and with Cohn and Ham<sup>17</sup> (all of whose data were obtained under similar conditions in hydrocarbon solutions), disagrees with the vapor phase value of both Pickett *et al.*<sup>10</sup> and Romand and Vodar<sup>11</sup> (whose results approximately agree). That our solution values of  $\epsilon$  for the strong transition of benzene ( $\epsilon = 45,000$ ) should be a little more than one-half the vapor phase value obtained by others ( $\epsilon = 80,000$ ) is difficult to explain, as it has been shown that spectra in solution and in vapor should have about the same molar extinction coefficient.<sup>14</sup>

### RESULTS

As a vivid example of the increased sharpening of benzene spectra one can obtain with a rigid glass at low temperature, some of the benzene plates have been reproduced in Figure 1. Figure 1a shows absorption of the 2,100Å transition; the lower exposure is at room temperature, the upper exposure is the identical solution frozen to a glass at liquid-nitrogen temperature. Figure 1b gives a similar picture for the 1,850Å

<sup>17</sup>Unpublished data of J. S. Ham, and of C. E. Cohn.

<sup>18</sup>J. R. Platt, *J. Chem. Phys.* **19**, 1418 (1951).

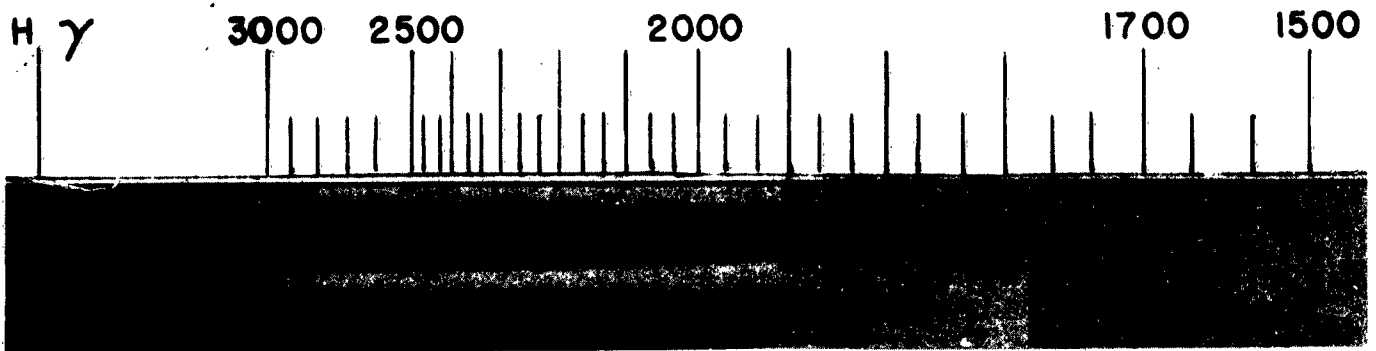


Fig. 1a. Comparison of room- and low-temperature spectra of benzene 2,100Å transition.

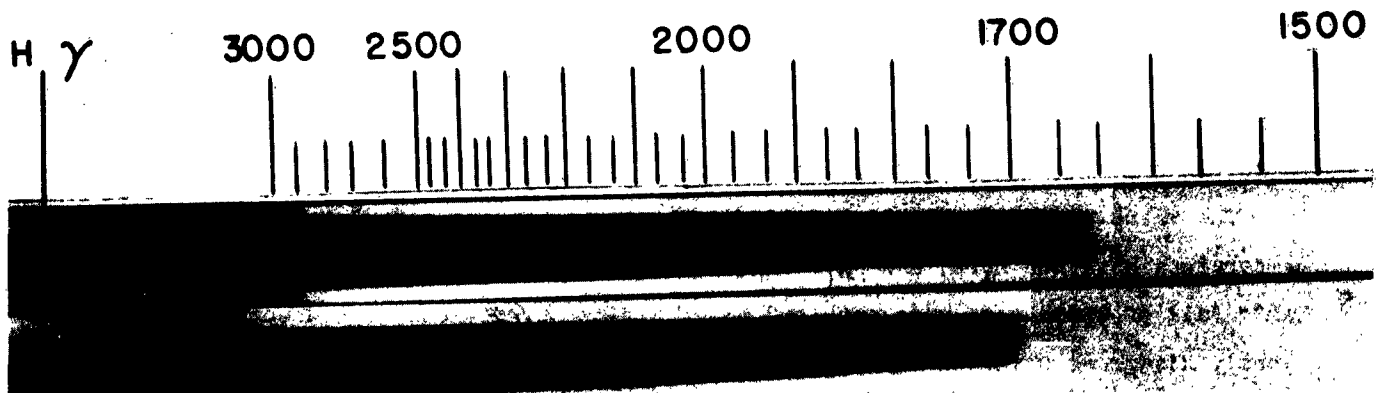


Fig. 1b. Comparison of room- and low-temperature spectra of benzene 1,850Å transition.

transition of benzene. That low temperatures are of value in this farther ultraviolet region is clearly shown by the effect on the 1,850Å transition; not even vapor spectra

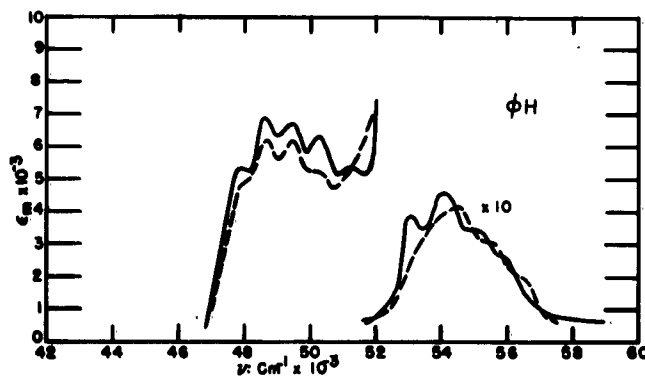


Fig. 2. Far ultraviolet absorption spectra of benzene.

have produced such sharpening of this transition.

In Figures 2, 3, and 4 are plotted the molar extinction coefficient of benzene, toluene, and para-xylene, respectively, against the frequency in wave numbers. The solid curve is the data at low temperature, the dashed curve is the data at room temperature. Figures 5, 6,

LOW-TEMPERATURE FAR UV SPECTRA OF BENZENE, TOLUENE, AND PARA-XYLENE

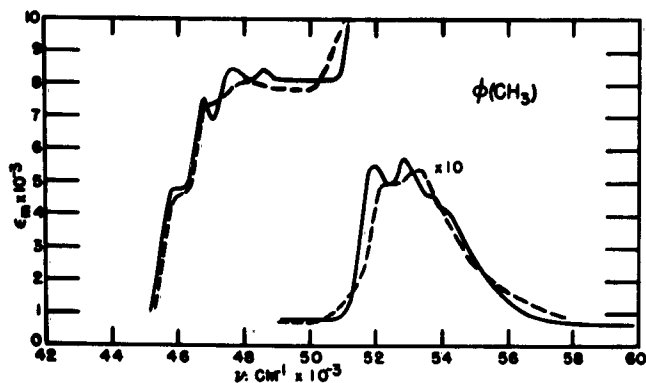


Fig. 3. Far ultraviolet absorption spectra of toluene.

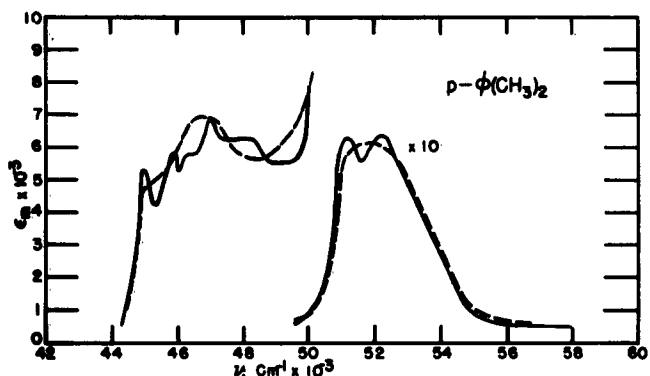


Fig. 4. Far ultraviolet absorption spectra of para-xylene.

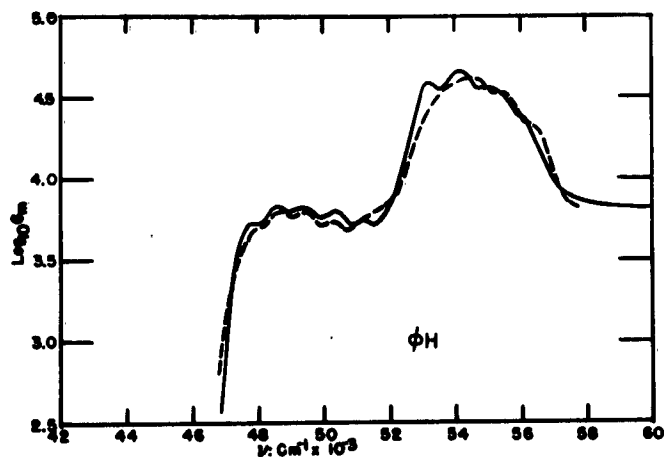


Fig. 5. Spectra of benzene on a log plot.

and 7 give the same data on a  $\log_{10}$  plot.

Because the molecular symmetries of benzene, toluene, and para-xylene differ, analogous spectral transitions in these molecules properly get different symmetry labels. Thus, to avoid confusion, for the present we shall designate the transition near  $2,100\text{\AA}$  ( $47,500\text{cm}^{-1}$ ) in all three molecules as the "2,100 $\text{\AA}$  transition," the much stronger transition near  $1,850\text{\AA}$  ( $54,000\text{cm}^{-1}$ ) as the "1,850 $\text{\AA}$  transition."

In Table I are tabulated the "electronic" features of the various transitions, data being given for both temperatures. The "centers" of the transitions are chosen as the points which divide in half the integrated absorption intensity, or oscillator strength,<sup>19</sup> of each transition. These values are uncertain to about  $\pm 250\text{cm}^{-1}$ . In a separate column are tabulated the (estimated) analogs of these positions in the vapor, using the data of Price *et al.*<sup>8,9</sup>

The molar extinction coefficients are for the strongest vibration peak in all cases. The error is roughly 15% or less.

The oscillator strengths,<sup>19</sup> or  $f$ -numbers, given are subject to some uncertainty not only from error of extinction coefficient, but also from the selection of cut-off points on either side of the

<sup>19</sup> $f$ -number, or oscillator strength, is defined as:  $f = 10^3(\log_{10} e) \frac{mc^2}{\pi e^2 N} \int \epsilon_v dv = 4.32 \times 10^{-9} \int \epsilon_v dv$ , where  $v$  is in  $\text{cm}^{-1}$ ,  $\epsilon_v$  is molar extinction coefficient.

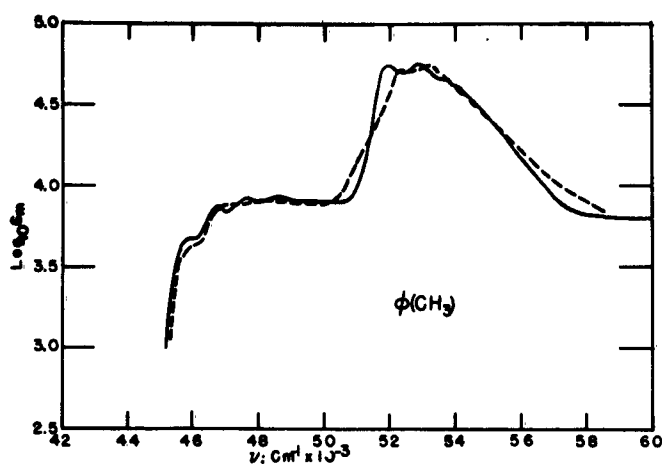


Fig. 6. Spectra of toluene on a log plot.

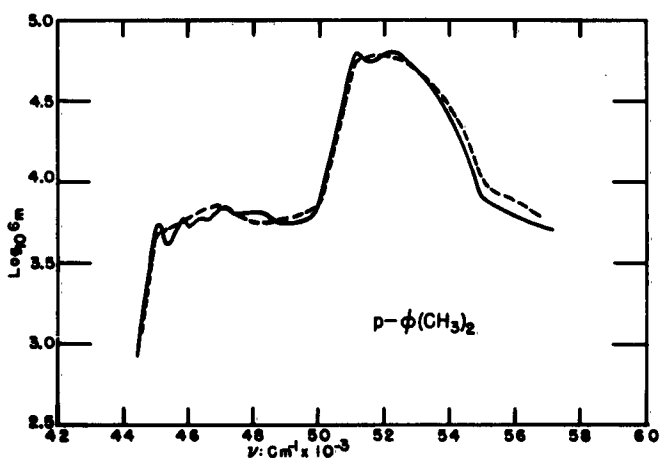


Fig. 7. Spectra of para-xylene on a log plot.

what lower than those reported by Platt and Klevens,<sup>12</sup> but within probably experimental error of both sets of data.

Table II gives the vibrational-structure features of the 2,100 $\text{\AA}$  and 1,850 $\text{\AA}$  transitions of the three molecules. Values are given for both room-temperature and low-temperature conditions. The positions of the vibration peaks have been obtained not from the absorption curves, but by two independent measurements of the plates themselves. They are believed to be accurate to  $\pm 100\text{cm}^{-1}$ . Those vibration peaks at room temperature followed by (?) are rather doubtful, and would not have been reported had not they had definite analogs at low temperature.

As is well known, spectra shift to the red as the refractive index of the medium increases;<sup>14</sup> thus the low-temperature vibration peaks are all shifted to the red of

transitions. This latter error may be particularly bad for the 2,100 $\text{\AA}$  transitions, in that they lie so close to the much stronger 1,850 $\text{\AA}$  transitions. The choice for the junction between the 2,100 $\text{\AA}$  and 1,850 $\text{\AA}$  transitions was the point where the slope of the log plot (see Figures 5, 6, and 7) was zero just before the steep rise of the 1,850 $\text{\AA}$  transition. In toluene, because this zero slope extends some  $1,500\text{cm}^{-1}$ , its mid-point, namely  $49,550\text{cm}^{-1}$ , was chosen as the junction between the 1,850 $\text{\AA}$  and 2,100 $\text{\AA}$  transitions. Hence the larger uncertainty tabulated for the  $f$ -number of the 2,100 $\text{\AA}$  transition of toluene. (Percentage-wise, this position uncertainty has little effect on the  $f$ -number of the 1,850 $\text{\AA}$  transition.)

The oscillator strengths for room and low temperature agree within experimental error, as theory demands. The room-temperature values tend to be some-

LOW-TEMPERATURE FAR UV SPECTRA OF BENZENE, TOLUENE, AND PARA-XYLENE

TABLE I.  
ELECTRONIC FEATURES OF AROMATIC SPECTRA

Compound	Transition center $\pm 250\text{cm}^{-1}$			Shift from benzene ( $\text{cm}^{-1}$ )		$\epsilon_{\text{max}}$		f-number	
	298°K	77°K	Vapor*	298°K	77°K	298°K	77°K	298°K	77°K
	2,100Å Transition								
Benzene	49,750	49,500	50,600			6,200	6,800	.10±.01	.11±.01
Toluene	48,400	48,300	49,000	1,350	1,200	8,100	8,500	.13±.03	.13±.03
Para-xylene	47,000	47,000	47,500	2,750	2,500	6,900	6,900	.12±.02	.12±.02
	1,850Å Transition								
Benzene	54,600	54,250	55,900			42,000	46,000	.60±.07	.63±.07
Toluene	53,000	52,850	54,100	1,600	1,400	55,000	57,000	.80±.08	.82±.08
Para-xylene	52,100	52,000	52,600	2,500	2,250	61,000	63,000	.89±.08	.89±.08

\*See text.

the values obtained at room temperature, which, in turn, are shifted to the red of what would be observed in the vapor phase. In a third column appear the low-temperature frequency values "corrected" to the vapor state. These "corrections" are made by comparison with selected values of vapor spectra of other authors,<sup>7,8,9</sup> assuming that in one given transition all peaks shift the same amount. That this assumption is reasonable is shown by the rather close agreement in positions between the calculated "vapor" peaks and those which are sufficiently resolved from actual observations in the vapor.<sup>7,9</sup> For the 1,850Å transitions a certain amount of personal judgment has been used to "correct" the vibration peaks, as they are not resolved in the vapor state. The vibrational separations of Table II are from these "vapor" listings.

DISCUSSION

Vibrational Structure

The low-temperature rigid-glass method produces decidedly increased sharpening of vibration structure, particularly in the 1,850Å transitions. The results given here are not sufficiently accurate to warrant a vibrational analysis of states, but there is good indication that sufficiently accurate spectra may be obtained if one uses an

## POTTS

TABLE II.

## VIBRATIONAL FEATURES OF AROMATIC SPECTRA

Compound	Vibration Peaks, $\pm 100\text{cm}^{-1}$			Separation, $\pm 150\text{cm}^{-1}$
	298°K	77°K	"vapor" (see text)	
	2,100Å Transition			
Benzene	47,960	47,720	48,970	
				810
	48,660	48,430	49,680	950
	49,630	49,380	50,630	1000
	50,630	50,380	51,630	770
	51,410(?)	51,150	52,400	
Toluene	46,080	45,980	46,700	
				970
	47,060	46,950	47,670	900
		47,850	48,570	810(?)
	48,660(?)	49,380(?)		
Para-xylene	45,050	45,050	45,650	
				820
	46,080(?)	45,870	46,470	430
		46,300	46,900	760
	47,050(?)	47,060	47,660	1020
	48,080 (diffuse)	48,680		
	1,850Å Transition			
Benzene		53,050	54,700	
				860
	54,350(?)	53,910	55,560	1040
	55,250(?)	54,950	56,600	1070
	56,020	57,670		
Toluene	52,080(?)	51,810	53,060	
				1100
	53,190(?)	52,910	54,160	1000
		53,910	55,160	1040(?)
	54,950(?)	56,200(?)		
Para-xylene	(not resolved)	51,020	51,620	
		52,220	52,820	1200

## LOW-TEMPERATURE FAR UV SPECTRA OF BENZENE, TOLUENE, AND PARA-XYLENE

instrument of higher dispersion and resolution than the small instrument used for this research.

In Table I the frequencies of the electronic transitions were taken as the approximate centers of integrated absorption in each transition. It is also desirable to know the frequencies of these transitions with respect to the equilibrium configurations of their nuclei; that is, the 0-0 band of the transition.<sup>20</sup>

The 2,100Å transition is forbidden in benzene, but allowed in toluene and para-xylene [see below]. In an allowed transition the 0-0 band is seen, but in a forbidden transition it is not; for it is vibrational interaction which makes the transition appear at all,<sup>21</sup> and the 0-0 band of course contains no vibrational interaction. Thus the first band appearing in the 2,100Å transition in toluene and para-xylene is probably the 0-0 band, but in benzene the 0-0 band is not seen.

Further, if one expects the 0-0 band of the 2,100Å transition to shift to the red at about the same rate as the "center" of the transition shifts as methyl groups are added to benzene, then the first observed vibrational band in the 2,100Å transition of benzene bears no correlation to the first band observed in toluene and para-xylene. However, if one subtracts about  $650\text{cm}^{-1}$  from the positions of the benzene vibration peaks, then the first two vibration peaks correlate well in all these compounds, both at room and low temperature and in the calculated vapor state. This  $650\text{cm}^{-1}$  is the value of the  $\epsilon_{2g}$  vibration which makes the transition allowed<sup>20,21,22</sup> [also see below] and is also the interval observed between the faint 0-0 band and first strong peak in the 2,600Å transition of benzene.<sup>5,21</sup> Thus, for the 2,100Å transition, it is probably safe to assert that the first vibrational peak in toluene and para-xylene are the 0-0 bands (allowed transitions), the first observed peak in benzene is the 0-0 band plus the  $650\text{cm}^{-1}$   $\epsilon_{2g}$  vibration which makes the transition allowed. (Correlation of higher vibrational bands is not possible, because there apparently is more than one vibrational level being excited in the 2,100Å transition of para-xylene, judging from the separations.)

The first two vibrational peaks in the 1,850Å transition of the three molecules seem to correlate fairly well with the shift of the transition "centers". As this transition is strongly allowed<sup>20,22</sup> [also see below] in all three molecules, the first

<sup>20</sup>Nordheim, Sponer, and Teller, J. Chem. Phys. **8**, 455 (1940).

<sup>21</sup>H. Sponer and E. Teller, Rev. Mod. Phys. **13**, 76 (1941).

<sup>22</sup>C. C. J. Roothaan and R. S. Mulliken, J. Chem. Phys. **16**, 118 (1948).

## POTTS

vibrational peak is quite probably the O-O band.

In Table III are given the positions of the electronic transitions, using the O-O band as a "point of reference." The O-O band of benzene ( $2,100\text{\AA}$  transition) is obtained by subtracting  $650\text{cm}^{-1}$  from the first observed band, assuming that the  $\epsilon_{2g}$  vibration in the  $2,100\text{\AA}$  transition has about the same energy as in the  $2,600\text{\AA}$  transition.<sup>20,22</sup>

TABLE III.

## O-O BANDS OF THE AROMATIC TRANSITIONS

Compound	O-O band position $\pm 100\text{cm}^{-1}$			Shift from benzene $\pm 300\text{cm}^{-1}$	
	298°K	77°K	"vapor"	298°K	77°K
	$2,100\text{\AA}$ Transition				
Benzene	ca. 47,310*	ca. 47,070*	ca. 48,320*		
Toluene	46,080	45,980	46,700	1,220	1,020
Para-xylene	45,050	45,050	45,650	2,250	1,950
	$1,850\text{\AA}$ Transition				
Benzene		53,050	54,700		
Toluene	52,080(?)	51,810	53,060		1,240
Para-xylene		51,020	51,620		2,030

\*Calculated. See text.

Group Theory Notation

In discussing the more theoretical aspects of these spectral states it will be necessary to list the symmetries, group theory notations, and selection rules of the three molecules. These are tabulated in Table IV. The reductions of symmetry from  $D_{6h}$  (benzene) to  $C_{2v}$  (toluene) and  $V_h$  (para-xylene) are made by rotating the (substituted) benzene molecule about the x symmetry axis (so that  $x \rightarrow x$ ,  $y \rightarrow z$ ,  $z \rightarrow y$ ). This is necessary to obtain  $C_{2v}$  symmetry for toluene, desirable to obtain  $V_h$  symmetry so that the symmetry axes of toluene and para-xylene have the same notation. (There are, of course, several alternative choices for axis assignment in reducing  $D_{6h}$  to  $V_h$ ; and, although each gives some different assignments for states, the same selection rules are obtained.) The corresponding spectral transitions have been placed in the same row. If the transition is symmetry forbidden, it is followed by "forb"; if allowed, it is followed by the moment in which direction it takes place in order to be allowed.<sup>21</sup>

LOW-TEMPERATURE FAR UV SPECTRA OF BENZENE, TOLUENE, AND PARA-XYLENE

TABLE IV.

SYMMETRY PROPERTIES OF BENZENE, TOLUENE, AND PARA-XYLENE\*

	Benzene	Toluene	Para-xylene
Symmetry	$D_{6h}$	$C_{2v}$	$V_h$
Method of Reduction	$C_2^z$		$C_2^y$
	$C_2^y$	$C_2^z$	$C_2^z$
	$C_2^x$		$C_2^x$
	$\sigma_h$	$\sigma_v^y$	$\sigma_v^y$
Transitions and Selection Rules	${}^1A_{1g} \rightarrow {}^1B_{1u}$ (forb)	${}^1A_1 \rightarrow {}^1A_1(T_z)$	${}^1A_g \rightarrow {}^1B_{1u}(T_z)$
	${}^1A_{1g} \rightarrow {}^1B_{2u}$ (forb)	${}^1A_1 \rightarrow {}^1B_1(T_x)$	${}^1A_g \rightarrow {}^1B_{3u}(T_x)$
	${}^1A_{1g} \rightarrow {}^1E_{1u}(T_y, T_x)$	${}^1A_1 \rightarrow \left\{ \begin{array}{l} {}^1A_1(T_z) \\ {}^1B_1(T_x) \end{array} \right\}$	${}^1A_g \rightarrow \left\{ \begin{array}{l} {}^1B_{1u}(T_z) \\ {}^1B_{3u}(T_x) \end{array} \right\}$
	${}^1A_{1g} \rightarrow {}^1E_{2g}$ (forb)	${}^1A_1 \rightarrow \left\{ \begin{array}{l} {}^1A_1(T_z) \\ {}^1B_1(T_x) \end{array} \right\}$	${}^1A_g \rightarrow \left\{ \begin{array}{l} {}^1A_g(\text{forb}) \\ {}^1B_{1g}(\text{forb}) \end{array} \right\}$

\*For a general treatment of group theory as applied to electronic spectra, see Sponer and Teller (reference 22).

The notations in Table IV will be frequently referred to in the following discussion.

In benzene there are only two group-theoretically allowed (singlet) transitions:  ${}^1A_{1g} \rightarrow {}^1E_{1u}$  and  ${}^1A_{1g} \rightarrow {}^1A_{2u}$ . The latter is unlikely as an electronic transition because its transition moment lies along the axis perpendicular to the plane of the benzene ring. Two other transitions,  ${}^1A_{1g} \rightarrow {}^1B_{1u}$  and  ${}^1A_{1g} \rightarrow {}^1B_{2u}$ , are forbidden in benzene but may be made allowed by interaction of a  $\epsilon_{2g}$  type of vibration:<sup>23</sup>

<sup>23</sup>Small Greek letters are used for vibrations or orbitals; capital Roman letters for electronic states.

$\epsilon_{2g} \times \begin{Bmatrix} 1B_{1u} \\ 1B_{2u} \end{Bmatrix} = E_{1u}$ .<sup>20</sup> Molecular orbital treatment of benzene<sup>24</sup> shows that the only one-electron (singlet) transitions likely in benzene are  $1A_{1g} \rightarrow 1B_{1u}$ ,  $\rightarrow 1B_{2u}$ ,  $\rightarrow 1E_{1u}$ , which all arise from an upper  $\epsilon_{1g}$  electron going to an unfilled  $\epsilon_{2u}$  orbital. All of these transitions become allowed in toluene and para-xylene.

Another possible transition for benzene is the  $1A_{1g} \rightarrow 1E_{2g}$  transition predicted by Sklar<sup>25</sup> from the Heitler-London approximation. It is forbidden in benzene, but could be made allowed by an  $\epsilon_{1u}$  vibration. Because of its even, or "g" character, the analogous transition is allowed in toluene, but forbidden in para-xylene. Further, if such a transition exists, according to MO theory<sup>24</sup> it must either be a two-electron transition (two  $\epsilon_{1g}$  electrons going to an  $\epsilon_{2u}$  orbital) or a one-electron transition from the lower  $\alpha_{2u}$  orbital to an  $\epsilon_{2u}$  orbital. In either case this requires more energy than the other one-electron transitions mentioned above, and thus would be found only in the very far ultraviolet if at all.

#### The 1,850Å Transitions

These transitions may now be assigned with certainty to the  $1A_{1g} \rightarrow 1E_{1u}$  transition for benzene, the  $1A_1 \rightarrow \begin{Bmatrix} 1A_1 \\ 1B_1 \end{Bmatrix}$  for toluene, and the  $1A_g \rightarrow \begin{Bmatrix} 1B_{1u} \\ 1B_{3u} \end{Bmatrix}$  transition for para-xylene. This one-electron transition is group-theoretically allowed and should be strong; it is the only allowed one-electron transition in benzene which has its transition moment in the plane of the molecule. It is noted from the character tables of benzene<sup>21</sup> that the  $1A_{1g} \rightarrow 1E_{1u}$  transition is doubly degenerate, and methyl substitution breaks down this degeneracy in toluene and para-xylene.

The assignment of  $1A_{1g} \rightarrow 1E_{1u}$  for the 1,850Å transition in benzene has been advocated before, especially by Mulliken.<sup>22</sup> The present work makes this assignment certain because the low-temperature methods, while obliterating the sharp Rydberg bands superimposed on this transition, have sharpened the transition to the point where vibrational structure is seen beyond question. Hence the 1,850Å transition is not a dissociation or predissociation band,<sup>20</sup> but a definite  $\pi$ - $\pi$  type electronic transition.

<sup>24</sup>Much of the MO theory discussed in this section has been borrowed from C. C. J. Roothaan, "New Developments in Molecular Orbital Theory, with Applications to Benzene," THIS TECHNICAL REPORT, 1949-50, Part Two.

<sup>25</sup>A. L. Sklar, *J. Chem. Phys.* **5**, 669 (1937).

## LOW-TEMPERATURE FAR UV SPECTRA OF BENZENE, TOLUENE, AND PARA-XYLENE

### The 2,100Å Bands

These transitions are group-theoretically allowed in toluene and para-xylene, but forbidden in benzene, whether one assigns  ${}^1A_{1g} \rightarrow {}^1B_{1u}$  or  ${}^1A_{1g} \rightarrow {}^1B_{2u}$  (and their analogs in toluene and para-xylene) to the transition. That they are allowed in the substituted benzenes but not in benzene itself is experimentally shown from the respective appearance and non-appearance of what have been tentatively assigned the O-O bands.

If these O-O band assignments are correct, then the transition may not be assigned to  ${}^1A_{1g} \rightarrow {}^1E_{2g}$  and its analogs as has been proposed by Sklar,<sup>25</sup> for these assignments predict the transition to be allowed in toluene, but not in benzene or para-xylene. Furthermore, as noted above, the energy of the  ${}^1A_{1g} \rightarrow {}^1E_{2g}$  transition must be at least more than the energy of the  ${}^1A_{1g} \rightarrow {}^1E_{1u}$ , or 1,850Å transition, thus ruling it out as an assignment for the 2,100Å transition.

The transition at 2,100Å must therefore be assigned to either  ${}^1A_{1g} \rightarrow {}^1B_{1u}$  or  ${}^1A_{1g} \rightarrow {}^1B_{2u}$  in benzene, to their analogs in toluene and para-xylene. Most authors have assigned it to  ${}^1A_{1g} \rightarrow {}^1B_{1u}$  and assigned the near ultraviolet transition (2,600Å bands) to  ${}^1A_{1g} \rightarrow {}^1B_{2u}$ . This matter will not be further discussed at present, but the results presented may be reconciled with the above assignment.

### SUMMARY

The absorption spectra of the 2,100Å and 1,850Å transitions of benzene, toluene, and para-xylene show sharp structure at low temperature. The sharp structure of the 1,850Å transition shows that it is a  $\pi$ - $\pi$  type transition, and not a predissociation band. Its correct assignment is  ${}^1A_{1g} \rightarrow {}^1E_{1u}$ , and analogous assignments in toluene and para-xylene. The 2,100Å transitions of these molecules can be assigned to  ${}^1A_{1g} \rightarrow {}^1B_{1u}$  and its analogs, while the 2,600Å transitions are assigned to  ${}^1A_{1g} \rightarrow {}^1B_{2u}$ . Evidence presented indicates that there is no  ${}^1A_{1g} \rightarrow {}^1E_{2g}$  transition in this region of the spectrum.

## MOLECULAR COMPOUNDS AND THEIR SPECTRA.

### IV. THE PYRIDINE-IODINE SYSTEM\*

C. Reid<sup>†</sup> and R. S. Mulliken<sup>‡</sup>  
Laboratory of Molecular Structure and Spectra  
Department of Physics  
The University of Chicago  
Chicago 37, Illinois

#### ABSTRACT

The visible and ultraviolet absorption spectra of dilute solutions of iodine plus pyridine in heptane have been studied, and the existence of an equilibrium with a 1:1 molecular complex  $\text{Py}\cdot\text{I}_2$  ("outer complex") was demonstrated [ $K = 290$  at  $16.7^\circ\text{C}$ , where  $K$  means  $(\text{Py}\cdot\text{I}_2)/(\text{Py})(\text{I}_2)$ ]. The corresponding changes in heat content, entropy, and free energy (at  $17^\circ$ ) in formation of the complex were determined to be  $-7.8\text{kcal/mole}$ ,  $-15.5\text{cal/deg. mole}$ , and  $-3.3\text{kcal/mole}$  respectively. The location and intensities of the  $\text{I}_2$  band ( $\lambda_{\text{max}} = 4,220\text{\AA}$ ,  $\epsilon_{\text{max}} = 1,320$ ) and of the charge-transfer band ( $\lambda_{\text{max}} = 2,350$ ,  $\epsilon_{\text{max}} = 50,000$ ) of  $\text{Py}\cdot\text{I}_2$  were determined.

The  $\lambda_{4,220}$  band shifts gradually, and increases in intensity, on adding pyridine to the aforementioned heptane solutions, until for pure pyridine solutions it has reached about  $\lambda_{3,890}$ , with  $\epsilon_{\text{max}} = 2,120$ , provided the solutions are not too dilute in iodine. These changes can most probably be attributed to a somewhat increased polarity and stability of the  $\text{Py}\cdot\text{I}_2$  "outer" complex in the polar solvent pyridine than in the nonpolar solvent heptane. There is no evidence of the presence of the "inner complex"  $(\text{PyI})^+\text{I}^-$  in more than small concentrations, but conductivity studies by Kortüm and Wilski indicate that appreciable small concentrations of its ions  $(\text{PyI})^+$  and  $\text{I}^-$  are present in pure pyridine solutions of iodine. Additional studies in very dilute solutions of iodine in pyridine show further interesting spectroscopic changes, which are discussed, but we feel that further experimental study will be needed using extreme precautions toward exclusion of side-reactions, moisture, or impurities.

#### INTRODUCTION AND SURVEY

RECENT STUDIES have confirmed older ideas that in its violet solutions, iodine exists essentially free, but that in its brown solutions it forms 1:1 molecular complexes

\*This work was assisted by the Office of Ordnance Research under Project TB2-0001(505) of Contract DA-11-022-ORD-1002 with The University of Chicago.

<sup>†</sup>On leave of absence from The University of British Columbia, 1952-1953. Present address: Department of Chemistry, The University of British Columbia, Vancouver, Canada

<sup>‡</sup>On leave of absence from The University of Chicago, 1952-1953; Fulbright Research Scholar at Oxford University, 1952-1953.

with the solvent.<sup>1</sup> The strong visible absorption of  $I_2$  vapor with maximum at  $\lambda 5,200$  is essentially unchanged in "violet" solvents, but in solutions where it forms complexes this peak is shifted toward shorter wavelengths; this accounts for the altered color. In addition, a new very intense peak characteristic of the complex, first noted by Benesi and Hildebrand for aromatic solvents, appears at shorter wavelengths, usually in the ultraviolet. The interpretation of this new peak as a charge-transfer spectrum has proved important for a clearer understanding of the electronic structure of these complexes.<sup>1</sup>

There is evidence<sup>2,3,4,5</sup> that iodine forms especially stable complexes with pyridine and related compounds. Waentig<sup>2</sup> reported golden crystals, which he attributed to  $Py \cdot I_2$ , crystallizing from a saturated solution of iodine in pyridine. From heats of solution Hartley and Skinner<sup>3</sup> estimated the heat of formation of  $Py \cdot I_2$  in solution to be about 7.95kcal/mole, much larger than for other types of iodine complexes. Similarly, the enhancement of the dipole moment in the formation of  $Py \cdot I_2$  is exceptionally large.<sup>4</sup> Further, the change in the infra-red spectrum of  $Py$  when it goes into  $Py \cdot I_2$  is much greater<sup>5</sup> than the corresponding effect in the case of complex-forming solvents of other types.

Audrieth and Birr<sup>6</sup> reported that solutions of iodine in pyridine show high electrical conductivities, which slowly increase with time to asymptotic values. According to them the molar conductivity based on  $I_2$  is so high in dilute solutions that it cannot be explained by simple dissociation into  $I^+$  (or  $PyI^+$ ) and  $I^-$ . They suggested instead the formation of a ternary electrolyte

<sup>1</sup>See R. S. Mulliken, (a) J. Am. Chem. Soc. 72, 600 (1950), and 74, 811 (1952); (b) J. Phys. Chem. 56, 801 (1952), for quantum-theoretical interpretation of molecular complexes and their spectra, and a comprehensive review. These are I, II, and III of the present series.

<sup>2</sup>P. Waentig, Z. physik. Chem. 68, 513 (1909); Chatelet, Ann. Chim. [11] 2, 12 (1934); H. Carlsohn, Z. angew. Chem. 45, 580 (1932), and 46, 747 (1933).

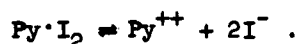
<sup>3</sup>K. Hartley and H. A. Skinner, Trans. Faraday Soc. 26, 621 (1950).

<sup>4</sup>Y. K. Syrkin and K. M. Anisimowa, Doklady Akad. Nauk. SSSR 59, 1457 (1948); G. Kortüm, J. Chim. Phys. 49, C127 (1952); G. Kortüm and H. Walz, Z. Elektrochem. 57, 73 (1953).

<sup>5</sup>D. L. Glusker, H. W. Thompson, and R. S. Mulliken, J. Chem. Phys. 21, 1407 (1953), and references given there; also further unpublished results of Mr. Glusker. Also W. Luck, Z. Elektrochem. 56, 870 (1952), especially Table 4.

<sup>6</sup>L. F. Audrieth and E. J. Birr, J. Am. Chem. Soc. 55, 668 (1933).

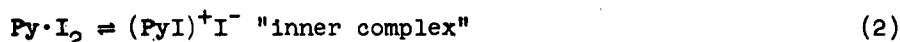
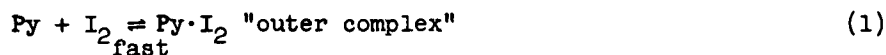
REID AND MULLIKEN



However, recent work of Kortüm and Wilski,<sup>7</sup> using very great precautions to keep moisture excluded, indicates that iodine in freshly prepared solutions in pure pyridine at concentrations in the neighborhood of  $10^{-4}$  molar gives only a small conductivity, though larger than for most iodine complexes.<sup>8</sup> They find, however, that this increases with time, and attribute the effect to a slow iodination in the ring; the effect is strongly catalyzed by platinum sponge.

Kleinberg, Van der Werf, and associates<sup>9</sup> have made a spectrophotometric investigation of solutions of iodine in pyridine (also in quinoline). They too conclude that a very slow iodination in the ring occurs; this should liberate  $\text{I}^-$  ions, which may form  $\text{I}_3^-$  ions with  $\text{I}_2$ .

Mulliken<sup>10</sup> in 1952 suggested that when  $\text{I}_2$  is dissolved in pyridine the following should be considered as the primary reactions:



The "outer complex"  $\text{Py} \cdot \text{I}_2$  in (1) would be a molecular complex of the usual type. The "inner complex" in (2) would be an essentially ionic structure (N-iodopyridinium iodide). It was suggested that, in iodine solutions in pyridine, the pyridine has a double role, acting as an electron donor toward  $\text{I}_2$  in reaction (1), and as a polar medium in assisting reactions (2) and (3).

The present research was undertaken in the hope of studying these two roles of

<sup>7</sup>G. Kortüm and H. Wilski, Z. physik. Chem. **202**, 35 (1953). See also Kortüm, ref. 4.

<sup>8</sup>They find an ionic dissociation constant  $(\text{PyI}^+)(\text{I}^-)/(\text{Py} \cdot \text{I}_2)$  of about  $4.6 \times 10^{-8}$ , which corresponds to about 2% ionization at  $10^{-4}$  molar iodine. This may be compared with  $1.2 \times 10^{-11}$  for  $(\text{H}_2\text{OI})^+(\text{I}^-)/(\text{H}_2\text{O} \cdot \text{I}_2)$  as determined by R. P. Bell and E. Gelles [J. Chem. Soc. 2734 (1951)] and smaller values (see reference 7) for the benzene and dioxane complexes. However, it seems not impossible that some of the alcohols may have larger values [cf. L. I. Katzin, J. Chem. Phys. **21**, 490 (1953)].

<sup>9a</sup>Kleinberg, Zingaro, and Van der Werf, J. Am. Chem. Soc. **73**, 88 (1951).

<sup>9b</sup>Kleinberg, Colton, Sattizahn, and Van der Werf, J. Am. Chem. Soc. **75**, 447 (1953).

<sup>10</sup>Reference 1a, p. 818; reference 1b, pp. 812, 819.

pyridine separately by a spectrophotometric investigation, first, of equilibrium (1) at varying low concentrations of Py and  $I_2$  in a non-polar solvent medium; second, of the combined equilibria (1), (2), and (3) in a polar medium (perhaps pyridine itself, or preferably a different polar solvent). These two phases of the present work are reported in Sections I and II below.

In Section I equilibrium (1) was successfully studied in heptane solution. The visible iodine band of the outer complex  $Py \cdot I_2$  was located at the exceptionally strongly shifted position of  $\lambda 4,220$  (for free iodine it is at  $\lambda 5,200$ ), and the expected charge-transfer band at  $\lambda 2,350$ . The equilibrium constant for (1), and the heat of formation of  $Py \cdot I_2$ , were determined.

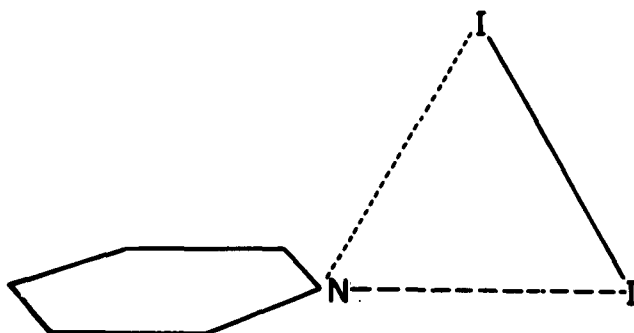


Fig. 1

much as perhaps 25 percent dative character. That is, in the type of formulation given by Mulliken,<sup>1</sup>

$$\psi(Py \cdot I_2) \approx a \psi_0(\text{no-bond } Py, I_2) + b \psi_1(\text{dative } Py^+ - I_2^-), \quad (4)$$

with  $a^2 \approx 0.75$ ,  $b^2 \approx 0.25$ . In Eq. (4), because of the asymmetry (Figure 1) and unusual strength of the complex, the dative function  $\psi_1$  may be already approximately of the structure  $C_5H_5N^+ - I^-$  with the  $N^+$  bonded to one I atom nearly in the Py plane (N-iodopyridinium ion) leaving the other I atom as an  $I^-$  above the plane.<sup>12</sup> An outer complex with an exceptionally large amount of dative character may well account for the fact<sup>5</sup>

<sup>11</sup>This is based on general considerations previously advanced by Mulliken (reference 1).

<sup>12</sup>The Py would then be acting as an n donor in the terminology of reference 1b. However, to a slight extent, it probably acts simultaneously also as a  $\pi$  donor (like benzene in its iodine complex; cf. footnote 42 on page 818 of reference 1a).  $\psi_1$  in Eq. (4) would then involve a mixture of mainly n with a little  $\pi$  donor action by the Py.

that complex formation causes greater changes in the infrared spectrum in the case of Py than for any other known cases (except the related picolines).

When the work reported in Section II was undertaken, it was with the thought,<sup>10</sup> suggested by the conductivity studies of Audrieth and Birr,<sup>6</sup> that in pure Py, acting as a polar medium, (a) equilibrium for reaction (2) lies almost completely to the right; but (b) the reaction proceeds only very slowly, over a high potential barrier; and that as fast as  $(\text{PyI})^+\text{I}^-$  is formed, reaction (3) proceeds largely to the right. However, the recent work of Kortüm and Wilski<sup>7</sup> indicates that ions  $\text{PyI}^+$  and  $\text{I}^-$  are formed at once in  $\text{I}_2$  solutions in Py, in definite relatively small equilibrium concentrations, and that a later slow increase in ionic concentration is due to slow side-reactions. Taken in connection with our spectrophotometric results in Sections I and IIA and the discussion presented in IIA, the work of Kortüm and Wilski indicates that in the absence of side-reactions most of the iodine would remain as  $\text{Py}\cdot\text{I}_2$ , but that a small portion of it has at once undergone reaction (2) followed by (3), or else perhaps the direct ionization



Further discussion will be given in Section IIA.

#### EXPERIMENTAL

C. P. pyridine was refluxed with chromium trioxide for several hours to remove traces of picolines, dried by NaOH, and distilled from magnesium perchlorate. C. P. iodine was sublimed and kept in a desiccator. Solvents were purified by the methods described by Potts.<sup>13</sup> Absorption measurements were made in a Beckman spectrophotometer, using 10cm, 1cm, 0.0296cm, and 0.0109cm cell thicknesses. Apart from the use of cells with fairly well fitting lids, no precautions were taken to avoid moisture uptake during a run. No lids at all were possible in experiments using spacers to decrease cell thickness.

#### I. THE $\text{Py}\cdot\text{I}_2$ COMPLEX IN A NON-POLAR SOLVENT

The equilibrium (1) was studied in very dilute solutions ( $<0.1\%$  Py +  $\text{I}_2$ ) in heptane ( $>99.9\%$  by weight). As pyridine in increasing but small amounts is added to a (violet) dilute solution of iodine in heptane, the solution goes through a reddish

<sup>13</sup>W. J. Potts, *J. Chem. Phys.* 20, 809 (1952).

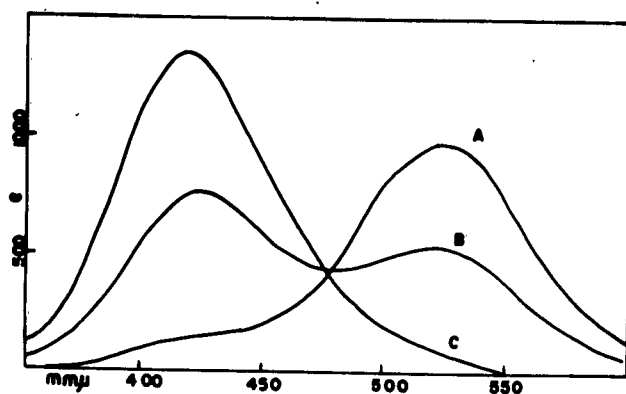


Fig. 2. Plot of extinction coefficient [ $\epsilon = (1/lc)\log_{10}(I_0/I)$ , where  $l$  = cell thickness, and  $c$  = formal molarity based on total iodine added] against wavelength for 0.0005M iodine solutions in heptane, with increasing amounts of pyridine. Room temperature. Cell thickness = 1.00cm.

- A. Pyridine 0.0005M  
 B. Pyridine 0.005M  
 C. Pyridine 0.25M

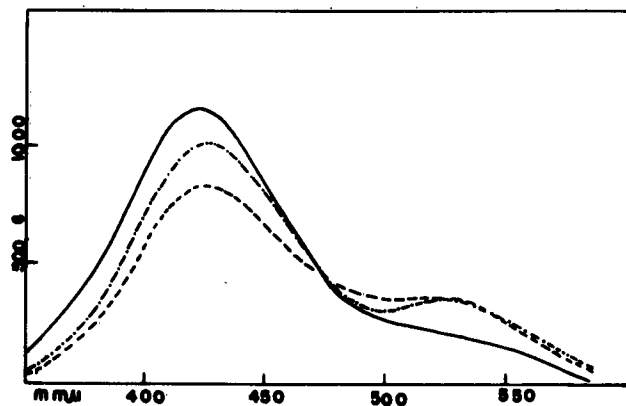


Fig. 3. Plot of formal extinction coefficient (see Fig. 2) against wavelength of  $I_2 + Py$  in heptane for a series of temperatures. Cell thickness = 1.00cm.

- 2°C Py = .005M  $I_2$  = .0005M  
 — 16.7°C Py = .025M  $I_2$  = .000625M  
 - - - 41°C Py = .025M  $I_2$  = .000625M

The equilibrium shifts strongly towards  $Py \cdot I_2$  as the temperature is lowered, but the pyridine concentration has been lowered in the 2°C experiment so that both peaks are measurable.

color to golden brown. The uncomplexed  $I_2$  peak at 5,200Å diminishes and is replaced by a new and somewhat higher but otherwise very similar peak at 4,220Å (cf. Figure 2). The peaks are well enough separated for a fairly accurate determination of the equilibrium constant  $K$ :

$$K = \frac{(Py \cdot I_2)}{(Py)(I_2)} \text{ litres/mol.}$$

From the  $K$  values at 2°C (649), 16.7°C (290), and 41°C (101)--cf. Figure 3--a graph was made (Figure 4) from which in the usual way the heat of dissociation of  $Py \cdot I_2$  was calculated to be  $7.8 \pm 0.2$  kcal/mole. It is of some interest that this result agrees closely with the value 7.95kcal/mole estimated from the heat of solution of  $I_2$  in pure  $Py$  by Hartley and Skinner.<sup>3</sup> From the available data the free energy and entropy

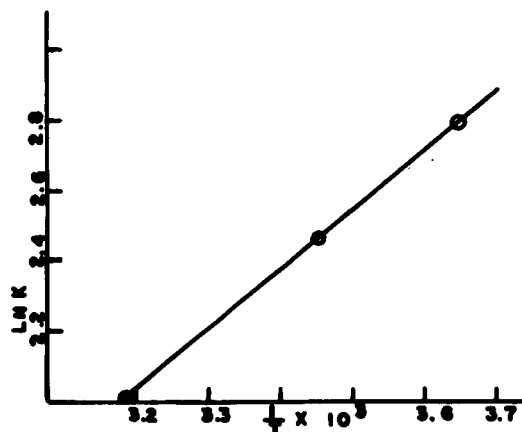


Fig. 4. Plot of  $K = (Py \cdot I_2) / (Py)(I_2)$  [litres/mole] against  $1/T$  for the equilibrium between iodine and pyridine in heptane.

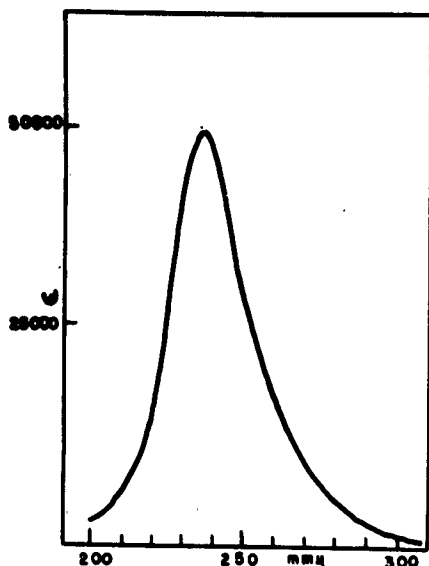


Fig. 5. The  $\text{Py}\cdot\text{I}_2$  charge-transfer spectrum at room temperature. The absorption of pyridine which lies in this region was cancelled out exactly by dividing a 0.05M pyridine solution in heptane into two parts, adding iodine (0.0005M) to one half, and using the other half as a blank. Cell thickness = 0.0296cm. Free  $\text{I}_2$  is negligible in its effect.

changes for reaction (1) were also computed, the results, in conventional units, at  $17^\circ\text{C}$ , being,  $\Delta F = -3.3$ ,  $\Delta H = -7.8$ ,  $\Delta S = -15.5$ .

McConnell, Ham, and Platt<sup>14</sup> have predicted that the charge-transfer peak of  $\text{Py}\cdot\text{I}_2$  should occur at 38,000K ( $2,635\text{\AA}$ ), on the basis of an electron impact value of 9.8 volts<sup>15</sup> for the ionization potential of pyridine. Use of the same ionization potential in an equation given by Hastings, Franklin, Schiller, and Matsen,<sup>16</sup> which fits a great number of iodine complexes closely, gives a similar prediction (38,300K or  $2,610\text{\AA}$ ). A search of this region using  $\text{Py}\cdot\text{I}_2$  in heptane at concentrations of 0.01M in Py and 0.0005M in  $\text{I}_2$ , with thin cells to avoid excessive pyridine absorption, showed such a band with peak at 42,600K ( $2,350\text{\AA}$ ). The extinction

coefficient is sufficiently large ( $\epsilon = 50,000$ ) that no difficulty was experienced in locating this band in spite of the considerable pyridine absorption in this region.

The charge-transfer band is shown in Figure 5, in which the pyridine absorption was automatically cancelled out by using as a blank part of the heptane + pyridine solution which had been used to dissolve iodine. No correction for free  $\text{I}_2$  was needed, in view of its very low concentration and small absorption near  $\lambda_{2,350}$ .

The fact that the observed charge-transfer band is at somewhat shorter wavelengths

<sup>14</sup>H. McConnell, J. S. Ham, and J. R. Platt, *J. Chem. Phys.* **21**, 66 (1953).

<sup>15</sup>Hustrulid, Kusch, and Tate, *Phys. Rev.* **54**, 1037 (1938). Stevenson and Schissler in unpublished work have recently obtained 9.85 volts (private communication from D. P. Stevenson).

<sup>16</sup>S. H. Hastings, J. L. Franklin, J. C. Schiller, and F. A. Matsen, *J. Am. Chem. Soc.* **75**, 2900 (1953). The form of their equation is based on Mulliken's theoretical discussion in reference 1a.

than predicted may perhaps be connected with the exceptionally high stability of the  $\text{Py}\cdot\text{I}_2$  complex. The validity of the predictions mentioned above is dependent on an approximate constancy of certain parameters in the equations used. Although this constancy is apparently surprisingly well fulfilled for most iodine complexes,<sup>16</sup> it has no obvious theoretical basis. Or on the other hand, possibly the reported ionization potential of 9.8 volts is inaccurate; a value of 10.3 volts would give a prediction corresponding to the observed position of the charge-transfer band.

Or, perhaps the observed 9.8 volts is the first  $\pi$  ionization potential, but the relevant potential, which should correspond not to a  $\pi$  but to a non-bonding (i.e., "onium" or n) ionization potential essentially of the N atom,<sup>12</sup> is at a higher voltage. However, the absorption spectrum of pyridine suggests that the  $\pi$  and n ionization potentials are actually almost equal. This statement is based on the fact that, taking the means of the frequencies of transitions to corresponding singlet and triplet states,<sup>17</sup> the frequencies of the first "n- $\pi$ " and " $\pi$ - $\pi$ " transitions are almost exactly equal. But here, one should bear in mind, it has never been proved that, in the so-called n- $\pi$  transitions in the aza-substituted aromatics, the transition is really from a true localized non-bonding (n) orbital of the N atom. It would be safer to call such transitions  $\sigma$ - $\pi$  transitions, where the  $\sigma$  orbital may be a fairly strongly delocalized orbital only partly localized on the N atom. The appropriate localized N atom true n ionization potential required in predicting the location of the charge-transfer band would then correspond to a weighted mean of several  $\sigma$  ionization potentials and might be appreciably greater than the minimum  $\sigma$  ionization potential.

## II. THE SYSTEM PYRIDINE PLUS IODINE IN POLAR SOLVENTS

### A. The Transition to Pure Pyridine as Solvent

When, in a dilute solution of iodine plus pyridine in heptane, the pyridine concentration is gradually increased, the  $\lambda_{4,220} \text{Py}\cdot\text{I}_2$  iodine band begins to shift toward shorter wavelengths, and its extinction coefficient increases. The relations between position and  $\epsilon$  of the band maximum, and pyridine concentration, are shown in Figure 6, for a fixed concentration (0.0005 molar) of iodine. (At these concentrations, practically all the iodine should be complexed.) The position of the band approaches a limiting value of  $3,890\text{\AA}$ , and  $\epsilon_{\text{max}}$  a limiting value of 2,120 in pure

<sup>17</sup>Cf., e.g., J. H. Rush and H. Sponer, J. Chem. Phys. 20, 1847 (1952), Table VII.

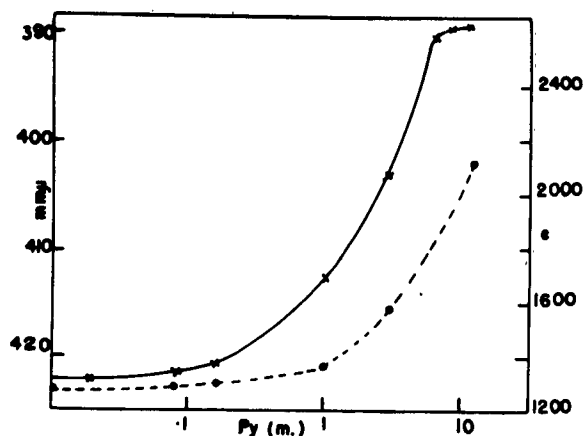


Fig. 6. Variation in position (x—x) and extinction coefficient (o---o) of the  $\text{Py} \cdot \text{I}_2$  absorption band with increasing pyridine concentration.  $\text{I}_2 = 0.0005\text{M}$ . Solvent heptane. Room temperature.

pyridine.<sup>18</sup> These changes, as distinct from some of the phenomena to be described in Part C of this Section, are reversible: dilution of the solution with heptane results in a return of the position of the band to  $\lambda_{4,220}$  with corresponding diminution in intensity.

Attempts were made also to see what happens to the "charge-transfer" band at  $2,350\text{\AA}$  as the pyridine concentration is increased. Unfortunately, even using special thin cells (0.001cm) constructed by putting a rolled lead spacer between quartz plates the experiments could be carried out only up to 1.5M Py (see Figure 7). At this Py concentration, with 0.06M iodine, the position of the charge-transfer band appears to be shifted to about  $2,450\text{\AA}$ . No appreciable change in the ratio of the pyridine molar absorption to that of the charge-transfer band could be detected.

In connection with the interpretation of the foregoing observations, some unpublished infrared work of Glusker<sup>5</sup> on solutions containing Py and  $\text{I}_2$  is highly relevant. He finds no appreciable difference between the modified Py infrared bands in  $\text{CS}_2$

<sup>18</sup>Kleinberg and collaborators (reference 9b), for iodine at  $2 \times 10^{-4}$  molar in pyridine, find  $\lambda_{\text{max}} = 383\text{-}380\text{m}\mu$  and  $\epsilon_{\text{max}} \approx 2,600\text{-}2,700$ . The moderate difference between their results and ours at  $5 \times 10^{-4}$  molar can be understood in terms of our findings at high dilution, as reported in Section IIC and Figure 8.

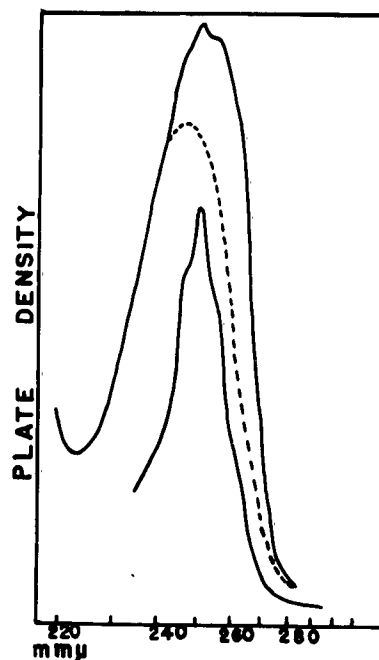


Fig. 7. Densitometer trace showing (a) 1.5M pyridine absorption, (b) 1.5M pyridine + 0.06M iodine showing charge-transfer peak shifted to about  $2,450\text{\AA}$  and superposed on the pyridine absorption. The dotted curve gives the estimated shape of the charge-transfer band.

solutions very dilute in Py and in those much more concentrated, up to  $I_2$  solutions in pure Py. This strongly indicates that these modified bands are due to essentially the same  $Py \cdot I_2$  entity whether the solvent is an inert one ( $CS_2$ ) or pure Py. The gradual shift of the  $\lambda_{4,220}$   $Py \cdot I_2$  band in heptane to  $\lambda_{3,890}$  in Py solvent may now probably be attributed to a gradual clustering of polar Py molecules around the strongly polar  $Py \cdot I_2$  molecules, causing these to become more polar [increased  $b$  in Eq. (4)] and more stable; but the infrared evidence indicated that these changes cannot be very large.<sup>19</sup>

It was suggested earlier<sup>10</sup> that the "inner complex" of structure  $(PyI)^+I^-$  may be so much stabilized by the polar solvent pyridine as to be present in predominant amount in that solvent. But according to the preceding paragraph, it appears that  $Py \cdot I_2$  remains predominant even in pure Py, and this suggests that  $(PyI)^+I^-$  if present is only in small amounts. The definite presence<sup>7</sup> of the ions of  $(PyI)^+I^-$  in small concentrations does, however, presumably indicate that a correspondingly small amount of the inner complex itself is present in accordance with Eq. (3).<sup>20</sup>

<sup>19</sup>Or perhaps the observed continuously shifting peak is the result of a superposition in changing proportions of two distinct bands; if so, these may most probably be attributed to unsolvated and fully solvated  $Py \cdot I_2$  molecules. The limiting positions  $\lambda_{4,220}$  and  $\lambda_{3,890}$  are so close together (unlike those of the  $Py \cdot I_2$  and free  $I_2$  iodine peaks in Figure 1) that the superposition of two such bands would give a single peak. Another conceivable explanation of the  $\lambda_{3,890}$  peak, namely that it might correspond to a superposition of the  $\lambda_{4,220}$   $Py \cdot I_2$  peak and the  $\lambda_{3,600}$   $I_3^-$  peak can almost certainly be ruled out because these peaks are too far apart. [A very small, probably negligible, amount of the very strongly absorbing ion  $I_3^-$  should be present in equilibrium in accordance with Eqs. (6) and (7) of Section IIC. In addition, the possible presence of a trace of water or other impurities should give rise to additional  $I_3^-$ , but probably not enough to affect the observed absorption appreciably except for the very low  $I_2$  concentrations discussed in Section IIC.]

<sup>20</sup>The present work does not throw doubts on the concept of an "inner complex" as discussed in reference 1b, but indicates that the inner complex of  $Py \cdot I_2$  is not so low in energy as was at first surmised. (Consideration of the system  $I_2 + H_2O$  similarly indicates that, there too, the inner complex  $(H_2OI)^+I^-$  in water solution is a structure of higher energy than the outer complex  $H_2O \cdot I_2$ .) It is conceivable, however, that the solvated inner complex or ion-pair  $(PyI)^+I^-$ , while separated by a considerable activation barrier from the lower-energy outer complex, may be somewhat unstable with respect to the interposition of a Py molecule between the  $(PyI)^+$  and  $I^-$  ions, so that instead of the equilibria (2) and (3) one has something like



### B. Pyridine Plus Iodine in Other Polar Solvents

In order to differentiate between specific effects due to excess pyridine and effects due to increasing polarity of the solvent as pyridine is added to heptane solutions of iodine, attempts were made to study the pyridine-iodine complexes in other polar solvents.

Experiments in which pyridine was added to iodine dissolved in methanol were inconclusive because the very strong  $\text{MeOH}\cdot\text{I}_2$  charge-transfer band showed that most of the iodine was complexed with methanol rather than with pyridine. This was true up to concentrations of 4-5% of pyridine, beyond which it was impracticable to go.

When  $\text{Py}\cdot\text{I}_2$  solutions in Py were diluted with water, precipitation of golden-yellow " $\text{Py}\cdot\text{I}_2$ " crystals resulted.<sup>21</sup> Examination of the resulting solutions after filtration showed no trace of the characteristic  $\text{Py}\cdot\text{I}_2$  bands, but only  $\text{I}_3^-$  bands and visible and charge-transfer bands attributable to small amounts of complexes of  $\text{I}_2$  with the solvent.<sup>22</sup> Apparently the solid  $\text{Py}\cdot\text{I}_2$ , or perhaps<sup>21</sup>  $(\text{PyI})^+\text{I}^-$ , phase is but little soluble in these solvents.

### C. Very Dilute Solutions of Iodine in Pure Pyridine

In pure pyridine at concentrations below about 0.001 molar in iodine, the position and particularly the intensity of the  $\lambda_{3,890}$  band become increasingly concentration-dependent (cf. Figure 8), a fact which was not observed by Kleinberg and his associates<sup>9b,18</sup> because their cell thickness could be changed only by a factor of two, whereas it was varied by a factor of  $> 1,000$  in the experiments here described.

Strong dilution of more concentrated pyridine solutions ( $> 0.07$  molar), or the preparation of more dilute ones from pyridine and solid iodine, results in an instantaneous shift in the band maximum, accompanied by an increase in extinction coefficient

---

all participants in (2') and (3') being of course solvated. If more than one Py is interposed between  $(\text{PyI})^+$  and  $\text{I}^-$ , the Py may be regarded simply as a dielectric medium separating the ions.

<sup>21</sup>An X-ray study of these crystals would be of interest. It seems possible that they may be built from  $(\text{PyI})^+$  and  $\text{I}^-$  ions (cf. reference 1b, Section VI, and the discussion of  $\text{NH}_4^+ + \text{Cl}^-$  crystals on p. 811 of Section VIII), although their insolubility in water seems to indicate the contrary.

<sup>22</sup>L. I. Katzin [*J. Chem. Phys.* **21**, 490 (1953)] has studied the spectra of solutions of iodine in water and the alcohols and has demonstrated the presence of  $\text{I}_3^-$ , probably due largely, however, to the presence or formation of  $\text{I}^-$  from impurities.

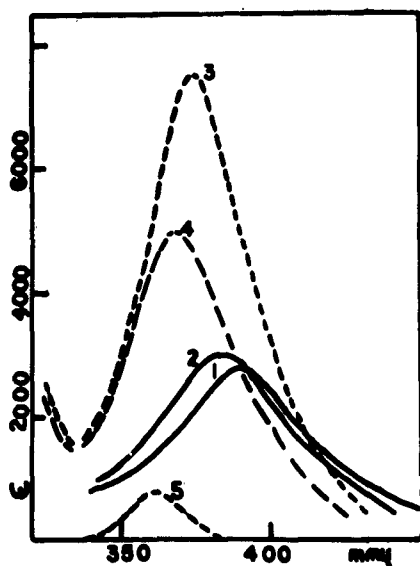


Fig. 8. Increasing dilution (1-5) of  $I_2$  solution in pure Py. Solid curves 1 and 2 are essentially due to  $Py \cdot I_2$ . Curve 3 shows the  $I_3^-$  curve nearing its maximum value. In curves 4 and 5 the  $I_3^-$  intensity falls again presumably because of dissociation into  $I^-$  ions. All  $\epsilon$  values are based on formal  $I_2$  concentration.

1. .025 Molar  $I_2$
2. .0005 Molar  $I_2$
3. .00005 Molar  $I_2$
4. .0000125 Molar  $I_2$
5. .00000612 Molar  $I_2$
6. .00000306 Molar  $I_2$

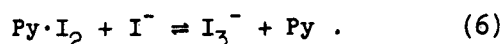
molar, a new phenomenon is observed. The  $I_3^-$  peak near  $\lambda 3,650$  diminishes rapidly in intensity (cf. Figure 8, curves 4 and 5), and no new band appears in the visible or ultraviolet to take its place. This change occurs just below the concentration range where Audrieth and Birr<sup>6</sup> reported the onset of anomalously high conductivity,<sup>24</sup> and

<sup>23a</sup>A. D. Awtrey and R. E. Connick, *J. Am. Chem. Soc.* **73**, 1842 (1951).

<sup>23b</sup>R. E. Buckles, J. P. Yuk, and A. I. Popov, *J. Am. Chem. Soc.* **74**, 4379 (1952).

<sup>24</sup>The occurrence of Eqs. (7)-(9) would account for the anomalously high conductivity observed by Audrieth and Birr without assuming the presence of  $Py^{++}$  ions as they did. However, since these results of Audrieth and Birr were obtained from aged solutions, after occurrence of what other investigators (references 7 and 9) consider to be a slow ring iodination liberating  $I^-$  ions, it would seem that their results may not be relevant to what occurs in pure Py without side-reactions.

(cf. Figure 8, curves 1-3). If the dilution is to between  $10^{-4}$  and  $10^{-5}$  molar, the maximum shifts to  $3,680\text{\AA}$  and the apparent extinction coefficient based on  $I_2$  rises to a maximum value of 9,000. The simultaneous appearance of a characteristic band of nearly double the extinction coefficient at  $2,875\text{\AA}$  makes it fairly certain that the maximum at  $3,680\text{\AA}$  is due to  $I_3^-$  ions. (The usual absorption spectrum of  $I_3^-$  consists of two peaks, one at  $\lambda 3,650$  and one of nearly double as great peak intensity at  $\lambda 2,950$ .<sup>23</sup>) The observed maximum extinction coefficient suggests that under optimum conditions about four  $I_2$  molecules yield one  $I_3^-$  group. This would indicate that about half the iodine remains as  $Py \cdot I_2$ , but that about half has reacted instantaneously in some way involving the formation of  $I^-$  followed by



If dilution is continued below  $10^{-5}$



MOLECULAR COMPOUNDS AND THEIR SPECTRA. IV

at higher dilutions according to Eq. (7) would be exactly what one should expect.

An interesting alternative possibility might be that the rise in  $I^-$ , hence in  $I_3^-$ , below  $10^{-4}$  molar, was due to Eqs. (8)-(9). To test the two possibilities, further investigations will be required, and it is planned to undertake them.

---

---

heptane solution, are not called in question by this possibility.